PHARMACOLOGICAL EFFECTS OF PAEONOL AGAINST ENDOPLASMIC RETICULUM STRESS AND INFLAMMATION-INDUCED ENDOTHELIAL DYSFUNCTION

CHOY KER WOON

FACULTY OF MEDICINE
UNIVERSITY OF MALAYA
KUALA LUMPUR

2018

PHARMACOLOGICAL EFFECTS OF PAEONOL AGAINST ENDOPLASMIC RETICULUM STRESS AND INFLAMMATION-INDUCED ENDOTHELIAL DYSFUNCTION

CHOY KER WOON

THESIS SUBMITTED IN FULFILMENT OF THE REQUIREMENTS FOR THE DEGREE OF DOCTOR OF PHILOSOPHY

FACULTY OF MEDICINE
UNIVERSITY OF MALAYA
KUALA LUMPUR

2018

UNIVERSITY OF MALAYA

ORIGINAL LITERARY WORK DECLARATION

Name of Candidate: Choy Ker Woon

Matric No: MHA140056

Name of Degree: Doctor of Philosophy

Title of Project Paper/Research Report/Dissertation/Thesis ("this Work"):

Pharmacological Effects of Paeonol against Endoplasmic Reticulum Stress and Inflammation-Induced Endothelial Dysfunction.

Field of Study: Pharmacology

I do solemnly and sincerely declare that:

(1) I am the sole author/writer of this Work;
(2) This Work is original;
(3) Any use of any work in which copyright exists was done by way of fair dealing and for permitted purposes and any excerpt or extract from, or reference to or reproduction of any copyright work has been disclosed expressly and sufficiently and the title of the Work and its authorship have been acknowledged in this Work;
(4) I do not have any actual knowledge nor do I ought reasonably to know that the making of this work constitutes an infringement of any copyright work;
(5) I hereby assign all and every rights in the copyright to this Work to the University of Malaya ("UM"), who henceforth shall be owner of the copyright in this Work and that any reproduction or use in any form or by any means whatsoever is prohibited without the written consent of UM having been first had and obtained;
(6) I am fully aware that if in the course of making this Work I have infringed any copyright whether intentionally or otherwise, I may be subject to legal action or any other action as may be determined by UM.

Candidate's Signature Date:

Subscribed and solemnly declared before,

Witness's Signature Date:

Name:

Designation:

PHARMACOLOGICAL EFFECTS OF PAEONOL AGAINST ENDOPLASMIC RETICULUM STRESS AND INFLAMMATION-INDUCED ENDOTHELIAL DYSFUNCTION

ABSTRACT

Endoplasmic reticulum (ER) stress and inflammation leads to endothelial dysfunction which are associated with the pathogenesis of cardiovascular diseases such as atherosclerosis, ischemic heart disease, cardiac hypertrophy and hypertension. Endothelial dysfunction is characterized by reduction of the endothelium-derived relaxing factors (EDRFs), particularly nitric oxide (NO), and/or an increase in endothelium-derived contracting factors (EDCFs), resulting in impairment of endothelium-dependent relaxation (EDR). Paeonol (20-hydroxy-40-methoxyacetophenone) is the most abundant phenolic component of Moutan cortex, the root of *Paeonia suffruticosa* Andrews which is widely used in traditional Chinese medicine. However, limited information is available concerning the pharmacological effects of paeonol in protecting against vascular endothelial dysfunction due to ER stress and inflammation. The present study investigates the pharmacological effects of paeonol against ER stress and inflammation-mediated endothelial dysfunction using *in vitro*, *ex vivo* and *in vivo* models. Our findings revealed that *ex vivo* and *in vivo* treatments with paeonol reversed the impaired EDR in C57BL/6J and peroxisome proliferator-activated receptor δ (PPARδ) wild-type mouse aortas following exposure with ER stress inducer, tunicamycin. Treatment with paeonol or tempol reversed the elevated blood pressure, ER stress and reactive oxygen species (ROS) as well as reduced NO bioavailability induced by tunicamycin in human umbilical vein endothelial cells (HUVECs), C57BL/6J and PPARδ wild-type mouse aorta. These protective effects of paeonol were diminished by co-incubation with PPARδ antagonist, GSK0660 and 5′ adenosine monophosphate-activated protein kinase (AMPK) antagonist, compound C as well as in aorta from PPARδ

knockout mouse. These findings suggest that paeonol protects against tunicamycin-induced endothelial dysfunction in mice by inhibiting ER stress and ROS production by elevating NO bioavailability via the AMPK/PPARδ pathway. The protective effect of paeonol was further examined against inflammation-induced endothelial dysfunction. Exposure of HUVECs to lipopolysaccharide (LPS), an inflammatory stimuli increased the protein expression of toll like receptor 4 (TLR4), bone morphogenic protein 4 (BMP4), BMP receptor type 1A (BMPR1A), nicotinamide adenine dinucleotide phosphate oxidase subunit 2 (NOX2), mitogen-activated protein kinases (MAPK), inducible nitric oxide synthase (iNOS) and cleaved caspase 3 and decreased the protein expression of phosphorylated endothelial nitric oxide synthase (eNOS). Co-treatment with paeonol reversed the LPS-induced inflammatory responses in HUVECs and in addition prevented the BMP4-induced apoptosis of the endothelial cells. In the mouse aorta, LPS impaired EDR was subsequently reversed by co-treatment with paeonol, noggin (BMP4 inhibitor), TAK242 (TLR4 inhibitor), apocynin (ROS scavenger), MAPK inhibitors and aminoguanidine (iNOS inhibitor). Blockade by BMP4 small interfering RNA (siRNAs) but not with TLR4 siRNA, abolished LPS-induced increases in BMP4 protein expression and vice versa. Silencing of TLR4 and BMP4 abolished the protective effects of paeonol on LPS-induced activation of cleaved caspase 3. The present findings imply that paeonol reduces LPS-induced endothelial dysfunction and cell apoptosis by inhibiting BMP4-triggered ROS production, independent of TLR4 signalling. Taken together, the results demonstrate the protective effects of paeonol against endothelial dysfunction induced by ER stress and inflammation. The present study further support other potential use of paeonol as a novel endothelial protective agent in cardiovascular diseases associated with ER stress and inflammation.

Keywords: paeonol, endoplasmic reticulum stress, inflammation, endothelial dysfunction, reactive oxygen species.

KESAN FARMALOGIKAL PAEONOL TERHADAP DISFUNGSI ENDOTELIAL YANG DISEBABKAN OLEH STRES RETIKULUM ENDOPLASMA DAN INFLAMASI

ABSTRAK

Stres retikulum endoplasma (ER) dan inflamasi menyebabkan disfungsi endotelial yang dikaitkan dengan patogenesis pelbagai penyakit jantung atau vaskular seperti aterosklerosis, penyakit iskemik jantung, hipertrofi jantung dan darah tinggi. Disfungsi endotelial dikaitkan dengan pengurangan faktor relaksi terbitan endotelium terutamanya nitrik oksida (NO) atau peningkatan faktor kontraksi terbitan endotelium pada tisu vaskular. Ketidakseimbangan ini menyebabkan kerosakan pada relaksi bergantungan endotelium. Paeonol (20-hydroxy-40-methoxyacetophenone) merupakan sebatian fenolik yang utama dalam Moutan cortex daripada akar *Paeonia suffruticosa* Andrews dan banyak digunakan dalam perubatan tradisional Cina. Namun, maklumat kesan farmakologikal paeonol terhadap disfungsi endotelial yang disebabkan oleh stres retikulum endoplasma dan inflamasi adalah terhad. Oleh itu, kajian ini berhasrat untuk menyiasat kesan farmakologi paeonol terhadap disfungsi endotelial yang disebabkan oleh stres retikulum endoplasma dan inflamasi dengan menggunakan model *in vitro*, *ex vivo* dan *in vivo*. Penemuan kami menunjukkan bahawa rawatan paeonol secara *ex vivo* dan *in vivo* mengurangkan gangguan relaksi bergantungan endotelium pada aorta yang diinduksi dengan tunicamycin (pencetus stres ER) pada tikus C57BL/6J dan *peroxisome proliferator-activated receptor δ* (PPARδ) *wild type*. Rawatan dengan paeonol dan tempol membalikkan peningkatan ER stress, darah tinggi, spesies oksigen reaktif dan pengurangan kandungan NO yang dicetuskan oleh tunicamycin pada sel endotelial vena umbilical manusia (HUVECs), aorta tikus C57BL/6J dan PPARδ *wild type*. Namun, paeonol tidak mempunyai kesan apabila aorta tikus C57BL/6J diinkubasikan dengan antagonis *peroxisome proliferator-activated receptor δ* (PPARδ), GSK0660 atau

antagonis *5' adenosine monophosphate-activated protein kinase* (AMPK), compound C dan pada aorta tikus PPARδ *knockout*. Keputusan kajian ini menunjukkan bahawa paeonol memulihkan disfungsi endotelium yang dicetuskan oleh tunicamycin dengan merencat stres ER dan oxidatif melalui laluan AMPK/PPARδ untuk meningkatkan bioavailabiliti NO. Kesan anti-inflamatori paeonol ke atas disfungsi endotelial yang disebabkan oleh inflamasi juga dikaji. Pendedahan kepada lipopolisakarida, (LPS, pencetus inflamasi) meningkatkan protein *toll like receptor 4* (TLR4), *bone morphogenic protein 4* (BMP4), *BMP receptor type 1A* (BMPR1A), *nicotinamide adenine dinucleotide phosphate oxidase subunit 2* (NOX2), *mitogen-activated protein kinases* (MAPK), *inducible nitric oxide synthase* (iNOS) dan *cleaved caspase 3* serta mengurangkan *phosphorylated endothelial nitric oxide synthase* (eNOS) dalam HUVECs. Kesan-kesan ini diperbalikkan dengan rawatan paeonol. Rawatan paeonol juga mengurangkan apoptosis yang dicetuskan oleh BMP4 pada HUVECs. Ganguan pada relaksi bergantungan endotelium oleh LPS juga diperbalikkan oleh paeonol, noggin (perencat BMP4), TAK242 (perencat TLR4), apocynin (perencat ROS), perencat MAPK dan aminoguanidine (perencat iNOS). Penyekatan laluan oleh BMP4 siRNAs memansuhkan peningkatan BMP4 dan *cleaved caspase 3* yang disebabkan oleh LPS pada sel. Sebaliknya, TLR4 siRNA tidak menyekat laluan BMP4 yang dirangsang oleh LPS. Penyekatan laluan oleh siRNAs BMP4 dan siRNAs TLR4 memansuhkan kesan paeonol ke atas pengaktifan *cleaved caspase 3* oleh LPS. Data ini mencadangkan bahawa paeonol mengurangkan disfungsi endotelial, apoptosis dan spesies oksigen reaktif yang dicetuskan oleh LPS dengan menghadang laluan TLR4 dan BMP4. Secara kesimpulannya, kajian ini menunjukkan kesan perlindungan paeonol terhadap disfungsi endotelial yang dicetus oleh stres retikulum endoplasma dan inflamasi. Kajian menyokong selanjutnya penggunaan paeonol sebagai agen terapeutik novel untuk

perlindungan kepada penyakit vaskular yang berpunca daripada stres retikulum endoplasma atau inflamasi.

Kata kunci: paeonol, stres retikulum endoplasma, inflamasi, disfungsi endotelial, spesies oksigen reaktif.

ACKNOWLEDGEMENTS

This thesis owes its existence with the help, support and inspiration of several people. Firstly, I would like to express my sincere gratitude to my supervisors, Professor Mohd Rais Mustafa and Dr Dharmani Murugan for their guidance during my research. They always engaged me in intellectual discussion as well as provided me opportunity to attend lab attachment and various conferences. Secondly, I would like to thank the help from post-doc, Dr. Lau Yeh Siang and Dr Liu Jian. They had patiently taught me the laboratory techniques and worked closely with me especially during the initial stage of the research. Additionally, I would also like to express my appreciation to Professor Huang Yu from Chinese University of Hong Kong (CUHK) who wholeheartedly supported me during my 5 months lab attachment in CUHK and his physical insight was instrumental for the completion of the first part of the project. I would also like to thank Professor Paul Vanhoutte (University of Hong Kong) for his constructive comments and motivation which enable me to complete the second part of the project. I would also like to thank the colleagues and staffs from University Malaya and CUHK who were the fundamental in supporting me during these stressful and difficult moments. In addition, I would like to thank My Brain 15 scholarship from Ministry of Higher Education for the financial support on academic fees and living allowances. I am also grateful for the funding sources for research: High Impact Research (HIR) grant, Postgraduate Research Grant (PPP) and Fundamental Research Grant Scheme (FRGS) for not only for providing the funding which allowed me to undertake this research, but also for the opportunity to attend conferences. Finally, my deepest gratitude does to my family and my husband for their unconditional support throughout my studies. I owe deep appreciation for them who had been helping to take care of my son during my attachment in Hong Kong. Thank you once again as all of you enable me to offer my humble contribution to science especially in the field of Vascular Biology.

TABLE OF CONTENTS

LIST OF FIGURES

LIST OF TABLES

LIST OF SYMBOLS AND ABBREVIATIONS

%	:	percentage
&	:	and
a.m.	:	ante meridiem
AA	:	arachidonic acid
ACh	:	acetylcholine
ADMA	:	asymmetric dimethylarginine
ADP	:	activating purinoceptors
ADP	:	adenosine diphosphate
AG	:	aminoguanidine hydrochloride
ALK3	:	activin receptor-like kinase 3
AMPK	:	5' adenosine monophosphate-activated protein kinase
ANOVA	:	analysis of variance
ASK	:	apoptosis signal-regulating kinase
ATF	:	activating transcription factor
BH_4	:	tetrahydrobiopterin
BiP	:	immunoglobin binding protein
BKC_a	:	calcium-activated potassium channels
BMP4	:	bone morphogenic protein 4
BMPER	:	BMP endothelial cell precursor-derived regulator
BSA	:	bovine serum albumin
bZIP	:	basic leucine zipper
Ca^{2+}	:	calcium ion
$CaCl_2$	:	calcium chloride
CAM	:	calmodulin

CaMKII	:	calmodulin-dependent protein kinase II
CGMP	:	cyclic nucleotide cyclic 3’, 5’-guanosine monophosphate
CHOP	:	C/EBP-homologous protein
CO_2	:	carbon dioxide
COX	:	cyclooxygenase
DAF-FM DA	:	4-amino-5-methylamino-2’,7’-difluorofluorescein
DETCA	:	diethylthiocarbamic acid
DHE	:	dihydroethidium
DMEM	:	Dulbecco's Modified Eagle Medium
DPI	:	diphenyleneiodonium
ECL	:	enhanced chemiluminescence
EDCF	:	endothelium-derived contracting factor
EDHF	:	endothelium-derived hyperpolarising factor
EDR	:	endothelium-dependent relaxation
EDRF	:	endothelium-derived relaxing factor
EDTA	:	ethylenediaminetetraacetic acid
EGM	:	endothelial cell growth medium
eIF2α	:	eukaryotic translation initiation factor 2α
ELISA	:	enzyme-linked immunosorbent assay
eNOS	:	endothelial nitric oxide synthase
ER	:	endoplasmic reticulum
ERAD	:	endoplasmic-reticulum-associated protein degradation
ERK	:	extracellular-signal-regulated kinase
ERO	:	endoplasmic reticulum oxidoreductin
et al.	:	*et alia* (and other people)
ET-1	:	endothelin-1

FBS	:	fetal bovine serum
g	:	gram
GAPDH	:	glyceraldehyde 3-phosphate dehydrogenase
GRP	:	glucose-regulated protein
GSH	:	glutathione
GSSG	:	glutathione disulphide
GTP	:	guanosine 5'-triphosphate
GTPCH	:	guanosine-5'-triphosphate cyclohydrolase
H_2O_2	:	hydrogen peroxide
HEPES	:	4-(2-hydroxyethyl)-1-piperazineethanesulfonic acid
HOG-LDL	:	heavily-oxidised glycated low-density lipoprotein
Hsp90	:	heat shock protein 90
HUVECs	:	human umbilical vein endothelial cells
i.p.	:	introperitoneal
I/R	:	ischemia/ reperfusion
IACUC	:	Institutional Care and Use Committee
ICAM	:	intercellular adhesion molecule 1
IL-1	:	interleukin- 1
IL-6	:	interleukin-6
IL-8	:	Interleukin-8
iNOS	:	inducible nitric oxide synthase
IP receptor	:	prostacyclin receptor
IRE1	:	inositol-requiring protein 1
JNK	:	cJUN NH_2-terminal kinase
K^+	:	potassium ion
K-ATP	:	ATP-sensitive potassium channel

KCl	:	potassium chloride
kg	:	kilogram
KH_2PO_4	:	monopotassium phosphate
KO	:	knockout
K_V	:	voltage-activated potassium channel
L-Arg	:	amino acid l-arginine
LEC	:	lucigenin-enhanced chemiluminescence
LPS	:	lipopolysaccharide
MAPK	:	mitogen-activated protein kinase
mg	:	milligram
$MgCl_2$	:	magnesium chloride
$MgSO_4$	:	magnesium sulfate
$MgSO_4.7H_2O$	:	magnesiumsulphate heptahydrate
mL	:	milliliter
mM	:	millimolar
mm	:	millimeter
mM	:	millimolar
MMP	:	mitochondrial membrane potential
mN	:	millinewton
Na_2HCO_3	:	sodium bicarbonate
NaCl	:	Sodium chloride
NADPH	:	nicotinamide adenine dinucleotide phosphate
$NaHCO_3$	:	sodium bicarbonate
NF-κB	:	nuclear factor-κB
nM	:	nanomolar
nm	:	nanometer

nNOS	:	neuronal nitric oxide synthase
NO	:	nitric oxide
NOS	:	nitric oxide synthase
NOx	:	total nitrite and nitrate concentration
NRF2	:	nuclear erythroid 2 p45-related factor 2
O_2	:	oxygen
OD	:	optical density
OH-	:	hydroxyl radicals
ONOO-	:	peroxynitrite
ox-LDL	:	oxidized low-density lipoprotein
P	:	phosphorylate
PBA	:	4-phenylbutyrate
PBS	:	phosphate buffered saline
PDI	:	protein disulfide isomerase
pEC_{50}	:	concentration that produces 50% of R_{max} (maximum effect)
PERK	:	protein kinase RNA-like endoplasmic reticulum kinase
PGD_2	:	prostaglandin D2
PGE_2	:	prostaglandin E2
$PGF_{2\alpha}$	:	prostaglandin F2α
PGI_2	:	prostacyclin
pH	:	potential of hydrogen
Phe	:	phenylephrine
PI	:	propidium iodide
PI3K	:	phosphatidylinositol 3-kinase
PLA_2	:	phospholipase A2
PPARδ	:	peroxisome proliferator-activated receptor δ

PVDF	:	polyvinylidene difluoride
RIPA	:	radioimmunoprecipitation
R_{max}	:	maximum response
ROS	:	radical oxygen species
rpm	:	revolutions per minute
S1P	:	serine protease site-1
S2P	:	metalloprotease site-2
SDS	:	sodium dodecyl sulphate
SEM	:	standard error of mean
sGC	:	soluble guanylate cyclase
SHRs	:	spontaneously hypertensive rats
siRNA	:	small interfering ribonucleic acid
SNP	:	sodium nitroprusside
SOD	:	superoxide dismutase
STZ	:	streptozotocin
TGF-β	:	transforming growth factor-beta
TLR	:	toll-like receptor
TNF-α	:	tumor necrosis factor alpha
TP	:	thromboxane-prostanoid
TRAF2	:	tumour necrosis factor receptor-associated factor 2
TUDCA	:	taurine-conjugated tursodeoxycholic acid
TXA_2	:	thromboxane A2
U	:	unit
UPR	:	unfolded protein response
V	:	volt
VCAM	:	vascular cell adhesion molecule

VEGF	:	vascular endothelial growth factor
vs.	:	versus
WT	:	wild-type
XBP	:	X-box binding protein
XBP1s	:	spliced form of XBP
μg	:	microgram
μL	:	microliter
μM	:	micromolar
μm	:	micrometer

LIST OF APPENDICES

CHAPTER 1: GENERAL INTRODUCTION

1.1 Endothelium and endothelial dysfunction

The vascular endothelium is the inner unicellular layer of the blood vessels which acts as an interface between the blood stream and the vessel wall (Vanhoutte, 1989). Vascular endothelial cells line the entire circulatory system, from the heart to the smallest capillaries (Augustin *et al.*, 1994). The endothelium serves a number of crucial roles in physiology and pathophysiology, including modulating vascular tone, platelet function, inflammatory responses, vascular smooth muscle cell growth and migration (Cines *et al.*, 1998). Under normal physiological condition, the healthy endothelium maintain the balance between vasoconstriction and vasodilation factors (Schwartz *et al.*, 2010). Nitric oxide (NO) which is released from the endothelial cells is a critical modulator of the local vascular tone (Cannon, 1998). Endothelial dysfunction is commonly associated with reduced NO bioavailability and represented by the loss of vasodilatory responses to stimuli such as acetylcholine or shear stress (Mudau *et al.*, 2012). Endothelial dysfunction is attributable to impaired release of endothelium-derived relaxing (EDR) and augmented production of endothelium-derived contracting (EDC) factors (Bijl, 2003). Endothelial dysfunction leads to the development of various cardiovascular diseases such as atherosclerosis, ischemic heart disease, hypertension and coronary heart disease (Zhang *et al.*, 2017).

1.2 Risk factors of endothelial dysfunction

Endoplasmic reticulum (ER) stress and inflammation have been identified as risk factors of endothelial dysfunction (Widlansky *et al.*, 2003). The endoplasmic reticulum is the cellular organelle where protein translation, folding and trafficking occurs (Galan *et al.*, 2014). Prolonged perturbation of the endoplasmic reticulum leads to ER stress and

unfolded protein response (UPR) (Shen *et al.*, 2004). ER stress and UPR pathways activation leads to increased oxidative stress in endothelial cells, resulting in endothelial dysfunction (Zeeshan *et al.*, 2016). The ER stress-induced oxidative stress involves activation of nicotinamide adenine dinucleotide phosphate (NADPH) oxidase (Santos *et al.*, 2009). Activation of CCAAT-enhancer-binding protein homologous (CHOP) from UPR induces NOX2 (a member of the NOX family of enzymes) which transfer electrons from NADPH to molecular oxygen (O_2), forming hydrogen peroxide (H_2O_2) or superoxides (Santos *et al.*, 2014). The superoxides interact with NO to form peroxynitrite which inactivates tetrahydrobiopterin (BH_4), an essential cofactor for endothelial nitric oxide synthase (eNOS), resulting in the uncoupling of eNOS from NO and reducing its bioavailability to cause endothelial dysfunction (Hamilton *et al.*, 2001; Loo *et al.*, 2000).

Besides ER stress, prolonged inflammation may similarly lead to endothelial dysfunction. Lipopolysaccharide (LPS), a major component of the outer membrane of gram-negative bacteria is a potent trigger of the inflammatory response (Wang *et al.*, 2009). LPS binds to toll-like receptors 4 (TLR4), a receptor in innate immunity which stimulate up-regulation of chemokines, adhesion molecules, and other inflammatory factors (Geng *et al.*, 2010) including high production of NO through the activation of inducible nitric oxide synthase (iNOS) (Chuaiphichai *et al.*, 2016). In LPS-induced endotoxemia of mice, iNOS-generated NO plays a key role in mediating endothelial dysfunction of conduit (aorta) and resistance (mesenteric) arteries. The iNOS-generated NO suppresses the expression of eNOS and inhibit the activity of guanylate cyclase, resulting in reduction of acetylcholine-induced relaxation (Chauhan *et al.*, 2003). Activation of TLR4 by LPS also augment the expression of NADPH oxidase triggering further oxidative stress (Kim *et al.*, 2010). Other than LPS, bone morphogenic protein 4 (BMP4) also induced pro-inflammatory response in endothelial cell through oxidative

stress pathway (Csiszar *et al.*, 2006). Increased level of reactive oxygen species (ROS) reduces eNOS coupling, reduces NO production, increases the activity of cyclooxygenase 1 (COX-1) and augmented EDCF-mediated contractions (Tang & Vanhoutte, 2009). These effects combine and contribute to endothelial dysfunction in arteries during inflammation (Liang *et al.*, 2013b).

1.3 Research justification

Various pharmacological agents are reported to ameliorate endothelial dysfunction and treat cardiovascular diseases. Metformin, a widely used antidiabetic drug with an insulin-sensitizing effect attenuated oxidative stress-induced cardiomyocyte apoptosis and prevented the development of heart failure in dogs, through activation of 5' adenosine monophosphate-activated protein kinase (AMPK) (Sasaki *et al.*, 2009). Pravastatin, a member of the drug class of statins, reduced cardiac remodelling due to pressure overload in mice, through inhibition of the ER stress signalling pathway (Zhao *et al.*, 2008). Amlodipine, inhibits the transmembrane influx of calcium ions (Ca^{2+}) into vascular smooth muscle and cardiac muscle, and has been used to treat angina and hypertension (Lee *et al.*, 2014a). However, prolonged usage of these drugs may cause adverse effects such as constipation, oedema, drowsiness, blurred vision, fatigue, nausea and vomiting (Mohebbi *et al.*, 2010). The present cardiovascular drugs remain ineffective in reducing mortality, for example, approximately 14 million individuals died of cardiovascular disease in 1990, and deaths are projected to rise to 25 million by 2020 in developing nations (Ohlstein, 2010). Large subgroups of patients with ischemia and arrhythmias underwent interventional procedures for treatment including angioplasty and ablation, but they are still left with significant morbidity (Wolfram & Donahue, 2013). There exists an unmet need for improved clinical outcomes in treating cardiovascular disease without side effects.

Recently, traditional Chinese medicine has rapidly regained interest amongst the pharmaceutical industries as new drug leads to provide innovative treatments for the benefits of human healthcare (Liu *et al.*, 2016b). Treatment option for cardiovascular diseases has extended to multitherapy which offers more *enormous potential* and holistic approach nowadays (Rodgers, 2003). Traditional Chinese medicine functions as a multi-target drug that act through a diversity of molecular mechanisms and therefore, more comprehensive in treating cardiovascular diseases (Liu *et al.*, 2016a).

Paeonol (2′-hydroxy-4′-methoxyacetophenone) is a major phenolic compound from the root bark of Chinese herb *Paeonia suffruticosa* (*Cortex Moutan*) (Matsuda *et al.*, 2001). In traditional Chinese medicine, *Cortex Moutan* is used to clear heat from blood, promote blood circulation and for the treatment of amenorrhea and dysmeorrhea (Zhu, 1998). Paeonol has been reported to have anti-oxidant (Ding *et al.*, 2016; Hsieh *et al.*, 2006), anti-apoptosis (Bao *et al.*, 2013; Wang *et al.*, 2011) and anti-inflammatory (Liao *et al.*, 2016; Liu *et al.*, 2017) effects both *in vitro* and *in vivo*. However, the pharmacological effects of paeonol on ER stress and inflammation related cardiovascular diseases has not been fully characterized.

1.4 Research Objectives and Hypothesis

Pharmacological therapies that can improve endothelial dysfunction may offer new potential therapeutic opportunities for treating cardiovascular diseases.

The first objective of this thesis is to investigate the effect of paeonol in ER stress-induced endothelial dysfunction, followed by a detailed investigation of the mechanisms through pharmacological approach *in vitro, ex vivo* and *in vivo.* We hypothesize that

paeonol improves EDR by alleviating ER stress and subsequently reduced ROS overproduction, normalized blood pressure and increased phosphorylation of eNOS.

The second objective of this study is to investigate the endothelial protective effect of paeonol and its underlying molecular mechanisms in inflammation-induced endothelial dysfunction and apoptosis *in vitro, ex vivo* and *in vivo.* We hypothesize that paeonol reduced inflammation-induced endothelial dysfunction by inhibiting BMP4 and TLR4, subsequently reducing ROS and iNOS-induced NO production as well as improving eNOS activity.

CHAPTER 2: LITERATURE REVIEW

2.1 Vascular Endothelium: structure and function

Endothelium comprised of a monolayer of endothelial cells that lines the inner wall of the blood vessel of the entire circulatory system (Rajendran *et al.*, 2013). The endothelium together with the extracellular matrix comprises the tunica intima in the blood vessel (Figure 2.1) (Waller *et al.*, 1992). The size of the endothelial cell is approximately 20-40 μm in length, 10-15 μm in width and 0.1-0.5 μm thickness (Cahill & Redmond, 2016). Under electron microscopy, the arterial endothelium appears as a continuous layer with tight junctions at the lateral borders of each cell which limit the movement of macromolecules (Bowyer *et al.*, 1977). Despite its apparent morphological simplicity and relative homogeneity, there is regional and species variations manifested by differences in permeability, responsiveness and biosynthesis (Cahill & Redmond, 2016).

Vascular endothelium functions as a selective permeable barrier between extravascular and intravascular compartments for the cardiovascular system (Rajendran *et al.*, 2013). Its anatomic location permits communication between circulating blood components and cells as well as interaction between the cells in the vessel wall (Deanfield *et al.*, 2007). It senses mechanical stimuli, such as pressure and shear stress, and hormonal stimuli, such as vasoactive substances. In response to these stimuli, it release mediators that regulate vasomotor function, trigger inflammatory processes, and affect haemostasis (Endemann & Schiffrin, 2004). The endothelium regulate the vascular tone by balancing the levels between the endothelium derived relaxing factors (EDRFs) and endothelium derived contracting factors (EDCFs) (Feletou, 2011). Therefore, endothelium is now perceived as

an organ which is important to maintain vascular health, and its dysfunction plays a key role in the development of several vascular diseases (Waller *et al.*, 1992).

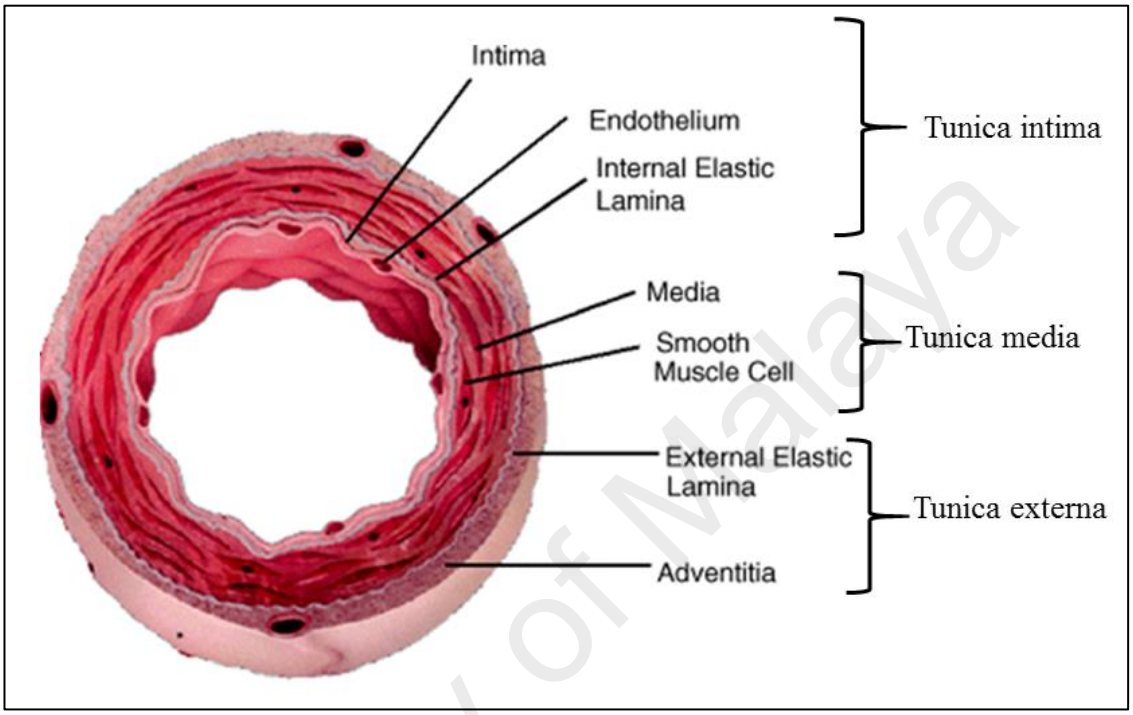

Figure 2.1: A general diagram illustrating the layers of the wall of blood vessel (Modified from Davis *et al*., 2003).

2.2 Endothelium-derived relaxing factors (EDRFs)

Triggered by several neurohumoral mediators and physical stimuli, endothelial cells influence the tone of the surrounding vascular smooth muscle cells by releasing vasodilator substances called EDRFs (Bassenge *et al.*, 1988; Vanhoutte *et al.*, 1995). Furchgott and Zawadzki (1980) were the first to conclude that the presence of endothelial cells is necessary to stimulate acetylcholine-induced endothelium-dependent relaxation of isolated arteries. The three main EDRFs released by the endothelium are (i) nitric oxide (NO), (ii) endothelium-derived hyperpolarizing factor (EDHF), and (iii) prostacyclin (PGI_2) (Figure 2.2). These EDRFs perform synergistically in a complex manner to maintain the vascular well-being and tone (Ozkor & Quyyumi, 2011). Studies have shown that the EDRFs are differently released in various vascular regions. Small resistance artery like mesentery arteries rely on EDHF while in larger conduit arteries like the aorta, NO is the predominant EDRF (Hwa *et al.*, 1994; White *et al.*, 1996).

Endothelium-derived NO is the main EDRFs in the vasculature. NO is formed from the conversion of a semi-essential amino acid, L-arginine to L-citrulline by an enzyme called nitric oxide synthase (NOS) in endothelial cells (Griffith *et al.*, 1988). There are three isoforms of NOS named according to their activity or type of tissue (Forstermann & Sessa, 2012). The isoforms of NOS are neuronal NOS (nNOS or type I NOS), inducible NOS (iNOS or type II NOS) and endothelial NOS (eNOS or type III NOS) (Forstermann & Sessa, 2012). This enzymatic transformation can be inhibited competitively by L-arginine analogs like NG-monomethyl-L-arginine and NG-nitro- L-arginine (Griffith *et al.*, 1988). The extend of NOS activation is determined by the Ca^{2+} concentration present in the endothelial cell, therefore it's calmodulin dependent (Moncada *et al.*, 1991). Once released, NO diffuses into the smooth muscle to activate a cytosolic enzyme called soluble guanylate cyclase (sGC) which accelerates the conversion of guanosine 5'-

triphosphate (GTP) to cyclic nucleotide cyclic 3', 5'-guanosine monophosphate (cyclic GMP) which ultimately leads to vasodilatation (Rapoport & Murad, 1983). Besides maintaining vascular tone, NO also plays a role in inhibiting the aggregation of platelets within the vessels to prevent thrombosis. In physiological environment, oxyhemoglobin in the erythrocytes instantly neutralizes the NO to prevent the adhesion of platelets and leukocytes to the endothelium (Vanhoutte *et al.*, 1995). In addition, NO act synergistically with prostacyclin to prevent platelet aggregations (Dalman & Porter, 1990) and growth of vascular smooth muscle cells (ScottBurden & Vanhoutte, 1993).

In smaller arteries, although NO is released, EDHF has been shown as the predominant EDRF (Hwa *et al.*, 1994; White *et al.*, 1996). Although the identify and exact role of EDHF is pathological as well as under normal conditions are not completely understood, K+ ion, gap junctions, eicosatrienoic acids (ETT) and hydrogen peroxide have been proposed as EDHF candidates (Kang, 2014). EDHF hyperpolarizes vascular smooth muscle cells by opening potassium (K^+) channels, closing voltage-dependent Ca^{2+} channels, thus allowing K^+ efflux along its chemical gradient and as a consequence, relaxes the vascular smooth muscle (Ozkor & Quyyumi, 2011). The release of EDHF by the endothelial cell is also controlled by the cytosolic Ca^{2+} concentration, and is inhibited by calmodulin antagonists (Nagao & Vanhoutte, 1993). Acetylcholine causes hyperpolarization of vascular smooth muscle in aorta with an intact endothelium but not in its absence (Ozkor & Quyyumi, 2011). In addition, increased in intracellular calcium activates phospholipase A2 (PLC) to produce arachidonic acid (AA). AA metabolites derived from cytochrome P450 monooxygenases that generates eicosatrienoic acids (EETs) and hyperpolarize the smooth muscle cells by activating large conductance calcium-activated potassium channels (BKC_a) in blood vessels including large and small coronary arteries (Feletou & Vanhoutte, 2006). EETs may also act in an autocrine manner

on endothelial cells by activating transient receptor potential (TRP) V4 channels, which promote Ca^+ influx further increasing the calcium concentration and activating calcium dependent potassium (K_{Ca}^+) channels to cause hyperpolarization and release of K^+ ions into the subendothelial space (Ozkor & Quyyumi, 2011). H_2O_2 has been reported to cause hyperpolarization by several mechanisms including the cGMPor cAMP-mediated pathway, activation of PKA/PLA2 to release PGI2, or direct activation of various K+ channels (Kang, 2014).

Another important EDRF that elicits vasodilation is prostacyclin (PGI_2). PGI_2 is the metabolite of AA formed by COX enzyme in endothelial cells (Moncada & Vane, 1978). It activates prostacyclin (IP) receptor on vascular smooth muscle to elicit relaxation in most normal arteries through cAMP stimulation (Feletou, 2006). Prostacyclin appears to be released more *in vivo* than *in vitro* (Shimokawa *et al.*, 1988). Endothelium-dependent relaxations potentiated by prostacyclin are most pronounced in the coronary and basilar arteries (Shimokawa *et al.*, 1988).

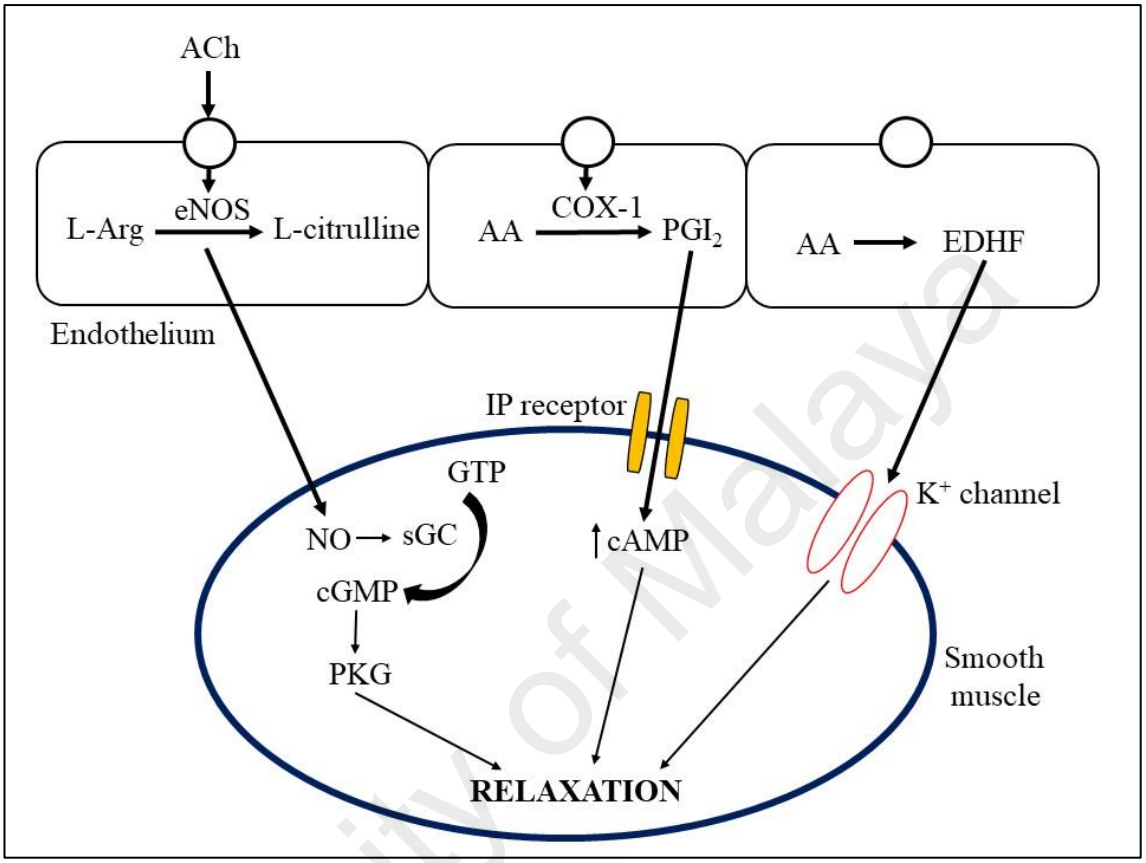

Figure 2.2: Endothelium-derived relaxing factors (EDRFs). The three EDRFs are: i) Nitric oxide (NO) which is produced from amino acid L-arginine (L-Arg) by NO synthase (NOS) enzyme diffuses to smooth muscle and activates soluble guanylate cyclase (sGC), causing increased production of guanosine 3′,5′-cyclic monophosphate (cGMP), which results in relaxation; ii) Prostacyclin (PGI_2) formed by cyclooxygenase-1 (COX-1) from arachidonic acid (AA), diffuses to vascular muscle where it activates adenylate cyclase, causing increased production of adenosine 3′,5′-cyclic monophosphate (cAMP) that relaxes smooth muscle; iii) Endothelium-derived hyperpolarizing factor (EDHF) is probably a product of AA metabolism, diffuses to vascular muscle to activate potassium (K^+) channels. Augmented potassium channels activity results in hyperpolarization and relaxation of vascular smooth muscle (Modified from Faraci and Heistad, 1998).

2.3 Endothelium-derived contracting factors

Other than EDRFs, the endothelium also release a variety of vasoconstrictor factors called endothelium-derived contracting factors (EDCFs) (Lüscher *et al.*, 1992). Among the EDCFs released by the endothelium are endothelin (ET)-1 and endoperoxidases (Figure 2.3).

The vasoconstrictor peptide ET was discovered as one of the major EDCF (Yanagisawa *et al.*, 1988). ET acts as a natural counterpart of NO (Luscher *et al.*, 1990). Several factors modulate ET production and release such as shear stress, angiotensin II, thrombin, adrenaline, oxidised low-density lipoproteins and inflammatory cytokines (Barton *et al.*, 1997; Kohno *et al.*, 1989; Woods *et al.*, 1998; Yoshizumi *et al.*, 1989). Three isoformes of the peptide (ET-1, ET-2 and ET-3) exist, which are converted by the endothelin converting enzyme (ECE) from their precursors big endothelin originating from pre-proendothelin peptides cleaved by endopeptidases (Ikegawa *et al.*, 1990; Shimada *et al.*, 1994). Among the several peptides, ET-1 is the most known, and its vasoactive properties have been extensively researched. ET-1 mediate vasoconstriction through the stimulation of receptors, namely ET_A and ET_B receptors, in the VSMC membrane (Virdis *et al.*, 2010). This peptide promotes a long-lasting vasoconstriction essential to the vessel tone control in coronary arterioles, as reduction ET-1 induces an elevation of coronary blood flow in increased demand situations such as increased metabolism (Merkus *et al.*, 2002).

Endoperoxidases are derived from the metabolism of AA by the enzymatic activity of cyclooxygenas (COX), which then transformed into several other prostanoids and various prostaglandins (Virdis *et al.*, 2010). Stimulation of specific membrane receptors such as muscarinic receptors for acetylcholine (Boulanger *et al.*, 1994), ADP (activating

purinoceptors) (Mombouli & Vanhoutte, 1993) or calcium-increasing agents, such as the calcium ionophore A23187 (Tang *et al.*, 2007) as the initial trigger of EDCFs. These EDCFs cause a raise in endothelial cytosolic Ca^{2+} entry activating phospholipase A2 (PLA_2) and makes AA available for metabolism (Tang *et al.*, 2007). COX-1 breakdown AA into endoperoxides, which is ultimately converted to prostanoids namely thromboxane A2 (TXA_2) and prostaglandins (PGs), such as prostacyclin (PGI_2), prostaglandin F2α ($PGF_{2\alpha}$), prostaglandin D2 (PGD_2), prostaglandin E2 (PGE_2) (Bos *et al.*, 2004; Vanhoutte *et al.*, 2005). These prostanoids and prostaglandins activate thromboxane-prostanoid (TP) receptors of the vascular smooth muscle cells to elicit contraction (Vanhoutte & Tang, 2008).

Oxygen-derived free radicals can facilitate the production and/or the action of EDCF (Figure 2.3) (Shi & Vanhoutte, 2008). ROS including superoxide anions, hydroxyl radicals (OH-) and H_2O_2 are formed as by-products during production of prostanoids by COX (Wong & Vanhoutte, 2010). ROS, in turn, can stimulate COX both in the endothelium and vascular smooth muscle (Vanhoutte & Tang, 2008). ROS formed in the endothelium may diffuses into the layer of smooth muscle via passive diffusion or myoendothelial gap junctions and subsequently stimulate COX-1 to amplify TP receptor-mediated contractions of the vascular smooth muscle (Vanhoutte & Tang, 2008). ROS can also either act directly as EDCF (Katusic & Vanhoutte, 1989) or indirectly potentiate EDCF-mediated responses by reducing the bioavailability of NO (Paolocci *et al.*, 2001) and stimulating COX in the vascular smooth muscle cells (Yang *et al.*, 2002).

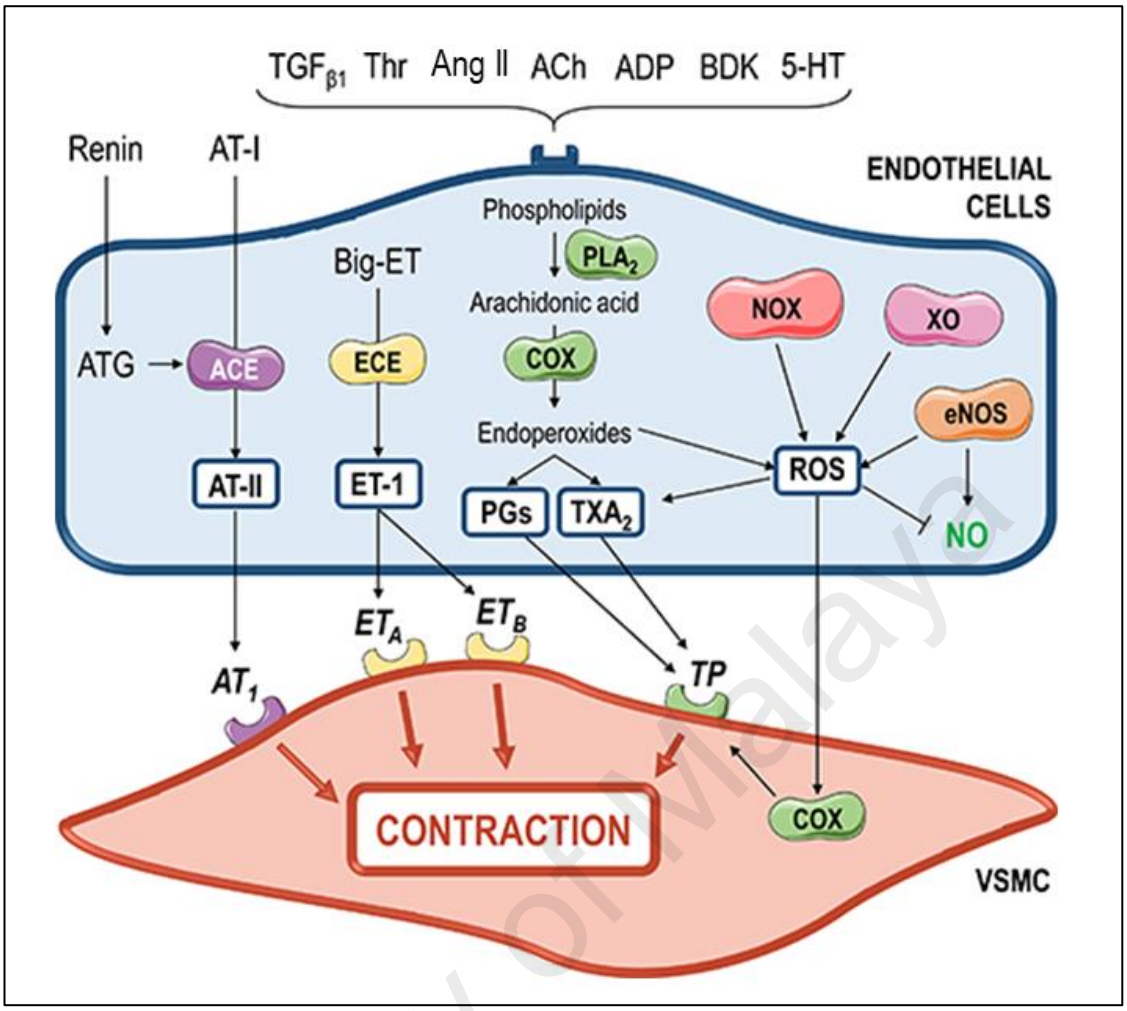

Figure 2.3: Schematic diagram shows action of endothelium-derived contracting factors (EDCF) produced in the blood vessel wall. Endothelin-1 (ET-1) which are converted by the endothelin converting enzyme (ECE) mediate vasoconstriction through the stimulation of receptors, namely ET_A and ET_B receptors, in the VSMC membrane. Besides, receptor-dependent agonists such as transforming growth factor ($TGF_{\beta 1}$), thrombin (Thr), angiotensin-II (Ang II), acetycholine (ACh), adenosine diphosphate (ADP), bradykinin (BDK) or 5-hydrotryptamine (5-HT) stimulated the increased in intracellular calcium and activates phospholipase A2 (PLA_2) to release arachidonic acid. The endothelial COX-1 isoform metabolizes the fatty acid into endoperoxides and ultimately to prostanoids namely thromboxane A2 (TXA_2) and prostaglandins (PGs) that subsequently causes contraction by activating the thromboxane-prostanoid (TP) receptors of the underlying vascular smooth muscle cells. Reactive oxygen species (ROS) produced in the endothelium may reach the smooth muscle layer via passive diffusion or through myoendothelial gap junctions, which activates the COX and eventually amplify TP receptor-mediated contractions of the vascular smooth muscle (Modified from Fonseca, 2016) .

2.4 Pathogenesis of Endothelial dysfunction: Molecular Mechanism of eNOS Uncoupling

Under physiological conditions, NO is produced mainly by the eNOS in the vasculature (Li & Förstermann, 2013). eNOS serves as a critical enzyme in maintaining vascular pressure by producing NO; hence, it has a crucial role in the regulation of endothelial function (Vanhoutte *et al.*, 2009). In endothelial cells, during resting stage, eNOS which is located at the plasma membrane caveolae is bound to caveolin 1 (cav-1) (Kietadisorn *et al.*, 2012). Upon activation, eNOS disassociates from cav-1 and binds with calmodulin (CAM), heat shock protein 90 (Hsp90) and together with phosphorylation of serine sites (e.g., Ser1177) (Kietadisorn *et al.*, 2012). This functional eNOS protein is called "coupled eNOS" (Figure 2.4). BH_4, an essential cofactor of eNOS generated from enzyme guanosine-5'-triphosphate cyclohydrolase (GTPCH), is required to maximise eNOS activity that convert L-arginine to NO and relaxes smooth muscle through the cGMP-dependent downstream signalling cascade (Kietadisorn *et al.*, 2012).

Under pathological conditions, eNOS can be converted from an NO-producing enzyme to a one that generates superoxide, a condition referred as "eNOS uncoupling" (Figure 2.4) (Li & Förstermann, 2013). As a consequence of eNOS uncoupling, NO production is attenuated (Li & Förstermann, 2013). The bioavailability of NO produced by eNOS depends on several factors such as a) eNOS mRNA or protein expression, b) availability of its substrate L-arginine, which may compete with asymmetric dimethylarginine (ADMA), c) decrease of BH_4 bioavailability from enhanced oxidation of BH_4, 4) protein-protein interaction such as cav-1 and Hsp90, 5) interaction between NO and superoxide to form peroxynitrite (Huang, 2009).

The bulk of ROS generated in the vasculature is derived from NADPH oxidases (NOX) and eNOS uncoupling. Activation of NOX is due to phosphorylation of the

oxidase components and translocation of the cytosolic components to the cell membrane, allowing complete oxidase complex assembly (Babior, 2004). Electron transfer from NADPH to O^2 to generate O^{2-}, which is rapidly converted to H_2O_2, and eventually to OH^- (Zorov *et al.*, 2014). Increased activity of NOX can impair endothelial function via several mechanisms (Santos *et al.*, 2009). For instance, the resulting superoxide interacts with NO which decreases its bioavailability (Hamilton *et al.*, 2001). This interaction forms peroxynitrite which oxidizes and inactivates BH_4 (Forstermann & Sessa, 2012). As the result, eNOS is uncoupled from NO production and augment the pre-existing oxidative stress (Loo *et al.*, 2000). Peroxynitrite also propagates oxidative stress by causing nitration of critical antioxidants, including superoxide dismutase (Macmillan-Crow & Cruthirds, 2001). Enhanced EDCFs also increase the production of superoxide anion and cause cellular oxidative damage (Pryor & Squadrito, 1995).

The phenomenon of uncoupling of eNOS eventually leads to endothelial dysfunction (Lerman & Burnett, 1992). Endothelial dysfunction has become a hallmark and a predictor of cardiovascular diseases (Landmesser et al., 2002). Endothelial dysfunction associated with eNOS uncoupling is reported both in animal models such as angiotensin II-induced hypertension (Mollnau *et al.*, 2002), streptozotocin (STZ)-induced diabetes (Hink *et al.*, 2001) and hypertension-induced heart failure (Takimoto *et al.*, 2005) as well as in patient with diabetes, hypertension, hypercholesterolemia and atherosclerosis (Hadi *et al.*, 2005).

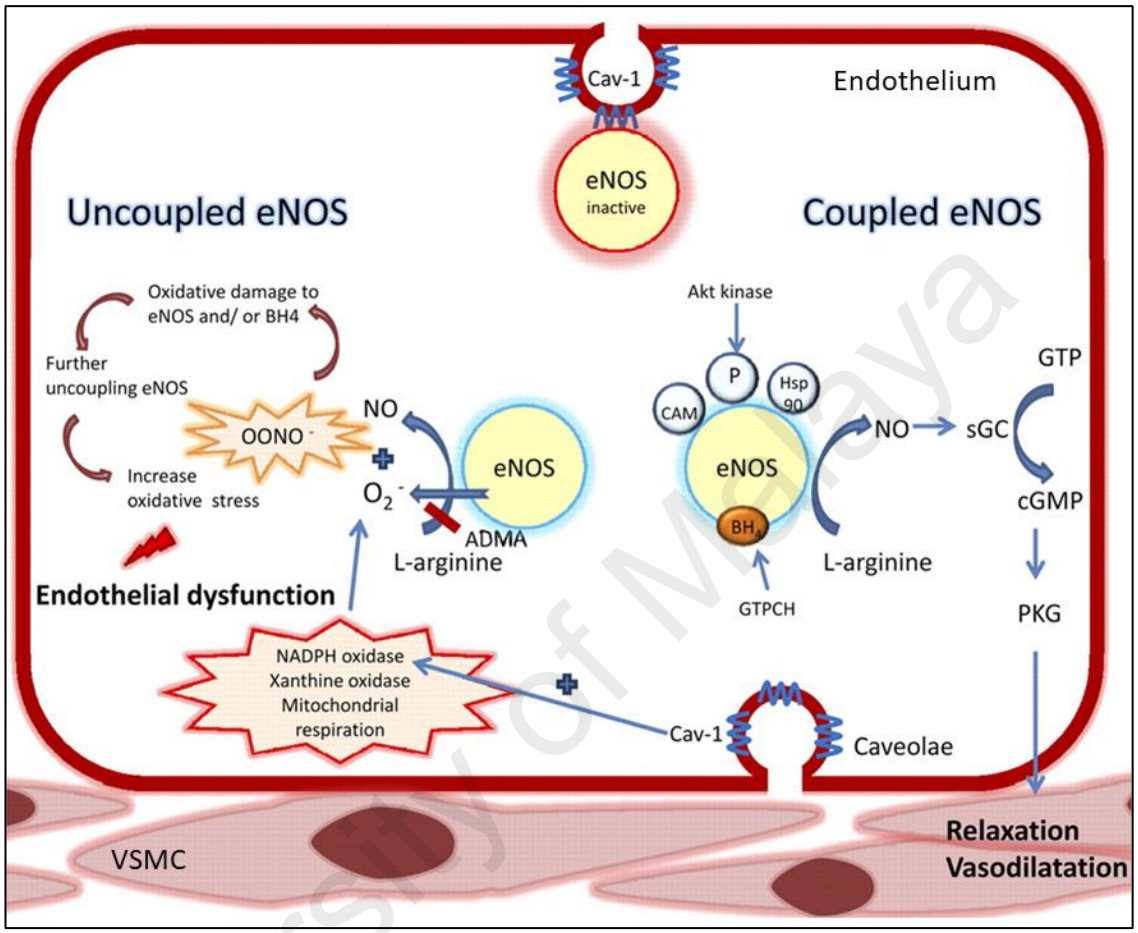

Figure 2.4: Role of endothelial nitric oxide synthase (eNOS) uncoupling in the pathogenesis of endothelial dysfunction. In the healthy endothelium, the eNOS play a key role in vascular nitric oxide (NO) production. However, in the pathological state, the L-arginine or tetrahydrobiopterin (BH_4) availability are reduced. Subsequently, eNOS becomes unstable and uncoupled, leading to less NO production and more superoxide (O_2^-) generation. In addition, interaction between NO and superoxide leads to formation of peroxynitrite ($ONOO^-$), a potent oxidant, which further oxidizes BH_4, resulting in eNOS uncoupling as a vicious cycle, with subsequent endothelial dysfunction (Source from Kietadisorn *et al.*, 2012).

2.5 Endoplasmic Reticulum stress and the unfolded protein response

The endoplasmic reticulum (ER) is an intracellular organelle covered by an extensive membrane network located in eukaryotic cells (Hong *et al.*, 2017). The ER lumen has a unique environment which contains high concentration of Ca^{2+} within the cell because of active transport of Ca^{2+} by Ca^{2+} ATPases (Schroder & Kaufman, 2005). ER is the primary site for controlling various intracellular physiological functions such as secretary protein translocation, protein folding, Ca^{2+} storage as well as biosynthesis of steroids, cholesterol and lipids (Duan *et al.*, 2009). Because of its role in protein folding and transport, the ER is also rich in Ca^{2+}-dependent molecular chaperones, such as glucose-regulated protein (GRP) 78, GRP94, and calreticulin, which stabilize protein folding intermediates (Shen *et al.*, 2004).

Aging, hypoxia, genetic mutations, nutrient deprivation, pathogen infection and overexpression of folding-defective proteins may disrupt ER homeostasis (Yoshida, 2007). Disturbances in ER function results in overexpression of unfolded and misfolded proteins which accumulate in the ER lumen and leads to potential cellular dysfunction and pathological consequences, namely ER stress (Minamino *et al.*, 2010). ER stress can similarly be induced using chemicals such as tunicamycin, dithiothreitol and thapsigargin which inhibit protein glycosylation, reduce formation of disulfide bonds or depleting Ca^{2+} from the ER lumen (Oslowski & Urano, 2011).

The initial response of the UPR is to adapt to the changing environment, and re-establish normal ER function by attenuating protein synthesis, inducing transcriptional ER chaperone genes to enhance folding capacity of the ER and promoting ER-associated degradation (ERAD) component genes to remove misfolded proteins (Yoshida, 2007). However, prolonged ER stress trigger three transmembrane sensors and initiates UPR in

the ER lumen, leading to oxidative stress, inflammation, and apoptotic response (Kadowaki & Nishitoh, 2013), which may be an important factor in the pathogenesis of cardiovascular diseases, such as ischemia/ reperfusion (I/R) injury, cardiomyopathy, cardiac hypertrophy, heart failure, and atherosclerosis (Zhang *et al.*, 2017). In general, ER stress-induced cell apoptosis and inflammation causing endothelial cells damage and dysfunction eventually leading to cardiovascular diseases (Tabas, 2010).

2.5.1 The adaptive and apoptotic pathway of unfolded protein response (UPR)

During unstressed conditions, the ER chaperone, GRP78 or immunoglobin binding protein (BiP) binds to the luminal domains of three ER transmembrane sensors: Inositol Requiring 1 (IRE1), PKR-like ER kinase (PERK), and Activating Transcription Factor 6 (ATF6), keeping them inactive (Oslowski & Urano, 2011). ER stress is triggered by cellular stresses such as perturbations in Ca^{2+} homeostasis, redox imbalance, altered protein glycosylation, or protein folding defects which leads to unfolded or misfolded proteins accumulating in the ER lumen (Senft & Ronai, 2015). During protein misfolding, the protein which gathered in the ER lumen activate an adaptive response to survive the ER stress conditions called UPR (Kadowaki & Nishitoh, 2013). BiP or GRP78 dissociates from these sensors permitting their oligomerization and thereby initiating the UPR to clear the accumulated unfolded proteins (Oslowski & Urano, 2011). This ER transmembrane sensors detect the unfolded proteins accumulated in the ER to initiate 3 distinct UPR branches mediated by IRE1, PERK and ATF6 (Figure 2.5). Activation of UPR results in regulation of the size, shape, and the components of the ER to re-establish homeostasis of protein folding in various physiological and pathological conditions (Schuck et al., 2009). If UPR is unable to normalise and regulate the ER, cell dysfunction and apoptosis occurs (Bhandary et al., 2012). ER sensor proteins including PERK and IRE1 plays a crucial role in both the adaptive and the pro-apoptotic pathways of UPR

(Bernales *et al.*, 2006). Once the adaptive UPR pathway is overcome by prolonged ER stress, it can no longer maintain ER homeostasis, the UPR-mediated proapoptotic signal becomes dominant, thereby inducing apoptotic cell death of the damaged cells (Inagi *et al.*, 2014).

2.5.1.1 IRE1

IRE1 is the most fundamental ER stress sensor of the UPR (Ron & Walter, 2007). Mammalian IRE1 has two homologues, IRE1α which is expressed in all cells or tissues, and IRE1β which is expressed specifically in the intestinal epithelium (Galan *et al.*, 2014). During ER stress, IRE1 autophosphorylation stimulate an endoribonuclease respond that cleaves the mRNA encoding the transcription factor X-box binding protein (XBP) 1 (Kim *et al.*, 2008; Minamino & Kitakaze, 2010; Ron & Walter, 2007). This results in the translation of transcriptionally active (spliced) XBP1s which merge to the ER stress response element in the promoter region of a various UPR-target genes to fold and degrade the proteins (Kim *et al.*, 2008; Minamino & Kitakaze, 2010; Ron & Walter, 2007). XBP1 translocate into the nuclear and targets many genes encoding proteins for ER membrane biogenesis, ER protein folding, ER-associated protein degradation (ERAD), and secretion of protein from the cell (Acosta-Alvear *et al.*, 2007; Lee *et al.*, 2003) (Figure 2.5). The nuclear translocation of XBP1 is accelerated by the regulatory subunit of phosphatidylinositol 3-kinase (PI3K) called p85α (Park *et al.*, 2010). In addition, IRE1α activation is related to apoptosis and inflammatory signalling (Minamino *et al.*, 2010). IRE1α causes the initiation of a apoptosis signal-regulating kinase (ASK)1 and cJUN NH_2-terminal kinases (JNK) by interacting with the adaptor protein tumor necrosis factor TNF receptor-associated factor (TRAF) 2 (Nishitoh *et al.*, 2002; Urano *et al.*, 2000). JNK has pro-apoptotic effects, including phosphorylation-induced activation

of the pro-apoptotic (Bak and Bax), and inactivation of the anti-apoptotic Bcl2 proteins (Malhi & Kaufman, 2011).

2.5.1.2 PERK

PERK is another ER stress sensor and is a serine threonine kinase. PERK activation phosphorylates eIF2α at Ser51 which decreases the synthesis of global protein and attenuate protein influx into the ER lumen for pro-survival (Scheuner *et al.*, 2001; Shi *et al.*, 1998). Additionally, it also phosphorylates nuclear erythroid 2 p45-related factor 2 (NRF2), an antioxidant transcription factor for initiation of antioxidant response genes such as heme oxygenase 1 and glutathione *S*-transferase (Cullinan *et al.*, 2003). Phosphorylation of eIF2α also lead to preferential translation of activating transcription factor-4 (ATF4) protein over other upstream reading frames in the mRNA (Harding *et al.*, 2000). ATF4, a transcription factor stimulate gene expression related to ER function, ER stress-mediated cell death, ER stress-associated oxidative stress and an inhibitory feedback loop to prevent hyperactivation of the UPR through dephosphorylation of eIF2α (Harding *et al.*, 2003) (Figure 2.5). ATF4 restores cap-dependent translation by binding to the promoter of the gene encoding GADD34, the regulatory subunit of the phosphatase that dephosphorylates eIF2α (Ma & Hendershot, 2003). ATF4 pathways regulates CCAAT/ enhancer-binding protein homologous protein (CHOP), the pro-apoptotic basic-leucine zipper transcription factor (Kim *et al.*, 2008; Minamino & Kitakaze, 2010; Ron & Walter, 2007). CHOP induce cell death by activating pro-apoptotic protein (Bax and Bak) and inhibit anti-apoptotic (Bcl-2) protein (Fu *et al.*, 2010; McCullough *et al.*, 2001). These proteins oligomerize in the mitochondrial membrane, induces the generation of cytochrome c from the mitochondria, forms a complex with other apoptosome components, stimulates caspase-3 and causes apoptosis (Scull & Tabas, 2011). Thus, the

PERK-eIF2α pathway functions to promote redox balance activation of ATF4 and NRF2 pathway during ER stress.

2.5.1.3 ATF6

ATF6, an ER-associated type 2 transmembrane basic leucine zipper (bZIP) transcription factor is the third ER stress member (Kim *et al.*, 2008; Minamino & Kitakaze, 2010; Ron & Walter, 2007). Upon activation of ER stress, GRP78 is released from ATF6 and allows ATF6 to translocate from the ER to the Golgi for cleavage by serine protease site-1 (S1P) and metalloprotease site-2 (S2P) to produce a transcriptionally active cytosolic fragment (Schindler & Schekman, 2009) (Figure 2.5). Dissociation of GRP78 and disulfide bond cleavage with ER assist the translocation of about 90-kDa ATF6 monomers to the Golgi lumen (Shen *et al.*, 2002). Cleaved ATF6 binds to the ER stress response element in the promoters of UPR target genes and activates transcription of ATF6-inducible ER stress response-element genes (Kondo *et al.*, 2005; Omori *et al.*, 2001). Major ATF6 targets include chaperone proteins, the transcription factor XBP1, and CHOP (Toth *et al.*, 2007).

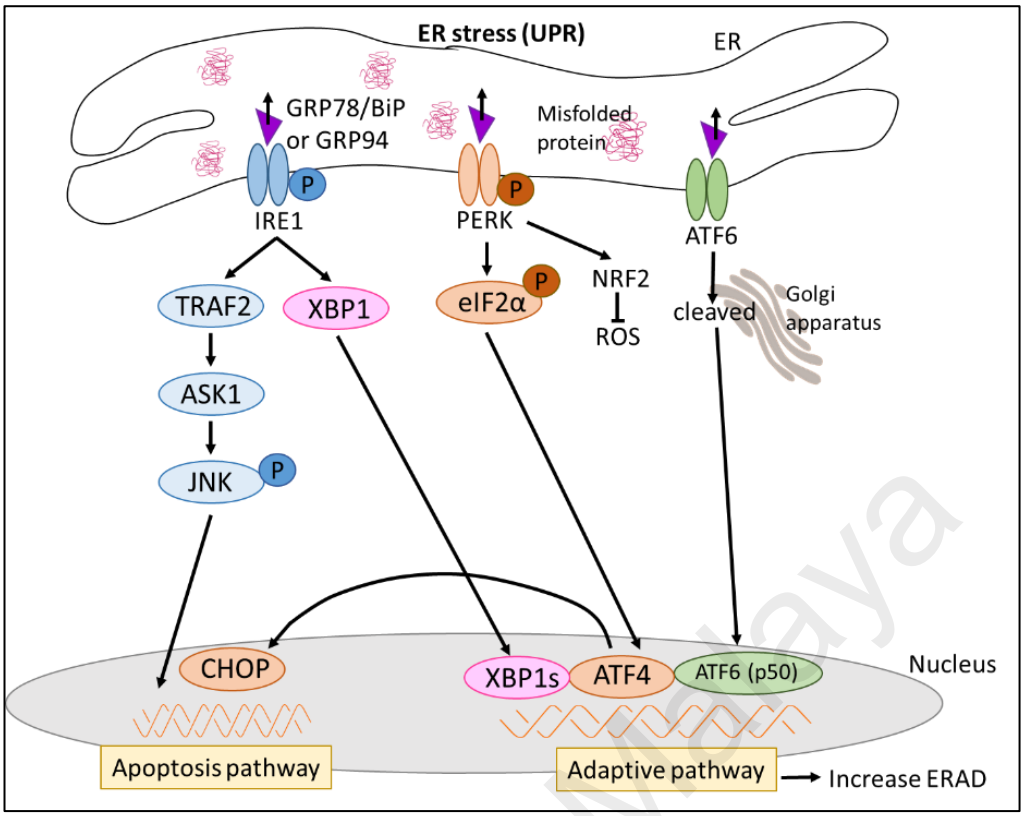

Figure 2.5: The unfolded protein response (UPR). During ER stress, ER chaperone (GRP78/BiP or GRP94) dissociates from 3 ER transmembrane sensors for the activation of IRE1, PERK and ATF6. Dimerization and phosphorylation of UPR modulators PERK and IRE1 as well as cleaved ATF6 in the Golgi apparatus inducing the activation of UPR transcription factors XBP1s, ATF4 and ATF6. These transcription factors initiate the adaptive UPR pathway and regulate the ER function via the IRE1-XBP1, PERK-eIF-2α-ATF4 or ATF6 pathways. Additionally, PERK also phosphorylates NRF2, an antioxidant transcription factor for initiation of antioxidant response genes. If the adaptive UPR pathway fails to normalize the cells, ER stress is prolong, inducing apoptotic UPR pathway involving IRE1-TRAF2-ASK1-JNK or PERK-eIF-2α-ATF4-CHOP pathway. Abbreviations: ASK1, apoptosis signal-regulating kinase 1; ATF, activating transcription factor; BiP, immunoglobin binding protein; CHOP, C/EBP-homologous protein; eIF-2α, ERAD, endoplasmic-reticulum-associated protein degradation; eIF2α, eukaryotic translation initiation factor 2α; ER, endoplasmic reticulum; GRP78, glucose-regulated protein 78; GRP94, glucose-regulated protein 94; IRE1, inositol-requiring protein 1; JNK, c-Jun N-terminal kinase; NRF2, nuclear erythroid 2 p45-related factor 2; P, phosphorilate; PERK, protein kinase RNA-like endoplasmic reticulum kinase; ROS, reactive oxygen species; TRAF2, tumour necrosis factor receptor-associated factor 2; UPR, unfolded protein response; XBP1, X-box binding protein 1; XBP1s, spliced form of XBP1 (Modified from Inagi *et al*., 2014).

2.5.2 ER stress and ROS

Accumulating evidence revealed that protein misfolding in the ER are closely linked to the production of ROS. Studies have suggested the interrelation of ER stress and ROS with redox signalling mediators such as i) protein disulfide isomerase (PDI)-endoplasmic reticulum oxidoreductin (ERO)-1, ii) glutathione (GSH)/glutathione disulphide (GSSG), iii) NADPH oxidase and iv) calcium (Figure 2.6) (Zeeshan *et al.*, 2016).

During enhanced protein folding, ROS are formed as a by-product of nonpathological protein folding in the ER, which are likely sources of oxidative stress (Santos *et al.*, 2009). Protein disulphide isomerase (PDI), a family of ER oxidoreductases, is an essential and well-characterized enzyme of disulfide bond formation in the ER (Braakman & Bulleid, 2011). During chaperone-assisted disulphide bond formation between polypeptide chain substrates, two electrons from thiol residues are provided to the cysteine residue within the PDI active site (Kramer *et al.*, 2001). This transfer of electrons results in the reduction of the PDI active site and oxidation of the substrate (Kramer *et al.*, 2001). The reduced PDI transfers its electrons through ER oxidoreductase 1 (ERO1) to molecular oxygen as the final electron acceptor (Tu & Weissman, 2004). The sequential action of PDI and ERO1 in transferring electrons from thiol groups in proteins to molecular oxygen formed H_2O_2 that can diffuse out of mitochondria into the cytoplasm (Tu & Weissman, 2004).

In addition, ROS may be formed as a consequence of the GSH depletion that occurs as GSH reduces unstable and improper disulphide bonds. The consumption of GSH would return thiols involved in non-native disulphide bonds to their reduced form so they may again interact with ERO1/PDI to be reoxidized (Zeeshan *et al.*, 2016). This would generate a futile cycle of disulphide bond formation and breakage in which each cycle

would generate ROS and consume GSH. As a consequence, it is expected that proteins that have multiple disulphide bonds may be more prone to generating oxidative stress (Malhotra *et al.*, 2008). The ROS generated by these processes appear to be a critical second signal to initiate apoptosis. In addition, ROS can further disrupt protein misfolding in the ER. Intriguingly, antioxidants can improve protein folding and reduce apoptosis under conditions of ER stress (Santos *et al.*, 2009).

Increasing evidence suggests that NOX NADPH oxidases are important ROS sources during the UPR in distinct cell types (Zeeshan *et al.*, 2016). The two NOX isoforms so far reported to be involved in ER stress are NOX2 and NOX4 which exists as a membrane-bound heterodimer with a lower molecular weight p22phox subunit (Touyz *et al.*, 2005). NADPH oxidase subunit, NOX2 is induced through a CHOP/CAMKII pathway to mediate oxidative stress and apoptosis while NOX4 plays a dual prosurvival/proapoptotic role (Laurindo *et al.*, 2014). ER stress-induced ROS formation is abolished in CHOP deficient cells and mice (Li *et al.*, 2010a). Activation of CHOP up-regulated NOX2 expression, which catalyze the transfer of electrons from NADPH to molecular O_2, forming H_2O_2 or superoxide (Li *et al.*, 2010a). The lumen of NOX2-containing vesicles is topologically analogous to the extracellular milieu regarding superoxide production (Laurindo *et al.*, 2014). Endothelium-dependent relaxations (EDR) improved when NADPH oxidase subunits, NOX1 and NOX4 mRNA expression were reduced by ER stress inhibitors in aortas and mesenteric arteries of Ang II-induced hypertensive mice (Kassan *et al.*, 2012). In contrast, NADPH oxidase subunit, NOX2 protected ER-stressed mice from renal dysfunction via the inhibition of CHOP-induced apoptosis pathway (Li *et al.*, 2010a). Several findings showed that ER stress inhibitor, taurine-conjugated tursodeoxycholic acid (TUDCA) blocked the superoxide anion production or NADPH oxidase activity in Ang II-induced hypertensive animals, implying

that ER stress might be upstream of the oxidant stress in hypertension (Kassan *et al.*, 2012; Young *et al.*, 2012).

ER stress may increase Ca^{2+} leak from the ER lumen to cytosol (Gorlach *et al.*, 2006). Increases in cytosolic Ca^{2+} leads to accumulation of Ca^{2+} near mitochondria, thereby increasing mitochondrial ROS production and leading to opening of the permeability transition pore (Jacobson & Duchen, 2002). Increased mitochondrial Ca^{2+} loading ultimately leads to cytochrome c release and ROS generation (Malhotra & Kaufman, 2007). Furthermore, ROS can also feedback to sensitize the Ca^{2+}-release channels at the ER membrane which further increase Ca^{2+} release from the ER (Viner *et al.*, 2000). For example, this may occur through ROS or reactive nitrogen species that can oxidize a critical thiol in the ryanodine receptor and cause its inactivation, thereby enhancing Ca^{2+} release from the sarcoplasmic reticulum (Favero *et al.*, 1995). The vicious cycle of Ca^{2+} release and ROS production becomes more threatening to cell survival.

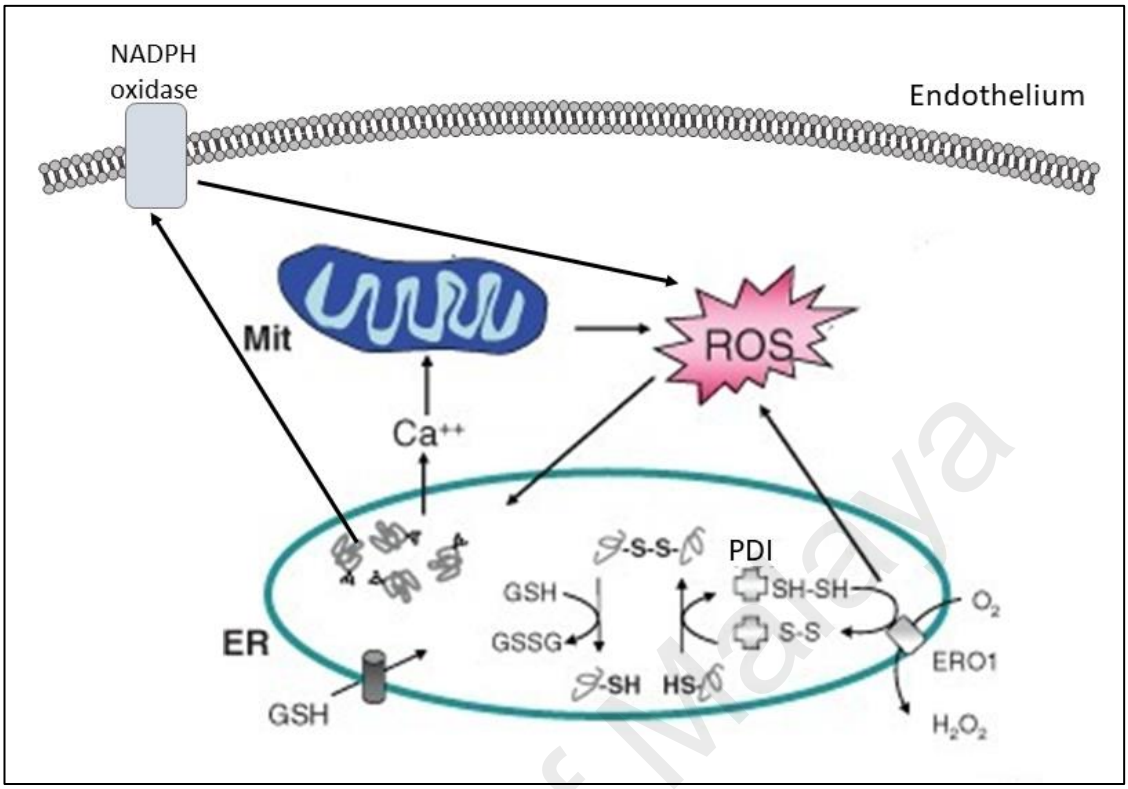

Figure 2.6: Endoplasmic reticulum (ER) stress-mediated oxidative stress pathway. ER stress causes the incorrect disulphide bonds formation which require breakage and reformation for proteins to attain the appropriate folded conformation. Protein disulphide isomerase (PDI) catalyses disulphide bond formation and isomerization, whereas glutathione (GSH) transported into the ER reduces improperly paired disulphide bonds. Reoxidation of PDI is mediated by ERO1; however, reactive oxygen species (ROS) are produced in the process. Cellular ROS can deplete GSH and increase the misfolded protein load in the ER. In turn, ROS can also cause ER stress through modification of proteins and lipids that are necessary to maintain ER homeostasis. ER stress also causes Ca^{2+} leak from the ER for accumulation in the inner mitochondrial matrix. This Ca^{2+} loading in the mitochondria can generate additional ROS through disruption of electron transport and opening of the mitochondrial permeability pore. ROS also produced by NADPH oxidase during ER stress. Thus, accumulation of misfolded protein in the ER increases ROS production that can further amplify ER stress and cause cell death (Source from Kaufman *et al*., 2010).

2.5.3 ER stress and endothelial dysfunction

Various studies have shown that ER stress promotes impairment of endothelium dependant relaxation (EDR). ER stress induce endothelial dysfunction by i) reduction of eNOS phosphorylation, ii) increased endothelin-1 (ET-1), iii) endothelial inflammation and iv) oxidative stress (Figure 2.7) (Battson *et al.*, 2017).

Study by Cheang *et al.*, (2014) have shown ER stress decreased expression and phosphorylation of eNOS in the vasculature and in isolated endothelial cells from mice, and this effects were reversed by ER stress inhibitors such as tauroursodeoxycholic acid (TUDCA) and 4-phenylbutyrate (PBA). In CHOP-/- mice, eNOS expression were elevated, indicating that CHOP inhibits NO production in endothelial cells by directly binding to the eNOS promoter (Loinard *et al.*, 2012).

Other than reduction of NO, ER stress inducers elevate the endothelial expression of ET-1, a potent vasoconstrictor (Lenna *et al.*, 2010). This is shown by restoration of ER stress-induced reductions in EDR by inhibition of ET-1 receptors in isolated rat aortic rings (Padilla & Jenkins, 2013).

In addition to its direct effects on endothelium- derived vasoactive substances, ER stress may also impair endothelial function indirectly by increasing pro-inflammatory mediators (Cao *et al.*, 2016). ER stress triggers inflammatory reaction through activation of the transcription factor nuclear factor-κB (NF-κB) (De Martin *et al.*, 2000). NF-κB is a negative regulator of eNOS expression and is increased in individuals with endothelial dysfunction (Lee *et al.*, 2014b). Inhibition of NF-κB restores EDR in experimental animals and humans (Pierce *et al.*, 2009; Read *et al.*, 1994). Besides NF-κB, increase in transcriptional regulator of inflammation MAP kinase, JNK has been demonstrated with

ER stress inducer, tunicamycin and inhibited by PBA in endothelial cells (Fiorentino *et al.*, 2015). In experimental animals and endothelial cells isolated from diabetic individuals, inhibition of JNK restored eNOS activation and endothelial function (Osto *et al.*, 2008). In liver cells, JNK inhibition prevented ER stress-induced insulin resistance (Ozcan *et al.*, 2004). Activation of both JNK and NF-κB triggers other inflammatory mediators including interleukin-6 (IL-6) and tumor necrosis factor-α (TNF-α) which both independently promote endothelial dysfunction (De Martin *et al.*, 2000; Zhang *et al.*, 2009). These findings indicate that ER stress activates various inflammatory pathways in the vasculature and consequently disrupt the endothelial function.

Oxidative stress is another recognised mechanism by which ER stress may impair endothelial function. Elevated cellular levels of H_2O_2 generated from the disulfide bond formation from PDI and ERO1 are sufficient to reduce NO bioavailability and impair endothelial function (Cai, 2005). Mitochondria-derived ROS resulted from Ca^{2+} leak from ER also lead to endothelial dysfunction (Walsh *et al.*, 2009). ER-stress induced superoxide act with NO to form peroxynitrite, which reduced availability of NO and BH_4 (Loo *et al.*, 2000). In addition, mice lacking the NOX p47phox subunit (p47phox$_{-/-}$) and treatment with NOX inhibitor apocynin also prevented tunicamycin-induced endothelial dysfunction in mesenteric arteries (Galan *et al.*, 2014).

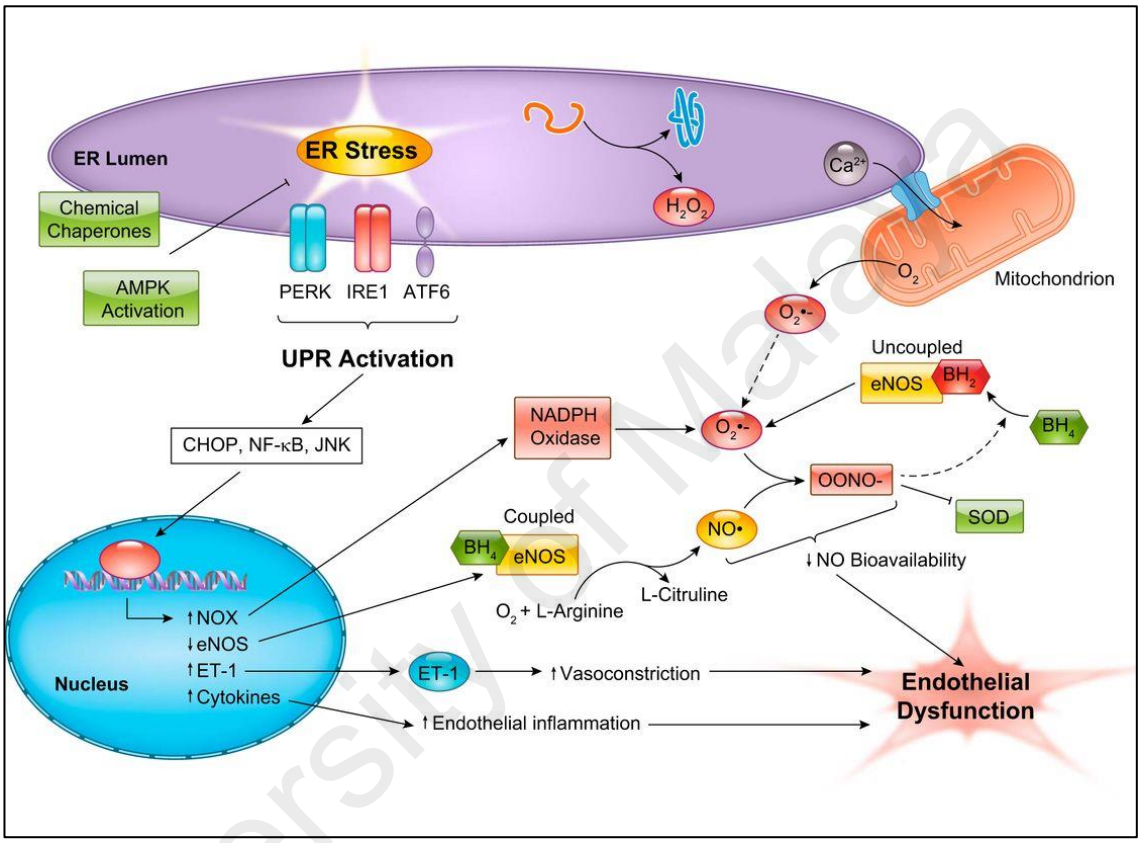

Figure 2.7. Mechanism of ER stress-induced endothelial dysfunction. NO, nitric oxide; eNOS, endothelial nitric oxide synthase; ET-1, endothelin-1; BH_4, tetrahydrobiopterin; NOX, NADPH oxidase; SOD, superoxide dismutase; $ONOO^-$, peroxynitrite, O_2^-, superoxide anion, H_2O_2; hydrogen peroxide (Source from Kaufman *et al.*, 2010).

2.5.4 ER stress and AMPK/PPARδ

5′ adenosine monophosphate-activated protein kinase (AMPK) is a physiological regulator that regulates cell's energy balance and metabolism (Hardie, 2007) by stimulating defensive response to stress (Hardie, 1999). Activation of AMPK may attenuate ER stress, suggesting that AMPK could be a novel therapeutic target for the treatment of ER stress-induced pathologies (Kim *et al.*, 2015). AMPK activation protected against hypoxic injury in cardiomyocytes by suppressing ER stress (Terai *et al.*, 2005) and suppressed heavily-oxidised glycated LDL (HOG-LDL) induced ER stress by inhibiting NADPH oxidase-derived ROS and sarcoplasmic/endoplasmic reticulum Ca^{2+} ATPase (SERCA) oxidation (Dong *et al.*, 2010b). In contrast, inhibition of AMPK promotes ER stress and atherosclerosis (Dong *et al.*, 2010a).

Besides AMPK, peroxisome proliferator-activated receptor δ (PPARδ) may also inhibit ER stress and improve endothelial function through various mechanisms. Recent finding demonstrated that PPARδ reduces ER stress and restore endothelial function via interaction with AMPK (Cheang *et al.*, 2014). Similarly, PPARδ prevents ER stress, inflammation and insulin resistance in skeletal muscle cells by activating AMPK (Salvado *et al.*, 2014). PPARδ attenuates palmitate-induced ER stress and induces autophagic markers, and subsequently reduced apoptotic cell death in myocardium of mice (Palomer *et al.*, 2014). PPARδ activation also protected pancreatic β-cells from ER stress by promoting oxidation of fatty acid (Cao *et al.*, 2012). PPARδ which are expressed universally in adipocytes and endothelial cells may protect against atherosclerosis and endothelial dysfunction (Piqueras *et al.*, 2007). Activation of PPARδ protects endothelial function in diabetic mice by mediating through PI3K and Akt with a subsequent increase of eNOS activity and NO production (Tian *et al.*, 2012a).

2.6 Inflammation

Vascular inflammation results from physical injury, lipid peroxidation, infection or risk factors including hypertension, diabetes, and smoking (Roifman *et al.*, 2011; Willerson & Ridker, 2004). Clinical and epidemiological research suggest a strong and consistent relationship between markers of inflammation and risk of future cardiovascular events (Kaplan & Frishman, 2001). The endothelium plays a vital role in normalising the inflammatory response in the vasculature (Levi *et al.*, 2002; Reinhart *et al.*, 2002). Dysregulation of the inflammatory response leads to capillary leak syndrome, hemodynamic instability and subsequently endothelial cell injury, apoptosis or loss of endothelial integrity (Assaly *et al.*, 2001; Haimovitz-Friedman *et al.*, 1997). As inflammation is a key process in the progression of cardiovascular diseases, targeting specific inflammatory proteins or pathways can be effective in reducing the risk of cardiovascular events (Golia *et al.*, 2014).

2.6.1 LPS/TLR4 signalling pathway

Lipopolysaccharide (LPS), a glycolipid component of the outer wall of gram-negative bacteria, has been demonstrated to expose vascular endothelial cells to systemic injury by causing systemic inflammatory response syndrome (Chakravortty *et al.*, 2000; Dunn, 1991). LPS is commonly used to mimic clinical septic syndrome by inducing a hyperinflammatory response in hosts (Van der Poll & Opal, 2008). LPS activates many of the proinflammatory and procoagulant responses in endothelial cells, leading to endothelial injury (Choi *et al.*, 1998).

In response to stimuli, LPS bind to membrane-localized toll-like receptors, and disrupt the endothelial barrier by activating intracellular signalling pathways that stimulate alteration to endothelial cell cytoskeletal architecture (Bannerman & Goldblum, 1999;

Cuschleri *et al.*, 2003). Toll-like receptor (TLR) family is a key set of innate immune receptors that recognize bacterial components, with TLR4 being the main receptor target for LPS (Faure *et al.*, 2000; Lien *et al.*, 2000). Recognition of LPS by TLR4 is necessary for the establishment of an immune response against bacteria (Ulevitch & Tobias, 1995). Mice deficient in TLR4 are associated with decreased inflammatory responses (Caso *et al.*, 2007). Activation of TLR4 initiate a variety of inflammatory process through activation of the three members of the MAPK family which are ERK (extracellular-signal-regulated kinase), JNK (c-Jun N-terminal kinase) and p38 and also activation of the NF-κB (Emre *et al.*, 2007) (Figure 2.8). NF-kB facilitates the pro-inflammatory cytokines release, such as TNF-α, interleukin- 1 (IL-1), IL-6, transforming growth factor-beta (TGF-β), and prostaglandins (Medvedev *et al.*, 2000; Sanlioglu *et al.*, 2001).

LPS induces ROS production, which constitutes a primordial signalling pathway potentiating MAPK activation (Cakir & Ballinger, 2005). In response to LPS, polymorphonuclear cells and macrophages produce ROS, such as O^{2-}, H_2O_2, and OH^- (Simon & Fernandez, 2009). One of the main sources of LPS-induced ROS generation in endothelial cells is the NADPH oxidase protein complex (DeLeo *et al.*, 1998). LPS-induced ROS production triggers apoptosis in HUVECs, which involved TLR4 and NOX2 as well as NOX4, independently from cytokine expression (Simon & Fernandez, 2009). NO generated by eNOS reacts with ROS to generate other reactive species such as nitric oxide radical and peroxynitrite (Bolisetty & Jaimes, 2013). The generation of peroxynitrite will cause substantial oxidation and destruction of host cellular constituents, which result in the dysfunction of critical cellular mechanism and the induction of cell apoptosis (Bonfoco *et al.*, 1995; Virag *et al.*, 2003). Although ROS are necessary for bacterial killing, it may induce oxidative stress within the tissues when present in excess (Gougerot-Podicalo *et al.*, 1996). As the result, this response may causes deleterious

effects, such as alteration of cell function, and exaggerated systemic inflammatory response (DeLeo *et al.*, 1998).

During the course of an inflammatory response, activation of several downstream kinase and transcription factors (JNK, p38 MAPK and NF-κB) by TLR4 leads to activation of immune molecules including inducible isoform of nitric oxide synthase (iNOS) (Kacimi *et al.*, 2011). iNOS is the enzyme which catalyzes the oxidation of one of the equivalent guanidino nitrogens of arginine to produce NO (Forstermann & Sessa, 2012). Large amounts of NO formed by the action of iNOS surpass the physiological amounts of NO, which are usually produced by the action of nNOS and eNOS, respectively (Xie *et al.*, 1994). NO generated by iNOS is a free radical species that accounts for cytotoxic and cytostatic effects against pathogenic microbes and tumor cells (Aktan, 2004; Hibbs *et al.*, 1988). Thus, iNOS-generated NO overproduction act as a ubiquitous mediator for inflammatory conditions and reflects the extent of inflammatory process (Farley *et al.*, 2006). Diseases such as septic shock, cerebral infarction, diabetes mellitus, neurodegenerative disorders, rheumatoid arthritis and other inflammatory events are associated with NO overproduction by iNOS (Moncada *et al.*, 1991). NO derived from iNOS causes an inhibitory effect on eNOS that impair the endothelium-dependent relaxation (Chauhan *et al.*, 2003).

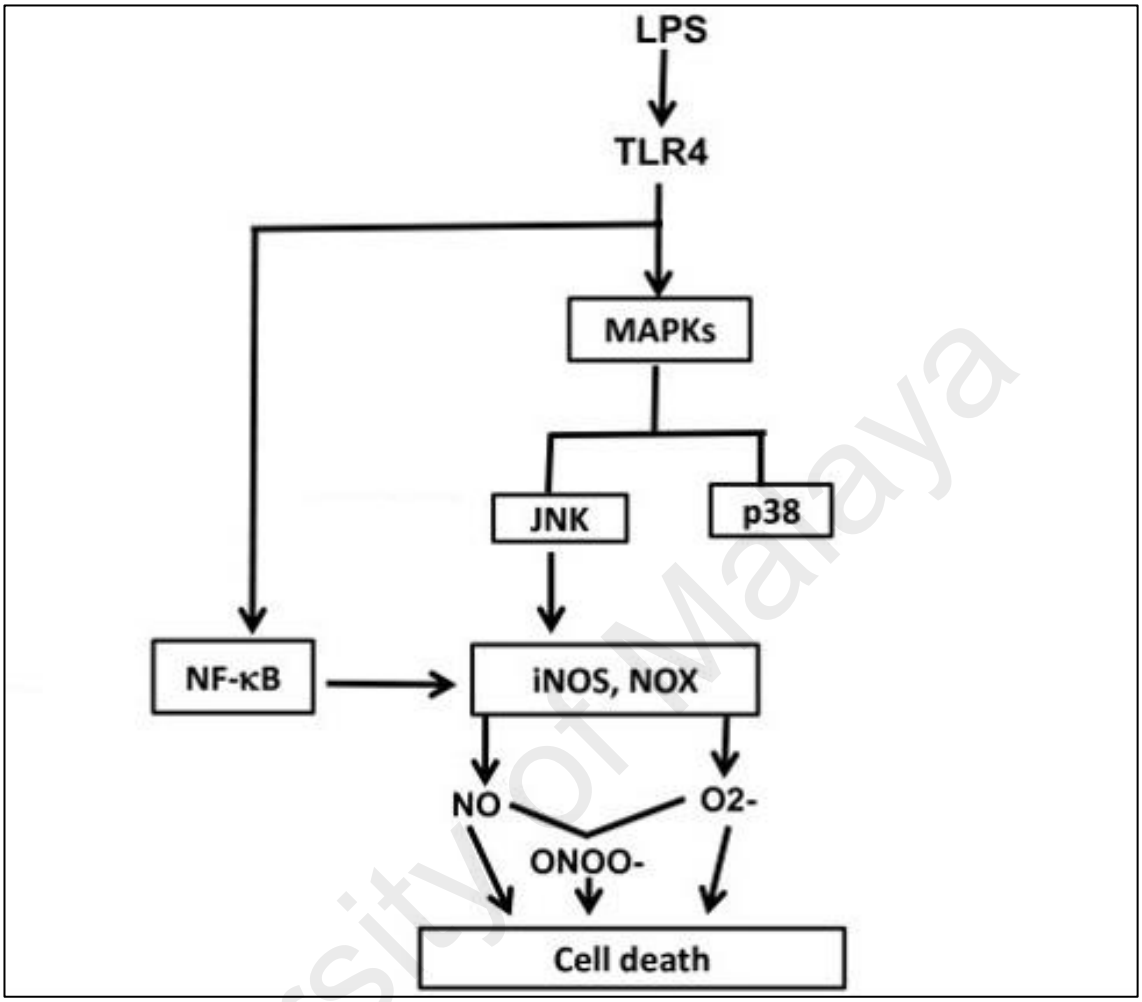

Figure 2.8: Proposed mechanism of LPS signalling leading to endothelial cell death. LPS binds toll-like receptor 4 (TLR4) on the surface of endothelial cells and activates several signalling pathways including NF-κB, the MAPKs and JAK-STAT. MAPKs then activate JNK (JNK kinase) and the p38 MAPK (p38). NF-κB, JAK-STAT and to a lesser extent, JNK lead to upregulation of immune factors iNOS and NADPH oxidase (NOX). These factors lead to the production of nitric oxide (NO) and superoxide (O2-), respectively. These molecules are themselves known to be directly cytoxic, but may also combine to form peroxynitrite (ONOO-) which can also kill cells (Modified from Kacimi *et al.*, 2011).

2.6.2 BMP4 signalling pathway

Bone morphogenic protein 4 (BMP4), a member of BMPs which belongs to the transforming growth factors-β superfamily, plays a vital role in embryonic development, cartilage formation, and bone mineralization (Hogan, 1996). BMP4 can be induced under the oscillatory shear stress stimulation (Sorescu *et al.*, 2003). BMP endothelial cell precursor-derived regulator (BMPER) controls bone morphogenetic protein BMP4 which exerts pro-inflammatory effects on the endothelium (Csiszar *et al.*, 2007) and decreased expression of eNOS in human umbilical vein endothelial cells (HUVECs) (Dyer *et al.*, 2014; Helbing *et al.*, 2011). BMP4 induced pro-inflammatory response and caused enhanced leukocyte adhesion to the endothelial surface *in vitro* (Csiszar *et al.*, 2006).

BMPs bind to 2 types of serine threonine kinase receptor: BMPR1 and BMPR2 (Figure 2.9) (Miyazono *et al.*, 2005). BMPR1 can be divided into 2 subgroups: activin receptor-like kinase 3 (ALK3 or BMPR1a) and ALK6 (BMPR1b) group and the ALK1 and ALK2 group (Cai *et al.*, 2012). BMP4 has a much higher affinity to bind with BMPR1a/ BMPR1b to form a binding complex and to stimulate the downstream signalling (Miyazono *et al.*, 2005). BMP4 signalling activation leads to SMAD-dependent and SMAD-independent pathways (Cai *et al.*, 2012). Activation of SMAD -dependent results in initiation of SMAD 1, 5, and 8 (SMAD 1/5/8) in the cytoplasm (Chen *et al.*, 2004). SMAD 1/5/8 associates with co- SMAD, SMAD 4, and translocate to the nucleus, where this SMAD complex will bind to the SMAD-responsive element and induce the transcription of SMAD-target genes (Dyer *et al.*, 2014). SMAD-independent pathway involves activation of mitogen-activated proteins kinases MAPKs (Guzman *et al.*, 2012).

Activation of BMP4 leads to activation of NADPH oxidases that increase production of ROS (Miriyala *et al.*, 2006), p38 mitogen-activated protein kinases activation (Yang

et al., 2005), and COX- 2 upregulation (Wong *et al.*, 2010). NADPH-dependent ROS production subsequently increase pro-inflammatory cytokines and adhesion molecules (Bostrom *et al.*, 2011; Sorescu *et al.*, 2003). BMP4-induced ROS production is mediated through the NOX1, NOX2, and NOX4 activation (Miriyala *et al.*, 2006; Sorescu *et al.*, 2004). In *db/db* diabetic mice and endothelial cells exposed to high glucose, ROS production are inhibited by BMP4 inhibitors, BMP4 silencing, and ROS scavengers (Zhang *et al.*, 2014). Besides, BMP4 induced up-regulation of NADPH oxidase also leads to initiation of NF-κB, increased intercellular adhesion molecule 1 (ICAM-1) expression, and subsequent elevated monocyte adhesively to endothelial cells (Jo *et al.*, 2006).

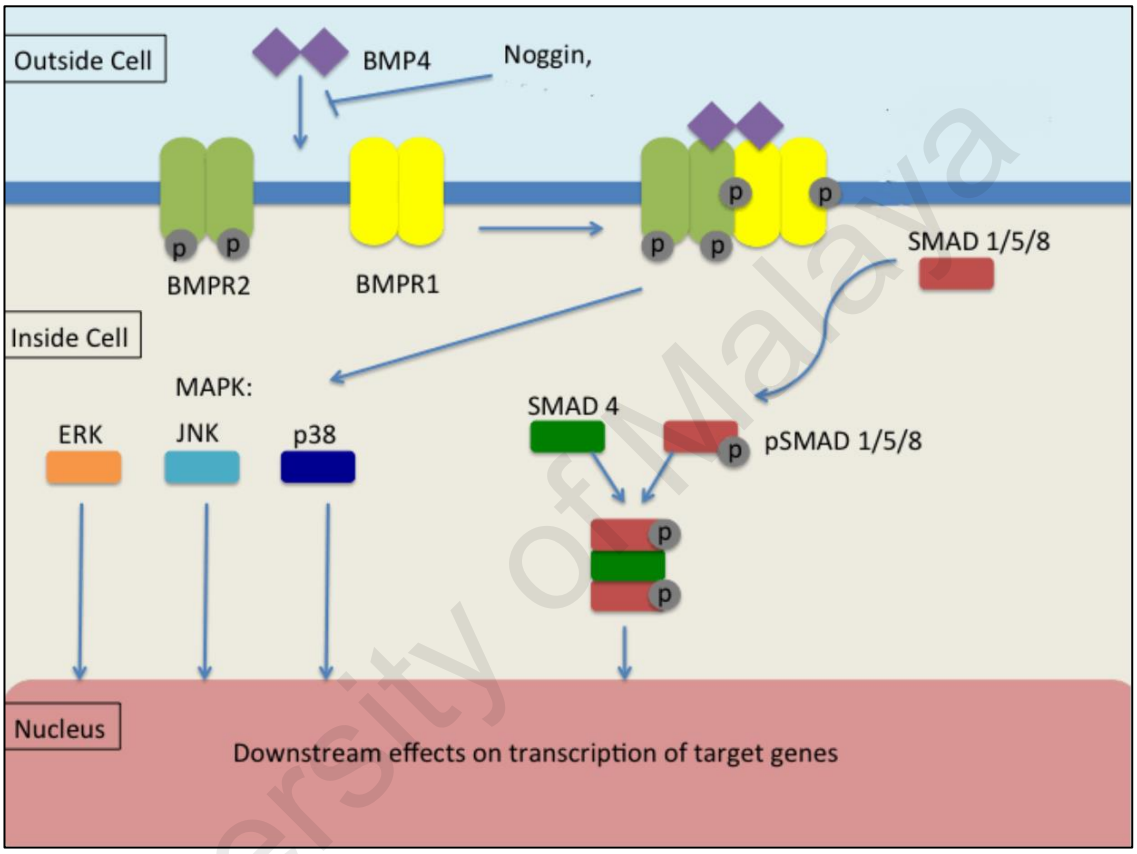

Figure 2.9: Bone morphogenetic protein (BMP4) signal transduction pathway. BMP4 binds to serine-threonine kinase receptors known as BMPR1 and BMPRl2, which induces the SMAD and the non-SMAD signal transduction pathways independently within the cell (Source from Miyazono *et al*., 2010).

2.6.3 Inflammation-induced apoptosis and endothelial dysfunction

Inflammation and apoptosis both play important roles in the pathophysiology of cardiovascular diseases such as atherosclerosis, heart failure, and hypertension (Diez, 2000; Richards, 2010). Apoptosis is a fundamental process that is important for homeostasis, but also contributes to diverse pathologic processes (Shioiri *et al.*, 2009). Apoptosis is a byproduct of inflammatory signalling probably due to the absence of sufficient antiapoptotic signals, or due to the presence of overwhelming proapoptotic triggers (Bannerman & Goldblum, 2003). Apoptosis is characterized by cell shrinkage, nuclear fragmentation and membrane blabbing (Kockx, 1998). Two major pathways involved in death receptors and cell stress pathway converge at caspase-3 activation to induce apoptosis, thus caspase-3 is recognised as a key enzyme in the pathogenesis of cell apoptosis (Sugawara *et al.*, 2004). LPS can interrupt the integrity of endothelial monolayer and cytoprotective mechanism through caspase cleavage of adherens junction proteins (Aliprantis *et al.*, 2000). The endothelial responds to LPS by reorganizing actin and cell detachment from the underlying matrix, thereby breaching the endothelial barrier (Aliprantis *et al.*, 2000; Szabo *et al.*, 1997). A minor breach in endothelial barrier may cause significant deleterious effects *in vivo* (Schwartz *et al.*, 1999). A widespread endothelial cell apoptosis has been shown in LPS-challenged mice and in cultured endothelial cells (Hull *et al.*, 2002; Szabo *et al.*, 1997). Meanwhile, BMP4 induce apoptosis by activating caspase-3 which is mediated through ROS-dependent p38 and JNK activation in the endothelial cells (Figure 2.10) (Tian *et al.*, 2012c). The knockdown of BMPR1A, NOX4, or JNK which interfere with BMP4 signalling abolished BMP4-induced endothelial cells apoptosis (Tian *et al.*, 2012c).

Inflammation and apoptosis is highly associated with endothelial dysfunction (Reinhart *et al.*, 2002). The endothelium regulate the inflammatory response by recruiting

leukocytes, and facilitating their transmigration into tissues (Pober, 1998). During inflammation, the microcirculation undergoes major changes which causes systemic vascular collapse, disseminated intravascular coagulation, and vascular leak syndrome (Pober, 1998; Reinhart *et al.*, 2002). LPS has functional effects on leukocytes that can directly or indirectly affect the viability of endothelium *in vivo* (Varani & Ward, 1994). Neutrophils activated by cytokine and mononuclear cells activated by LPS can elicit endothelial damage (Figure 2.10) (Lindner *et al.*, 1997). Key mediator of inflammation-induced endothelial dysfunction is due to high levels of NO expressed by iNOS during LPS stimulation (Chauhan *et al.*, 2003; McNeill *et al.*, 2015). Endothelial dysfunction in aorta and mesenteric arteries of mice showed an increased iNOS protein expression (Chauhan *et al.*, 2003). In the endothelium and vascular smooth muscle, proinflammatory stimuli up-regulated BH_4 levels followed by an increase in iNOS mRNA and protein (Gross & Levi, 1992; Radomski *et al.*, 1990). Induction of iNOS in cerebral arteries reduced NO-mediated vasodilation initiated by eNOS (Mathewson & Wadsworth, 2004). Mice with deficiency of global iNOS were shown to be protected against LPS-induced vascular dysfunction and hypotension (MacMicking *et al.*, 1995). Vascular tissues from experimental models of severe septic shock showed attenuation of eNOS expression, suggesting that vascular eNOS expression is dependent on the severity of disease induced by LPS (Chauhan *et al.*, 2003). LPS exposure increased iNOS-derived NO, which down-regulated sGC activity in the vascular smooth muscle and demonstrated an inhibitory effect on eNOS, thereby inhibiting acetylcholine-induced relaxation in conduit (aorta) and resistance (mesenteric) arteries in mice (Chauhan *et al.*, 2003).

Similar to LPS, BMP4 also impairs endothelium-dependent vasodilatation (Figure 2.10) (Wong *et al.*, 2010). BMP4 has been shown to induce endothelial dysfunction through ROS-dependent p38 MAPK activation and COX-2 upregulation in endothelial

cells (Wong *et al.*, 2010). Miriyala *et al.* (2006) has shown that chronic exposure of BMP4 triggers endothelial dysfunction and arterial hypertension in mice. Noggin, a negative regulator binds to and inactivates BMP4 has been shown to improve BMP4 induced endothelial dysfunction and hypertension in mice, and counteracts the proatherogenic effects of BMP4 in endothelial cells (Chang *et al.*, 2007). BMP4 inhibition also reversed endothelial dysfunction in *db/db* diabetic mice by attenuating oxidative stress production in endothelial cells and eventually increases NO bioavailability in blood vessels through BMP4 receptor 1a (ALK3) (Zhang *et al.*, 2014).

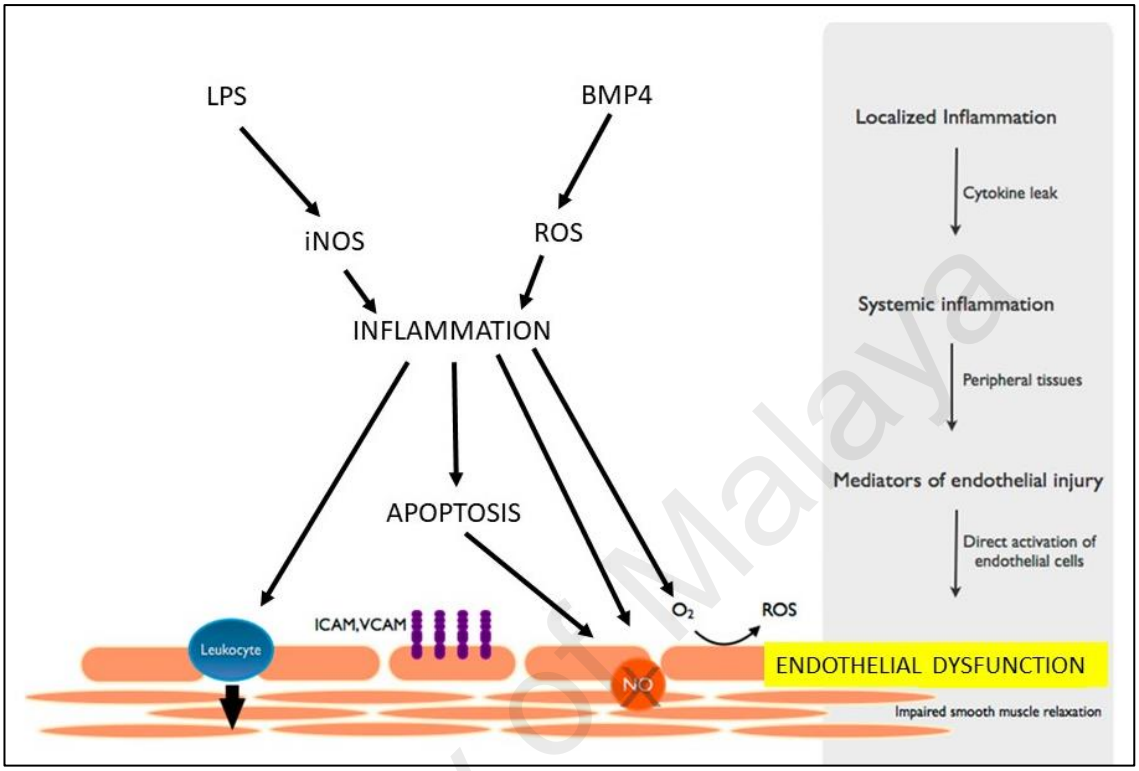

Figure 2.10: From local inflammation to systemic endothelial dysfunction. Inflammatory cytokines spread from the local inflammation into the systemic circulation to propagate a systemic inflammatory response. The byproducts of systemic inflammation elicit independent and complementary effects on the endothelium, leading to a state of endothelial dysfunction characterized by increased adhesion molecule expression (VCAM, ICAM), leukocyte diapedesis, ROS production and decreased NO-mediated smooth muscle relaxation and vascular dilation. Abbreviations: VCAM, vascular cell adhesion molecule; ICAM, intercellular adhesion molecule; BMP4, bone morphogenetic protein 4; ROS, reactive oxygen species; iNOS, NO, nitric oxide; O_2^-, superoxide anion; LPS, lipopolysaccharides (Modified from Steyers & Miller, 2014).

2.7 Paeonol

The root bark of Chinese herb *Paeonia suffruticosa* Andrew (Moutan Cortex), has been widely used in traditional Chinese medicine for centuries as remedies to alleviate sickness in humans by eliminating heat, promoting blood flow, and removing blood stasis (Zhu, 1998). Paeonol (2'-hydroxy-4'-methoxyacetophenone, $C_9H_{10}O_3$) (Figure 2.11) is a main active phenolic compound extracted from this plant. Paeonol exists as white needle crystal with relatively low melting point of 51°C to 52°C (Wu *et al.*, 2014).

Paeonol is used in traditional oriental medicines in treating various diseases and inflammatory diseases including hepatitis (Wu, 1966; Zhang *et al.*, 1996) and subsequently identified to have various pharmacological and physiological effects. It has been reported that paeonol possesses an anti-inflammatory property such as attenuating airway inflammation and hyperresponsiveness in a murine model of asthma (Du *et al.*, 2010), protect against cigarette smoke-induced lung inflammation (Liu *et al.*, 2014b) and protecting rat vascular endothelial cells from oxidized low-density lipoprotein (ox-LDL)-induced injury (Liu *et al.*, 2014c). Accumulating evidence suggests that paeonol exhibits free-radical scavenging properties by reducing the superoxide anion and microglia activation in ischemia-reperfusion injured rats which reduced cerebral infarction (Hsieh *et al.*, 2006), suppressed cigarette smoke-induced interleukin-8 (IL-8) *in vitro* via its antioxidant function by inhibiting both ROS-sensitive 5' AMPK/MAPK signalling pathway and the downstream transcriptional factors NF-κB and improve lung inflammation (Liu *et al.*, 2014a). Paeonol and "danshensu" combination attenuate apoptosis in myocardial infarction in rat models by inhibiting oxidative stress (Li *et al.*, 2016). Recent literature has revealed that paeonol possess anti-apoptotic effects by reducing the expression of caspases 3, 8, 9, and Bax, and increasing Bcl-2 (Gong *et al.*, 2017). Paeonol also suppressed ox-LDL by suppressing sequential events such as lectin-

like low density lipoprotein receptor-1 (LOX-1) up-regulation, reactive oxygen species (ROS) overproduction, caspase-3 activation and B-cell lymphoma 2 (Bcl-2) down-regulation (Bao *et al.*, 2013).

Despite the wide spread traditional medicinal use of paeonol, very few scientific evaluation has been undertaken to investigate its vascular protective effects against ER stress and inflammation-induced endothelial dysfunction. The present study would provide further information on protective effects of paeonol against ER stress and inflammation-induced endothelial dysfunction.

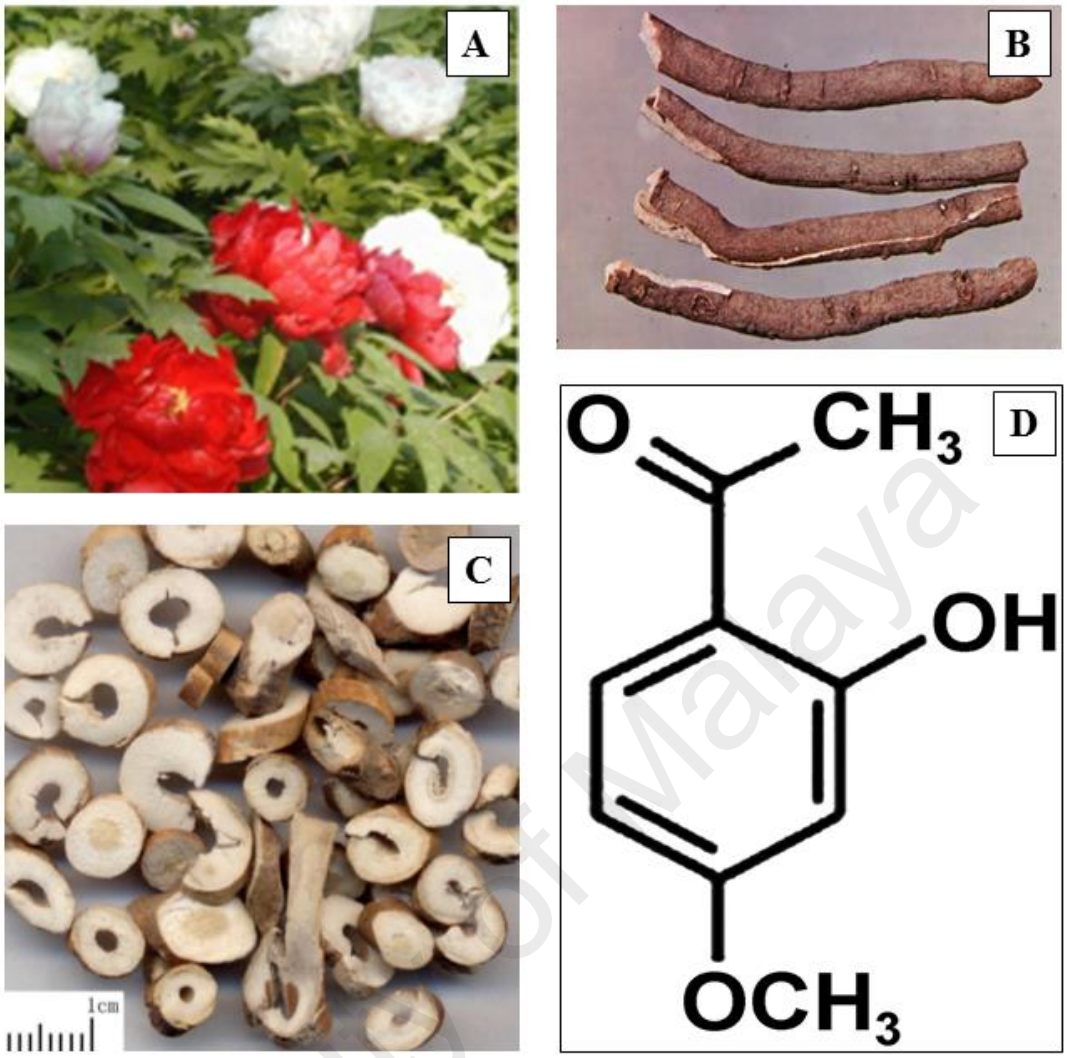

Figure 2.11: (A) The plants of Moutan Cortex (*Paeonia suffruticosa* Andrew), (B) root bark, (C) decoction pieces and (D) chemical structure of paeonol (Modified from Li *et al*., 2010b).

CHAPTER 3: EFFECT OF PAEONOL IN ENDOPLASMIC RETICULUM STRESS-INDUCED ENDOTHELIAL DYSFUNCTION

3.1 Introduction

The ER is the cellular site for protein translation, translocation, folding and post-translational modifications including glycosylation, disulfide bond formation, and chaperone-mediated protein folding processes (Hampton, 2002). When the function of the ER is disturbed by oxidative stress, ischemia or disturbances in Ca^{2+} homeostasis, unfolded proteins will accumulate within ER and leads to ER stress (Kim *et al.*, 2008; Minamino *et al.*, 2010). Activation of ER stress will release GRP78 from ER and activate transcriptional and translational pathways known as the UPR to regulate the buildup of unfolded protein (Ron & Walter, 2007). Activation of UPR triggers 3 distinct UPR called protein kinase-like ER kinase (PERK), inositol requiring kinase 1 (IRE1), and activating transcription factor 6 (ATF6) (Minamino *et al.*, 2010). Pro-apoptotic pathway is activated through IRE1 and CHOP (C/EBP-homologous protein) (Scull & Tabas, 2011) when UPR is prolonged. Excessive and prolonged UPR contribute to the development of cardiovascular diseases such as arteriosclerosis (Scull & Tabas, 2011), hypercholesterolemia (Sozen & Ozer, 2017) and diabetes (Demirtas *et al.*, 2016). There are also compelling evidence showing that ER stress is involved in vascular endothelial dysfunction (Galan *et al.*, 2014; Kassan *et al.*, 2012). Thus, targeting UPR component molecules and reducing ER stress offers a favourable strategy to treat cardiovascular diseases.

Peroxisome proliferator-activated receptor (PPAR) δ is a member of nuclear receptor proteins located in numerous tissues such as vascular endothelial and smooth muscle cells (Katusic *et al.*, 2012). PPARδ activation increases vascular endothelial growth factor

(VEGF), triggers PI3K-Akt pathway in the vascular walls and control the genes involved in lipid and glucose metabolism indirectly (Wang *et al.*, 2006). In the endothelial cells lining of the vasculature, activation of PPARδ increases Bcl-6 expression and the regulators of G protein-coupled signalling pathway to exhibit anti-inflammatory, anti-atherosclerotic, and stimulate angiogenesis (Piqueras *et al.*, 2007; Takata *et al.*, 2008). PPARδ activation is shown to reduce ER stress and mitigate endothelial dysfunction in diet-induced obese mice (Cheang *et al.*, 2014).

AMP-activated protein kinase (AMPK) is the central regulator of cellular and organismal metabolism in eukaryotes which regulate the energy balance of the cells (Hardie, 2007), and initiate protective reaction to combat cellular stresses (Hardie *et al.*, 1994). AMPK has been demonstrated to enhance the target transcriptional activity of PPARδ in transcriptional regulation of skeletal muscle metabolism directly (Narkar *et al.*, 2008). AMPK activation reduced ER stress by inhibiting NADPH oxidase-derived ROS (Dong *et al.*, 2010b) in atherosclerosis, insulin resistance, obesity and type 2 diabetes mellitus (Ozcan *et al.*, 2004). On the other hand, AMPK inhibition has been shown to augment ER stress and increase aortic lesions in $LDLr^{-/-}/AMPK\alpha2^{-/-}$ mice (Dong *et al.*, 2010a).

ER stress and oxidative stress are closely associated in the pathogenesis of cardiovascular diseases (Liang *et al.*, 2013a; Minamino *et al.*, 2010). Oxidative stress is triggered by activation of NADPH oxidase induced by ER stress and this involves Ca^{2+} and Ca^{2+}/calmodulin-dependent protein kinase II (CaMKII) (Li *et al.*, 2010a; Zhang & Ren, 2011). Activation of NADPH generates reactive oxygen species (ROS) such as superoxide anion in the blood vessels (Kalinowski & Malinski, 2004; Santos *et al.*, 2009). Superoxide anion reacts rapidly with NO released by the endothelium to generate

peroxynitrite which in turn leads to eNOS uncoupling to produce more superoxide anion (Harrison *et al.*, 2012). Besides, ROS-producing enzymes such as NADPH, xanthine oxidase, COX, inactivation of the antioxidant system, and uncoupling of endothelial NO synthase also cause oxidative stress (Higashi *et al.*, 2014). Oxidative stress induces accumulation of intracellular calcium, inflammatory signalling pathways initiation and elevated extracellular matrix deposition, leading to endothelial dysfunction (Baradaran *et al.*, 2014; Tabet *et al.*, 2004; Touyz, 2004).

Earlier study reported that paeonol increase the efficacy of chemotherapeutic drugs efficacy by reversing the ER stress-induced resistance to doxorubicin in human hepatocellular carcinoma cells (Fan *et al.*, 2012). Despite this pharmacological findings, the effects of paeonol on ER stress-induced endothelial dysfunction remains obscure. Thus, the present study seek to investigate the protective effects of paeonol against ER stress-induced endothelial dysfunction in mice. We hypothesized that paeonol protects against ER stress-induced endothelial dysfunction via up-stream activation of PPARδ leading to the inhibition of superoxide generation and elevation of NO bioavailability in the vascular walls. The results of this investigation will provide new insights on the role of paeonol to mitigate endothelial dysfunction related to ER stress.

3.2 Methods

3.2.1 Cell culture

HUVECs (Lonza, Basel, Switzerland, No. CC-2517) were grown in endothelial cell growth medium (EGM, Gibco, Invitrogen) supplemented with 10% FBS, 100 U/mL penicillin, 100 μg/mL streptomycin and endothelial cell growth supplement (50 μg/L, BD Transduction Laboratory, San Diego, CA, USA). The cells were cultured in a humidified atmosphere containing 5% carbon dioxide (CO_2) at 37 °C. Cells from passages between 4

and 6 were used. Once the cells reached 90% confluency, experiments were performed. The cells were made quiescent by incubation in FBS-free EGM for 4 hours before treatment with tunicamycin (ER stress inducer, 0.5 μg/mL), paeonol (0.001, 0.01, 0.1 μM), tauroursodeoxycholic acid (TUDCA, 10 μM), compound C (AMPK inhibitor, 5 μM), GSK0660 (PPARδ antagonist, 500 nM) and tempol (ROS scavenger, 100 μM) for 16 hours. The concentration and time duration were chosen based on previously reported effective concentration and time (Choy *et al.*, 2016; Murugan *et al.*, 2015).

3.2.2 Gene Reporter Assay

Mouse heart microvascular endothelial cell line H5V were seed in 48 well plates. The PPAR reporter plasmid PPRE-LUC (100 ng) were co-transfected with Renilla (5 ng) internal control pRL, plasmid over-expression PPAR heterodimer RXR (50 ng) as well as plasmid over-expression PPARδ (50 ng) with Lipofectamine™ 3000 according to manufacturer's instructions (Invitrogen, USA). After transfection for 16 hours, cells were treated with paeonol (0.1 μM) with or without compound C (5 μM) and GW1516 (100 nM, a PPARδ receptor agonist) for 24 hours. Cells were lysed and luciferase activity was measured by Dual-Luciferase Reporter Assay System (Promega, USA). Values are means ± SEM of fold changes of luciferase activity over controls after normalization to the renilla luciferase activity.

3.2.3 *Ex-vivo* study

3.2.3.1 Animal preparation

Approval for animal care and experimental protocol was gained from the Animal Research Ethics Committee of the Chinese University of Hong Kong and performed in compliance with the Guide for the Care and Use of Laboratory Animals (National Institutes of Health publication, eighth edition, updated 2011). In this study, 10 weeks old

male PPARδ wild-type (WT) and PPARδ knockout (KO) mice generated from C57BL/6N x Sv/129 background, (Peters *et al.*, 2000) and C57BL/6J mice were used. Mice were housed in a well-ventilated room with 12 h light/dark cycles at constant temperature of 24 ± 1°C and provided with normal rat chow (Specialty Feeds Pty Ltd., Glen Forrest, Australia) and tap water *ad libitum*. Mice were given 2 weeks to acclimate to the housing facility. Mice were killed by CO_2 inhalation for subsequent experiment.

3.2.3.2 *Ex vivo* culture of mouse aortic rings

The isolated mouse thoracic aorta from C57BL/6J, PPARδ WT or PPARδ KO mice was carefully isolated and cleaned from adjacent connective tissues in sterile phosphate buffered saline (PBS). The aortas were cut into several ring segments of around 2 mm in length each. Aortic rings were incubated in Dulbecco's Modified Eagle's Media (DMEM; Gibco, Gaithersburg, MD, USA) with 10% fetal bovine serum (FBS; Gibco), 100 µg/mL streptomycin and 100 U/mL penicillin and co-incubated with tunicamycin (ER stress inducer, 0.5 µg/mL), paeonol (0.001, 0.01, 0.1 µM), tauroursodeoxycholic acid (TUDCA, 10 µM), compound C (AMPK inhibitor, 5 µM) and GSK0660 (PPARδ antagonist, 500 nM) at 37 °C for 16 hours and subsequently, functional studies were carried out. Some of the rings were snap frozen in liquid nitrogen and stored in -80 °C for protein analysis.

3.2.4 *In vivo* study

All experiments were conducted with approval from Institutional Animal Care and Use Committee (IACUC) of University of Malaya (Ethics reference no: 2016-170531/PHAR/R/MRM). A total of 48 C57BL/6J male mice aged 10 weeks old purchased from Monash University (Sunway Campus, Malaysia) were randomly divided into the following groups: 1) control group; 2) group that received intra-peritoneal injection of ER stress inducer, tunicamycin (Tu, 1 mg/kg, 2 injections/week for 2 weeks) and vehicle

(saline, oral gavage, daily for 2 weeks); 3) group that received tunicamycin and oral administration of paeonol (20 mg/kg/day for 2 weeks) (Tu + Paeonol); 4) group that received only oral administration of paeonol (20 mg/kg/day for 2 weeks); 5) group that received tunicamycin and daily oral administration of a ROS scavenger, tempol (20 mg/kg/day) for 2 weeks (Tu + Tempol); 6) group that received tunicamycin and daily intra-peritoneal injection of ER stress inhibitor, TUDCA (150 mg/kg/day) for 2 weeks (Tu + TUDCA). The dose of paeonol was determined from literature (Hsieh *et al.*, 2006; Lee *et al.*, 2013; Shi *et al.*, 2016) and our preliminary data (Figure 3.16B & C) that showed paeonol treatment at 20 mg/kg improved endothelium-dependent relaxation in mice treated with tunicamycin.

During the experimental period, body weights were taken daily while systolic blood pressure of the mice was measured at day 0, day 7 and before sacrifice (day 14) using the tail-cuff blood pressure system (NIBP Monitoring System, IITC Inc., Woodland Hills, CA, USA). Prior to the blood pressure measurement, the mice were restrained in a pre-warmed chamber (28-30 °C) for at least 30 minutes. The arterial blood pressure measurements were performed at the same time of the day (between 9 a.m. and 11 a.m.) to avoid the influence of the circadian cycle. The value of systolic blood pressure was reported as the average of 6 successive measurements.

Mice were anaesthetized with CO_2 inhalation at the end of the treatment period, and blood samples were collected. Blood samples were centrifuged at 2500 rpm for 10 minutes at 4 ºC to obtain serum and was stored at -80 ºC immediately until further use. Then, mouse aorta was isolated immediately and processed accordingly for subsequent experiments.

3.2.5 Functional study with wire myograph

Isometric tone changes in aortic rings were measured by Multi Wire Myograph System (Danish Myo Technology, Aarhus, Denmark) in oxygenated Krebs solution containing (mM) NaCl 119, $NaHCO_3$ 25, KCl 4.7, KH_2PO_4 1.2, $MgSO_4.7H_2O$ 1.2, glucose 11.7 and $CaCl_2.2H_2O$ 2.5. Two mounting wires were threaded through the isolated mouse aorta rings and secured to two supports in a Multi Wire Myograph System (Danish Myo Technology, Aarhus, Denmark). One support was attached to a micrometer for the adjustment of vessel circumference and application of tension. The other support was attached to an isometric transducer. The rings were stretched to an optimal baseline tension of 3 milinewton (mN) with continuously oxygenated of 95% O_2 and 5% CO_2 at 37°C. After equilibration for 45 minutes, rings were pre-contracted with 60 mM KCl to prime the tissues and then were rinsed with Krebs solution for 3 times. Once tissues were stabilised, phenylephrine (Phe, 3 μM) was added to induce a stable contraction. Endothelium-dependent relaxation (EDR) was generated by cumulative addition of acetylcholine (3 nM to 10 μM; Sigma-Aldrich) and α2-adrenoceptor agonist, UK14304 (3 nM to 10 μM; Sigma-Aldrich). Endothelium-independent relaxation to sodium nitroprusside (SNP, 1 nM to 10 μM) was also constructed. The changes of isometric tension were recorded using the PowerLab LabChart 6.0 recording system (AD Instruments, Bella Vista, NSW, Australia). Concentration-response curves for both endothelium-dependent and -independent relaxation were expressed as the percentage of reduction in contraction induced by Phe before the application of acetylcholine, UK14304 or SNP independently. The maximum effect (R_{max}) and concentration inducing 50% of R_{max} (pEC_{50}) were determined from the cumulative concentration-response curves.

3.2.6 Western blotting

Treated mouse aortas and HUVECs were homogenized in ice-cold 1X RIPA buffer containing leupeptin 1 μg/mL, aprotonin 5 μg/mL, PMSF 100 μg/mL, sodium orthovanadate 1 mM, EGTA 1 mM, ethylenediaminetetraacetic acid (EDTA) 1 mM, NaF 1 mM, and β-glycerolphosphate 2 mg/mL. The lysates were centrifuged at 20,000 g for 20 minutes at 4°C. The supernatant was collected and the protein concentrations were measured using Lowry assay (Bio-Rad Laboratories, Hercules, CA, USA). Protein samples (15 μg) was electrophoresed through 7.5% or 10% sodium dodecyl sulphate (SDS)-polyacrylamide gels and transferred to an immobilon-P polyvinylidene difluoride (PVDF) membrane (Millipore, Billerica, MA, USA) at 100 V using wet transfer (Bio-Rad). Non-specific binding sites were blocked by 3% bovine serum albumin (BSA) in 0.05% Tween-20 phosphate-buffered saline with gentle shaking. After blocking, the membranes were incubated with primary antibodies against GRP78 (1:1000, Santa Cruz), ATF6 (1;1000, Abcam, Cambridge, UK), phosphorylated eIF2α at Ser^{52} (1;1000, Invitrogen, Carlsbad, CA, USA), eIF2α (1;1000, Cell Signaling), phosphorylated AMPKα at Thr^{172}, AMPKα (1;1000, Cell Signaling Technology, Danvers, MA, USA), PPARδ (1;1000, Cayman Chemcial, Ann Arbor, MI, USA), phosphorylated endothelial nitric oxide synthase (eNOS) at Ser^{1177} and at Ser^{1176} (1;1000, Abcam), eNOS (1;1000, BD Transduction laboratory, San Diego, CA, USA), NOX2 (1;1000, Abcam, Cambridge, UK), nitrotyrosine (1;1000, Abcam, Cambridge, UK) and glyceraldehyde 3-phosphate dehydrogenase (GAPDH, Ambion, Austin, TX, USA), at 4°C overnight. The membrane were then washed three times with TBS-T (Tris-buffered saline with 0.1% Tween 20), followed by incubation with respective horseradish peroxidase-conjugated secondary antibodies (DakoCytomation, Carpinteria, CA, USA) for 2 hours at room temperature. The membranes were developed with an enhanced chemiluminescence detection system (ECL reagents, Millipore Corporation, Billerica, MA) and exposed on X-ray films.

Densitometric analysis was performed using Quantity One analysis software (Bio-Rad). Equal protein loading was verified with use of GAPDH as housekeeping protein. The respective protein expression levels for ATF6, PPARδ, GRP78, NOX2 and nitrotyrosine were normalized to GAPDH, peNOS to eNOS, peIF2α to eIF2α, pAMPK to AMPK and then compared with control.

3.2.7 Immunofluorescence

Treated aortic rings were fixed with 4% paraformaldehyde and permeabilized by 0.01% TritonX100 for 15 minutes as previously described (Lau, 2013). Following rinsing three times with PBS, the aortic rings were blocked with 5% normal donkey serum in PBS at room temperature for 2 hours. Then, the rings were incubated with primary antibody against ATF6 (1:100, anti-rabbit, Abcam) and VE-cadherin (CD144, 1:100, anti-goat, Santa Cruz Biotechnology). After incubation at 4ºC overnight, the aortic rings were incubated with secondary antibody Alexa Fluor 488 anti-rabbit and 546 anti-goat for 2 hours at room temperature in dark. Non-specific control for immunofluorescence was done by omitting the primary antibody (ATF6) only and then incubated the isolated mouse aorta with secondary antibody to check for unspecific binding or for cross-reaction between the secondary antibodies. The rings were cut open carefully and laid between two coverslips with the endothelium placing upside down on the microscope. The fluorescent images were taken with the Fluoview FV1000 laser scanning confocal system (Olympus, Tokyo, Japan) with sequential excitation 488 nm to 546 nm and emission 520 nm to 585 nm. The endothelial cells was confirmed with positive staining with endothelial cell-specific marker VE-cadherin. The images were merged to identify the localization of target protein. The average fluorescence intensity in an area of interest was analyzed using Fluoview FV10-ASW software (Olympus) and was normalized to the control.

3.2.8 Detection of ROS formation in HUVECs and *en face* endothelium of mouse aortas

The level of oxidative stress in HUVECs and *en face* endothelium of mouse aorta was assessed using dihydroethidium (DHE) dye by confocal microscopy (San Cheang *et al.*, 2015). The treated HUVECs and aortic rings were incubated with DHE (5 μM, Invitrogen, Carlsbad, CA, USA) for 15 minutes in normal physiological saline solution (NPSS, composition in mM: NaCl 140, KCl 5, $CaCl_2$ 1, $MgCl_2$ 1, glucose 10 and HEPES 5) with pH 7.4. After incubation, cells and the aortic rings were rinsed 3 times with NPSS. The aortic rings were cut open and the endothelium was placed upside down between two coverslips on the microscope. Fluorescence intensity was captured by confocal microscope Leica TCS SP5 II (Leica Microsystems, Mannheim, Germany) with 515 nm excitation and 585 nm long pass filter. Background autofluorescence of elastin in aortic rings were taken at excitation 488 nm and emission 520 nm separately to avoid overlapping of the emission spectrum. DHE fluorescence intensity was analyzed by Leica LAS-AF software version 2.6.0.7266 as represented by the fold change in fluorescence intensity relative to the control group.

3.2.9 Detection of vascular superoxide formation

The vascular superoxide anion formation was quantified with lucigenin-enhanced chemiluminescence method (Lau *et al.*, 2013). Aortic rings were pre-incubated for 45 minutes at 37 °C in Krebs-HEPES buffer (in mM: NaCl 99.0, $NaHCO_3$ 25, KCl 4.7, KH_2PO_4 1.0, $MgSO_4$ 1.2, glucose 11.0, $CaCl_2$2.5 and Na-HEPES 20.0) in the presence of diethylthiocarbamic acid (DETCA, 1 mM) to inactivate superoxide dismutase (SOD) and β-NADPH (0.1 mM) as substrate for NADPH oxidase. Inhibitor of NADPH oxidase, diphenylene iodonium (DPI; 5 mM) was used as the positive control. A 96-well Optiplate containing lucigenin (5 mM) and β-NADPH (0.1 mM) in 300 mL of Krebs-HEPES buffer

per well was loaded into the Hidex plate CHAMELEONTM V (Finland). Background photo emission reading was measured with 30 seconds intervals over 20 minutes. The rings were then transferred into wells and measurement was taken again. Upon completion of measurement, the rings were dried for 48 hours at 65 °C and weighed. The data are expressed as average counts per mg of vessel dry weight.

3.2.10 Measurement of NO production and total nitrite/nitrate level in HUVECs and mouse aortas

Treated HUVECs were incubated with 1 μM 4-amino-5-methylamino-2',7'-difluorofluorescein (DAF-FM DA; Molecular Probes) at 37°C for 15 minutes (Tian *et al.*, 2012b). Then, the cells were rinsed with NPSS and stimulated with 1 μM calcium ionophore A23187 (Sigma-Aldrich, St Louis, MO, USA). The intensity of the fluorescence excited at 495 nm and emitted at 515 nm was determined using Olympus Fluoview FV1000 laser scanning confocal system. The differences in intracellular NO level were calculated as relative fluorescence intensity (F1/F0, where F0 = average fluorescence signals before addition of A23187 and F1 = fluorescence signal at defined time intervals when A23187 was added).

Total nitrite and nitrate level from media of cultured HUVECs and mouse aorta were detected using Nitrate/Nitrite Colorimetric Assay Kit (Cayman Chemical Company, Ann Arbor, MI, USA) according to manufacturer protocol. Absorbance was measured at 540 nm using Hidex plate CHAMELEON™ V (Turku, Finland) and compared with a standard nitrite curve. Results were expressed in μM.

3.2.11 Data analysis

Results are represented as means ± SEM from n experiments. Concentration-response curves were fixed to a sigmoidal curve using non-linear regression using statistical software GraphPad Prism version 4 (GraphPad Software Inc., San Diego, CA, USA). Statistical significance was determined using two-tailed Student's t-test for comparison of two groups and one-way ANOVA followed by Bonferroni multiple comparison tests when more than two treatments were compared. $P<0.05$ was considered statistically significant.

3.3 Results

3.3.1 Paeonol inhibited tunicamycin-induced endothelial dysfunction in mouse aorta *ex vivo*

Incubation with tunicamycin (0.5 μg/ml) for 16 hours impaired EDR to acetylcholine in aortic rings from C57BL/6J. The impaired relaxation were reversed by co-incubation with paeonol in a concentration dependent manner, with 0.1 μM being the most significant concentration (Figure 3.1A, Figure 3.1B & Table 3.1). Treatment with paeonol alone did not affect acetylcholine-induced relaxations. In addition, co-incubation with TUDCA (10 μM, ER stress inhibitor) also reversed the endothelial dysfunction induced by tunicamycin (Figure 3.1A, Figure 3.1C & Table 1). Compound C (5 μM, AMPK inhibitor) and GSK0660 (500 nM, PPARδ antagonist) inhibited paeonol-induced improvement of EDR in tunicamycin-treated aortas (Figure 3.1A, Figure 3.1C & Table 3.1). SNP-induced endothelium-independent relaxations was not affected in all groups (Figure 3.2 & Table 3.1). Removal of endothelium abolished acetylcholine -induced relaxations in all groups (Figure 3.3).

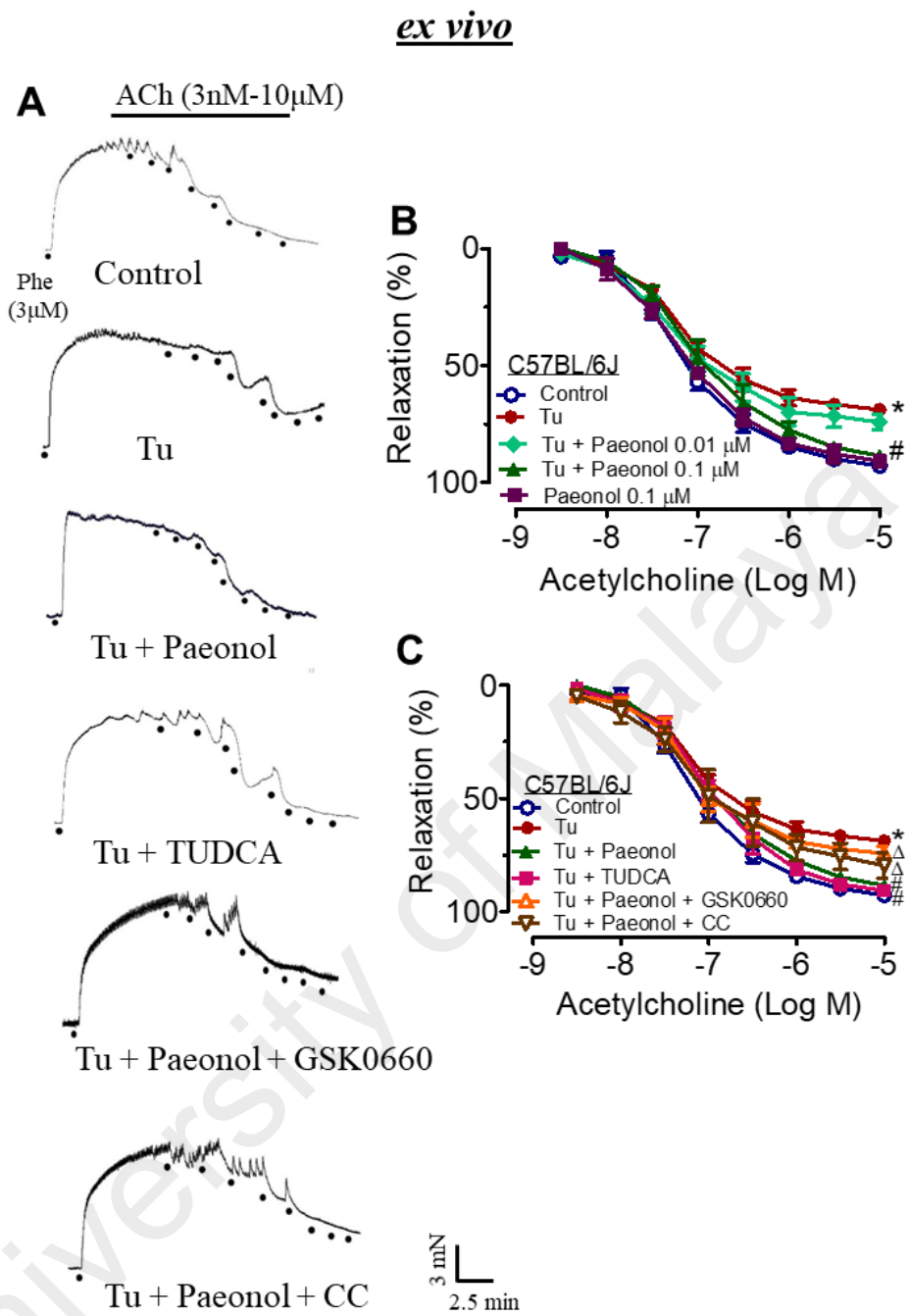

Figure 3.1: The effects of paeonol in improving endothelial dysfunction induced by tunicamycin (Tu, 0.5 μg/ml) for 16 hours. (A) Representative traces showing acetylcholine-induced endothelium-dependent relaxation in C57BL/6J mouse aortas precontracted with phenylephrine (Phe). (B) *Ex vivo* treatment with paeonol improved acetylcholine-induced endothelium-dependent relaxation in a concentration-dependent manner in C57BL/6J mouse aorta. (C) The effects of paeonol (0.1 μM) in reversing tunicamycin-induced impairment of acetylcholine-induced relaxations was inhibited by compound C (5 μM) and GSK0660 (500 nM). Results are means ± SEM of 6 experiments. *P< 0.05 vs. control, # P< 0.05 vs. Tu, Δ P< 0.05 vs. Tu plus paeonol.

ex vivo

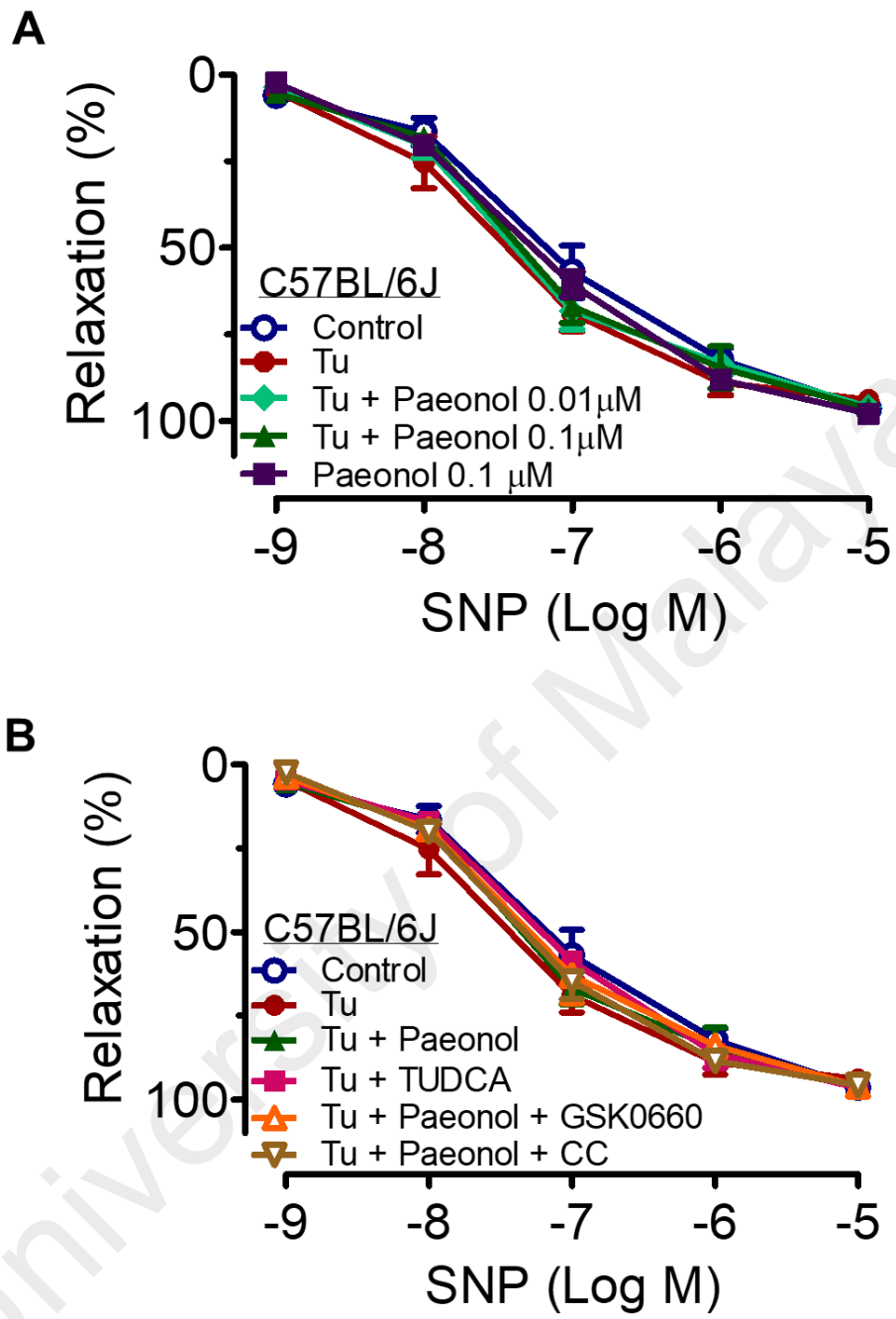

Figure 3.2: The effects of paeonol on sodium nitroprusside induced relaxation following tunicamycin (Tu, 0.5 μg/ml) incubation for 16 hours. Endothelium independent relaxations were not altered in all groups after *ex vivo* incubation to tunicamycin (0.5 μg/ml), paeonol (0.01 μM and 0.1 μM), TUDCA (10 μM), compound C (5 μM), GSK0660 (500 nM) for 16 hours.

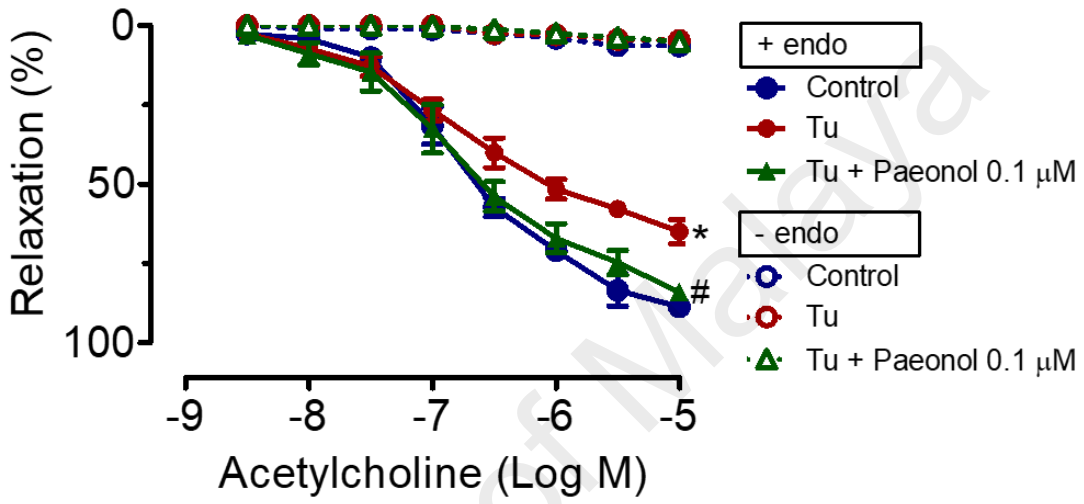

Figure 3.3: The effect of paeonol in reversing ER stress induced by tunicamycin (0.5 µg/ml) was present in mice aortas with endothelium but not in those without endothelium. Results are shown as means ± S.E.M. (n= 6). *P<0.05 compared with control, # P< 0.05 compared with Tu.

Table 3.1: Agonist sensitivity (pEC_{50}) and % maximum response (R_{max}) of endothelium-dependent and -independent vasodilators by acetylcholine and sodium nitroprusside (SNP), respectively, in C57BL/6J mouse aortic rings incubated with Tu, paeonol, CC, GSK0660 and TUDCA for 16 hours in DMEM. Results are means ± SEM (n=6). *P<0.05 compared with control, # P<0.05 vs. Tu, ΔP< 0.05 compared with Tu plus paeonol.

Groups	Acetylcholine		SNP	
	pEC_{50} (log M)	R_{max} (%)	pEC_{50} (log M)	R_{max} (%)
Control	7.18 ± 0.06	91.84 ± 1.48	7.12 ± 0.14	96.38 ± 1.27
Tu (0.5 μg/ml)	7.16 ± 0.07	68.70 ± 1.15 *	7.50 ± 0.14	93.81 ± 2.41
Tu + Paeonol (0.01 μM)	7.24 ± 0.12	74.24 ± 3.28	7.40 ± 0.11	95.91 ± 0.98
Tu + Paeonol (0.1 μM)	7.09 ± 0.09	87.78 ± 1.21 #	7.35 ± 0.11	96.42 ± 0.98
Tu + TUDCA (10 μM)	6.99 ± 0.08	90.79 ± 0.50 #	7.19 ± 0.08	96.56 ± 1.21
Tu + Paeonol + GSK0660 (500 nM)	7.17 ± 0.10	71.76 ± 3.13 Δ	7.33 ± 0.14	95.98 ± 0.98
Tu + Paeonol + CC (5 μM)	7.15 ± 0.21	79.72 ± 4.71 Δ	7.34 ± 0.09	95.65 ± 1.63
Paeonol (0.1 μM)	7.20 ± 0.07	90.78 ± 2.22	7.28 ± 0.08	97.85 ± 0.52

3.3.2 Paeonol upregulated PPARδ transactivation activity in H5V cells

To explore whether paeonol stimulates PPARδ activation, PPARδ reporter gene activity was quantified in H5V cells treated with paeonol. The result demonstrated that paeonol upregulated PPARδ transactivation activity in H5V cells significantly, signifying that PPARδ can be regulated by paeonol. Incubation with AMPK inhibitor, compound C reversed paeonol induced PPARδ activation, indicating that AMPK mediated paeonol induced PPARδ activity. As a positive control, GW1516 significantly increased PPARδ reporter activity (Figure 3.4).

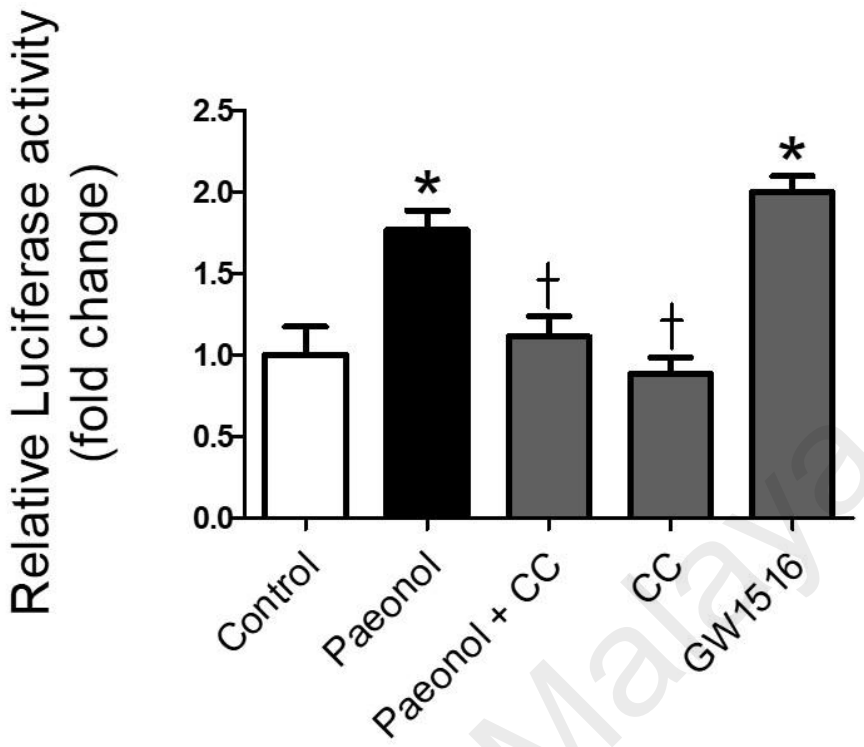

Figure 3.4: Paeonol promotes PPARδ activation through AMPK. H5V cells were transfected with PPAR reporter plasmids and exposed to paeonol (0.1 µM), compound C (CC, 5 µM) or GW1516 (100 nM) as positive control. Paeonol significantly increased PPARδ activity compared to the control, which was reversed by compound C, an AMPK inhibitor. Values are expressed as means ± SEM of fold change over control after normalization to the renilla luciferase activity of 6 experiments. *P< 0.05 vs. control, †P< 0.05 vs. paeonol alone.

3.3.3 Paeonol inhibited ER stress via AMPK/PPARδ signalling in mouse aortas and HUVECs

Tunicamycin exposure for 16 hours reduced the AMPKα phosphorylation (Figure 3.5A and 3.6A), PPARδ (Figure 3.5B & 3.6B) and phosphorylation of endothelial NO synthase (eNOS) at Ser^{1177} (Figure 3.5F & 3.6F), whereas ER stress proteins, namely phosphorylated of eukaryotic translation initiation factor 2 alpha (eIF2α), ATF6 and GRP78 (Figure 3.5C-3.5E & 3.6C-3.6E) were all elevated in mouse aortas isolated from C57B/6J and HUVECs respectively compared to control. Treatment with paeonol augmented the reduced AMPK phosphorylation, PPARδ protein expression and phosphorylation of eNOS at Ser^{1177} in mouse aortas (Figure 3.5A, 3.5B & 3.5F) and HUVECs (Figure 3.6A, 3.6B & 3.6F). However, phosphorylation of AMPK was unaffected by co-incubation of paeonol with GSK0660 in mouse aortas and HUVECs (Figure 3.5A & 3.6A). Co-treatment of paeonol with compound C (AMPK inhibitor) and GSK0660 (PPARδ inhibitor) respectively reduced the expression of PPARδ and phosphorylation of eNOS at Ser^{1177} in mouse aortas and HUVECs. Co-treatment with paeonol or TUDCA (ER stress inhibitor) reduced the expression of ER stress proteins elevated by tunicamycin in mouse aortas and in HUVECs. Co-incubation with compound C (AMPK inhibitor) and GSK0660 (PPARδ inhibitor) inhibited the protective effects of paeonol against tunicamycin-upregulated ER stress proteins in mouse aortas (Figure 3.5C- 3.5E) and in HUVECs (Figure 3.6C - 3.6E).

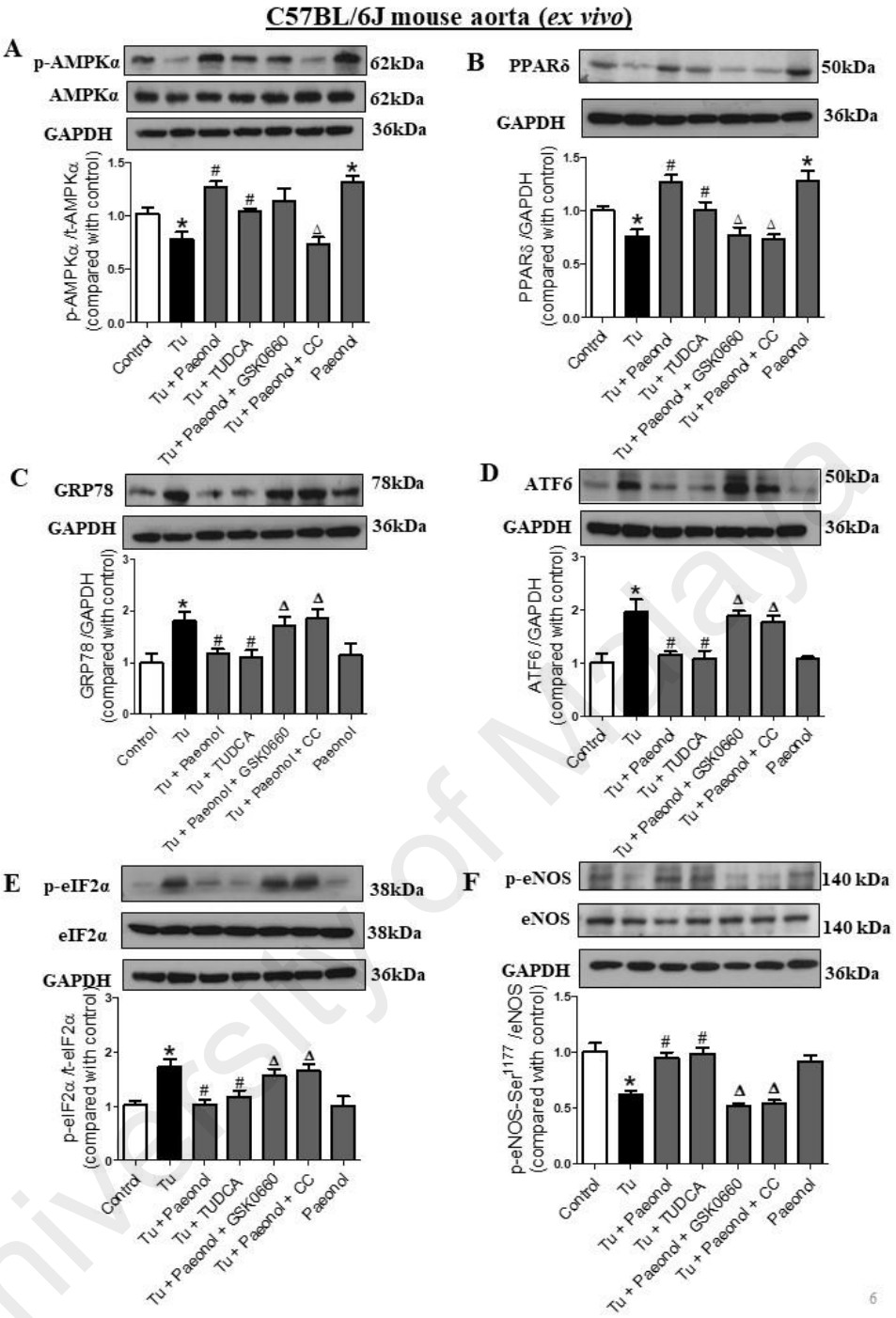

Figure 3.5: Inhibition of ER stress by paeonol via AMPK and PPARδ up-regulation in C57BL/6J mouse aorta. Western blot and quantitative data showing phosphorylation of AMPKα (A), PPARδ (B) and ER stress markers (C,D,E) and phosphorylation of eNOS (F) in C57BL/6J mouse aorta during *ex vivo* incubation with tunicamycin, (Tu, 0.5 μg/ml), paeonol (0.1 μM), compound C (5 μM), GSK0660 (500 nM) and TUDCA (10 μM) for 16 hours. Results are means ± SEM of 4-5 separate experiments. *P< 0.05 compared with control, # P< 0.05 compared with Tu, ΔP< 0.05 compared with Tu plus paeonol.

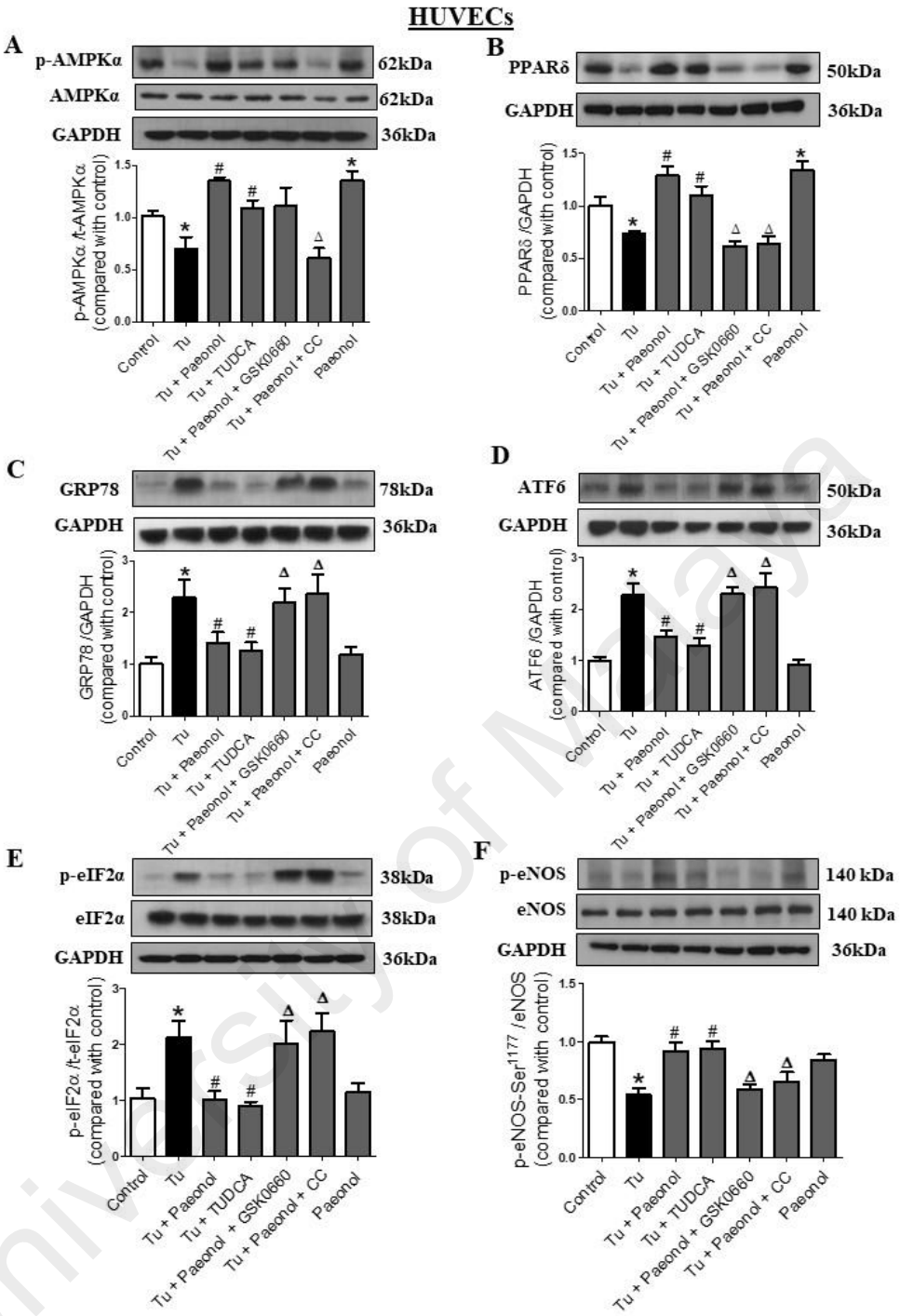

Figure 3.6: Paeonol reduces ER stress via activation of AMPK and PPARδ in HUVECs. Western blot and quantitative data showing the phosphorylation of AMPKα (A), PPARδ (B) and ER stress markers (C,D,E) and phosphorylation of eNOS (F) in HUVEC treated with tunicamycin (Tu, 0.5 μg/ml), paeonol (0.1 μM), compound C (5 μM),: GSK0660 (500 nM) and TUDCA (10 μM) for 16 hours. Results are means ± SEM of 4-5 separate experiments. *P< 0.05 compared with control, # P< 0.05 compared with Tu, **Δ**P< 0.05 compared with Tu plus paeonol.

3.3.4 PPARδ contributes to the beneficial effect of paeonol on endothelial function

Ex vivo exposure of tunicamycin was performed in PPARδ WT and KO mice to confirm the mechanism associated with the protective effects of paeonol against ER stress. Exposure to tunicamycin (0.5 μg/ml) for 16 hours impaired EDR in aortas from both PPARδ WT (Figure 3.7A) and PPARδ KO mice (Figure 3.7B) compared with control. Co-treatment with paeonol (0.1 μM) reversed endothelial dysfunction induced by tunicamycin in PPARδ WT mice (Figure 3.7A), but not in PPARδ KO mice (Figure 3.7B). TUDCA significantly improved EDR in both PPARδ WT and KO mice (Figure 3.7A & 3.7B). SNP-induced endothelium-independent relaxations were similar in all treatment groups in PPARδ WT or PPARδ KO mice (Figure 3.8).

Tunicamycin reduced AMPKα phosphorylation, PPARδ and phosphorylation of eNOS at Ser^{1177}, whereas ER stress markers such as GRP78, ATF6 and eIF2α were increased in aortas from PPARδ WT and KO mice (Figure 3.9A-F). Co-incubation with paeonol (0.1 μM) enhanced PPARδ protein expression in aortas from PPARδ WT mice, while AMPKα phosphorylation was increased in aortas of both PPARδ WT and KO mice. Paeonol reduced the expression of ER stress markers in aortas from PPARδ WT mice, but these inhibitory effects of paeonol were absence in PPARδ KO mice. Paeonol promoted phosphorylation of eNOS at Ser^{1177} in aortas from PPARδ WT mice but not from PPARδ KO mice (Figure 3.9A & G).

Immunofluorescence staining showed that paeonol reduced ATF6 protein upregulated by tunicamycin in endothelial cells *en face* of PPARδ WT mouse aorta (Figure 3.10). However, this effect of paeonol was diminished in endothelial cells *en face* of PPARδ KO mouse aortas. TUDCA reversed the effect of tunicamycin in both PPARδ mouse genotypes.

Ex vivo

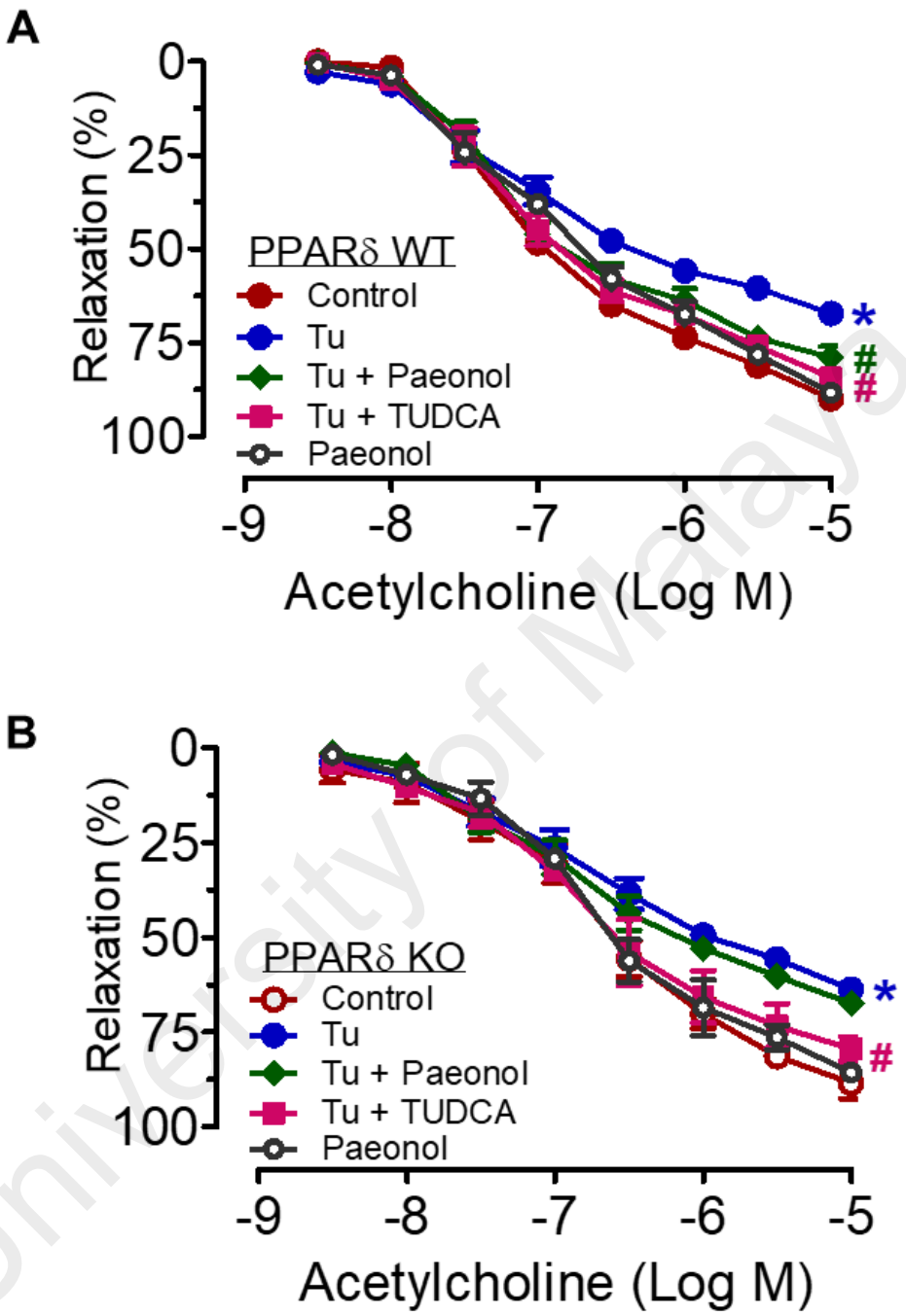

Figure 3.7: PPARδ plays a role in the vascular benefits of paeonol. Paeonol (0.1 µM) reversed endothelial dysfunction induced by tunicamycin (Tu, 0.5 µg/ml) for 16 hour in aortas of PPARδ WT mice (A) but not in PPARδ KO mice (B). Results are means ± SEM of 6 separate experiments. *P< 0.05 compared with control; #P< 0.05 compared with Tu from each genotype respectively.

Ex vivo

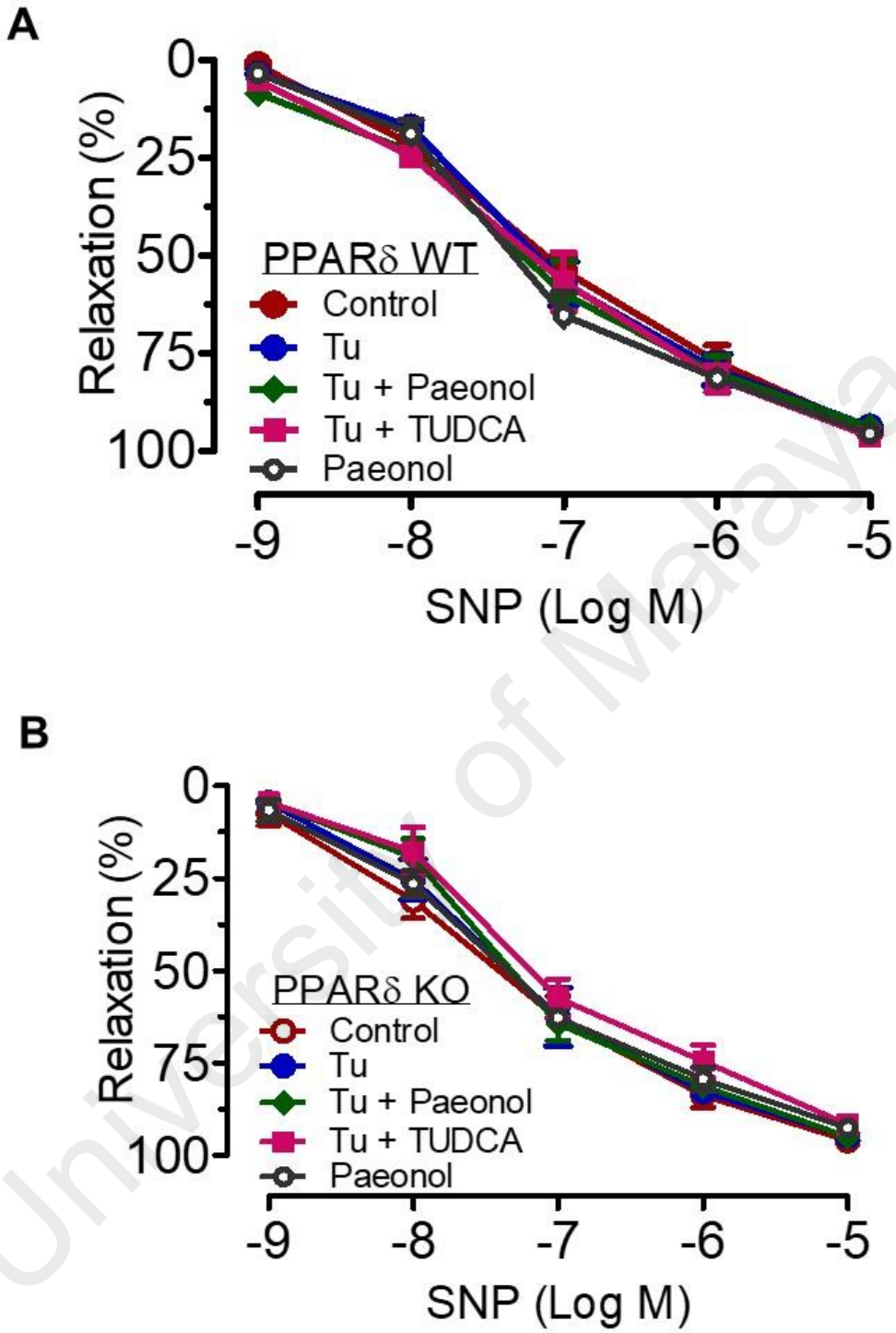

Figure 3.8: SNP-induced endothelium-independent relaxations were similar in all treatment groups in PPARδ WT or PPARδ KO mice. Results are means ± SEM of 6 separate experiments.

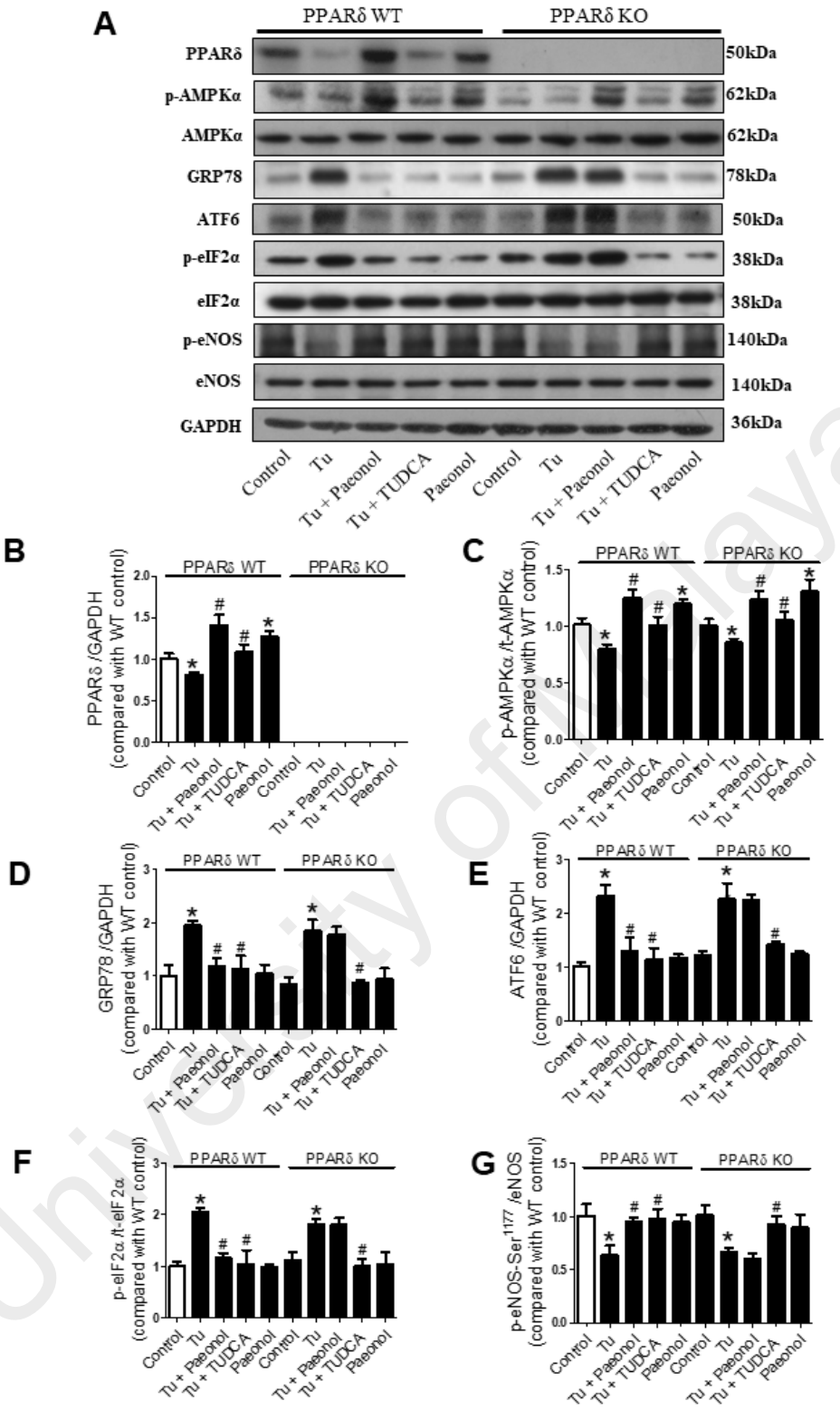

Figure 3.9: Representative bands and densitometry of Western blotting showing the level of p-AMPKα, PPARδ and ER stress markers in PPARδ WT and KO mouse aorta during *ex vivo* incubation with tunicamycin (Tu, 0.5 µg/ml), paeonol (0.1 µM) and TUDCA (10 µM) for 16 hours. Results are means ± SEM of 6 separate experiments. *P < 0.05 compared with control; #P < 0.05 compared with Tu from each genotype respectively.

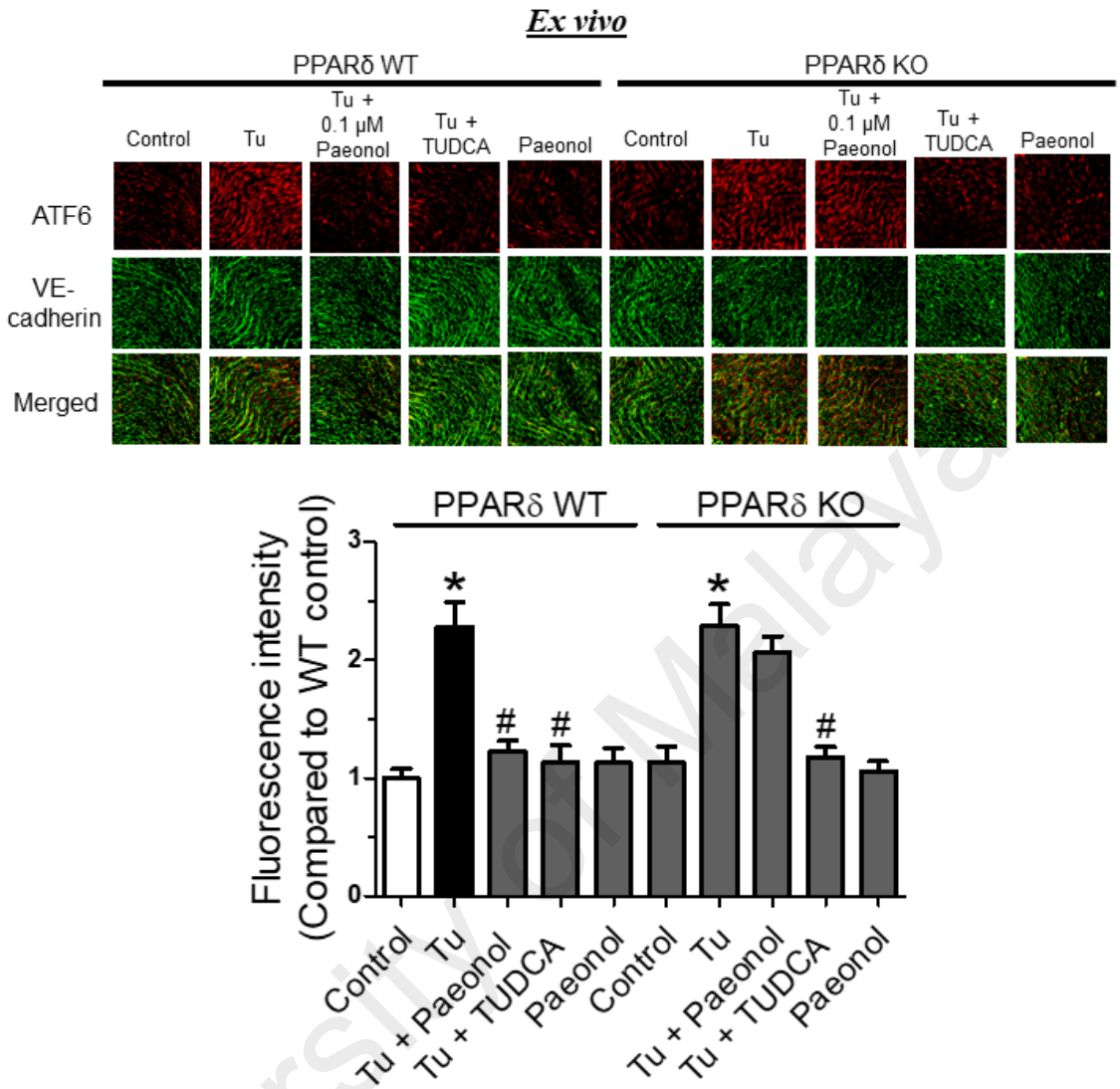

Figure 3.10: Paeonol reduced tunicamycin-induced ATF6 protein expression in PPARδ WT mice but not in PPARδ KO mice treated with tunicamycin (Tu, 0.5 µg/ml), paeonol (0.1 µM) and TUDCA (10 µM) for 16 hours during *ex vivo* incubation. In *en face* immunofluorescence staining assay, endothelium of thoracic aorta was stained with anti-vascular endothelial-cadherin (VE-cadherin) antibody for endothelial cell-cell junction staining (green) and anti-ATF6 antibody (red) and photographed under a confocal microscope. Results are means ± SEM of 6 separate experiments. Bar: 100 µm. *P < 0.05 compared with control; #P < 0.05 compared with Tu from each genotype respectively.

3.3.5 Paeonol reduced superoxide production through AMPK/PPARδ signalling pathway

Exposure with tunicamycin increased oxidative stress level in HUVECs and *en face* of mouse aortas (Figure 3.11) as measured by DHE fluorescence. Acute treatment with paeonol (0.1 μM) and TUDCA for 16 hours reduced the elevated ROS in HUVECs (Figure 3.11A & C) and *en face* endothelium of mouse aortas (Figure 3.11B & D), which were prevented by co-treatment with compound C (AMPK inhibitor) and GSK0660 (PPARδ antagonist).

In aortas of PPARδ WT and PPARδ KO mice, intracellular ROS and superoxide anion were measured using DHE (Figure 3.12A & 3.12B) and LEC (Figure 3.12C). Tunicamycin elevated DHE fluorescence intensity and superoxide anion production in both genotypes. Incubation with paeonol reduced tunicamycin-induced ROS (Figure 3.12A & 3.12B) and superoxide anion levels (Figure 3.12C) in PPARδ WT mouse aorta but paeonol's effect was ineffective in PPARδ KO mouse aorta. TUDCA reduced tunicamycin-induced ROS and superoxide anion levels while paeonol alone was comparable to control in both genotypes (Figure 3.12).

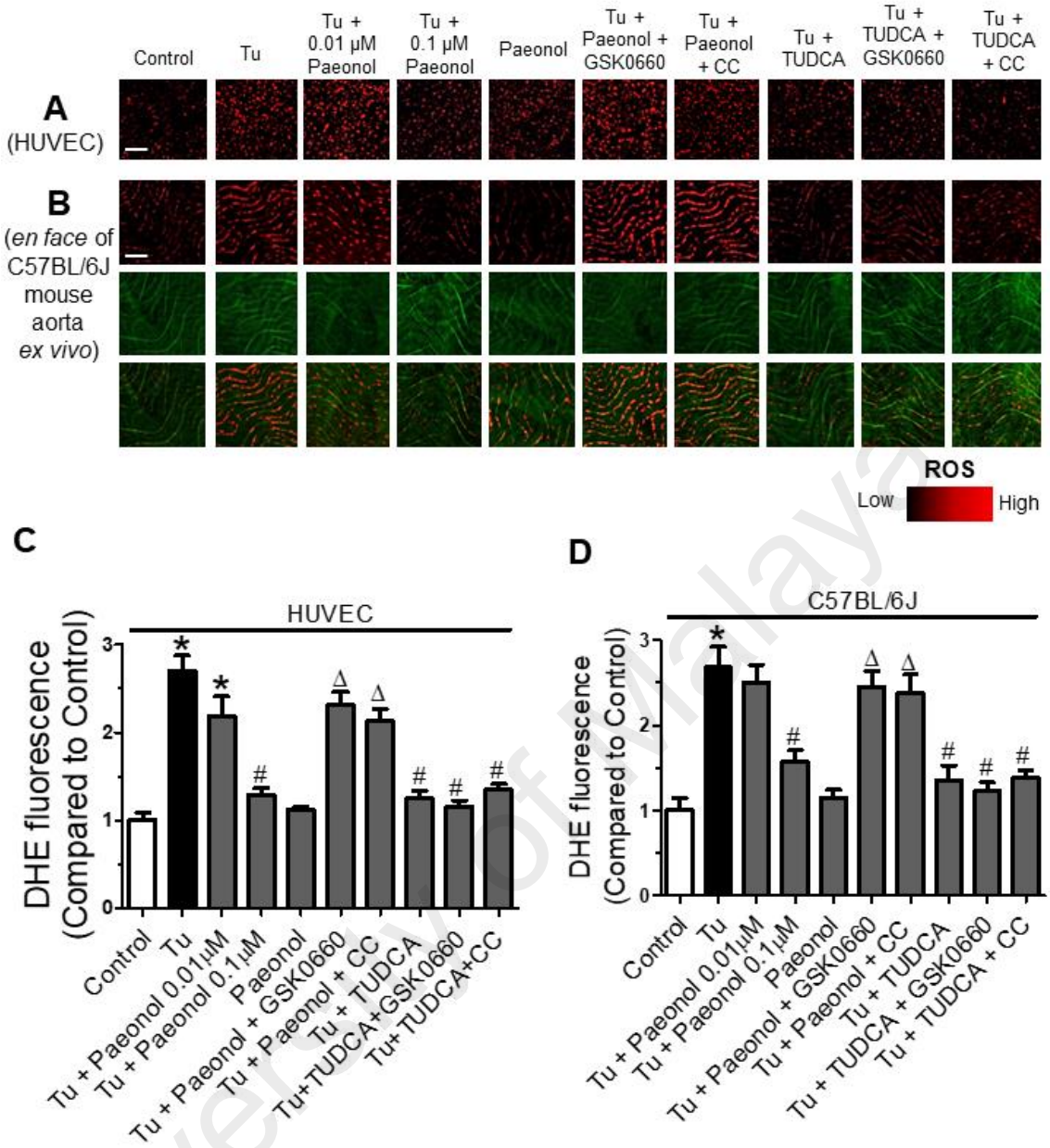

Figure 3.11: Paeonol reduces tunicamycin-stimulated superoxide production but its effect was normalized by co-incubation with AMPK inhibitors compound C (5 μM) and PPARδ antagonist GSK0660 (500 nM). Representative images and summarized results of superoxide production measured by DHE in (A&C) HUVECs and (B&D) *en face* endothelium of aorta of C57BL/6J aortic rings incubated with tunicamycin, (Tu, 0.5 μg/ml) for 16 hours. Red: DHE fluorescence (excitation: 515 nm) in the nucleus. Green: autofluorescence of elastin underneath the endothelium (excitation: 488 nm). Lower panel, merged images. Bar: 100μm. Results are means ± SEM of six separate experiments. *P<0.05 compared with control, # P<0.05 compared with Tu, ΔP< 0.05 compared with Tu plus paeonol.

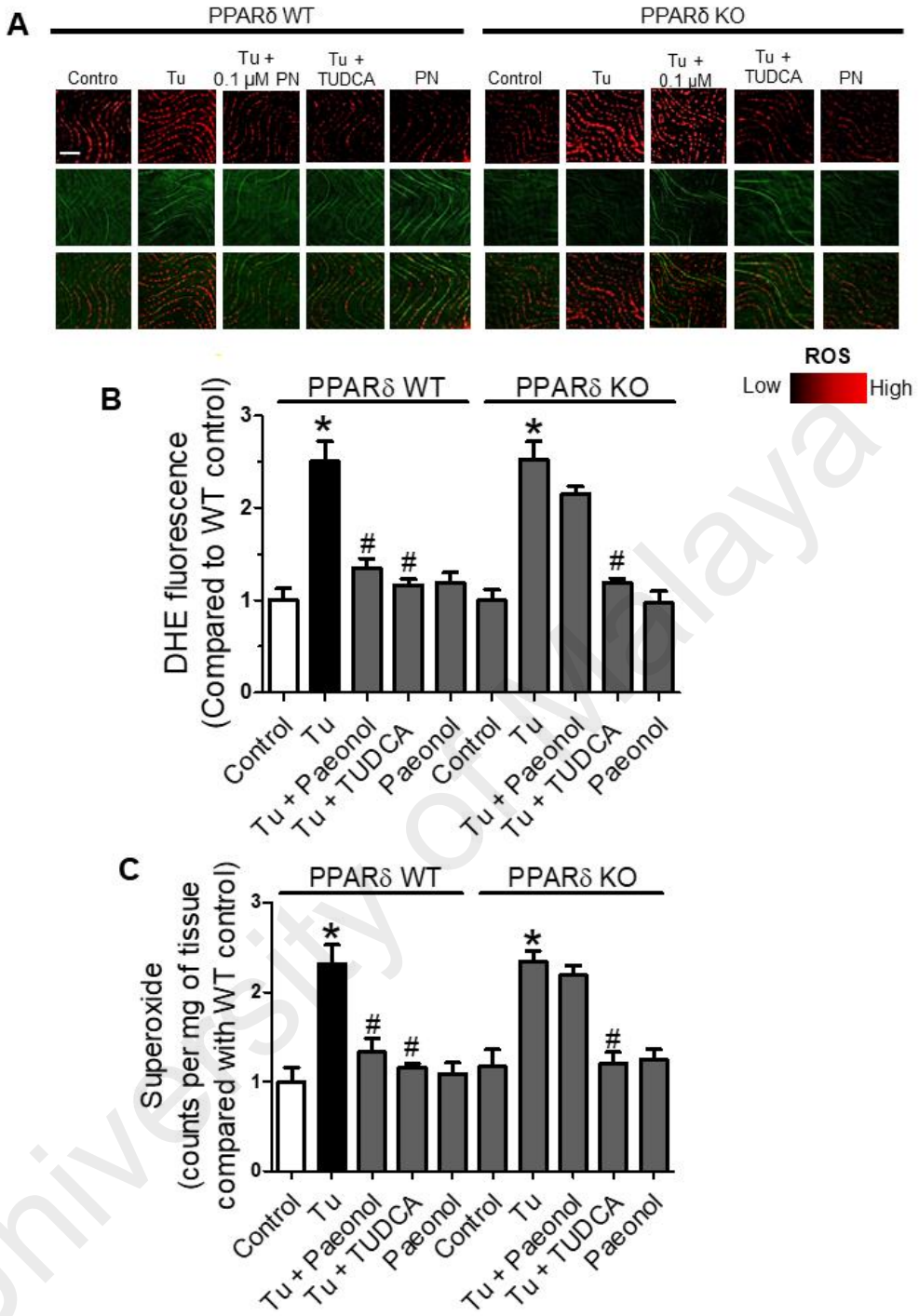

Figure 3.12: Acute paeonol treatment inhibits the increased generation of superoxide anion in tunicamycin-treated aortas of PPARδ WT mice but not in those from PPARδ KO mice as detected by (A&B) DHE fluorescence in the *en face* endothelium of aorta and (C) LEC method. Red: DHE fluorescence (excitation: 515 nm) in the nucleus. Green: autofluorescence of elastin underneath the endothelium (excitation: 488 nm). Lower panel, merged images. Bar: 100 μm. Results are means ± SEM of six separate experiments. *P<0.05 compared with control, # P< 0.05 compared with Tu.

3.3.6 Paeonol enhanced NO bioavailability in HUVECs

NO production is indicated by the increase of 4-amino-5-methylamino-2',7' difluorofluorescein fluorescence (DAF-FM DA) signal stimulated by addition of A23187, an Ca^{2+} ionophore in HUVECs. HUVECs incubated with tunicamycin showed reduction of NO production, which was normalized by co-incubation with paeonol and TUDCA (Figure 3.13A, B & C). However, this effect of paeonol was abolished by compound C (AMPK inhibitor) and GSK0660 (PPARδ inhibitors). Treatment with paeonol alone did not show any difference from the control.

Additionally, treatment with paeonol significantly increased the reduction of total NO metabolites (nitrite and nitrate) level induced by tunicamycin in the cultured media. However, the elevated level of NO induced by paeonol was significantly inhibited by compound C (AMPK inhibitor) and GSK0660 (PPARδ inhibitors) (Figure 3.14).

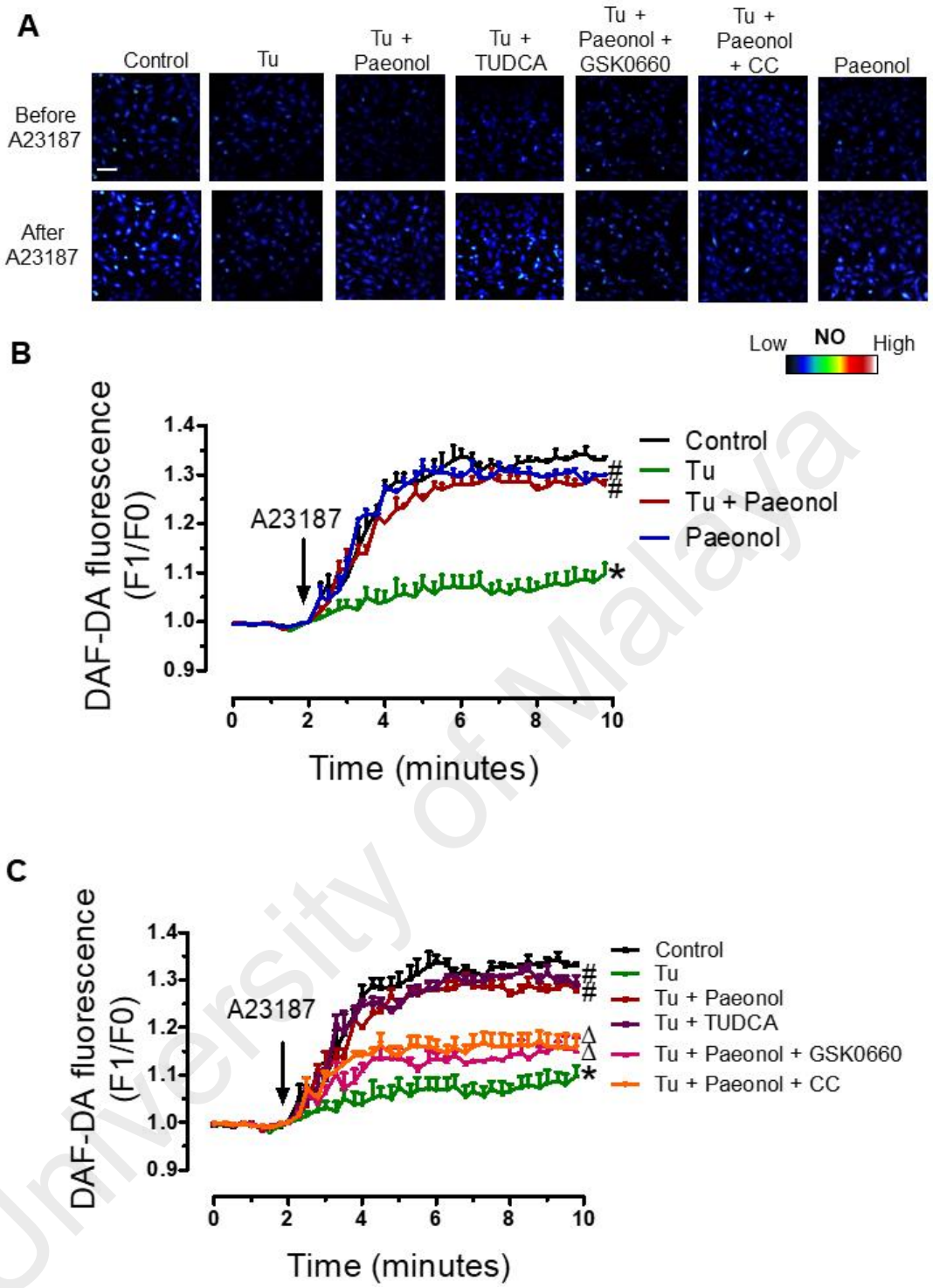

Figure 3.13: Paeonol increased NO bioavailability in endothelial cells. Representative images (A) and summarized results (B & C) of fluorescence imaging of 4-amino-5-methylamino-2',7'-difluorofluorescein (DAF-FM DA) which measures intercellular NO production before and after addition of calcium ionophore A23187 (1 μM) for 10 minutes in HUVEC incubated with tunicamycin (Tu; 0.5 μg/mL), paeonol (0.1 μM), GSK0660 (500 nM), compound C (5 μM) and TUDCA (10 μM) for 16 hours. Results are means ± SEM (n=5-6). *P<0.05 compared with control, # P<0.05 compared with Tu, ΔP< 0.05 compared with Tu plus paeonol.

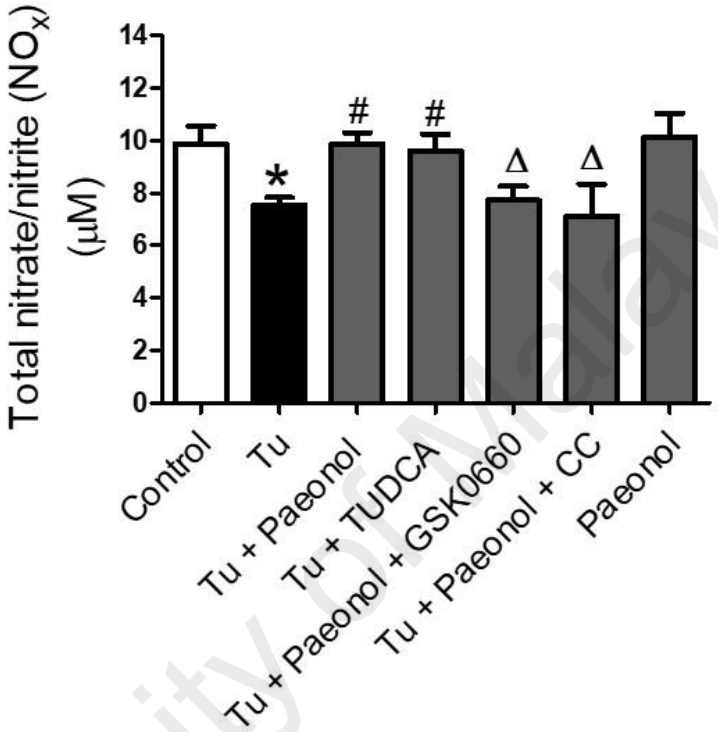

Figure 3.14: Paeonol increased total NO metabolites (nitrite and nitrate) level in HUVECs. Changes in total nitrate and nitrite level in HUVECs cultured with tunicamycin (Tu; 0.5 μg/mL), paeonol (0.1 μM), GSK0660 (500 nM), compound C (5 μM) and TUDCA (10 μM) for 16 hours. Results are means ± SEM (n=5-6). *P< 0.05 compared with control, # P< 0.05 compared with Tu, ΔP< 0.05 compared with Tu plus paeonol.

3.3.7 General parameters: systolic blood pressure and body weight in mice *in vivo*

Chronic treatment with tunicamycin in mice demonstrated a significant increase in systolic blood pressure compared with the control group (125.20 ± 3.01 versus 94.03 ± 3.36 mmHg; $P<0.05$) at the end of two weeks. Increment in blood pressure was significantly alleviated by chronic treatment with paeonol (103.70 ± 6.83 mmHg), TUDCA (103.70 ± 6.19 mmHg) and tempol (98.84 ± 1.53 mmHg) as shown in Figure 3.15A.

Mice treated with tunicamycin for two weeks demonstrated a reduction in body weight, which was prevented following co-treatment with paeonol, TUDCA and tempol (Figure 3.15B). There were no significant changes in both systolic blood pressure and body weight between the paeonol only and control group (Figure 3.15 A and B).

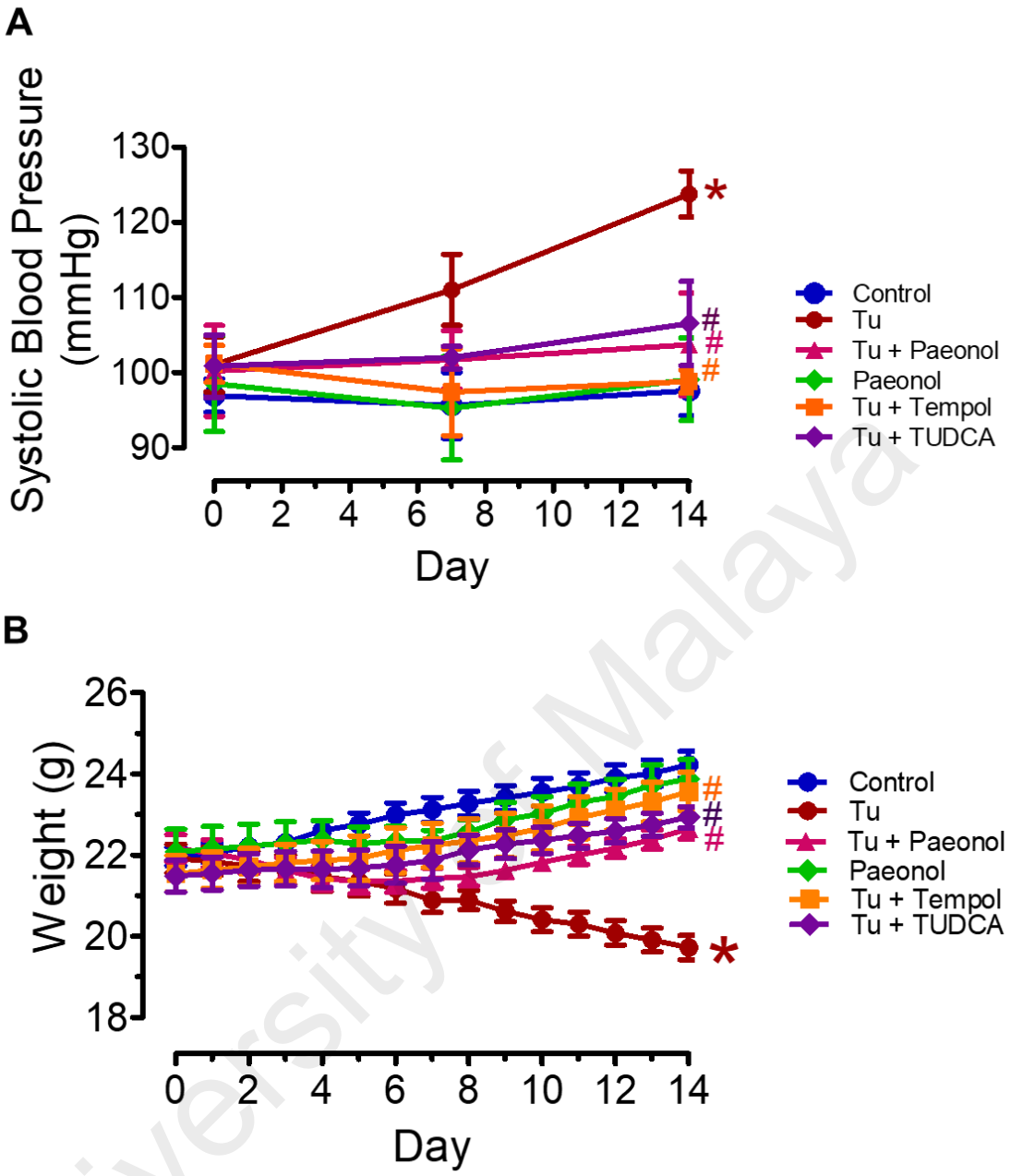

Figure 3.15: (A) Systolic blood pressure and (B) body weight (g) measured in all groups of C57BL/6J mice treated 2 weeks with or without tunicamycin (Tu, 1 mg/kg, 2 injections/week/i.p.), paeonol (20mg/kg/2 weeks/oral gavage), tempol (20 mg/kg/day/oral gavage) or TUDCA (150 mg/kg/day/ip) respectively. Results are means ± SEM of 6-7 separate experiments. *P< 0.05 compared with control, # P< 0.05 compared with tunicamycin.

3.3.8 Chronic treatment with paeonol protects against tunicamycin-induced endothelial dysfunction *in vivo*

To evaluate the effect of chronic treatment with paeonol in ER stress-induced endothelial dysfunction in mice, we examined EDR and endothelium-independent relaxation produced by acetylcholine, UK14304 and SNP in aorta respectively in a concentration dependent manner. Mice exposed with tunicamycin for 2 weeks showed reduction of acetylcholine and UK14304-induced EDR compared to the aorta from the control group. Chronic treatment with paeonol (Figure 3.16A-C & Table 3.2) and TUDCA significantly improved EDR impaired by tunicamycin (Figure 3.16A, D, E & Table 3.2). To identify the involvement of vascular oxidative stress in mice during tunicamycin exposure, the mice was treated chronically with tempol, a superoxide scavenger. Co-treatment with tempol prevented the tunicamycin-induced impairment of relaxations to acetylcholine and UK14304 in mice (Figure 3.16A, D, E & Table 3.2). The EDR of the paeonol only group were similar to the control group (Figure 3.16A-E & Table 3.2). Sodium nitroprusside induced endothelium-independent relaxation were not altered in all treatment groups, suggesting the sensitivity of vascular smooth muscle to NO remained intact (Figure 3.17 & Table 3.2).

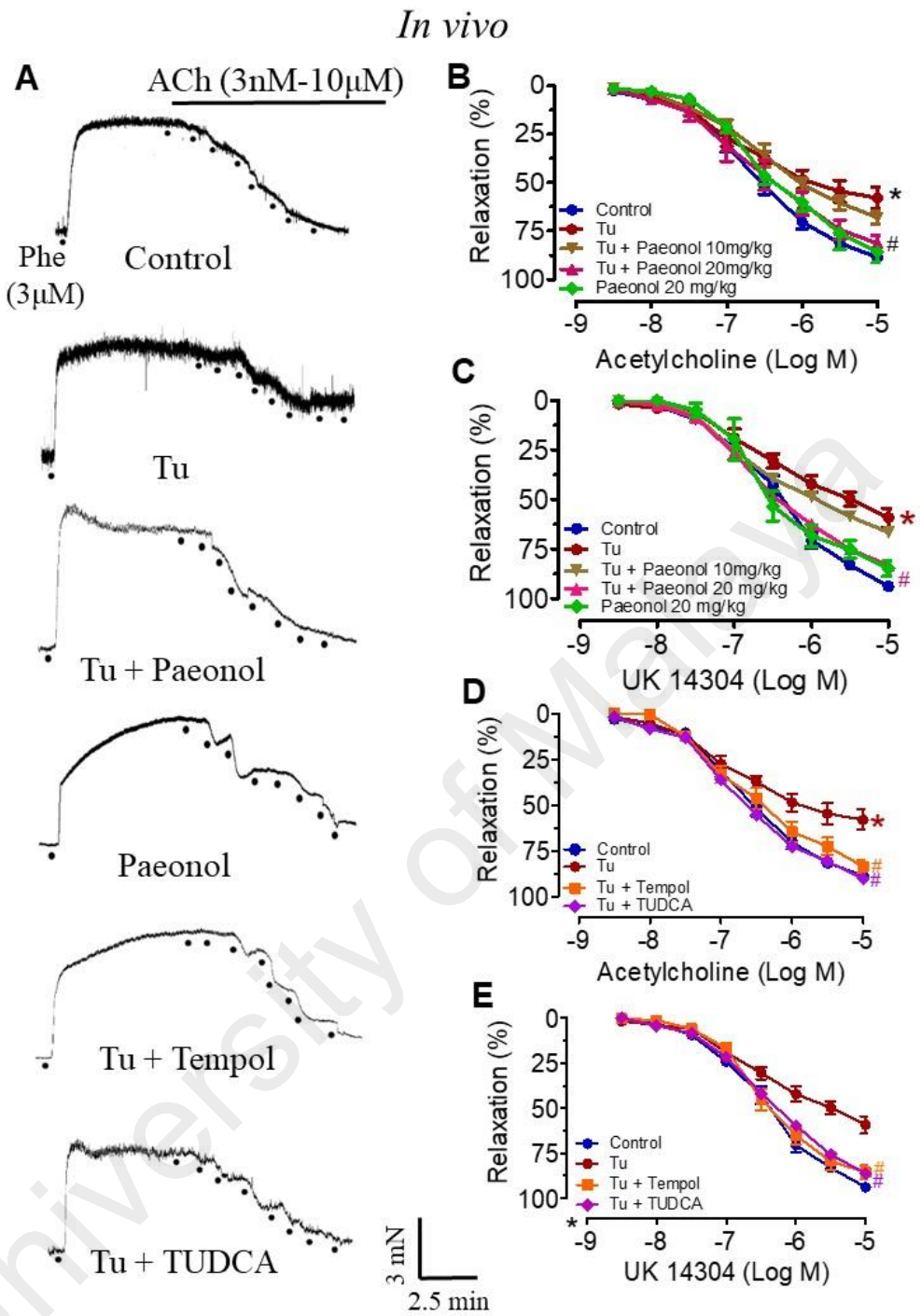

Figure 3.16: Chronic treatment with paeonol reversed endothelial dysfunction induced by tunicamycin for two weeks. (A) Representative traces showing acetylcholine-induced endothelium-dependent relaxation in C57BL/6J mouse aortas precontracted with phenylephrine (Phe). (B-E) Endothelium-dependent relaxations (EDR) induced by acetylcholine or UK14304 of aortae rings in mice exposed to chronic treatment of tunicamycin (Tu, 1 mg/kg, 2 injections/week/i.p.), paeonol (10 or 20 mg/kg/day/oral gavage), tempol (20 mg/kg/day/oral gavage) and TUDCA (150 mg/kg/day/i.p.) for 2 weeks. Results are means ± SEM of seven experiments. * P< 0.05 when compared with control, #P< 0.05 when compared with tunicamycin.

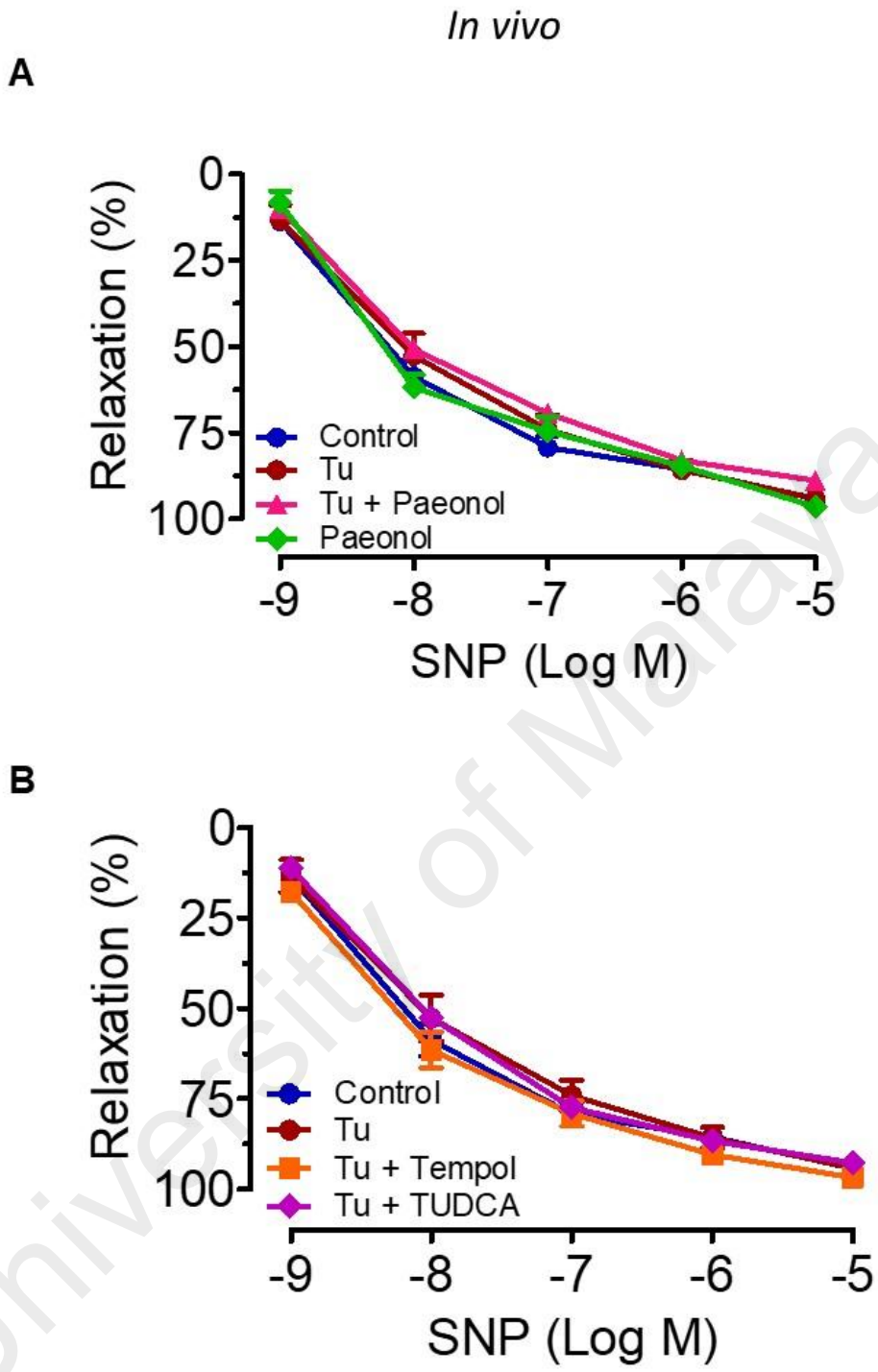

Figure 3.17: Endothelium-independent relaxations induced by sodium nitroprusside (SNP) of aortae rings in mice with or without 2 weeks chronic treatment of tunicamycin (Tu, 1 mg/kg, 2 injections/week/i.p.), paeonol (20 mg/kg/day/oral gavage), tempol (20 mg/kg/day/oral gavage) and TUDCA (150 mg/kg/day/i.p.). Results are means ± SEM of 6-7 experiments.

Table 3.2: Agonist sensitivity (pEC_{50}) and % maximum response (R_{max}) of endothelium-dependent vasodilators, acetylcholine (ACh), UK14304 and endothelium-independent vasodilator sodium nitroprusside (SNP), in isolated aorta from C57BL/6J mice treated with tunicamycin (Tu), paeonol, tempol and TUDCA for 2 weeks. Results are means ± SEM (n=6-7). *P<0.05 compared with control, # P<0.05 vs. tunicamycin.

Groups	ACh		UK14304		SNP	
	pEC_{50} (log M)	R_{max} (%)	pEC_{50} (log M)	R_{max} (%)	pEC_{50} (log M)	R_{max} (%)
Control	6.64 ± 0.07	89.73 ± 1.64	6.42 ± 0.07	93.30 ± 1.95	7.22 ± 0.52	94.30 ± 1.66
Tu	6.87 ± 0.18	55.20 ± 4.29 *	6.44 ± 0.19	60.50 ± 5.40 *	7.30 ± 0.26	94.12 ± 1.93
Tu + Paeonol	6.72 ± 0.18	85.08 ± 1.99 #	6.40 ± 0.12	86.67 ± 2.95 #	7.24 ± 0.52	95.91 ± 2.97
Paeonol	6.47 ± 0.12	90.10 ± 2.16	6.67 ± 0.10	91.24 ± 2.05	7.25 ± 0.43	92.76 ± 2.45
Tu + Tempol	6.72 ± 0.14	84.50 ± 3.49 #	6.50 ± 0.07	87.83 ± 4.22 #	7.39 ± 0.28	96.82 ±0.94
Tu + TUDCA	6.74 ± 0.15	85.75 ± 4.69 #	6.36 ± 0.14	85.05_ 3.92 #	7.40 ± 0.18	96.51 ± 2.22

3.3.9 Chronic treatment with paeonol inhibited ER stress-induced oxidative stress in mouse aorta

Chronic exposure of tunicamycin in mice elevated GRP78 (Figure 3.18A), ATF6 (Figure 3.18B) and phosphorylation of eukaryotic translation initiation factor 2 alpha (eIF2α) (Figure 3.18C) protein. The increase of these proteins were reversed following co-treatment with paeonol and TUDCA. In addition, co-treatment with either paeonol or tempol inhibited the increase of NADPH subunit, NOX2 and nitrotyrosine (marker for peroxynitrate, an index for increased oxidative stress) in mice induced with tunicamycin compared with the control group (Figure 3.18D & 3.18E). The protein presence of ER and oxidative stress markers were similar between the control and the paeonol only groups (Figure 3.18A - E).

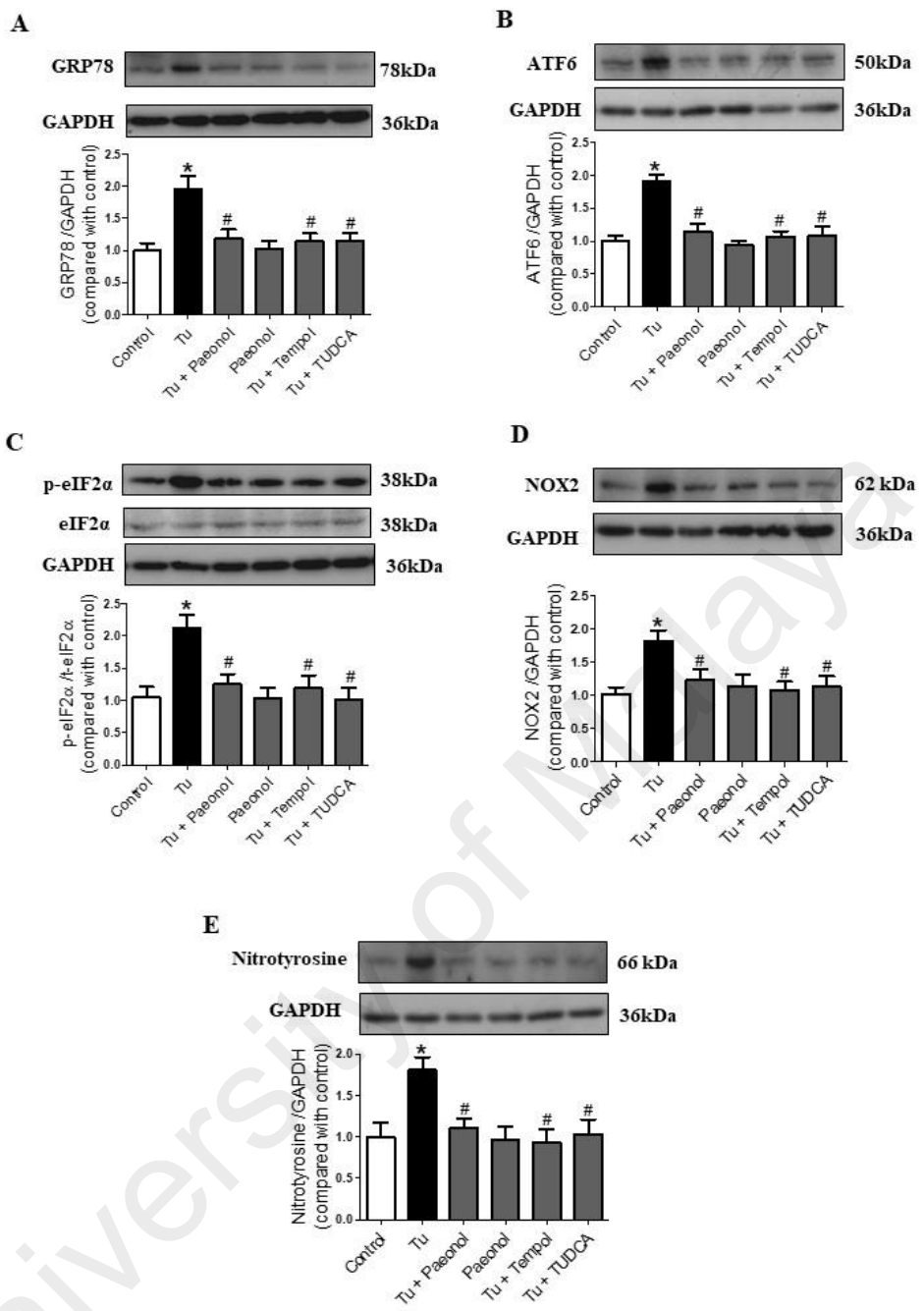

Figure 3.18: Western blot and quantitative data showing the ER stress markers, (A) glucose-regulated protein 78 (GRP78), (B) activating transcription factor-6 (ATF6), (C) phosphorylation of eukaryotic translation initiation factor 2 alpha (eIF2α) and oxidative stress markers, (D) NOX2 and (E) nitrotyrosine in C57BL/6J mice treated with or without tunicamycin (Tu, 1 mg/kg, 2 injections/week/i.p.), paeonol (20 mg/kg/day/oral gavage), tempol (20 mg/kg/day/oral gavage) and TUDCA (150 mg/kg/day/i.p.) for 2 weeks. Results are means ± SEM of 6-7 separate experiments. *P< 0.05 compared with control, # P< 0.05 compared with tunicamycin.

3.3.10 Chronic treatment with paeonol reduced the superoxide production in mouse aorta *in vivo*

Mice treated with tunicamycin for 2 weeks increased the ROS formation in *en face* endothelium and O_2^- level compared to control group as reflected by the intensity of DHE fluorescence staining (Figure 3.19A & B) and LEC (Figure 3.19C) respectively. Co-treatment with paeonol, TUDCA or ROS scavenger, tempol normalized the elevated ROS production in mice treated with tunicamycin (Figure 3.19). The NADPH oxidase inhibitor diphenyleneiodonium (DPI, 10 mM) as a positive control abolished the generation of superoxide anion in all groups (Figure 3.19C).

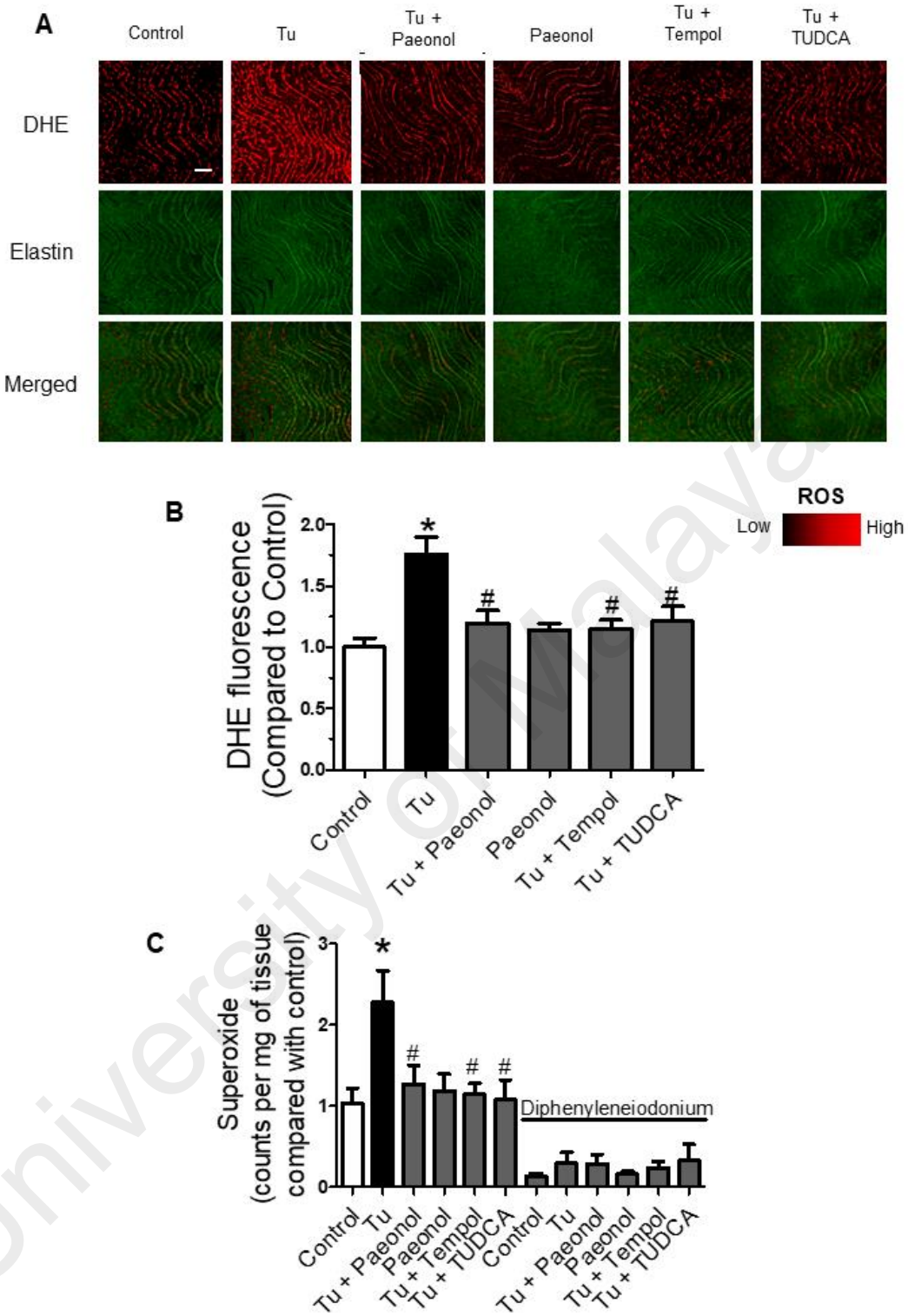

Figure 3.19: Representative images and summarized results of superoxide production measured by (A&B) DHE fluorescence in the *en face* endothelium of aorta and (C) LEC method in the aorta of C57BL/6J mice of all groups. Red: DHE fluorescence (excitation: 515 nm) in the nucleus. Green: autofluorescence of elastin underneath the endothelium (excitation: 488 nm). Lower panel, merged. Bar: 100µm. Results are means + SEM of 6-7 separate experiments. *P< 0.05 compared with control, # P< 0.05 compared with tunicamycin.

3.3.11 Chronic treatment with paeonol enhanced nitric oxide bioavailability in mouse aorta

Chronic exposure to tunicamycin in mice showed a significant decrease in tissue total nitrate/nitrite level compared to the control mice (Figure 3.20A), which was reversed by chronic co-treatment with paeonol, TUDCA and tempol respectively. In addition, chronic paeonol treatment increased phosphorylation of eNOS at Ser^{1176} in aortas which was reduced in tunicamycin treated mice (Figure 3.20B). Similarly, chronic exposure of tempol and TUDCA increased phosphorylation of eNOS at Ser^{1176} compared to mice induced with tunicamycin (Figure 3.20B). There were no significant differences in mice treated with paeonol only and control group (Figure 3.20).

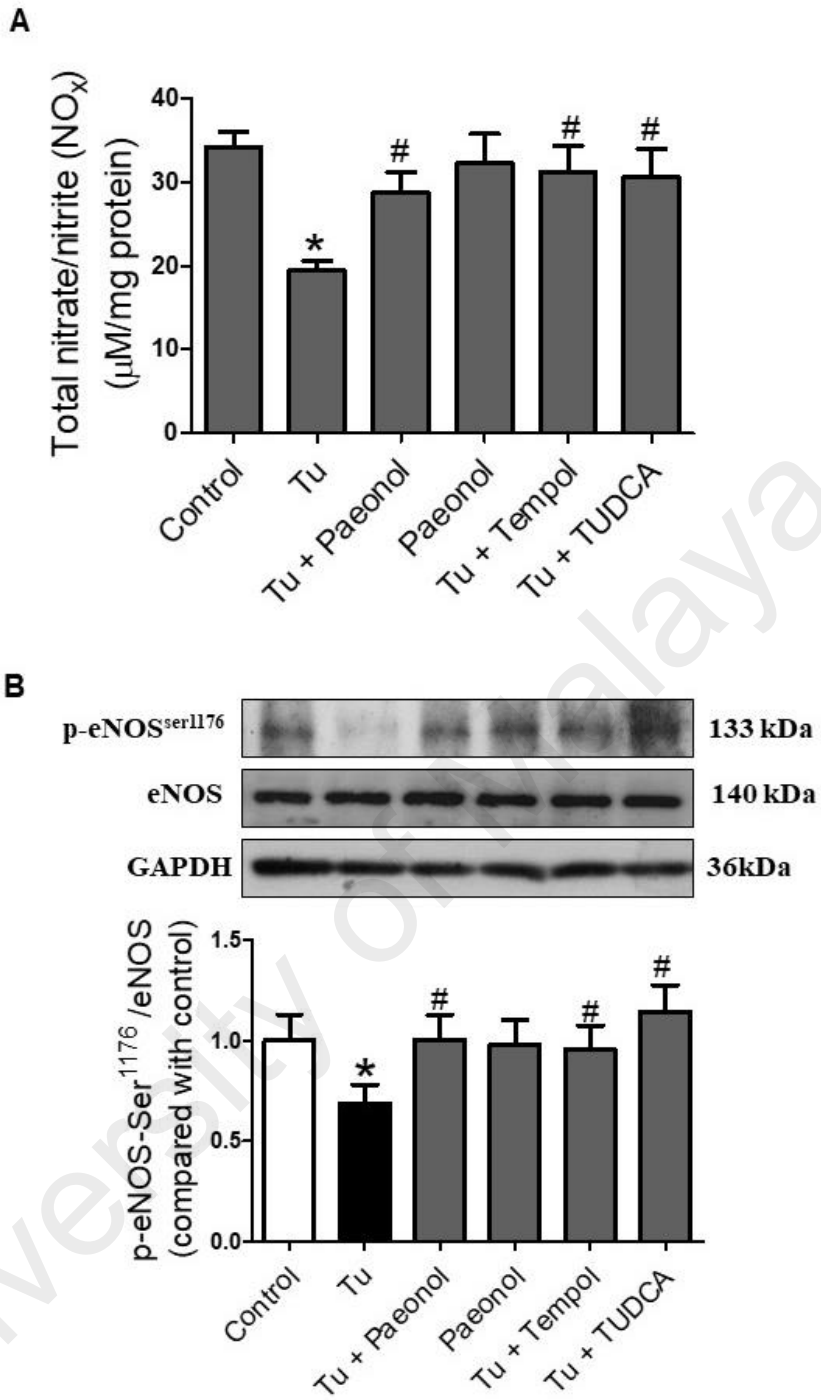

Figure 3.20: Paeonol (20 mg/kg/day/oral), tempol (20 mg/kg/day/oral) and TUDCA (150 mg/kg/day/i.p.) treatment for two weeks increased (A) tissue total nitrite/nitrate level and (B) phosphorylation of eNOS which was reduced in C57BL/6J mice induced with intra-peritoneal injection of tunicamycin (Tu, 1 mg/kg, 2 injections/week for two weeks) as measured by colorimetric assay kit and western blot respectively. Data are expressed as means ± SEM of 6-7 separate experiments. *P< 0.05 compared to control; #P <0.05 compared to mice induced with tunicamycin.

3.4 Discussion

The main findings of this study was paeonol reverse tunicamycin-induced endothelial dysfunction by inhibiting ER stress via activation of AMPK/PPARδ/ROS pathway. The present study demonstrated that acute and chronic treatment with paeonol reversed the deleterious effects of tunicamycin as evident by an improvement of endothelium-dependent relaxations, increased NO production, reduced superoxide production and normalized systolic blood pressure in C57BL/6J and PPARδ WT mouse, respectively. These protective effects of paeonol is inhibited by co-treatment with AMPK inhibitor and PPARδ antagonist and was absent in PPARδ KO mouse aortas, suggesting the involvement of AMPK and PPARδ signalling in attenuating ER stress by paeonol (Yoon *et al.*, 2016). In addition, these beneficial effects of paeonol were comparable to those produced by tempol, indicating that chronic treatment of paeonol inhibited ER stress-mediated oxidative stress pathway. TUDCA, a specific antagonist of ER stress reduced tunicamycin-induced endothelial dysfunction in C57BL/6J and PPARδ mouse via Akt-dependent cellular prion protein and Akt-Manganese-dependent superoxide dismutase pathway, therefore was used as a positive control in this study (Yoon *et al.*, 2016).

There is growing evidence that AMPK is an important regulator of vascular homeostasis (Zou & Wu, 2008). AMPK controls the balance of systemic energy and metabolism, and exerts its protective effects by inhibiting proliferation of vascular smooth muscle cell and elevating NO production (Davis *et al.*, 2006). Activation of AMPK phosphorylated PPARδ and reduced ER stress in high-fat-induced obesity (Cheang *et al.*, 2014) and hypertension (Liu *et al.*, 2015). Activation of PPARδ regulate various pro-inflammatory pathways to suppress atherosclerosis (Barish *et al.*, 2008), function as a versatile regulator of lipid homeostasis (Bojic & Huff, 2013) and protects against cardiac dysfunction and organ inflammation in septic mice (Kapoor *et al.*, 2010). PPARδ also

inhibited palmitate induced-ER stress through initiation of autophagic markers in human cardiac cells (Palomer *et al.*, 2014) and by increasing fatty acid oxidation (Cao *et al.*, 2012). Previously, paeonol has been described to reduce ER stress-induced resistance to doxorubicin in human hepatocellular carcinoma cells (Fan *et al.*, 2013), to reduce neuro-inflammation by activating AMPK-α in microglial cells (Lin *et al.*, 2015) and to activate PPARγ in diabetic rats (Ou *et al.*, 2014). In our study, paeonol improved endothelial function impaired by tunicamycin, and its effect were inhibited by selective AMPK inhibitor, compound C and PPARδ antagonist, GSK0660. These results are in line with the effect of paeonol which increased the tunicamycin-induced downregulation of AMPK phosphorylation and PPARδ protein expression in HUVECs and aortas from C56BL/6J and PPARδ WT mice, proposing that paeonol attenuate ER stress via AMPK/PPARδ pathway. In addition, AMPKα phosphorylation was not affected in the presence of GSK0660 in HUVECs and isolated mouse aortic rings, suggesting that AMPKα phosphorylation is an up-stream event of PPARδ similar to the previously reported literature by Cheang *et al*. (2014).

ER stress triggers an augmentation in oxidative stress in ER lumen by increasing cytosolic Ca^{2+} and maximize ROS production above basal levels (Bhandary *et al.*, 2012). Increased unfolded proteins in the ER stimulates Ca^{2+} leakage into the cytosol and further augment oxidative phosphorylation of the electron transport chain, increase cytochrome c release, impairing electron transfer, altering mitochondrial membrane potential and increasing the generation of ROS (Bhandary *et al.*, 2012; Malhotra & Kaufman, 2007). ROS generation (Kassan *et al.*, 2011) and increased NADPH oxidase activity (Minamino *et al.*, 2010) causes eNOS uncoupling in endothelial cells. AMPK has been shown to reduce ER stress through inhibition of NADPH oxidase-derived ROS (Dong *et al.*, 2010b). Inhibition of AMPK enhances NOX4 and NADPH oxidase activity in epithelial

cells (Eid *et al.*, 2010). Meanwhile, PPARδ agonist reduced superoxide production, NADPH oxidase activity, and mRNA expression of prepro-endothelin-1, phox22, phox47, and NOX-1 which eventually improved endothelial dysfunction in type 1 diabetic rats (Quintela *et al.*, 2012). Current finding demonstrates that acute treatment of paeonol relieved the ROS induced by tunicamycin by activating the AMPK and PPAR signalling pathway. The protective effects of paeonol was blocked by compound C and GSK0660 in HUVECS and in aortas from C57BL/6J and PPARδ WT mice, but not in those from PPARδ KO mice, which further supports that paeonol inhibits ER stress-induced ROS via AMPK/PPARδ activation. In addition, ER stress inhibitor, TUDCA reduced tunicamycin-mediated superoxide generation further supports the relationship between ER stress and its downstream activation of oxidative stress. During ER stress, NADPH oxidase (NOX) family, especially NOX2 increased ROS production and was reported to involve in blood pressure regulation (Montezano & Touyz, 2012) and augmentation of pro-apoptotic signalling (Laurindo *et al.*, 2014). Silencing of NOX2 has been demonstrated to suppress two atherosclerosis-relevant inducers of ER stress, cholesterol loading and 7-ketocholesterol in macrophages, indicating that NOX2 plays an important role in the oxidative stress and apoptotic responses of macrophages subjected to ER stress (Li *et al.*, 2010a). In our study, chronic treatment with paeonol inhibited the tunicamycin-induced vascular expression of NOX2 and nitrotyrosine, a marker for peroxynitrite in a similar manner to tempol, a free radical scavenger. The alleviation of ROS following paeonol treatment was accompanied with increased bioavailability of NO.

ER stress has a negative impact on endothelium-dependent relaxation in large and small arteries (Kassan *et al.*, 2012; Spitler *et al.*, 2013). ER stress increases the contractility of vascular smooth muscle in hypertension (Liang *et al.*, 2013a), activates caspase-12 and triggers apoptosis (Xie *et al.*, 2002), increases inflammatory signalling

(Hotamisligil, 2010), reduces eNOS phosphorylation (Galan *et al.*, 2014) and subsequently leads to endothelial dysfunction (Galan *et al.*, 2014). ER stress causes an increase in ROS generation via activation of NF-κβ and transforming growth factor beta 1 which results in vascular dysfunction and hypertension (Santos *et al.*, 2014). PPARδ agonists GW1516 elevated eNOS activity and NO production in endothelial cells (Tian *et al.*, 2012a). Paeonol reversed the tunicamycin-induced reduction of eNOS phosphorylation in only PPARδ WT mouse aortas, suggesting that the improved endothelial function by paeonol is attributable to increase NO bioavailability via PPARδ activation. In *p47phox−/−* mice, tunicamycin did not show impairment of EDR to acetylcholine in mouse aorta compared to wild type control mice which indicate that ER stress is associated with enhanced NADPH oxidase-ROS activity (Galan *et al.*, 2014). During UPR, disulfide bond formation dysregulation leads to ROS accumulation and induced oxidative stress (Cao & Kaufman, 2014). Some UPR components such as CHOP causes apoptosis, release ROS and impairs the endothelium (Wang & Kaufman, 2012). Our results showed that acute and chronic exposure of tunicamycin causes endothelial dysfunction and increased ER stress proteins in isolated C57BL/6J and PPARδ WT mouse aortas, which were reversed by paeonol and tempol independently. These effects of paeonol was inhibited by compound C and GSK0660 in C57BL/6J mice and abolished in PPARδ KO mouse aortas. These indicate that paeonol improves EDRs probably through activation of AMPK and PPARδ which leads to inhibition of ER stress-mediated ROS.

Prolonged ER stress will lead to advanced lesional macrophage death, plaque necrosis and increases contractility of vascular smooth muscle contributing to increase blood pressure (Liang *et al.*, 2013a; Scull & Tabas, 2011). Previous study reported that ER stress may increase blood pressure by increasing cardiac output and peripheral vascular

resistance (Liang *et al.*, 2013a). In addition, ER stress has been reported to be associated with hypertensive patients (Xu *et al.*, 2009), animals with metabolic syndrome (Galan *et al.*, 2012), high salt intake-induced hypertensive rats (Isodono *et al.*, 2010) and angiotensin II-induced hypertensive mice (Kassan *et al.*, 2012). Recent literature have shown that ER stress inhibitor, TUDCA reduced blood pressure and improved vascular activity in spontaneously hypertensive rats (SHRs) through inhibition of ER stress (Choi *et al.*, 2016), suggesting that ER stress is involved in hypertension. Besides, oxidative stress contributes to the development of hypertension (Baradaran *et al.*, 2014; Taniyama & Griendling, 2003). ROS causes vascular cell inflammation and apoptosis as well as extracellular matrix alterations (Dornas *et al.*, 2017; Mihalj *et al.*, 2016). Inhibition of ER stress in hypertension improved macrovascular endothelial function by transforming growth factor-β1 (TGF-β1)-dependent mechanism and microvascular endothelial function by an oxidative stress-dependent mechanism (Kassan *et al.*, 2012). Similarly, our results demonstrated that mice exposed to tunicamycin showed elevated blood pressure and reduction in body weight (Kassan *et al.*, 2011; Liang *et al.*, 2013a). Chronic treatment of paeonol normalised the blood pressure and body weight comparable to those produced by ER stress inhibitor (TUDCA) and antioxidant (tempol) or both, suggesting that paeonol may work by inhibiting ER stress-mediated oxidative stress pathway (Brozovic *et al.*, 2013; Zuo *et al.*, 2015).

3.5 Conclusion

In summary, the current study shows that paeonol improves EDR through activation of AMPK and PPARδ pathway; the latter alleviates ER stress, reduced ROS overproduction, increased phosphorylation of eNOS and normalized the blood pressure (Figure 3.21). Our finding further suggests a therapeutic potential of paeonol to protect vascular function in ER stress-related cardiovascular diseases such as hypertension.

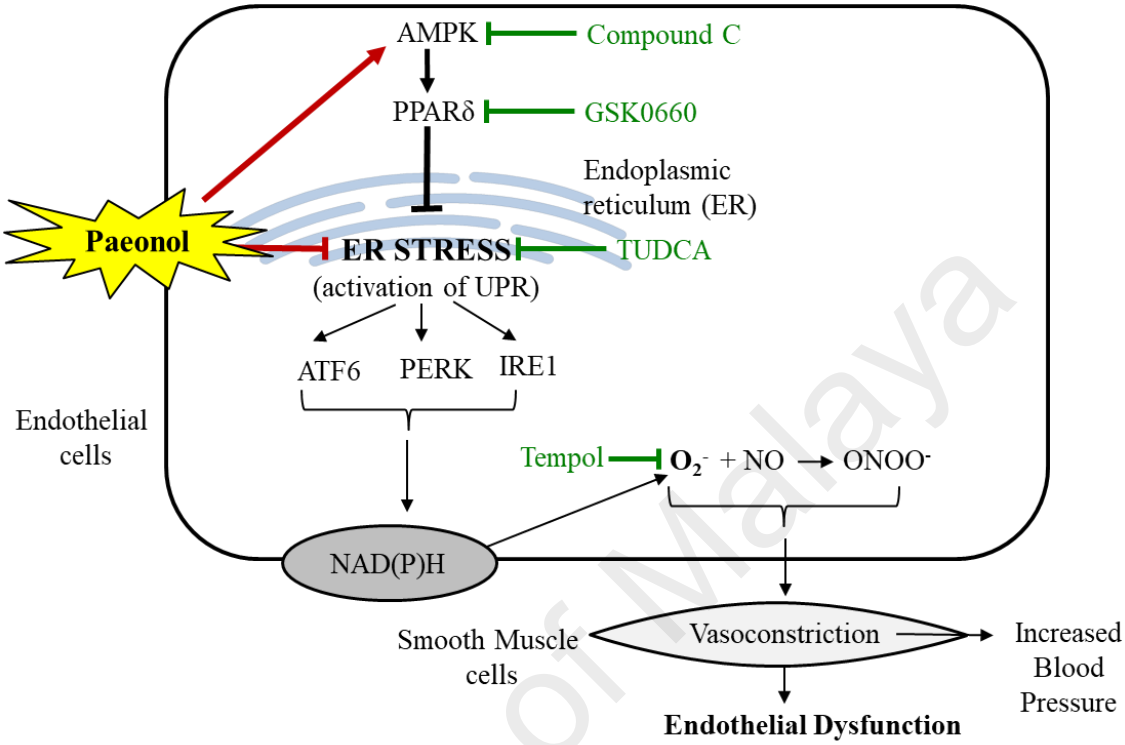

Figure 3.21: Schematic diagram showing paeonol treatment alleviates endoplasmic reticulum (ER) stress, inhibits reactive oxygen species (ROS) production and improves NO bioavailability via AMPK/PPARδ signalling. Subsequently, it reverses the endothelial dysfunction and normalized blood pressure in mice. AMPK, 5' AMP-activated protein kinase; PPARδ, Peroxisome proliferator-activated receptors delta; ER, endoplasmic reticulum; ATF6, activating transcription factor 6; PERK, PKR-like eukaryotic initiation factor 2 kinase; IRE1, inositol-requiring enzyme-1; O^{2-}, superoxide; NO, nitric oxide; $ONOO^-$, peroxynitrite; NOS; NADPH, Nicotinamide adenine dinucleotide phosphate.

CHAPTER 4: EFFECTS OF PAEONOL IN INFLAMMATION-INDUCED ENDOTHELIAL DYSFUNCTION

4.1 Introduction

When the vasculature is exposed to injury, lipid peroxidation and infection, a sequential of pro-inflammatory cascades is activated (Willerson & Ridker, 2004). Endotoxaemia is a systemic response to infection characterised by inflammation and microvascular leakage leading to widespread hypotension and cardiovascular collapse (Staehr *et al.*, 2011). A key mediator of these phenomena is the excessive generation of NO by iNOS, triggered by endotoxin such as LPS (McNeill *et al.*, 2015). LPS bind to TLR4, stimulate intracellular signalling pathways that alter the cytoskeletal architecture of the endothelial cells and eventually disrupt the endothelial barrier (Bannerman & Goldblum, 1999; Cuschleri *et al.*, 2003). The low grade chronic inflammation present within the vessel wall transiently increased the risk of cardiovascular diseases, including carotid artery disease and atherosclerosis (Aljada, 2003; Virdis & Schiffrin, 2003).

LPS induces severe microvascular injury and endothelial cells detachment, subsequently leading to apoptosis (Bannerman & Goldblum, 2003). Apoptosis contributes to a diversity of pathological processes including tissue injury and its attendant complications such as disseminated intravascular coagulation, systemic vascular collapse, multiorgan failure, vascular leaks or acute respiratory distress (Kockx, 1998). The main enzyme associated with the pathogenesis of cell apoptosis is activation of caspase-3 (Sugawara *et al.*, 2004). Subsequently, it leads to endothelial dysfunction, a condition defined as incapability of arteries and arterioles to dilate fully when triggered by vasodilator stimuli such as acetylcholine or shear stress (Cai & Harrison, 2000). LPS-

stimulation of iNOS also leads to impairment of endothelium-dependant vasodilatation (Chauhan *et al.*, 2003).

BMP4, a proinflammatory protein was reported to enhance leukocyte adhesion to the endothelial surface *in vitro* (Csiszar *et al.*, 2006). BMP4 impairs endothelial function in the mouse aorta via oxidative stress signalling pathway by generation of NADPH subunits (Csiszar *et al.*, 2007; Miriyala *et al.*, 2006). BMP4 induces endothelial cells apoptosis by binding to type I receptors called BMPR1A-receptors which triggers SMAD-independent pathways, leading to oxidative stress-dependent p38 MAPK and JNK pathway (Tian *et al.*, 2012c).

Paeonol reduced LPS-induced lung inflammation and fibrosis in mice and rats (Li *et al.*, 2012; Liu *et al.*, 2014a). Similarly, paeonol reduced inflammation and injury triggered by LPS in N9 microglia cells and in murine kidneys by inhibiting the TLR4 and nuclear factor κB (NF-κB) signalling pathways both *in vitro* and *in vivo* (Fan *et al.*, 2016; Tseng *et al.*, 2012). However, the effect of paeonol on inflammation-mediated apoptosis and endothelial dysfunction, as well as its effects on LPS/TLR4 and BMP4 signalling pathways are yet to be fully elucidated. Therefore, the objectives of the study is to explore the endothelial protective effect of paeonol and identify the involvement of BMP4 as possible pharmacological target of paeonol in LPS-induced endothelial cell apoptosis and endothelial dysfunction in HUVECs, isolated mouse aorta and *in vivo*.

4.2 Methods

4.2.1 Human endothelial cell culture

HUVECs (*ScienCell, Corte Del Cedro* Carlsbad, CA, USA) were cultured in endothelial cell medium (ECM) composed of 5% fetal bovine serum, 1% penicillin-streptomycin and 1% endothelial cell growth supplement at 37 °C with 5% CO_2 and 95%

O_2. HUVECs from passage four to six were used. For all experiments, HUVECs were seeded and grown overnight to sub-confluence before incubation (24 hours), in ECM, with LPS (0.1, 0.5 and 1 μg/mL), H_2O_2 (200 μM) and various concentrations of paeonol (0.01, 0.1 and 1 μM,) before collection for apoptosis and protein assays. For other drug treatments, HUVECs were co-treated with one of the following: recombinant BMP4 (100 ng/mL, dissolved in 4 mM HCl with 0.1% BSA), noggin (BMP4 antagonist, 100 ng/mL), apocynin (NADPH oxidase inhibitor, 20 μM), SP600125 (JNK inhibitor, 10 μM), SB202190 (p38 MAPK inhibitor, 10 μM), aminoguanidine (selective inhibitor of iNOS, 100 μM) and TAK242 (TLR4 inhibitor, 1 μM) for 24 hours.

4.2.2 Flow cytometry quantification of apoptosis

Annexin V-FITC apoptosis assay were performed according to manufacturer's instructions (BD Biosciences, San Jose, CA, USA) to evaluate the percentage of apoptotic cells. In brief, HUVECs were seeded in six-well plates and were treated with various concentrations of either LPS (0.1, 0.5 and 1 μg/mL) or H_2O_2 (200 μM; serving as a positive control) together with paeonol (0.01, 0.1 and 1 μM). After 24 hours, the cells were trypsinized, washed and re-suspended in 1 mL of binding buffer (1×10^6 cells/mL). Then, 1×10^5 cells were stained with propidium iodide (PI) and Annexin-V FITC, incubated for 15 minutes in the dark at room temperature and analysed with a FACSort flow cytometer (BD Biosciences). Results were analysed with the Cell Quest Pro software (BD Biosciences). The amount of apoptosis was determined as the percentage of annexin V-positive cells over PI-negative cells (Bao *et al.*, 2013).

4.2.3 Measurement of mitochondrial membrane potential

Mitochondrial depolarization is an early event in the apoptosis cascade. The changes in mitochondrial membrane potential (MMP) were determined using potential-sensitive

JC-1 (5, 5', 6, 6'-tetrachloro-1,1',3,3'- tetraethyl benzimidazolylcarbocianine iodide) cationic dye (Molecular probes), which displays potential-dependent accumulation in mitochondria. JC-1 monomers assemble into J-aggregates with red fluorescence (emission 590 nm) in healthy cells with high MMP (metabolically active mitochondria with polarized inner membranes), whereas JC-1 non-specifically accumulates in the cytosol as a green fluorescent monomer (emission 525 nm) in apoptotic cells with low MMP. HUVECs were seeded in 12 well plates and were treated with LPS (0.1, 0.5 and 1 μg/mL) or paeonol (0.01, 0.1 and 1 μM) for 24 hours. Then, the cells were washed twice with NPSS and loaded with JC1 (5 μg/mL) for 15 min at 37◦C in the dark. The cell images were analysed by confocal microscope FluoView FV10-ASW software (Olympus). The changes in MMP was expressed as the red/green JC-1 fluorescence intensity of ratio.

4.2.4 Transient transfection with small interfering ribonucleic acid (siRNA)

HUVECs were seeded into six-well plates at 2 x 10^4 per well and were grown overnight. The amount of siRNA was optimized following the manufacturer's instructions. The siRNA targeting TLR4 or BMP4 (ON-TARGETplus SMART pool small interfering RNA; Dharmacon, Thermo Scientific, Lafayette, CO) or scrambled siRNA (ON-TARGETplus Control Nontargeting pool; Dharmacon) were transfected into the cells using Dharmafect 1 transfection reagent (Dharmacon). The specific siRNA-concentration (5, 25, 50 nM) and time duration (24, 48 and 72 hours) resulting in more than 60% knockdown in protein levels compared to control siRNAs and scrambled siRNAs as determined by Western blotting were chosen. The media were refreshed post-transfection with BMP4 siRNAs or TLR4 siRNAs and treated with vehicle, LPS (1 μg/mL) or paeonol (1 μM) for 24 hours before being harvested for Western blotting.

4.2.5 Animals

C57BL/6J male mice were obtained from Monash University (Sunway Campus, Selangor, Malaysia) and housed in well ventilated room at a constant temperature of 23 ºC with a 12 hours light/dark cycle. They were fed with normal mice chow (Specialty Feeds Pty Ltd., Glen Forrest, Australia) and tap water *ad libitum.* All of the experiments were conducted according to the Guide for the Care and Use of Laboratory Animals as approved by University of Malaya Animal Care and Ethics Committee (Ethics reference no: 2016-170531/PHAR/R/MRM).

4.2.5.1 Induction of inflammation in mice *in vivo*

Twelve weeks-old mice were randomly assigned into six groups receiving: (a) vehicle [phosphate buffered saline, PBS, intraperitoneal injection] only (control); (b) an intraperitoneal injection of LPS (15 mg/kg) and vehicle (saline, 100 µL by oral gavage) (LPS); (c) LPS plus oral administration of paeonol (20 mg/kg) (LPS+ paeonol); (d) oral administration of paeonol (20 mg/kg) (Paeonol); (e) LPS plus intraperitoneal injections of noggin (0.5 mg/kg/day; BMP4 antagonist) one hour before and two, four and six hours after the LPS injection (LPS + Noggin); (6) LPS plus an intraperitoneal injection of TAK242 (3 mg/kg; TLR4 antagonist) one hour before the LPS injection (LPS + TAK242). The doses of LPS and paeonol were determined from the literature (Hsieh *et al.*, 2006; Lee *et al.*, 2013; Shi *et al.*, 2016) and our preliminary which showed that 20 mg/kg paeonol improved relaxations to the endothelium-dependent vasodilator acetylcholine in mice treated with LPS (15 mg/kg) (Figure 4.24). The animals were humanely sacrificed by CO_2 inhalation at the end of the 24 hours of treatment and blood samples were collected. Blood samples was allowed to clot at room temperature, and then centrifuged at 1 000 x g for 15 min to obtain the serum for NO and ELISA assay. Then, mouse aorta was isolated immediately for functional studies and Western blotting.

4.2.5.2 Organ culture of isolated aortae

The isolated aortae rings from C57BL/6J mouse were cultured in Dulbecco's Modified Eagle Medium (DMEM; Gibco, Gaithersburg, MD, USA) supplemented with 10% FBS (Gibco), containing 100 U/mL penicillin and 100 μg/mL streptomycin (Gibco) in incubator with atmosphere of 5% CO_2 and 37°C. The rings were incubated with or without LPS (1 μg/mL), paeonol (1 μM), recombinant BMP4 (100 ng/mL), noggin (100 ng/mL), SP600125 (10 μM), SB202190 (10 μM), apocynin (20 μM), aminoguanidine (100μM), TAK242 (1 μM) and indomethacin (10 μM, non-selective COX inhibitor) for 24 hours and thereafter transferred to wire myographs for functional examination.

4.2.5.3 Functional Studies

The aortae were excised, cleaned of adjacent connective tissues and were cut into several ring segments approximately 2mm in length. The rings were suspended in a Multi-Wire Myograph System (Danish Myo Technology, Aarhus, Denmark) and bathed in oxygenated modified Krebs physiological salt solution (pH 7.4) of the following composition (in mM): NaCl 119, $NaHCO_3$ 25, KCl 4.7, KH_2PO_4 1.2, $MgSO_4.7H_2O$ 1.2, glucose 11.7 and $CaCl_2.2H_2O$ 2.5. All rings were stretched to an optimal baseline tension of 3 mN and maintained at 37 °C with continuous oxygenation with 95% O_2 and 5% CO_2. After equilibration for 30 minutes, the rings were contracted with 60 mM KCl to prime the tissues until an equal contractions were attained. The rings were washed three times in Krebs solution and then contracted with Phe (1 μM, α-adrenergic agonist) to establish a stable tension. The presence of functional endothelium in pre-contracted aortic rings was confirmed by a relaxant response to acetylcholine (10 mM). Thereafter, cumulative concentration-relaxation curves were obtained for both endothelium-dependent relaxation with acetylcholine (3nM to 10 μM) and UK14304 (3nM to 10 μM) as well as endothelium-independent relaxation with SNP (1nM to 10 μM). Changes in isometric

tension were recorded with a PowerLab LabChart 6.0 recording system (AD Instruments, Bella Vista, NSW, Australia).

4.2.6 Western blotting

HUVECs and aortae were homogenized and lysed in ice-cold radioimmunoprecipitation assay (RIPA) buffer containing leupeptin 1 μg/mL, aprotinin 5 μg/mL, PMSF 100 μg/mL, sodium orthovanadate 1 mM, EGTA 1 mM, EDTA 1 mM, NaF 1 mM, and β-glycerolphosphate 2 mg/mL (Sigma Aldrich; St.Louis, MO, USA). The lysates were then centrifuged at 15,000 X g for 30 minutes at 4°C to collect supernatants. Protein concentrations of the supernatant were determined by a modified Lowry assay (Bio-Rad Laboratories, Hercules, CA, USA). Samples of protein (15 μg) loaded on 7.5 or 15% SDS polyacrylamide gels and transferred to an immobilon- PVDF membrane (Millipore, Billerica, MA, USA) at 100 V. The non-specific binding was blocked with 3% BSA in Tris-buffered saline containing 0.1% Tween-20 (TBS-T) for one hour at room temperature with gentle shaking. After washing in TBS-T, the blots were incubated with primary antibodies against phospho-p38 MAPK/ p38 MAPK (1:1000, Cell signaling Technology, Beverly, MA, USA), phospho-JNK/JNK, (1:1000, Cell signaling Technology, Beverly, MA, USA), caspase-3 (1:1000, Abcam, Cambridge, UK), NOX 2 (1:1000, Abcam, Cambridge, UK), TLR4 (1:1000, Abcam, Cambridge, UK), iNOS (1:1000, Abcam, Cambridge, UK), cleaved caspase-3 (1:500, Cell signaling Technology), BMPR1A (Santa Cruz, Dallas, Texas, USA), housekeeping GAPDH (1:10000, Santa Cruz), nitrotyrosine (1:500, Abcam), BMP4 (1:500, Sigma), phosphorylated eNOS at Ser^{1177} (p-eNOS-Ser^{1177}; 1:500, Cell Signaling Technology) and eNOS (1:1000, BD Transduction Laboratory, Oxford, UK) overnight at 4 °C. The next day, the membranes were washed three times in TBS-T and incubated with appropriate secondary antibodies conjugated to horseradish peroxidase for two hours at room temperature. The membranes

were developed with enhanced chemiluminescence (ECL) plus Western blotting detection system (Amersham, Buckinghamshire, UK). The densitometric analysis was performed using Quantity One 1D analysis software (Bio-rad). The protein levels were normalized to the housekeeping protein GAPDH and expressed relative to control.

4.2.7 Vascular superoxide anion production

To measure vascular superoxide anion formation at *en face* endothelium in mouse aortas, DHE (D1168, Invitrogen, Carlsbad, USA) fluorescence staining was performed by confocal microscopy. The aortic rings were incubated with 5 µM DHE (Molecular Probes, Eugene, OR, USA) in normal physiological solution (NPSS, composition in mM: NaCl 140, KCl 5, $CaCl_2$ 1, $MgCl_2$ 1, glucose 10 and HEPES 5) for 15 minutes at 37 °C. The aortae rings were then washed twice in PBS, cut open and were placed upside down between two coverslips on the microscope. Fluorescence intensity was measured with a confocal microscope [Leica TCS SP5 II (Leica Microsystems, Mannheim, Germany)] with 515 nm excitation and 585 nm long pass filters. Background autofluorescence of elastin was measured at excitation 488 nm and emission 520 nm separately to avoid overlapping of the emission spectra. DHE fluorescence intensity was evaluated with Leica LAS-AF software (version 2.6.0.7266) and was represented as fold changes in fluorescence intensity relative to control.

Other than DHE staining, the amount of superoxide anions at aortae rings was quantified using the LEC method (Choy *et al.*, 2017). The aortic rings from each groups were pre-incubated for 45 min at 37 °C in Krebs-HEPES buffer (in mM: NaCl 99, $NaHCO_3$ 25, KCl 4.7, KH_2PO_4 1, $MgSO_4$ 1.2, glucose 11, $CaCl_2$ 2.5 and Na-HEPES 20) in the presence of DETCA (1 mM) to inactivate superoxide dismutase (SOD) and β-NADPH (0.1 mM) as a substrate for NADPH oxidase. The inhibitor of NADPH oxidase; diphenylene iodonium (DPI; 5 mM) was used as a positive control. Then, the rings were

transferred to a 96-well Optiplate containing lucigenin (5 mM, Sigma Aldrich) and β-NADPH (0.1 mM, Sigma Aldrich) in 300 ml of Krebs-HEPES buffer per well and the signal was read with Hidex plate CHAMELEONTM V (SisLab, Turku, Finland) in luminescent detection mode for repetitive measurements of photo emission at 30 seconds intervals over 20 minutes. Upon completion of the measurements, the rings were dried during 48 hours at 65 °C and weighed. The data are expressed as average counts per mg of vessel dry weight.

4.2.8 Determination of NO level

NO level was determined by measuring its stable metabolites nitrite and nitrate in the mouse serum using Nitrate/Nitrite Colorimetric Assay Kit (Cayman Chemical Company, Ann Arbor, MI, USA) as described by manufacturer protocol. Typically, a nitrate standard solution was serially diluted and duplicated in a 96-well, flat-bottomed, polystyrene microtiter plate. The plate was rapidly loaded with sample to each well and followed by the addition of the Griess reagents. Absorbance was measured at 540 nm using Hidex plate CHAMELEON™ V (Turku, Finland) and NO production was determined by comparison with a sodium nitrite standard curve. Results were expressed in μM.

4.2.9 Measurement of IL-6 and TNFα cytokines

The circulating TNFα and IL-6 cytokines levels in the mouse serum were determined by enzyme-linked immunosorbent assay (ELISA) assay, using cytokine-specific mouse monoclonal antibodies and recombinant mouse cytokines purchased from Elabscience (Houston, Texas) according to the manufacturers' instructions. The ELISA plates provided in the kits had been pre-coated with an antibody specific to IL-6/TNF-α. Standards or samples are then added to the appropriate micro ELISA plate wells and

combined to the specific antibody for 90 minutes at 37°C. Then a biotinylated detection antibody working solution specific for IL-6/TNF-α was added to each micro plate well and incubated for 1 hour. Solution was aspirated and wash for three times. Then, horseradish peroxidase (HRP) conjugate working solution was added before adding substrate reagent and stop solution independently. The optical density (OD) was measured spectrophotometrically at a wavelength of 450 nm using Hidex plate CHAMELEONTM V (SisLab, Turku, Finland). The OD value was proportional to the concentration of IL-6 and TNF-α. The calculation of concentrations of IL-6/TNF-α in the samples was done by comparing the OD value of the samples to the standard curve.

4.2.10 Statistical analysis

Results are shown as means ± SEM; *n* reflects the number of individual experiments. Concentration-response data were fitted to a sigmoidal curve using non-linear regression with a statistical software [GraphPad Prism version 4 (GraphPad Software Inc., San Diego, CA, USA)]. Statistical significance was determined using Student's *t*-test for unpaired observations and, for multiple value comparison, one-way analysis of variance (ANOVA) for groups with one independent variable and two way ANOVA for groups that has two independent variable followed by Bonferroni's multiple comparison test were carried out. A value of P less than 0.05 was considered to indicate statistically significant differences.

4.3 Results

4.3.1 Paeonol inhibited LPS-induced apoptosis and depolarization of MMP

Annexin V/PI flow cytometry and JC-1 staining analysis were performed to investigate the inhibitory effects of paeonol on LPS-induced cell apoptosis and decreased MMP. LPS (0.1, 0.5 & 1 μg/mL) increased the percentage of apoptosis (Figure 4.1A & B), augmented

the presence of cleaved caspase 3 protein (Figure 4.1C) and decreased the MMP (Figure 4.2) in a concentration-dependent manner compared with control, with 1 μg/mL LPS being the optimal concentration to induce apoptosis in HUVECs. In HUVECs exposed to LPS (1 μg/mL), co-treatment with paeonol (0.01, 0.1, 1 μM) reduced apoptosis (Figure 4.3) and restored MMP (Figure 4.2) in a concentration-dependent manner, with 1 μM exerting the most significant effect. Therefore, paeonol at 1 μM was chosen for subsequent experiments. However, paeonol (1 μM) did not reduce apoptosis induced by H_2O_2 (200 μM), which served as oxidative stress inducer and a positive control (Figure 4.3). The effects of paeonol (1 μM) alone is similar to the control.

To further confirm the inhibitory effects of paeonol on LPS-induced cell apoptosis, Western blotting was performed. LPS (1 μg/mL) increased the protein levels of cleaved caspase 3, which was reversed in a concentration-dependant manner when co-treated with paeonol (0.001, 0.1, 1 μM) (Figure 4.4A). Paeonol (0.001, 0.1, 1 μM) also reduced LPS-induced BMP4 (Figure 4.4B) and TLR4 (Figure 4.4C) protein level in a concentration-dependant manner.

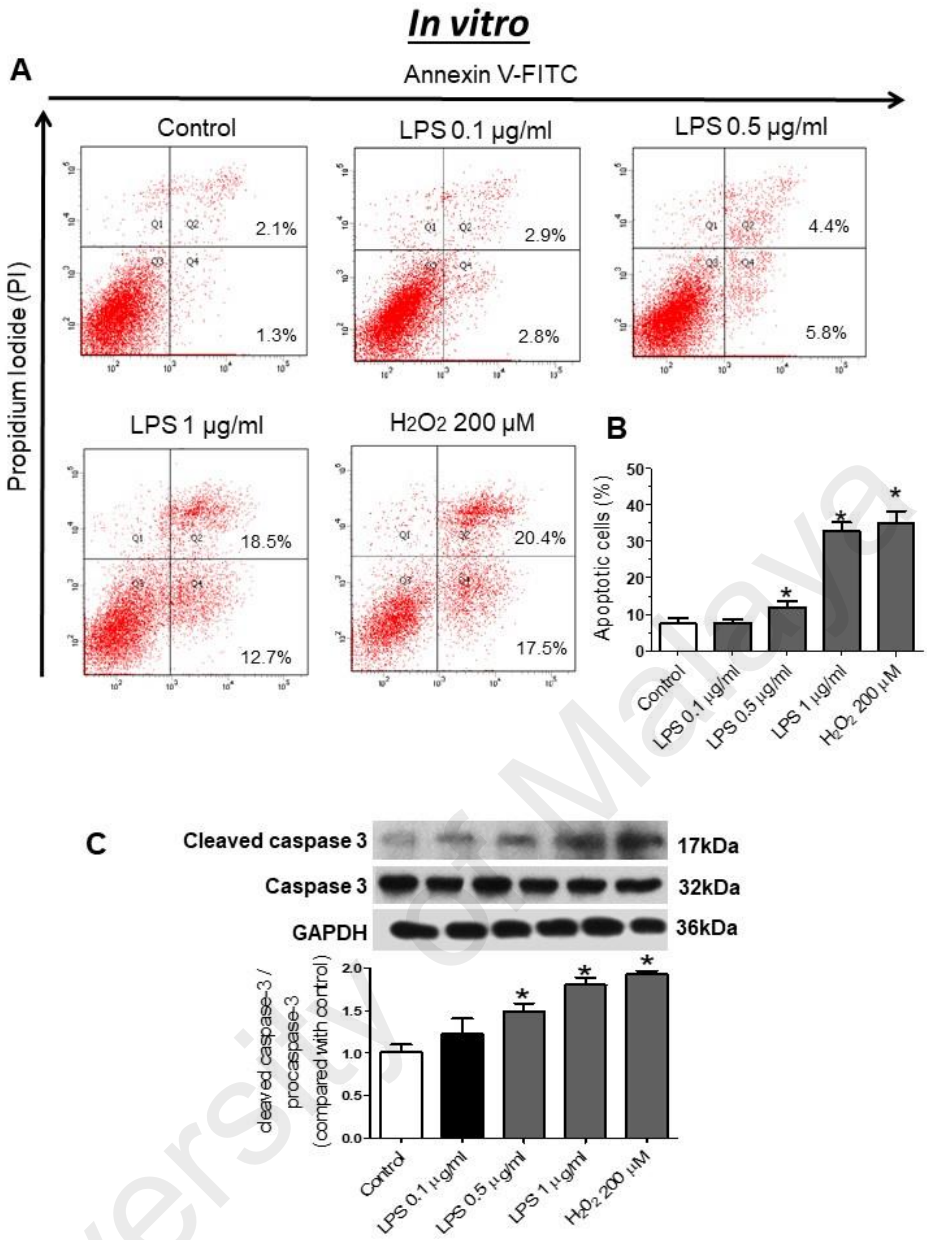

Figure 4.1: Flowcytometric analysis showing LPS-induced apoptosis in a concentration dependant manner in HUVECs after 24 hours. (A) Flow cytometry dot plots of apoptotic cells. In each dot plot figure, the upper left quadrant corresponds to necrotic cells; the upper right quadrant contains the late apoptotic cells, which are positive for Annexin V and propidium iodide (PI); the lower left quadrant shows viable cells, which exclude PI and Annexin V; the lower right quadrant represents the early apoptotic cells, Annexin V positive and PI negative. (B) Percentage of apoptotic cells quantified by flow cytometry. (C) Western blot and quantitative data showing the protein presence of cleaved caspase 3 in HUVECs treated with various concentration of LPS. Values are means ± SEM from four independent experiments. * P< 0.05 vs. control.

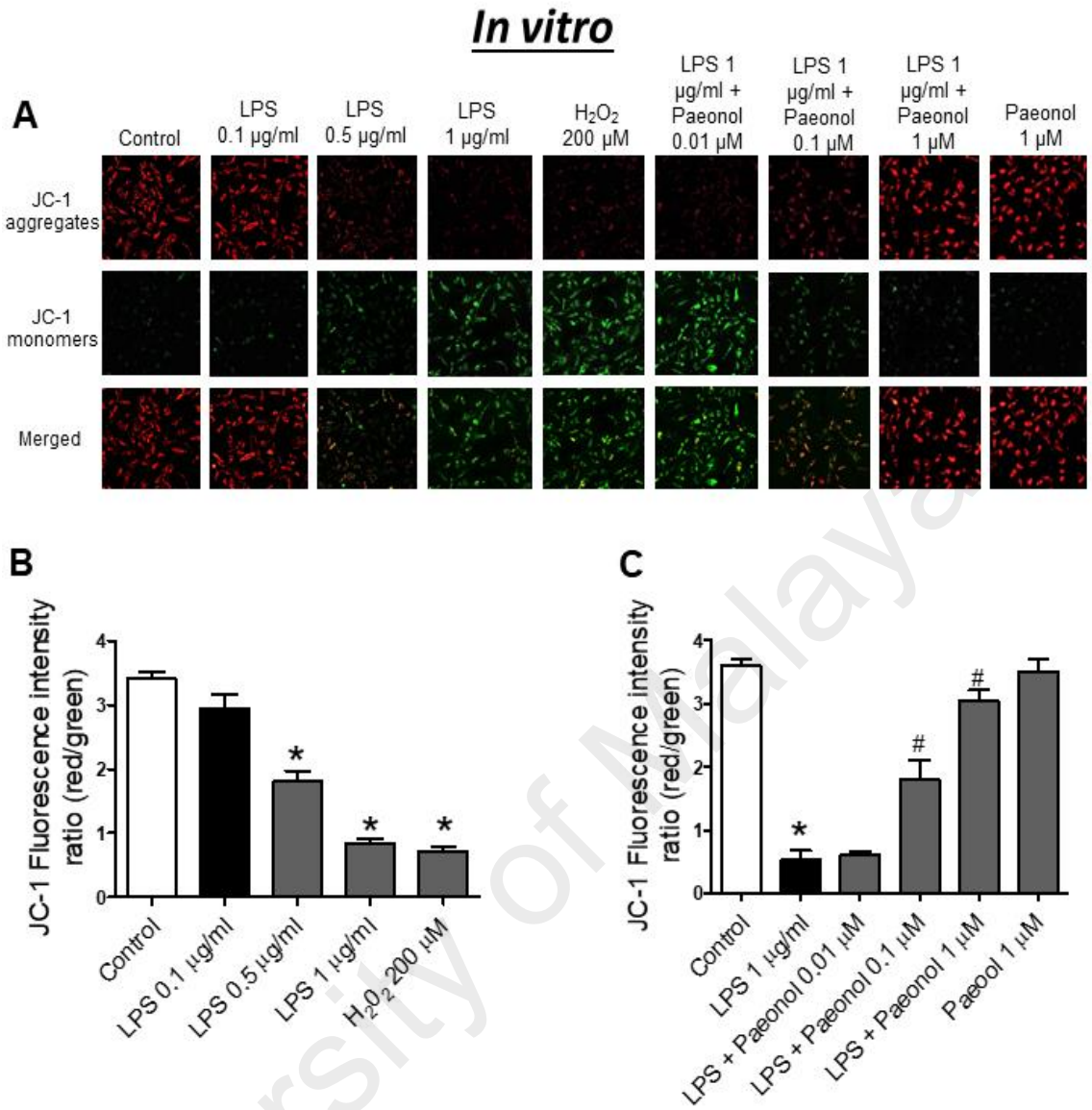

Figure 4.2: The mitochondrial membrane potential monitored with JC-1 dye in HUVECs treated with or without LPS, paeonol or H_2O_2 for 24 hours. The red fluorescence indicates healthy cells with high mitochondrial transmembrane potential, whereas the green fluorescence indicates apoptotic cells with low mitochondrial transmembrane potential. Data are presented as means ± SEM by four independent experiments. *P< 0.05 versus the control, # P< 0.05 compared with LPS.

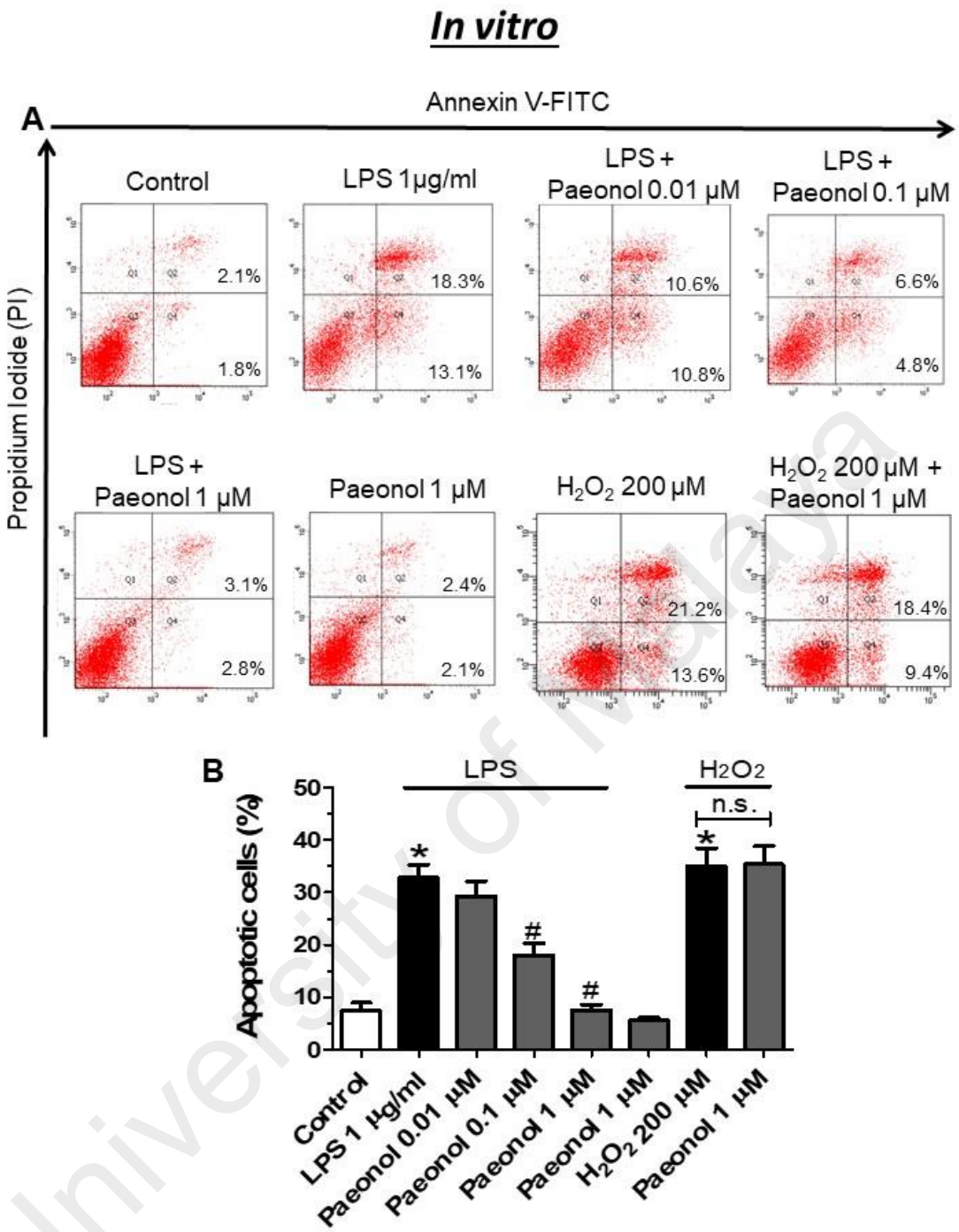

Figure 4.3: Paeonol reduced HUVECs cell apoptosis induced by LPS in a concentration dependant manner, except in cell apoptosis induced by H_2O_2 for 24 hours. (A) Flow cytometry dot plot figures showing percentage of apoptotic cells in HUVECs treated with LPS (1 µg/ml) or H_2O_2 (200 µM) and various concentration of paeonol (0.01, 0.1 and 1 µM). (B) Percentage of apoptotic cells quantified by flow cytometry. Values are means ± SEM from three independent experiments. * P< 0.05 vs. control, #P< 0.05 vs. LPS.

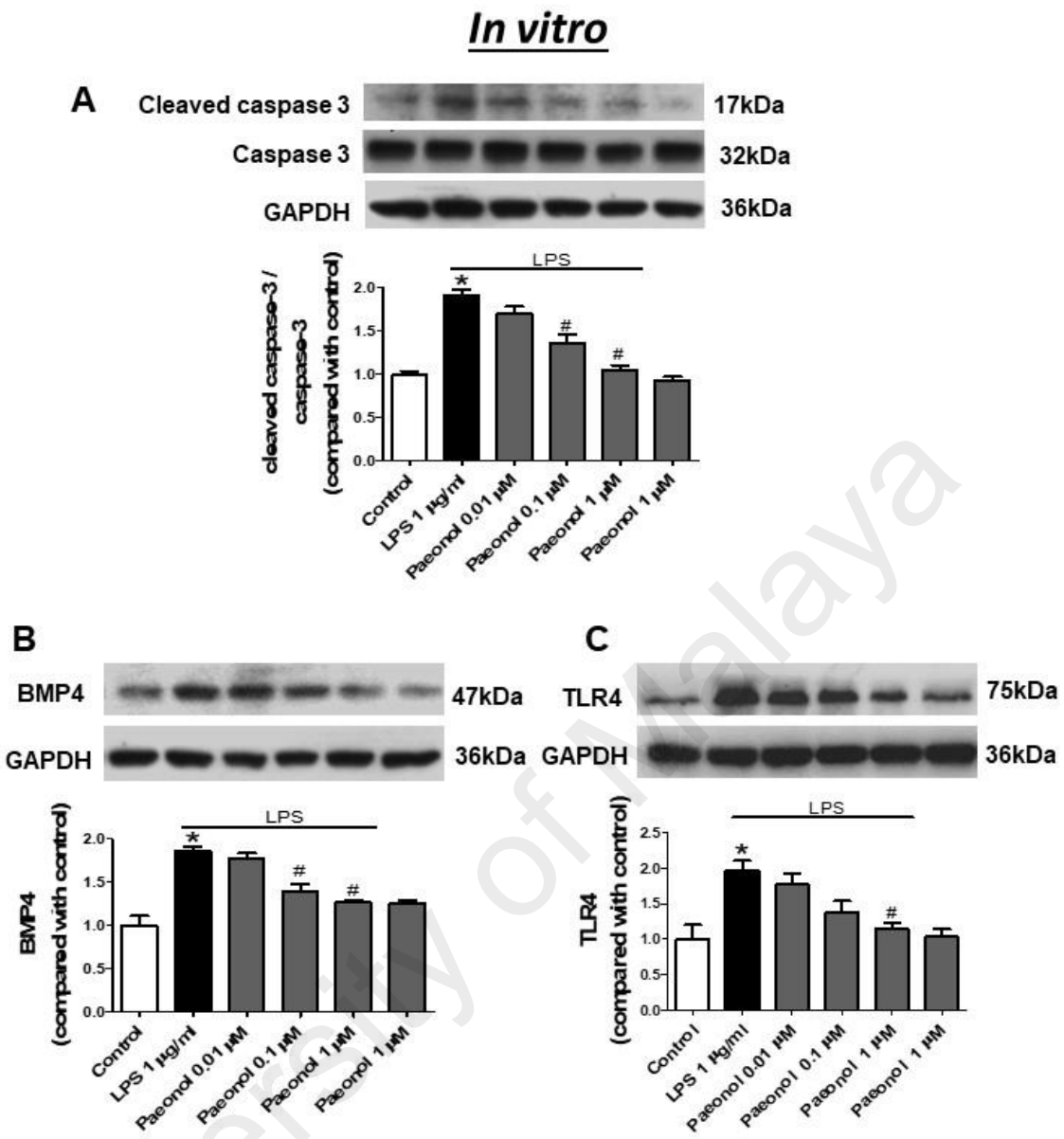

Figure 4.4: Paeonol reduced LPS-induced up-regulation of cleaved caspase 3, BMP4 and TLR4 in HUVECs in a concentration-dependant manner. Western blot and quantitative data showing the protein expression of (A) cleaved caspase 3, (B) BMP4, (C) TLR4 in HUVECs treated with LPS (1 µg/ml) and various concentration of paeonol (0.01, 0.1 and 1 µM). Values are means ± SEM from three independent experiments. * P< 0.05 vs. control, #P< 0.05 vs. LPS.

4.3.2 Paeonol reversed LPS-induced endothelial dysfunction *ex vivo*

Aortic rings exposed with LPS (1 μg/mL) during *ex vivo* culture in DMEM for 24 hours showed impairment of endothelium-dependent relaxation by acetylcholine (Figure 4.15A). Co-treatment with paeonol (0.1, 0.3 and 1 μM) for 24 hours significantly reversed this impairment in a concentration-dependant manner, with paeonol at 1 μM being the effective concentration (Figure 4.15A).

To determine the signalling pathway involved in LPS-induced endothelial dysfunction, aortic rings exposed with LPS were co-incubated with the following pharmacological inhibitors: SB202190 (10 μM), SP600125 (10 μM), TAK242 (1 μM), AG (100 μM), noggin (100 ng/mL) and apocynin (20 μM) for 24 hours. These inhibitors significantly reversed the LPS-induced impairment of the relaxation to acetylcholine (Figure 4.15B & C). However, co-incubation with indomethacin (10 μM) for 24 hours did not reverse the acetylcholine-induced relaxations impaired by LPS (Figure 4.6). Endothelium-independent relaxations induced by SNP were similar in all experimental groups (Figure 4.7).

To elucidate whether or not the endothelium-protective effect of paeonol is BMP4-dependent, aortic rings were exposed with BMP4 (100 ng/mL). The results displayed that BMP4 induced impairment of the relaxation to acetylcholine and this impairment was reversed by co-incubation with paeonol, noggin, apocynin, SB202190 and SP600125 (Figure 4.8). Relaxations to SNP were comparable in the different experimental groups (Figure 4.9).

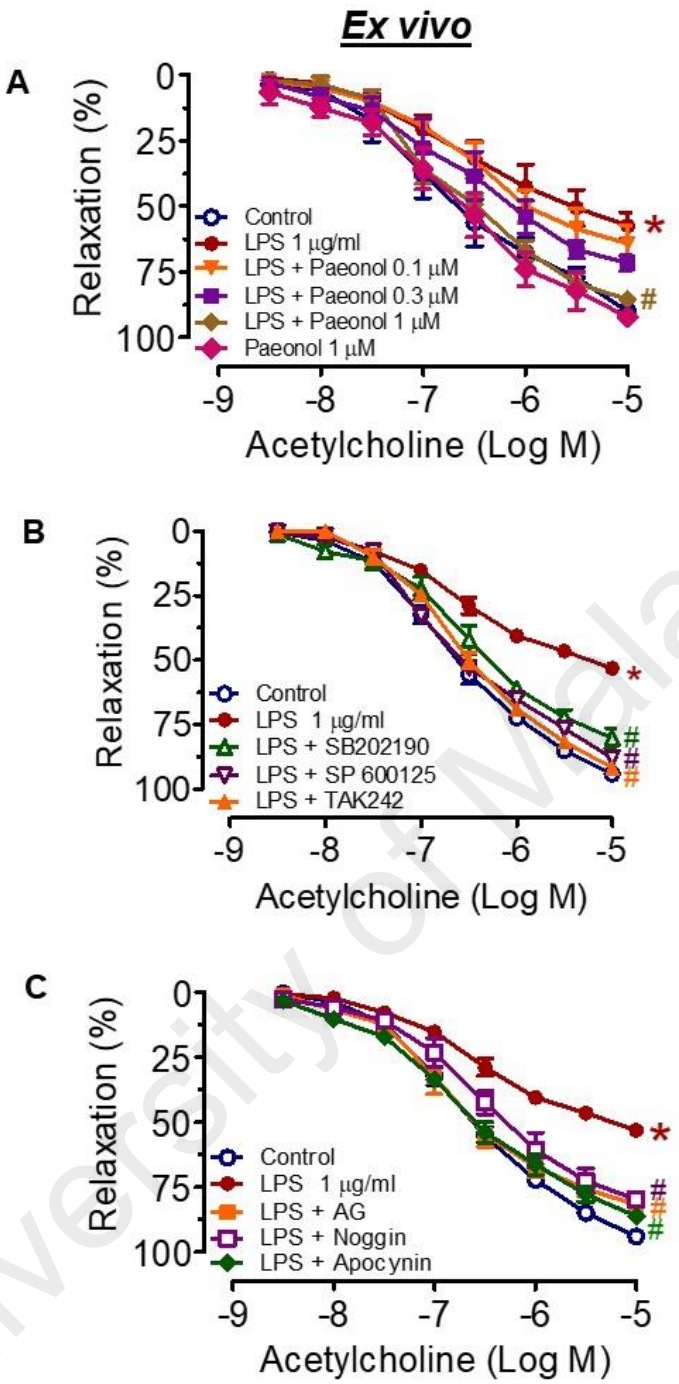

Figure 4.5: The effects of paeonol and various inhibitors in LPS-induced impairment of the relaxation to acetylcholine in mouse aorta. (A) Paeonol improved relaxations to acetylcholine in mouse thoracic aortae incubated with LPS (1 µg/mL) for 24 hours in a concentration-dependent manner. (B & C) Co-incubation of LPS with SB202190 (10 µM), SP600125 (10 µM) and TAK242 (1 µM) or (C) aminoguanidine (AG, 100µM), noggin (100 ng/ml) and apocynin (20 µM) for 24 hours improved the impairment of relaxations to acetylcholine induced by LPS in mouse aortae. Results are means± SEM of seven experiments. * P< 0.05, compared to control; # P< 0.05, compared to LPS and Δ, P< 0.05 compared to BMP4.

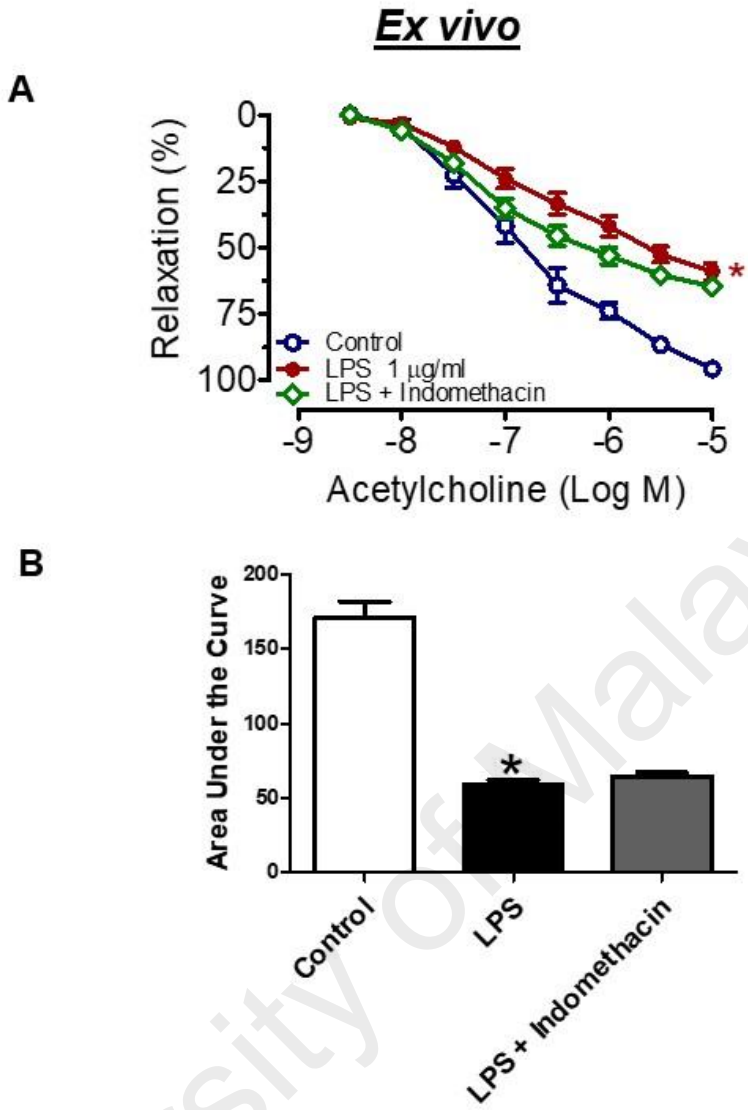

Figure 4.6: The effect of indomethacin in LPS-induced endothelial dysfunction in mouse aorta. (A) *Ex vivo* incubation with indomethacin (10 µM, cyclooxygenase inhibitor) for 24 hours did not improve the impairment of acetylcholine-induced relaxation induced by 1 µg/mL LPS in the aortae. (B) Area under the curve. Results are means± SEM of six to experiments. * P< 0.05, compared to control.

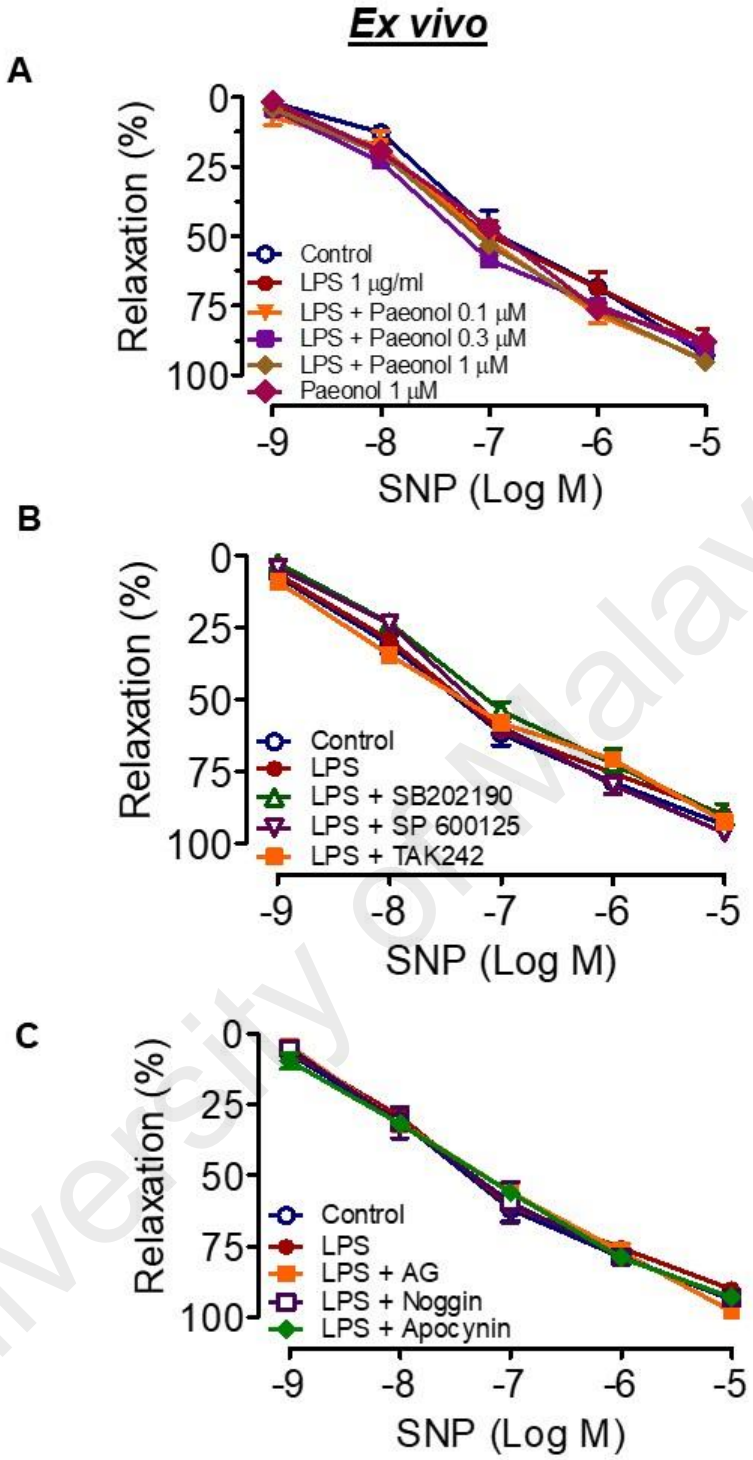

Figure 4.7: Endothelium-independent relaxations induced by SNP were similar in all groups. Endothelium-independent relaxations of mouse aortic rings treated in the presence or absence of LPS (1 µg/mL), paeonol (0.1, 0.3, 1 µM), SB202190 (10 µM), SP600125 (10 µM), TAK242 (1 µM), aminoguanidine (AG, 100µM), noggin (100 ng/ml) and apocynin (20 µM) for 24 hours. Results are means ± SEM of seven experiments.

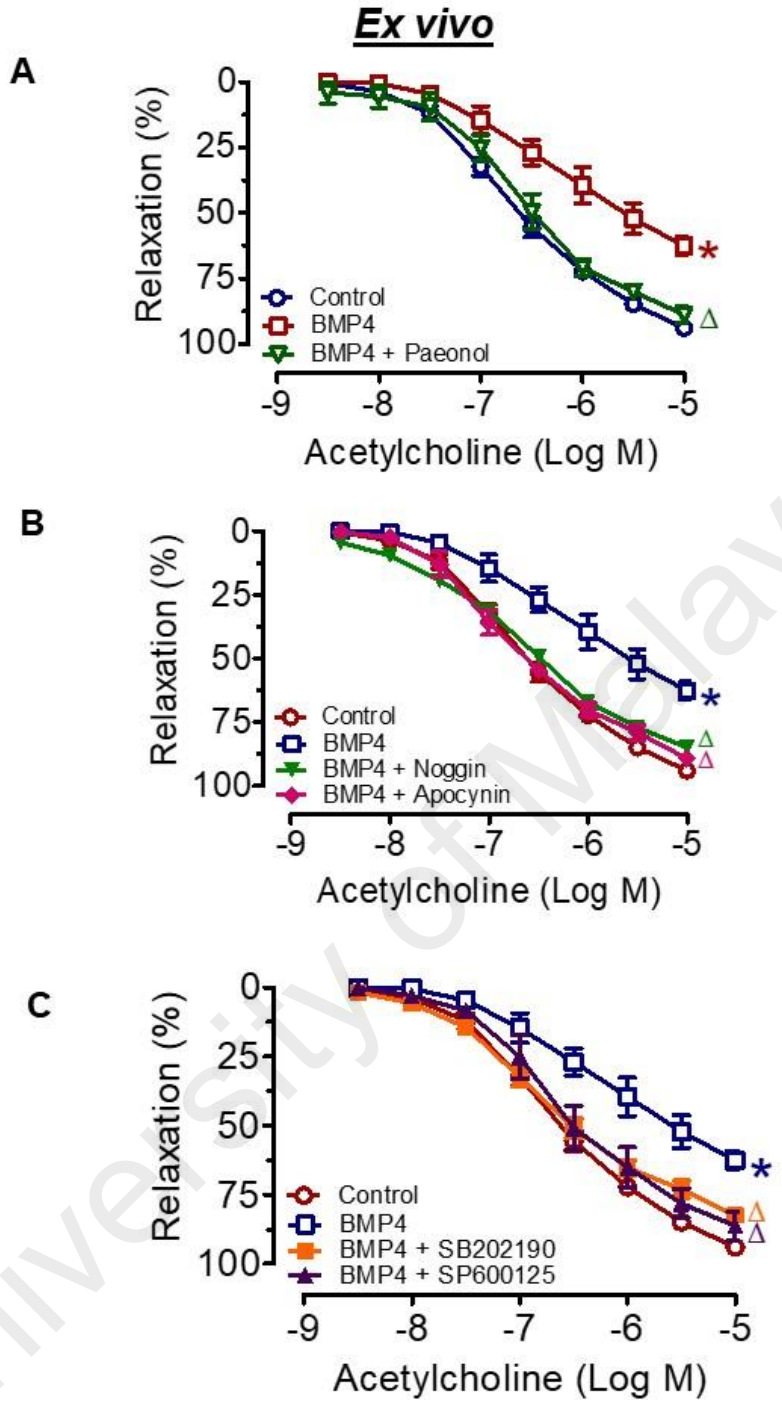

Figure 4.8: The effects of paeonol and various inhibitors in BMP4-induced impairment of the relaxation to acetylcholine in mouse aorta. (A) Paeonol (1 µM) improved the impaired response to acetylcholine in aortae exposed to BMP4 (100 ng/mL) for 24 hours. (B & C) Co-incubation of BMP4 with noggin (100 ng/ml), apocynin (20 µM), SB202190 (10 µM), SP600125 (10 µM) during 24 hours improved acetylcholine-induced relaxation. Results are means± SEM of seven experiments. *P< 0.05, compared to control; Δ, P< 0.05 compared to BMP4.

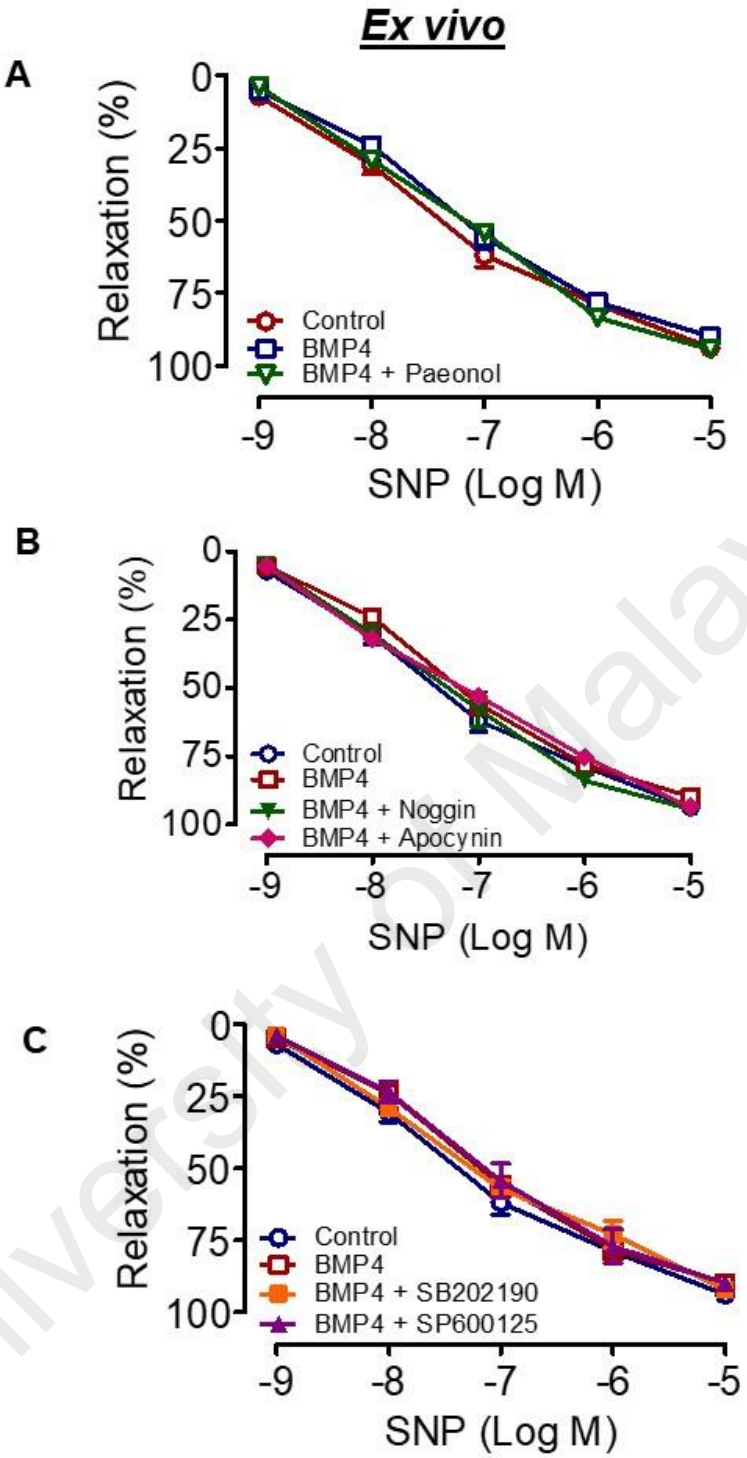

Figure 4.9: Endothelium-independent relaxations induced by SNP were similar in all groups. Endothelium-independent relaxations induced by SNP of aorta rings in mice treated with or without BMP4 (100 ng/mL), paeonol (1 µM), noggin (100 ng/ml), apocynin (20 µM), SB202190 (10 µM), SP600125 (10 µM) for 24 hours. Results are means ± SEM of seven experiments.

4.3.3 Paeonol attenuated LPS-induced inflammation and apoptosis in HUVECs through inhibition of TLR4 and BMP4 signalling pathway.

To characterize further the mechanism of anti-inflammatory action of paeonol, we studied the expression of inflammation and apoptosis markers via Western blotting. As shown in Figure 4.10, TLR4 (Figure 4.10A & B), phosphorylated p38 MAPK (Figure 4.10A & C), phosphorylated JNK (Figure 4.10A & D), BMP4 (Figure 4.10A & E), BMPR1A (Figure 4.10A & F), iNOS (Figure 4.10A & I), cleaved caspase 3/caspase 3 (Figure 4.10A & J) and NOX 2 (Figure 4.10A & K) were markedly increased after LPS treatment. However, co-treatment with paeonol (1 μM) suppressed these proteins levels. Phosphorylation of eNOS (Figure 4.10A & G) and eNOS (Figure 4.10A & H) was down-regulated with LPS treatment, which were reversed with paeonol treatment. There are no differences between control and treatment with paeonol alone.

To elucidate the signalling pathway involved in LPS-induced inflammation and apoptosis in HUVECs, specific inhibitors of p38 MAPK (SB202190), JNK (SP600125), TLR4 (TAK242), inducible NOS (AG, aminoguanidine hydrochloride), BMP4 (noggin), and NADPH oxidase (apocynin) were used. LPS-induced TLR4 up-regulation was inhibited significantly by TAK242 but not affected by the other inhibitors tested (Figure 4.11A & B). The phosphorylation of p38 MAPK protein in response to LPS was prevented by SB202190, noggin, TAK242 and apocynin without changes in total p38 MAPK protein presence (Figure 4.11A & C). The phosphorylation of JNK activated by LPS was inhibited by SP600125, noggin, TAK242 and apocynin without changes in total JNK protein presence (Figure 4.11A & D). Up-regulation of BMP4 (Figure 4.12A & B) and BMPR1A (Figure 4.12A & C) protein levels were inhibited by noggin but not by SB202190, SP600125, TAK242, aminoguanidine or apocynin. LPS reduced both the total eNOS (Figure 4.13A & B) as well as the phosphorylated eNOS (4.13A & C) protein

levels with no difference in their ratio, while increasing iNOS levels (4.14A & B) and caspase 3 activation (4.14A & C); these effects of LPS were reversed by all the inhibitors tested. Noggin, TAK242 and apocynin inhibited the increased of NADPH oxidase subunit 2 (NOX 2) induced by LPS (4.14A & D).

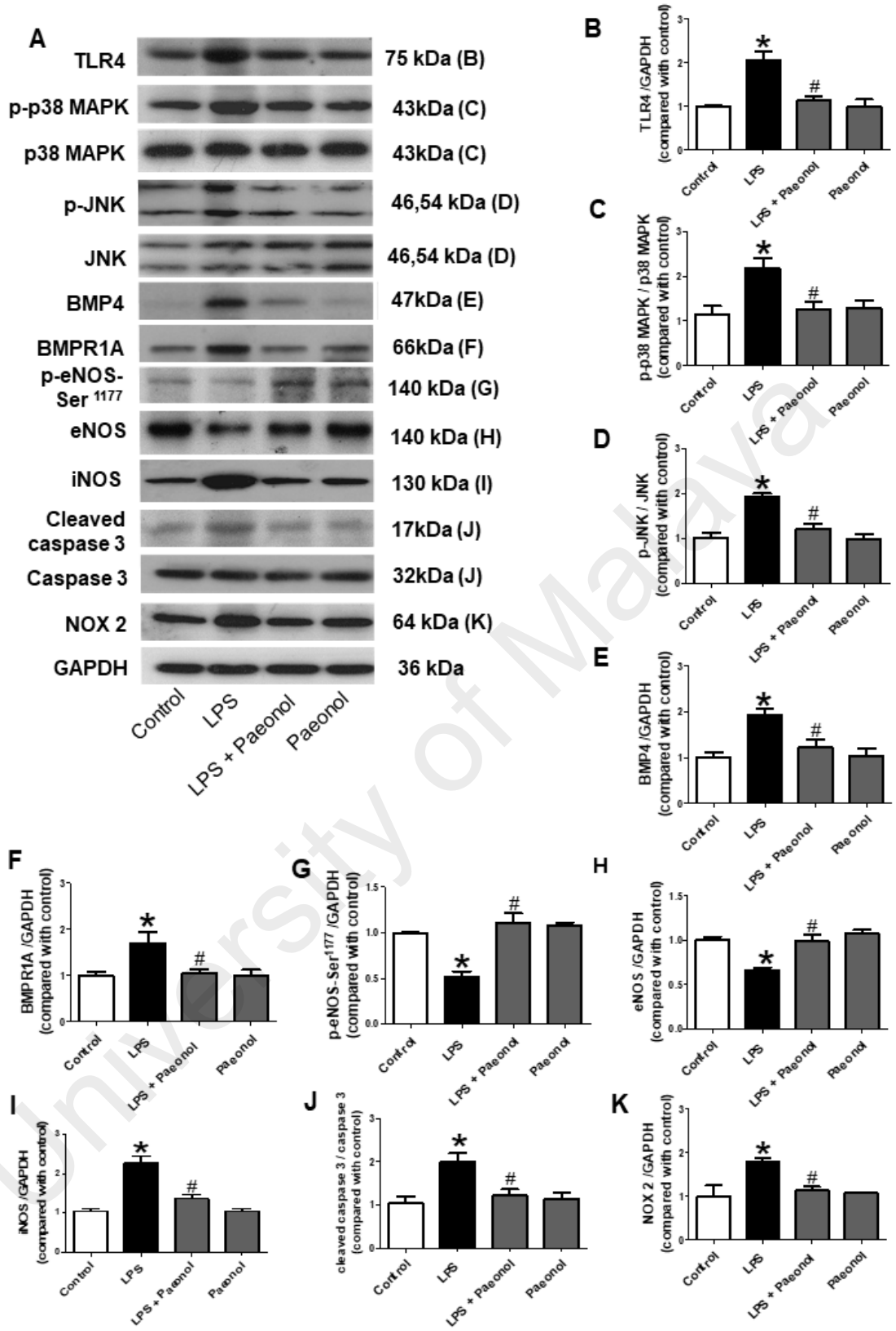

Figure 4.10: (A) Western blot and (B-K) quantitative data showing the protein expression in HUVECs treated with LPS (1 µg/mL) and paeonol (1 µM). Results are means ± SEM of four separate experiments. *P< 0.05 compared with control, #P< 0.05 compared with LPS.

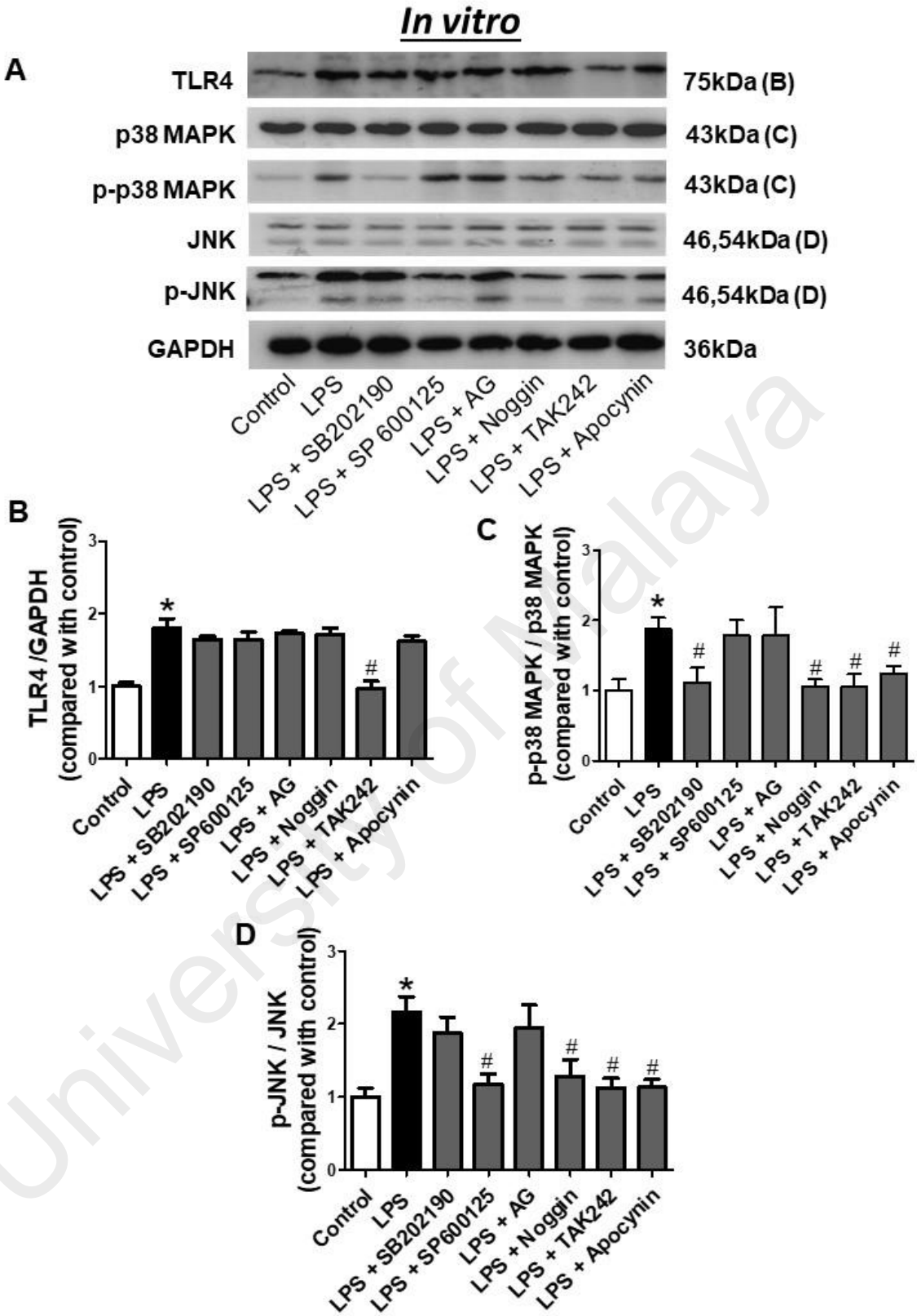

Figure 4.11: (A) Western blots and (B-D) quantitative data showing protein presences of TLR4, p38 MAPK and JNK in HUVECs treated with LPS (1 µg/mL) and paeonol (1 µM). Results are means ± SEM of five separate experiments. *P< 0.05 compared with control, # P< 0.05 compared with LPS.

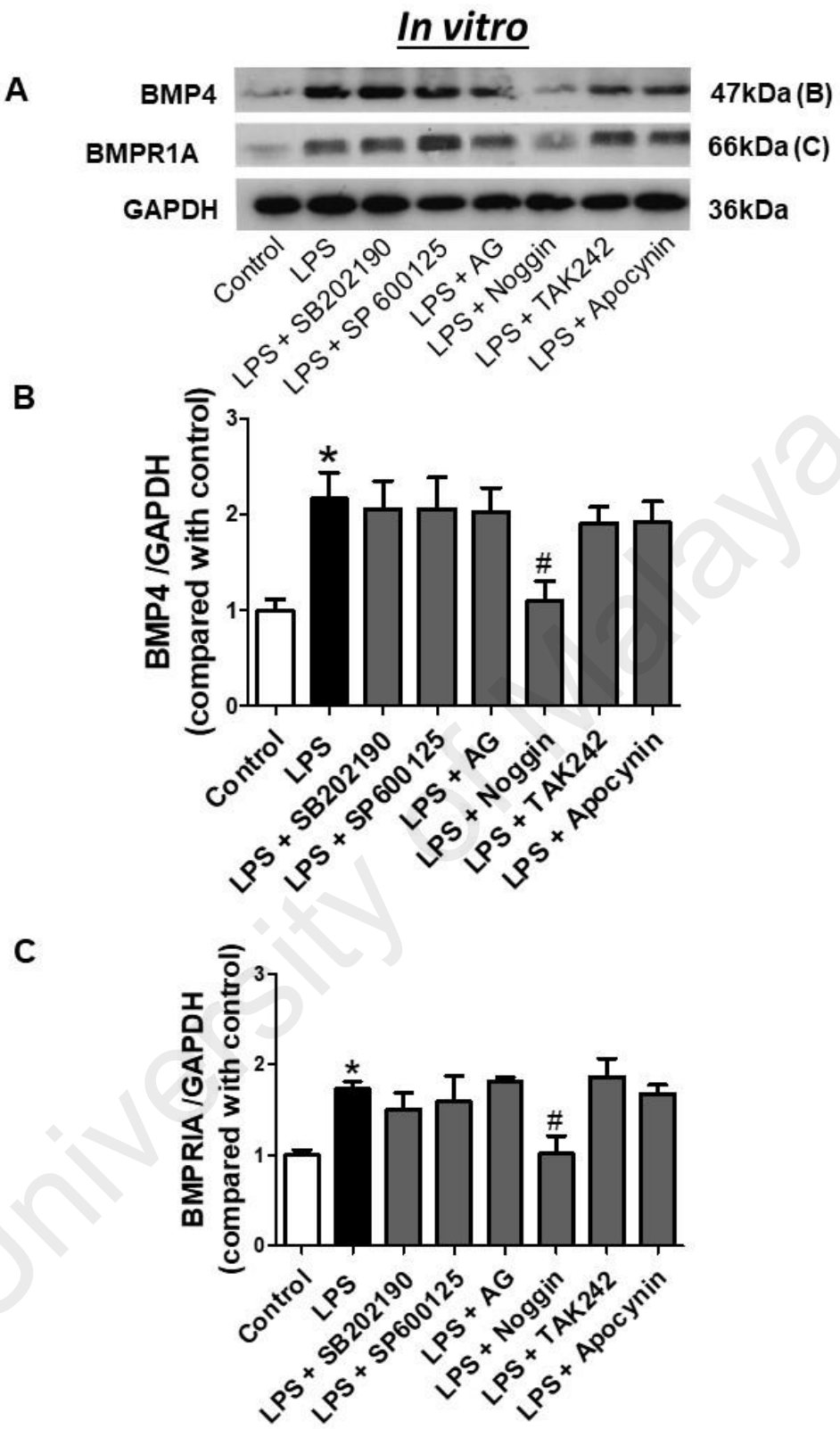

Figure 4.12: (A) Western blots and (B-C) quantitative data showing protein presences of BMP4 and BMPR1A in HUVECs treated with LPS (1 µg/mL) and paeonol (1 µM). Results are means ± SEM of five separate experiments. *P< 0.05 compared with control, # P< 0.05 compared with LPS.

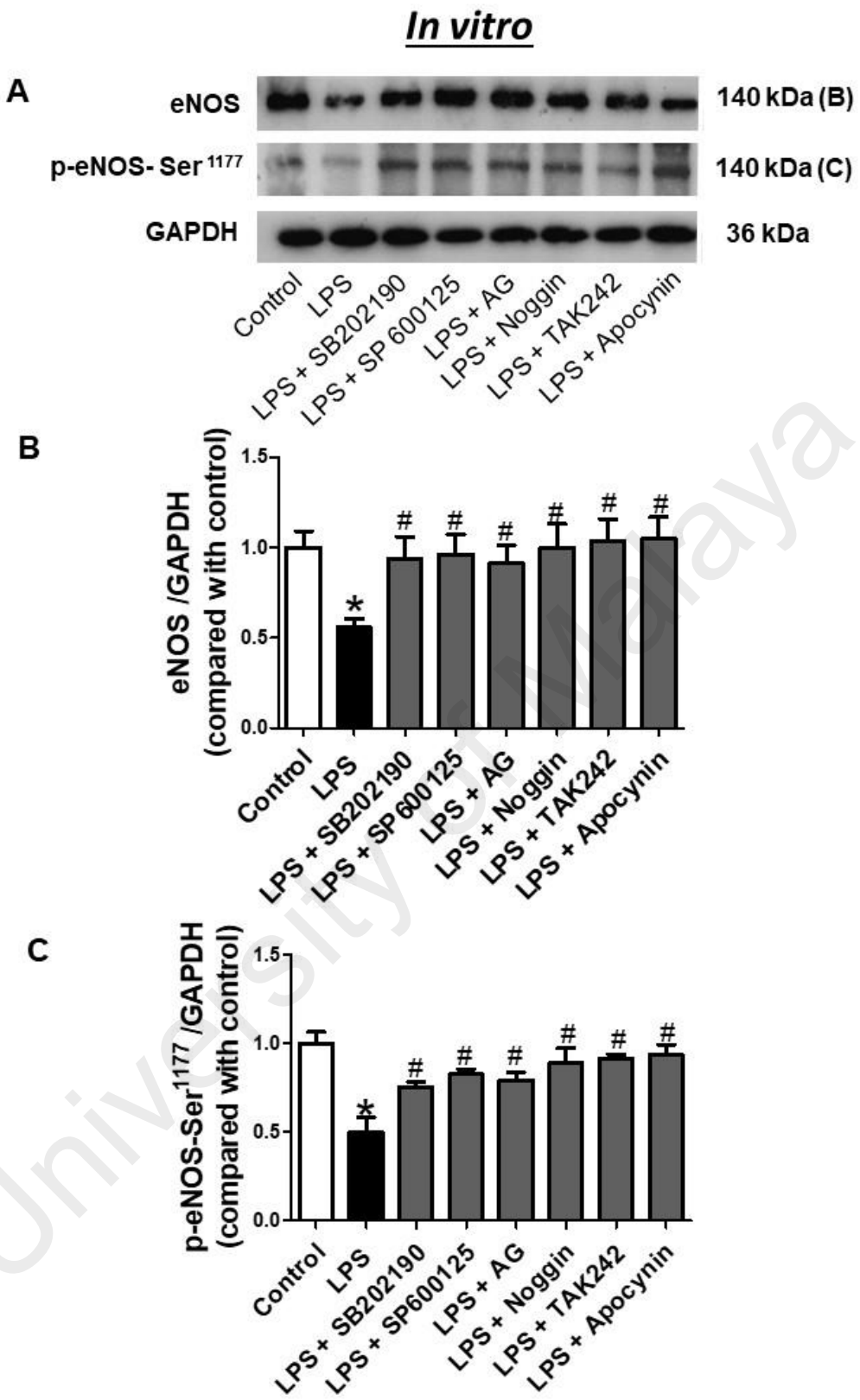

Figure 4.13: (A) Western blots and (B-C) quantitative data showing protein presences of eNOS and p-eNOS in HUVECs treated with LPS (1 µg/mL) and paeonol (1 µM). Results are means ± SEM of five separate experiments. *P< 0.05 compared with control, # P< 0.05 compared with LPS.

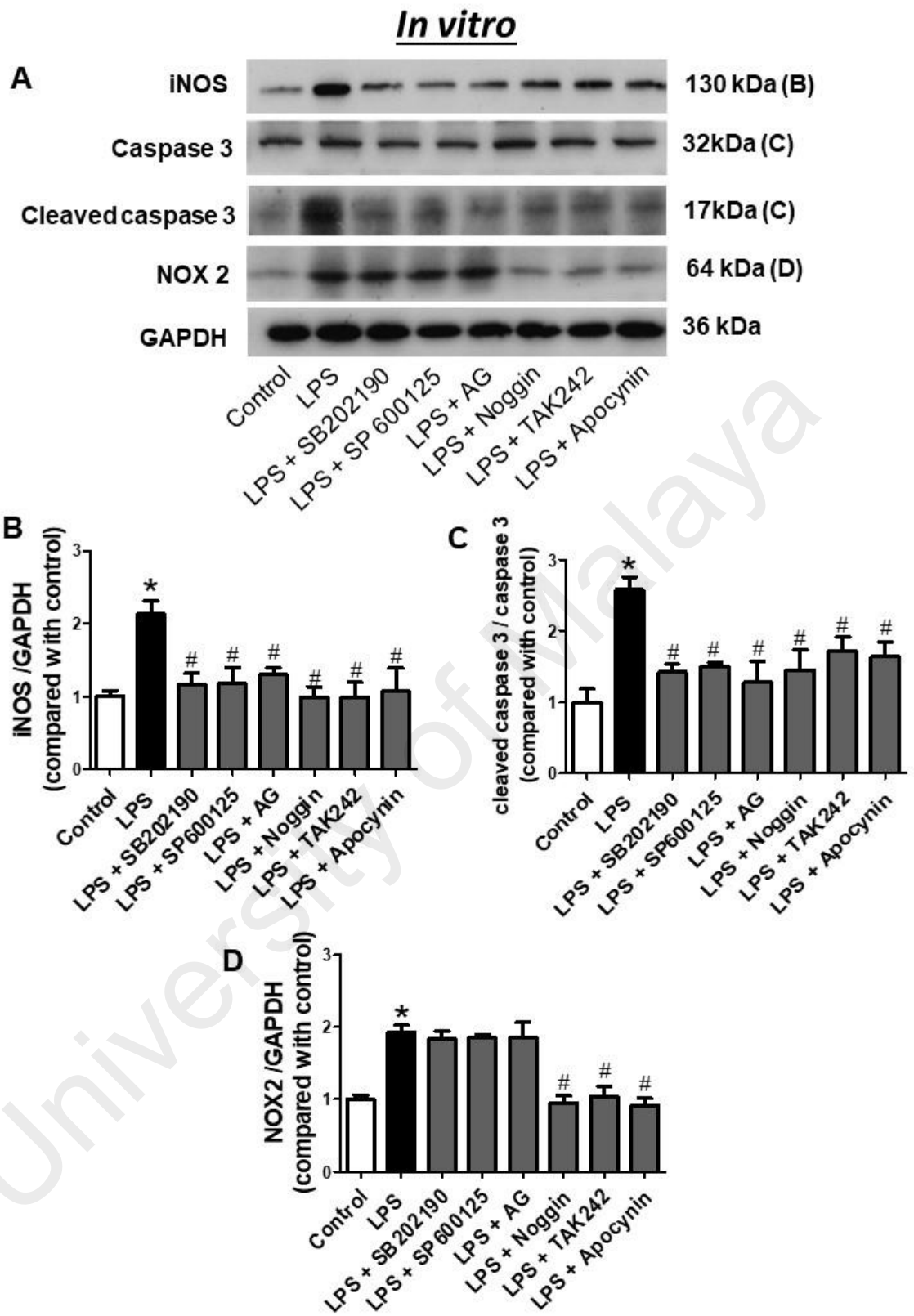

Figure 4.14: (A) Western blots and (B-C) quantitative data showing protein presences of iNOS, cleaved caspase 3 and NOX 2 in HUVECs treated with LPS (1 µg/mL) and paeonol (1 µM). Results are means ± SEM of five separate experiments. *P< 0.05 compared with control, # P< 0.05 compared with LPS.

4.3.4 Paeonol protected against BMP4-induced inflammation and apoptosis in HUVECs.

To evaluate the effect of paeonol on the BMP4 signalling cascade leading to cell apoptosis, HUVECs exposed to BMP4 were co-incubated with paeonol, noggin, SB202190, SP600125, apocynin and TAK242. Result from western blotting showed that BMP4 treated cells increased phosphorylated p38 MAPK (Figure 4.15A & B), phosphorylated JNK (Figure 4.15A & C), BMPR1A (Figure 4.15A & D), cleaved caspase 3 (Figure 4.16A & C), and NOX 2 (Figure 4.16A & D) while reduced the phosphorylation of eNOS (Figure 4.16A & B) without affecting the total eNOS level; co-treatment with paeonol normalised the presence of these proteins. Phosphorylation of p38 MAPK induced by BMP4 was abolished by noggin, SB202190 and apocynin without changes in total p38 MAPK protein presence (Figure 4.15A & B). Similarly, phosphorylation of JNK stimulated by BMP4 was also prevented by noggin, SP600125 and apocynin without changes in total JNK (Figure 4.15A & C). BMPR1A activated by BMP4 was inhibited by noggin but not by the other inhibitors tested (Figure 4.15A & D). Moreover, all inhibitors except for TAK242 normalised BMP4-induced downregulation of phosphorylated eNOS (Figure 4.16A & B) and the activation of caspase 3 (Figure 4.16A & C). BMP4 induced activation of NOX2 was inhibited only by noggin and apocynin (Figure 4.16A & D).

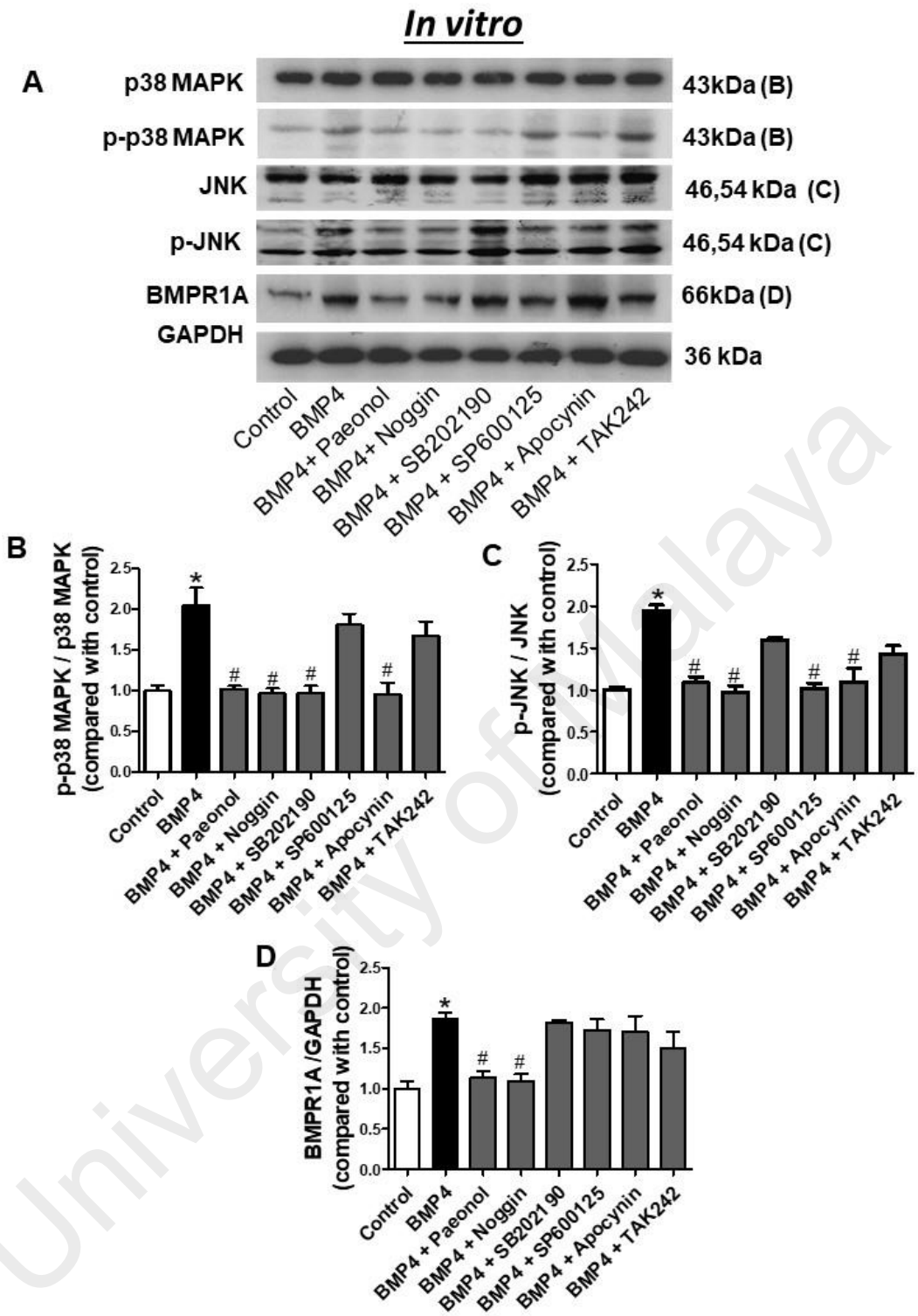

Figure 4.15: (A) Western blots and (B-D) quantitative data showing protein presences of p38 MAPK, JNK and BMPR1A in HUVECs treated with BMP4 (100 ng/mL), paeonol (1 µM), noggin (100 ng/mL), SB202190 (10 µM), SP600125 (10 µM), apocynin (20 µM) and TAK242 (1 µM). Results are means ± SEM of four separate experiments. *P< 0.05 compared with control, # P< 0.05 compared with BMP4.

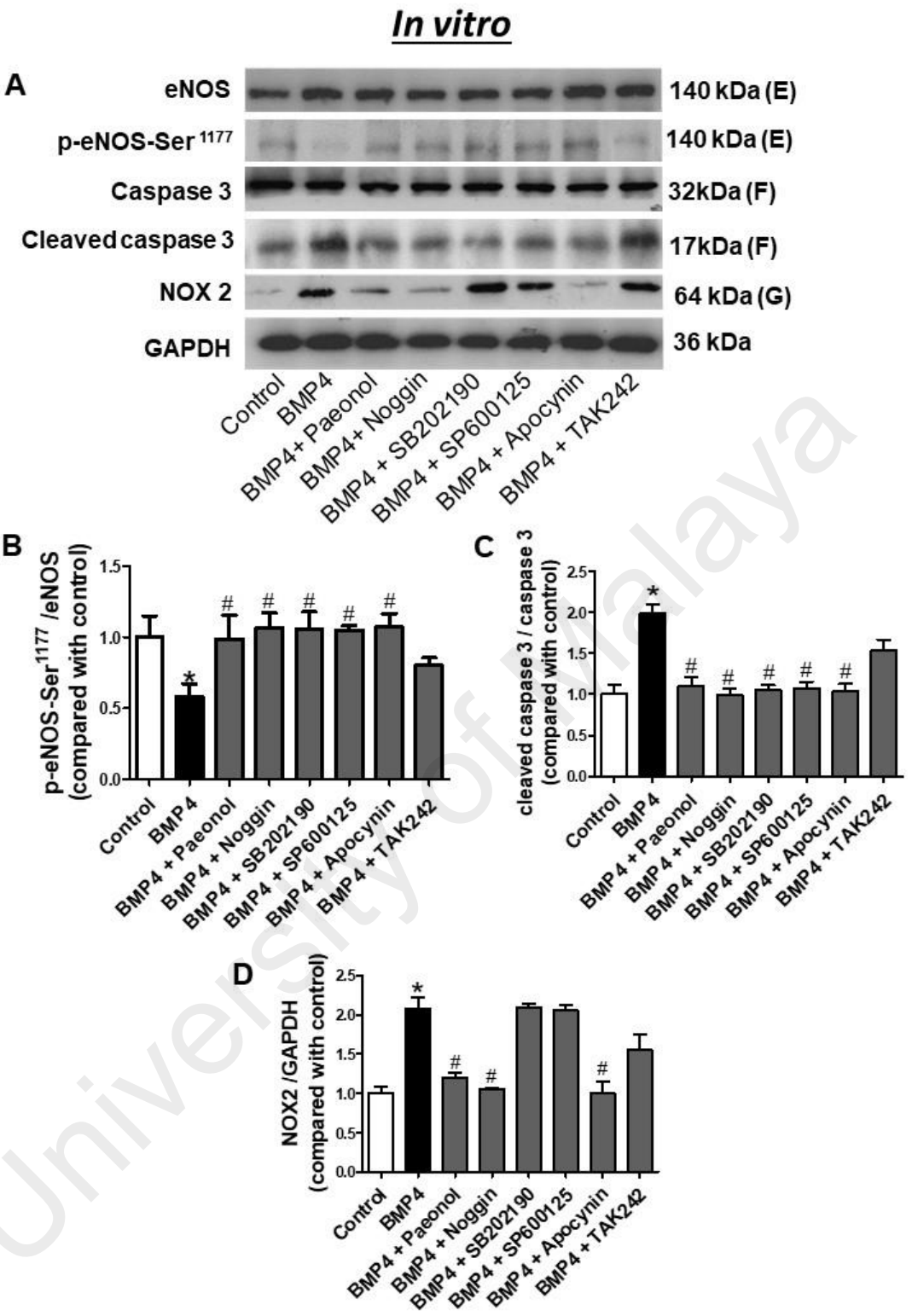

Figure 4.16: (A) Western blots and (B-D) quantitative data showing protein presences of p-eNOS, cleaved caspase 3 and NOX2 in HUVECs treated with BMP4 (100 ng/mL), paeonol (1 µM), noggin (100 ng/mL), SB202190 (10 µM), SP600125 (10 µM), apocynin (20 µM) and TAK242 (1 µM). Results are means ± SEM of four separate experiments. *P< 0.05 compared with control, # P< 0.05 compared with BMP4.

4.3.5 Paeonol reversed LPS-induced apoptosis in HUVECs via BMP4 which is independent of TLR4 signalling pathway.

To confirm the connection between TLR4 and BMP4 signalling pathways in LPS-induced apoptosis, the expression of BMP4 and TLR4 were knocked down respectively using BMP4 siRNAs (Figure 4.17) and TLR4 siRNAs (Figure 4.18) in HUVECs at concentration of 5, 25 or 50 nM for 24, 48 or 72 hours respectively. BMP4 siRNAs at 50 nM for 72 hours (Figure 4.17B) and TLR4 siRNAs at 50 nM for 48 hours (Figure 4.18B) reduced TLR4 and BMP4 protein presence respectively by approximately 60% compared with scrambled siRNAs.

The siRNAs against BMP4 reduced the LPS-induced increases in BMP4 (Figure 4.19A & C), BMPR1A (Figure 4.19A & D), and cleaved caspase 3 (Figure 4.19A & E) proteins levels, but did not affect that of TLR4 (Figure 4.19A & B), suggesting TLR4 and BMP4 activation by LPS is independent of each other. Knockdown of BMP4 abrogated paeonol-mediated protection of the cells from LPS-induced cell death, which indicate that the anti-apoptotic effects of paeonol is mediated via BMP4 signalling pathway.

Our results showed that the expression of TLR4 (Figure 4.20A & B) and cleaved caspase 3 (Figure 4.20A & E) was significantly blocked in HUVECs transfected with TLR4 siRNA compared with scrambled siRNA treated with or without LPS. LPS-induced BMP4 (Figure 4.20A & C) and BMPR1A (Figure 4.20A & D) protein level was similar in both scrambled siRNA and TLR4-siRNA-transfected cells, indicating that BMP4 signalling pathway is not medicated via TLR4. Paeonol treatment decreased TLR4, BMP4, BMPR1A and cleaved caspase 3 proteins level in LPS-treated cells transfected with scrambled siRNA. Silencing of TLR4 completely blocked the inhibitory effects of paeonol on LPS induced activation of TLR4 (Figure 4.20A & B) and cleaved caspase 3

(Figure 4.20A & E), suggesting that the anti-apoptotic effect of paeonol is also mediated through TLR4.

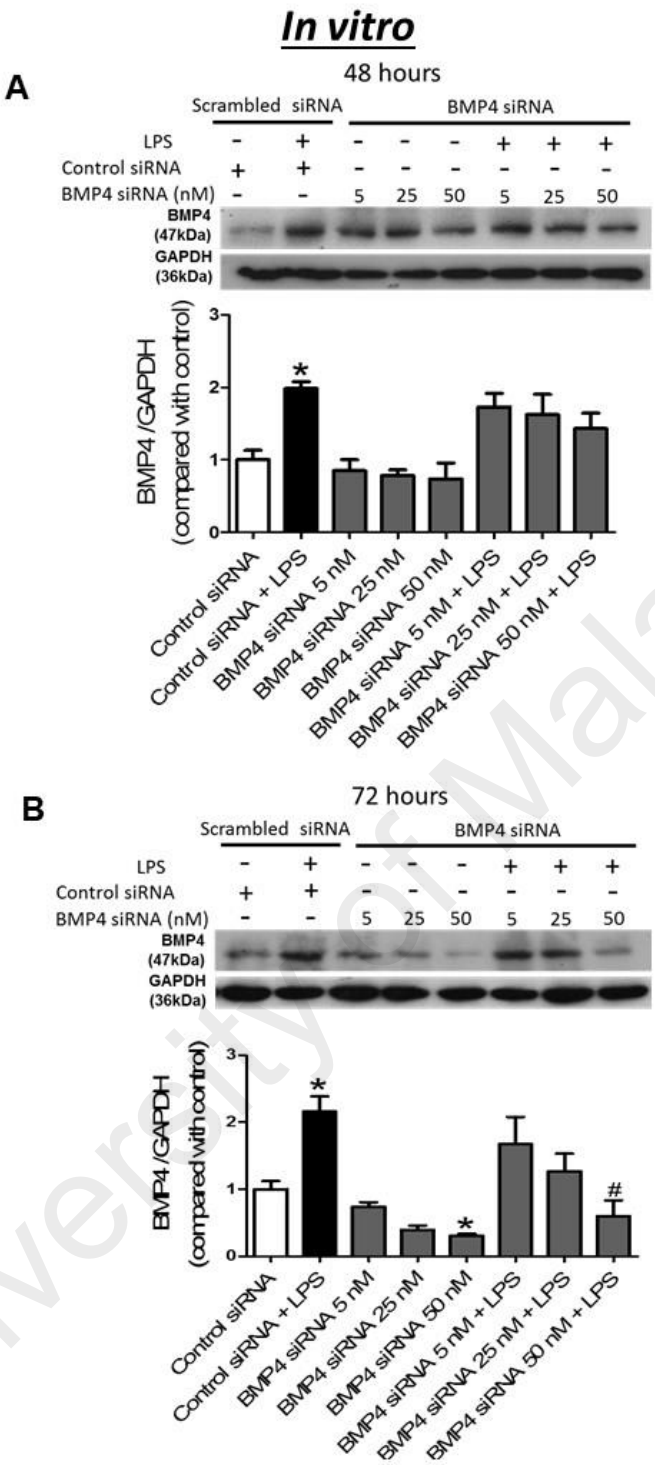

Figure 4.17: The extents of BMP4 knockdown assessed by Western blotting. BMP4 siRNA (5, 25 or 50 nM) or control siRNA were transfected into HUVECs for (A) 48 and (B) 72 hours, respectively, before incubation with LPS (1 μg/mL) for 24 hours. Results are expressed as means ± SEM of three separate experiments, *P< 0.05 vs. control BMP4 siRNA, # P< 0.05 vs. control BMP4 siRNA+ LPS.

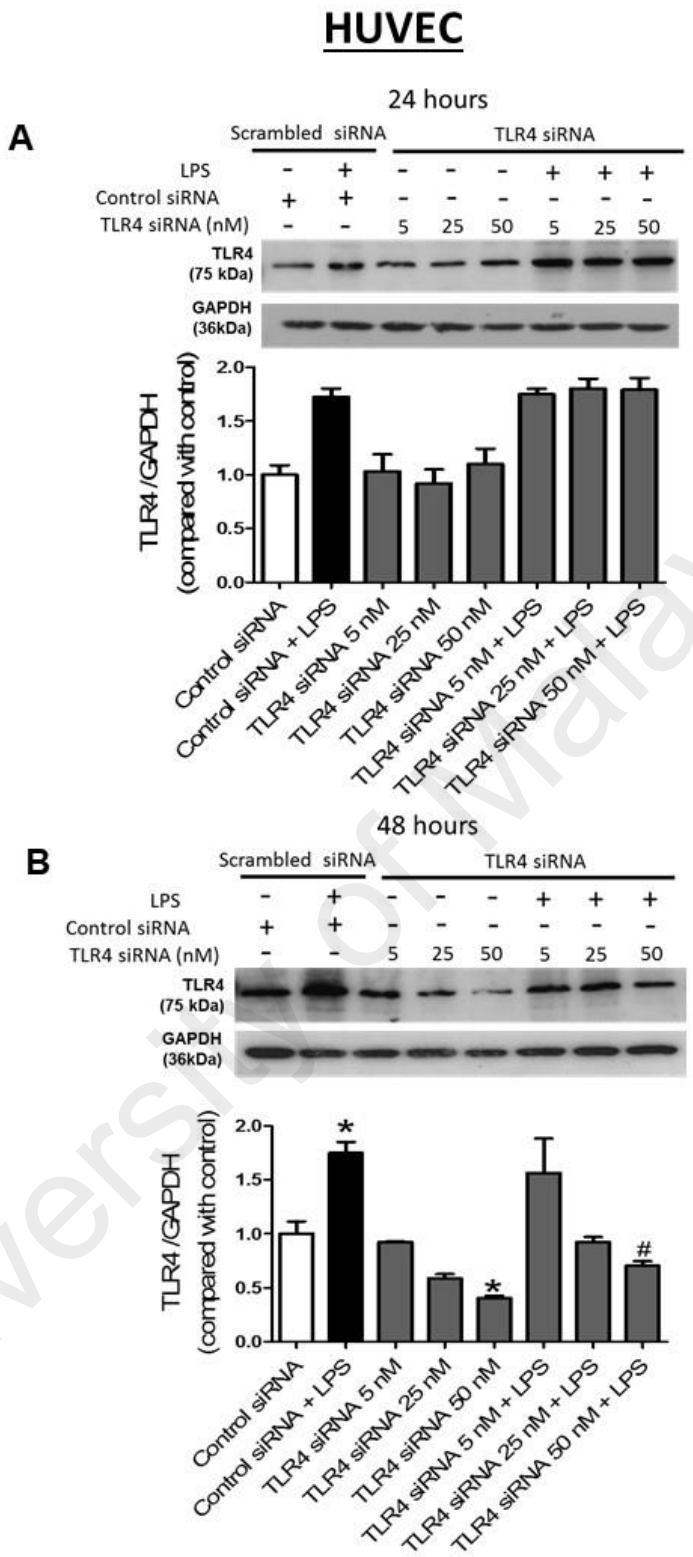

Figure 4.18: The extents of TLR4 knockdown assessed by Western blotting. TLR4 siRNA (5, 25 or 50 nM) or control siRNA were transfected into HUVECs for (A) 24 and (B) 48 hours, respectively, before incubation with LPS (1 μg/mL) for 24 hours. Results are expressed as means ± SEM of three separate experiments, *P< 0.05 vs. control TLR4 siRNA, # P< 0.05 vs. control TLR4 siRNA+ LPS.

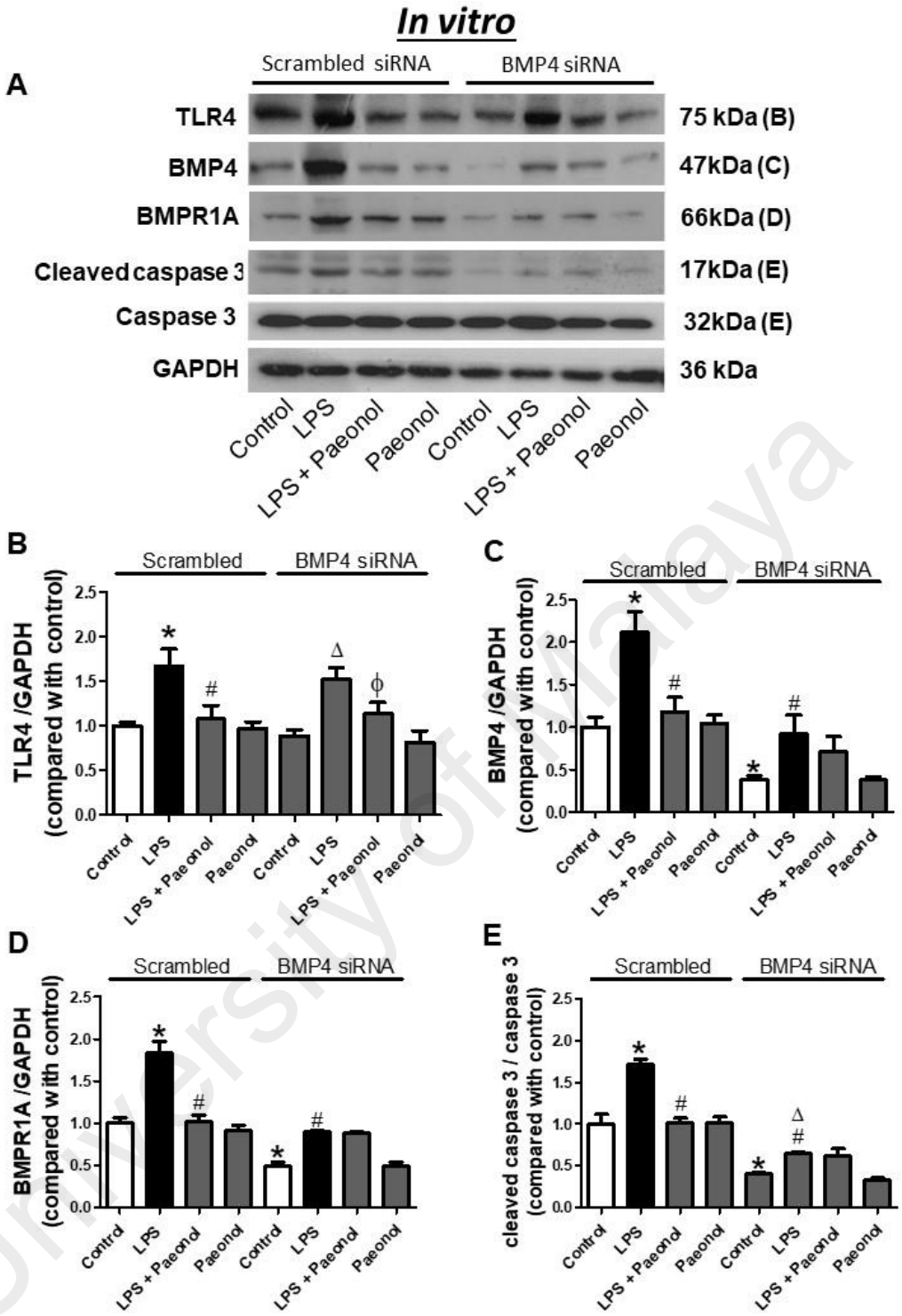

Figure 4.19: Effects of BMP4 knockdown on the paeonol- induced suppression of pro-inflammatory and apoptotic markers induced by LPS. BMP4 siRNA (50 nM/well) were transfected into HUVECs for 72 hours before exposed to LPS (1 μg/mL) and paeonol (1 μM) for 24 hours. Results are means ± SEM of four separate experiments; *P< 0.05 vs. control siRNA, # P< 0.05 vs. siRNA control + LPS, Δ P< 0.05 vs. BMP4 siRNA, ϕ P< 0.05 vs. BMP4 siRNA + LPS.

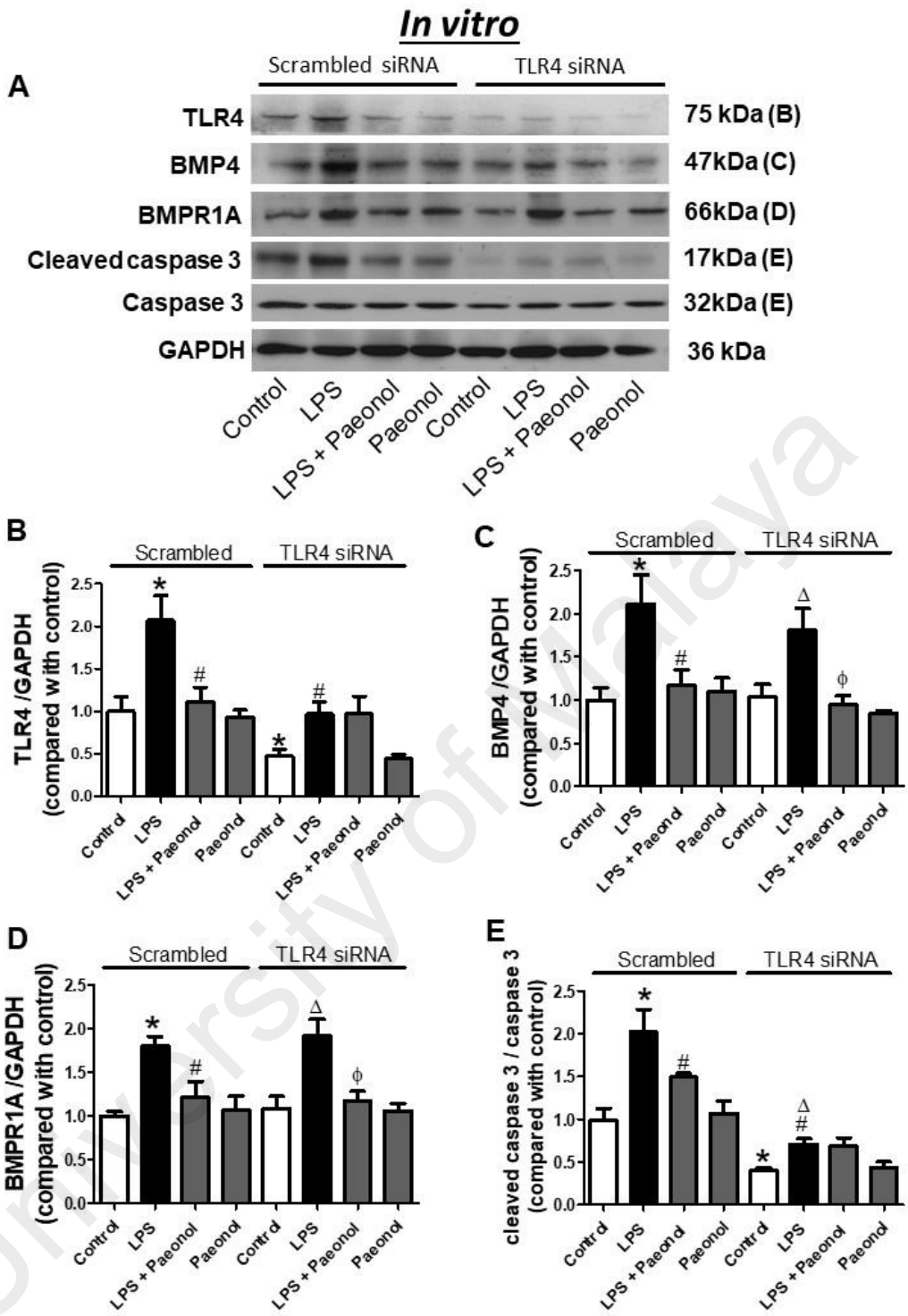

Figure 4.20: Effects of TLR4 knockdown on the paeonol- induced suppression of pro-inflammatory and apoptotic markers induced by LPS. TLR4 siRNA (50 nM/well) were transfected into HUVECs for 48 hours before exposed to LPS (1 μg/mL) and paeonol (1 μM) for 24 hours. Results are means ± SEM of four separate experiments; *P< 0.05 vs. control siRNA, #P< 0.05 vs. siRNA control + LPS, ΔP< 0.05 vs. TLR4 siRNA, ϕP< 0.05 vs. TLR4 siRNA + LPS.

4.3.6 General parameters: Body weight and systolic blood pressure in mice *in vivo*

Mice exposed to LPS (5, 10, 15 mg/kg), paeonol (10, 15, 20 mg/kg), noggin (0.5 mg/kg/day) and TAK242 (3 mg/kg) for 24 hours had no changes in body weight within groups (Figure 4.21).

Mice exposed to LPS (15 mg/kg) also demonstrated reduced blood pressure compared to the control group (86.7 ± 4.9 versus 107.4 ± 4.9 mmHg; $P<0.05$) at the end of 24 hours, which was alleviated by chronic treatment with paeonol (107.0 ± 8.0 mmHg), noggin (105.7 ± 7.1 mmHg) and TAK242 (102.5 ± 7.2 mmHg) (Figure 4.22). Blood pressure of mice exposed to paeonol only (103.4 ± 6.3 mmHg) was similar to control.

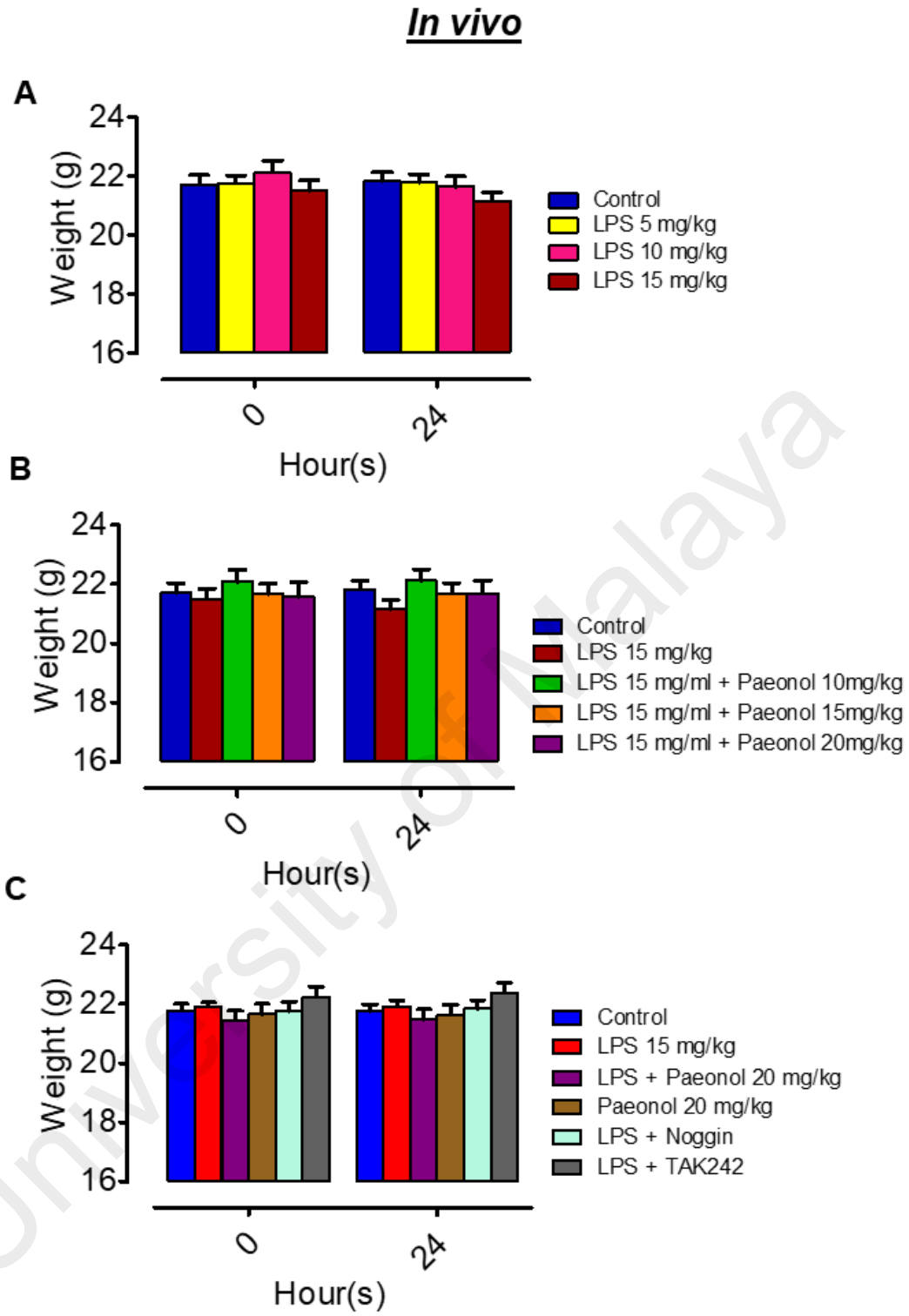

Figure 4.21: Body weight (g) measured in all groups of mice. Results are means ± SEM of seven separate experiments.

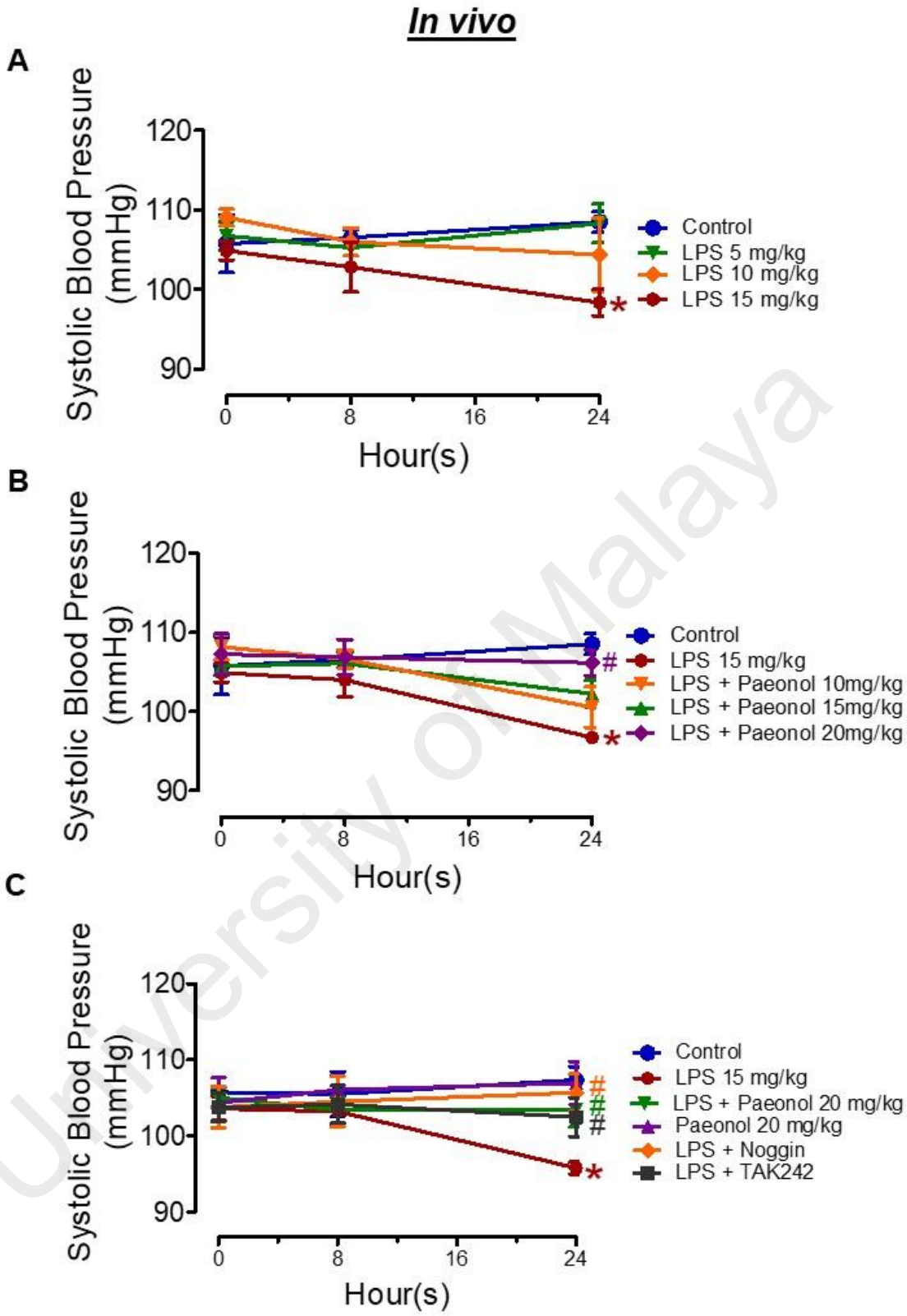

Figure 4.22: Systolic blood pressure (mmHg) measured in all groups of mice. Results are means ± SEM of seven separate experiments. *P< 0.05 compared with control, #P< 0.05 when compared with LPS.

4.3.7 Paeonol protected against LPS-induced endothelial dysfunction *in vivo*

Mice exposed to LPS (5, 10, 15 mg/kg) exhibited attenuated acetylcholine and UK14304-induced relaxations in a dose-dependent manner, with LPS at 15mg/kg being the optimum dose to impair the EDR (Figure 4.23). The impairment was reversed by paeonol co-treatment with paeonol (10, 15, 20 mg/kg) in a dose-dependent manner, with paeonol at 20 mg/kg being the most effective dose (Figure 4.24). Mice treated with paeonol only has similar EDR compared to control (Figure 4.24). Meanwhile, co-treatment with noggin or TAK242 also improved the acetylcholine and UK14304-induced relaxations (Figure 4.25). Sodium nitroprusside-induced relaxations were unchanged in all treatment groups (Figure 4.26).

Mice exposed to LPS also demonstrated increased protein levels of BMP4 (Figure 4.27A), TLR4 (Figure 4.27B), cleaved caspase 3 (Figure 4.27C) and iNOS (Figure 4.27D). These effects were reversed by paeonol, noggin and TAK242.

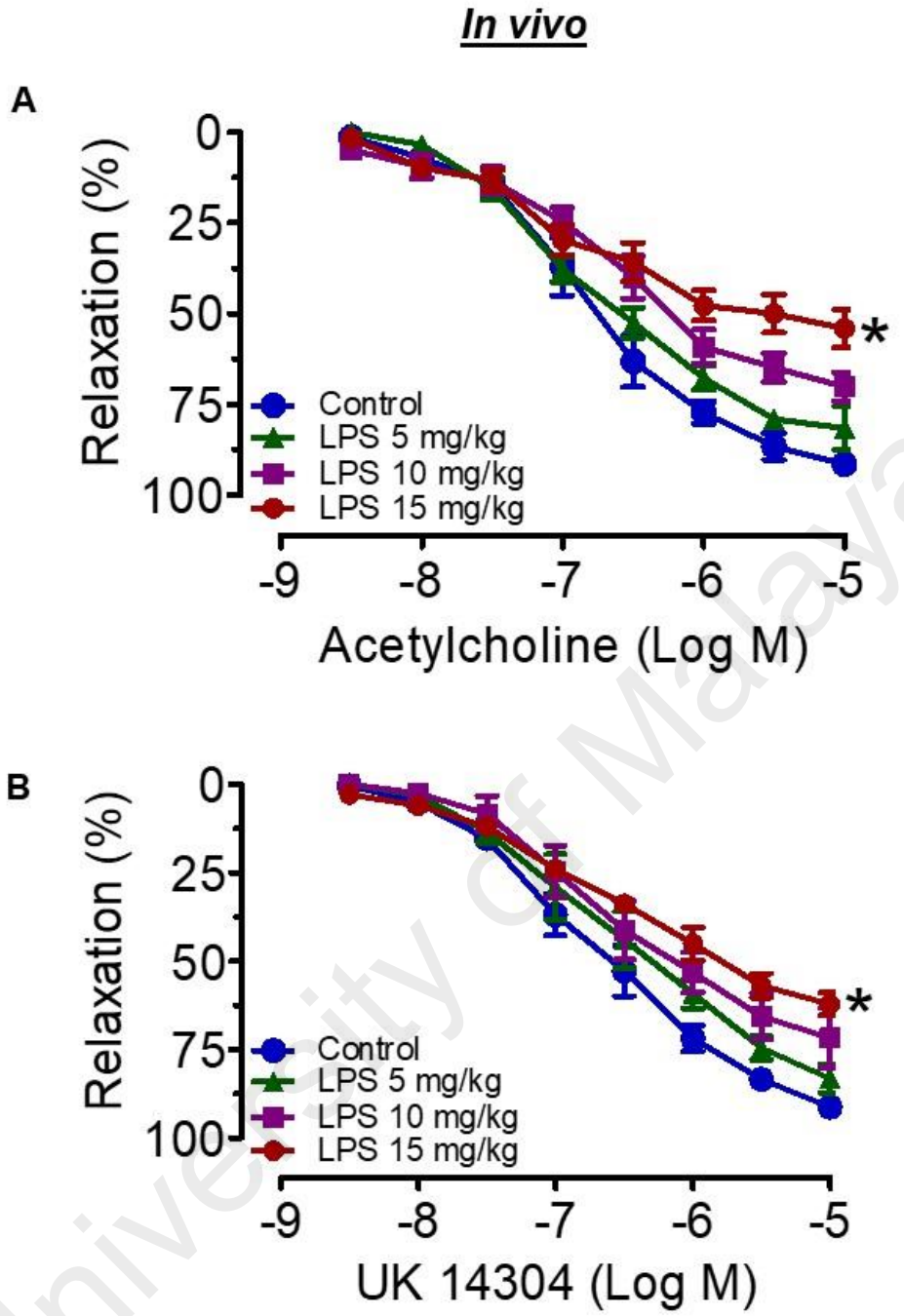

Figure 4.23: The effect of various doses of LPS (5, 10, 15 mg/kg) in impairment of acetylcholine and UK14304-induced endothelium-dependent relaxation (EDR) in C57BL/6J mice. Results are mean ± SEM of six experiments. *P< 0.05 compared with control.

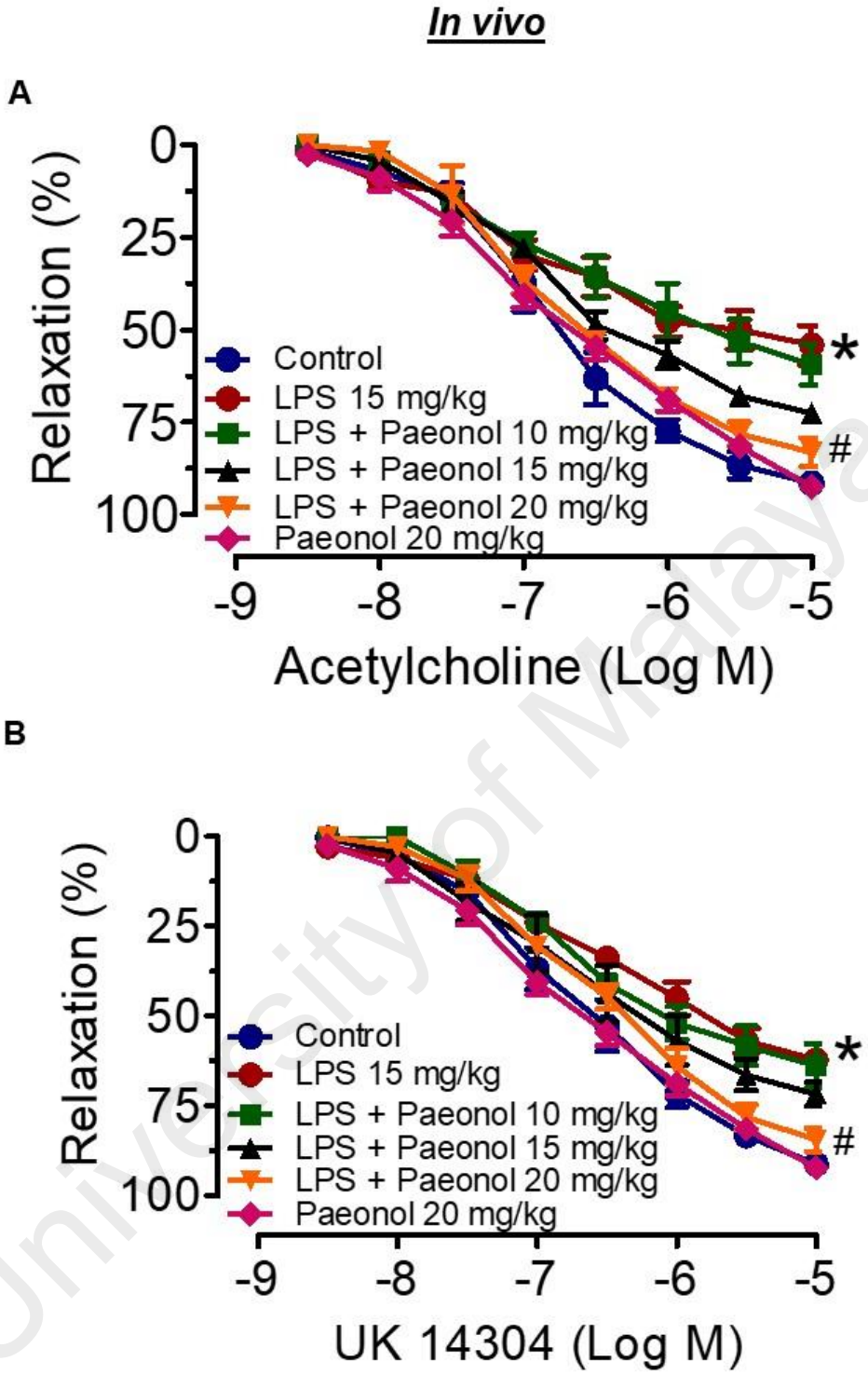

Figure 4.24: **The effect of various doses of paeonol (10, 15, 20 mg/kg) in acetylcholine and UK14304-induced endothelium-dependent relaxation impaired by LPS in C57BL/6J mice.** Results are mean ± SEM of seven experiments. *P< 0.05 compared with control, #P< 0.05 when compared with LPS.

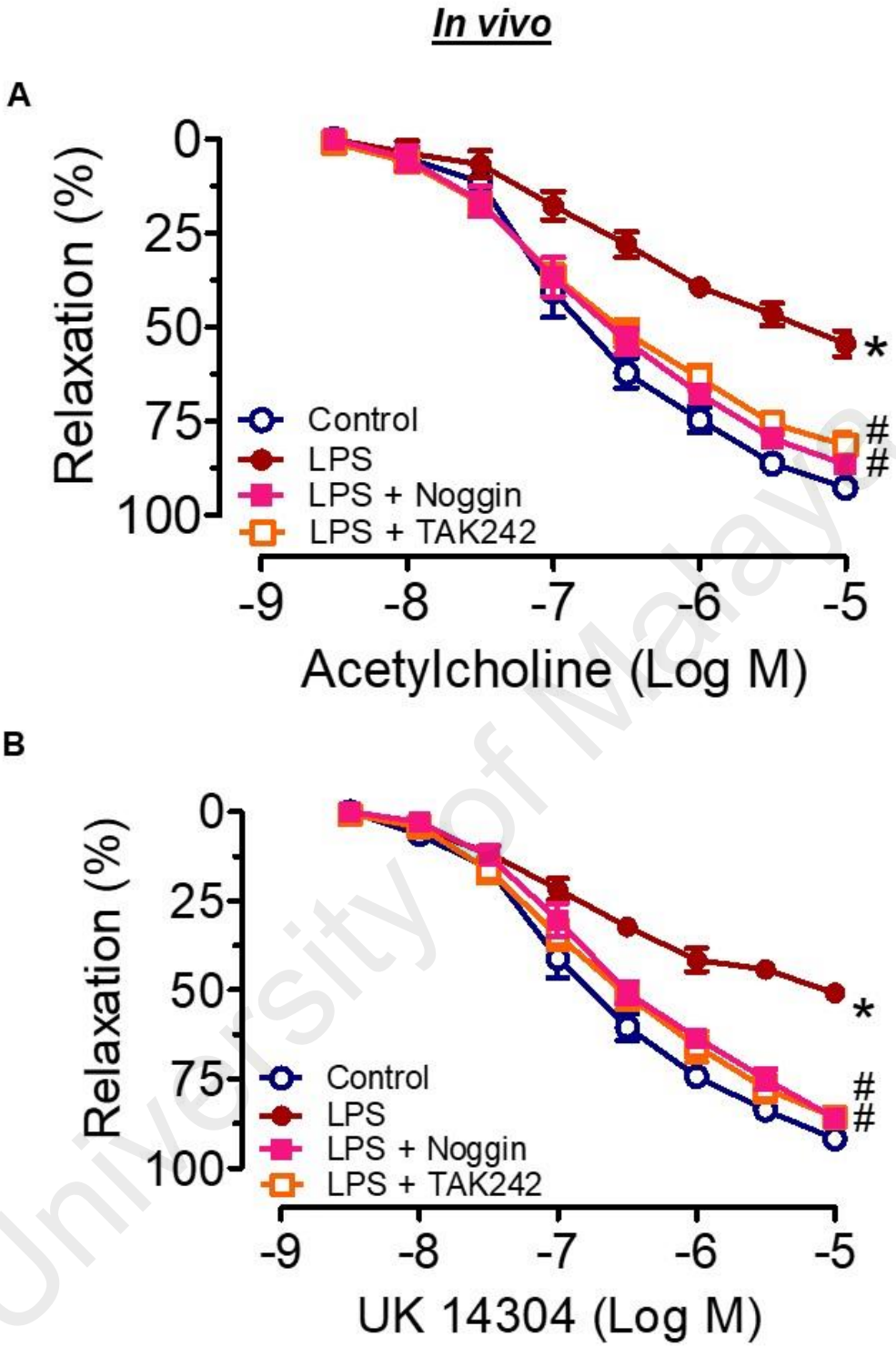

Figure 4.25: The effect of noggin (0.5 mg/kg/day) and TAK242 (3 mg/kg) in acetylcholine and UK14304-induced endothelium-dependent relaxation impaired by LPS in C57BL/6J mice. Results are means ± SEM of seven experiments. *P< 0.05 when compared with control, #P< 0.05 when compared with LPS.

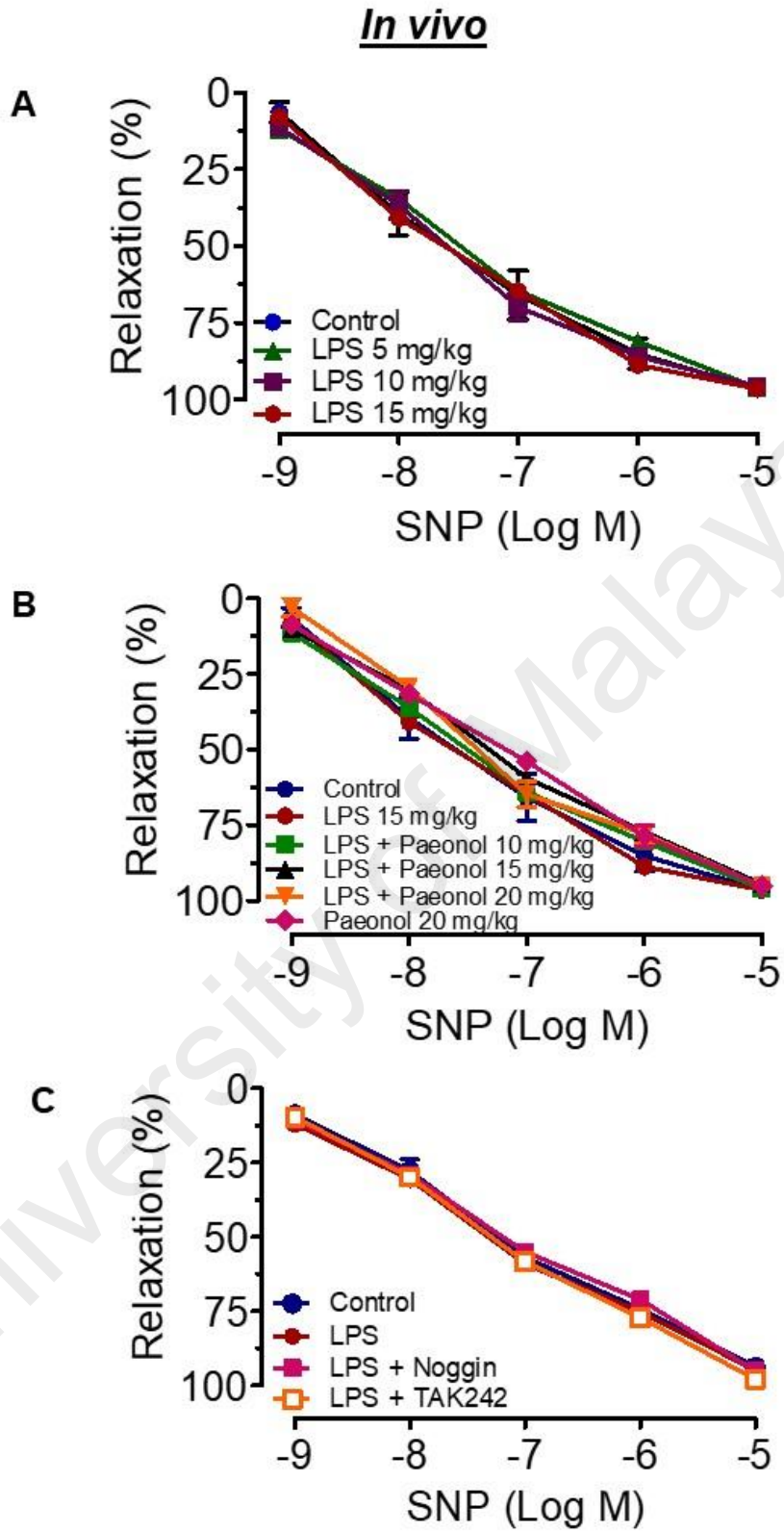

Figure 4.26: Endothelium-independent relaxations induced by SNP were similar in all treatment groups in C57BL/6J mice. Results are means ± SEM of seven experiments.

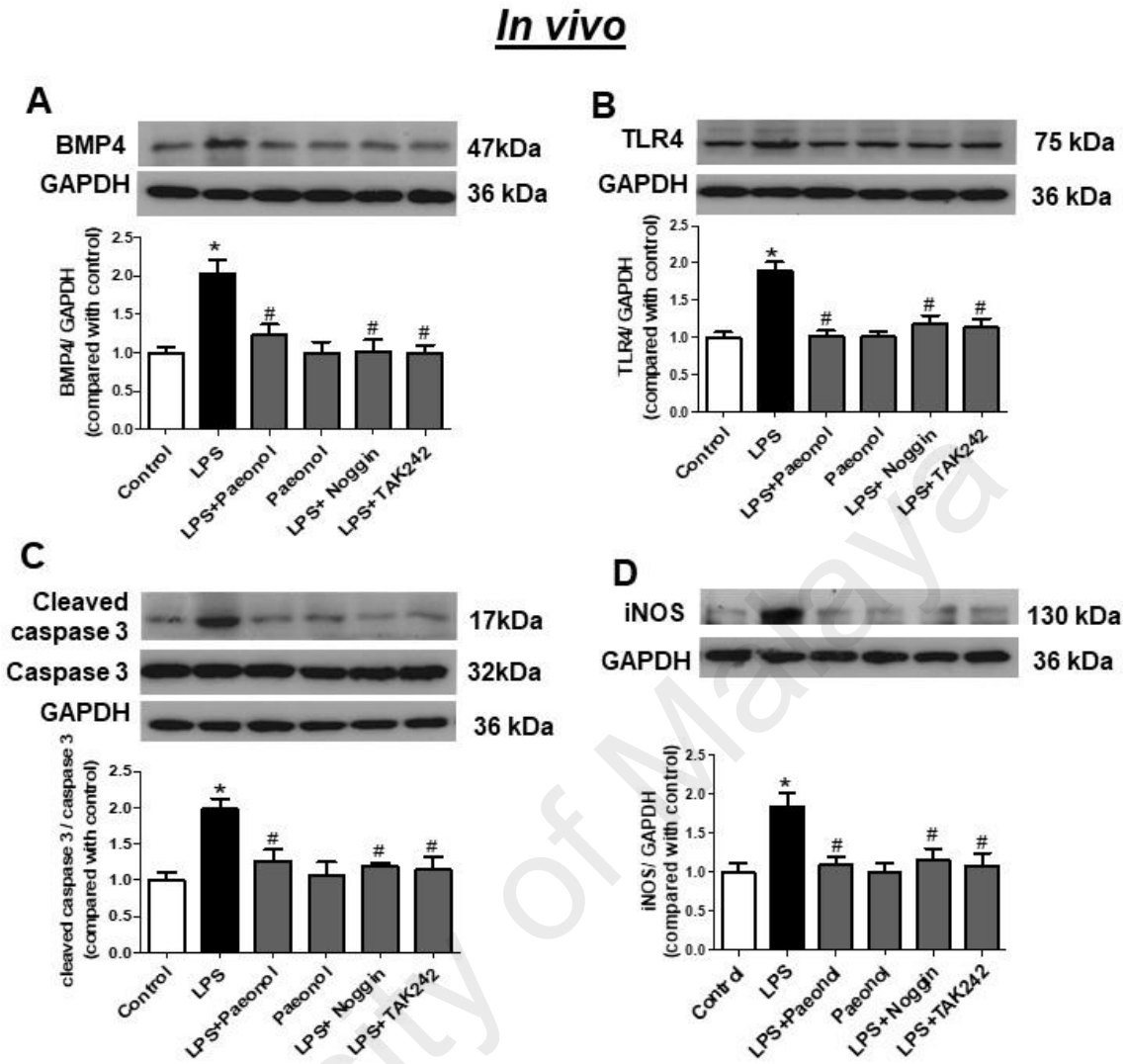

Figure 4.27: Western blots and quantitative data showing (A) BMP4, (B) TLR4, (C) cleaved caspase 3 and (D) iNOS protein in all groups of mice. Results are means ± SEM of seven experiments. *P< 0.05 compared with control, #P< 0.05 when compared with LPS.

4.3.8 Paeonol decreased ROS in HUVECs and mice

Intracellular ROS formation in HUVECs was markedly increased in LPS treated group compared to control group (Figure 4.28). Co-treatment with paeonol, SB202190, SP600125, TAK242, AG, noggin and apocynin normalized the elevated ROS production in LPS treated group in HUVECs. Paeonol treatment alone is similar to the control group.

Mice exposed to LPS *in vivo* showed significant increase in ROS formation and superoxide anion levels in the *en face* endothelium, as shown by the intensity of DHE fluorescence staining (Figure 4.29A & B) and LEC (Figure 4.29C). Co-treatment with paeonol, noggin and TAK242 normalized the LPS-stimulated increase of ROS formation in mice aorta. The ROS level in the paeonol only group was similar to that observed in aortae of the control group in mice. The NADPH oxidase inhibitor, DPI (10 mM) abolished the generation of superoxide anions.

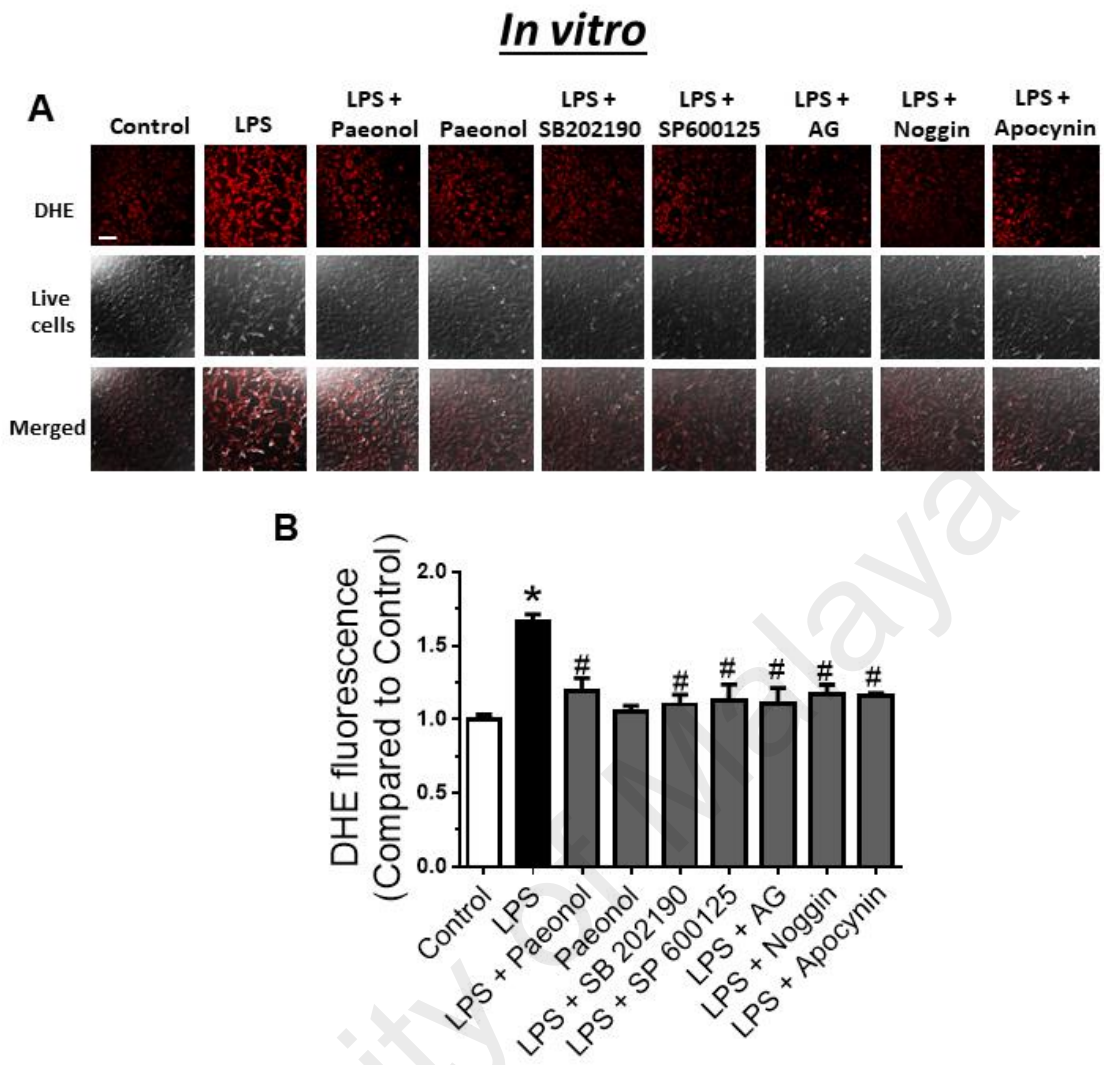

Figure 4.28: Paeonol reduced superoxide production in HUVECs. (A) Representative images and (B) summarized results of superoxide production measured by DHE in HUVECs incubated with LPS (1 µg/mL), paeonol (1 µM), SB202190 (10 µM), SP600125 (10 µM), Aminoguanidine hydrochloride (AG, 100 µM) and Noggin (100 ng/mL) and apocynin (20 µM). Bar: 100 µm. Results are means ± SEM of three separate experiments. *P< 0.05 compared with control, # P< 0.05 compared with LPS.

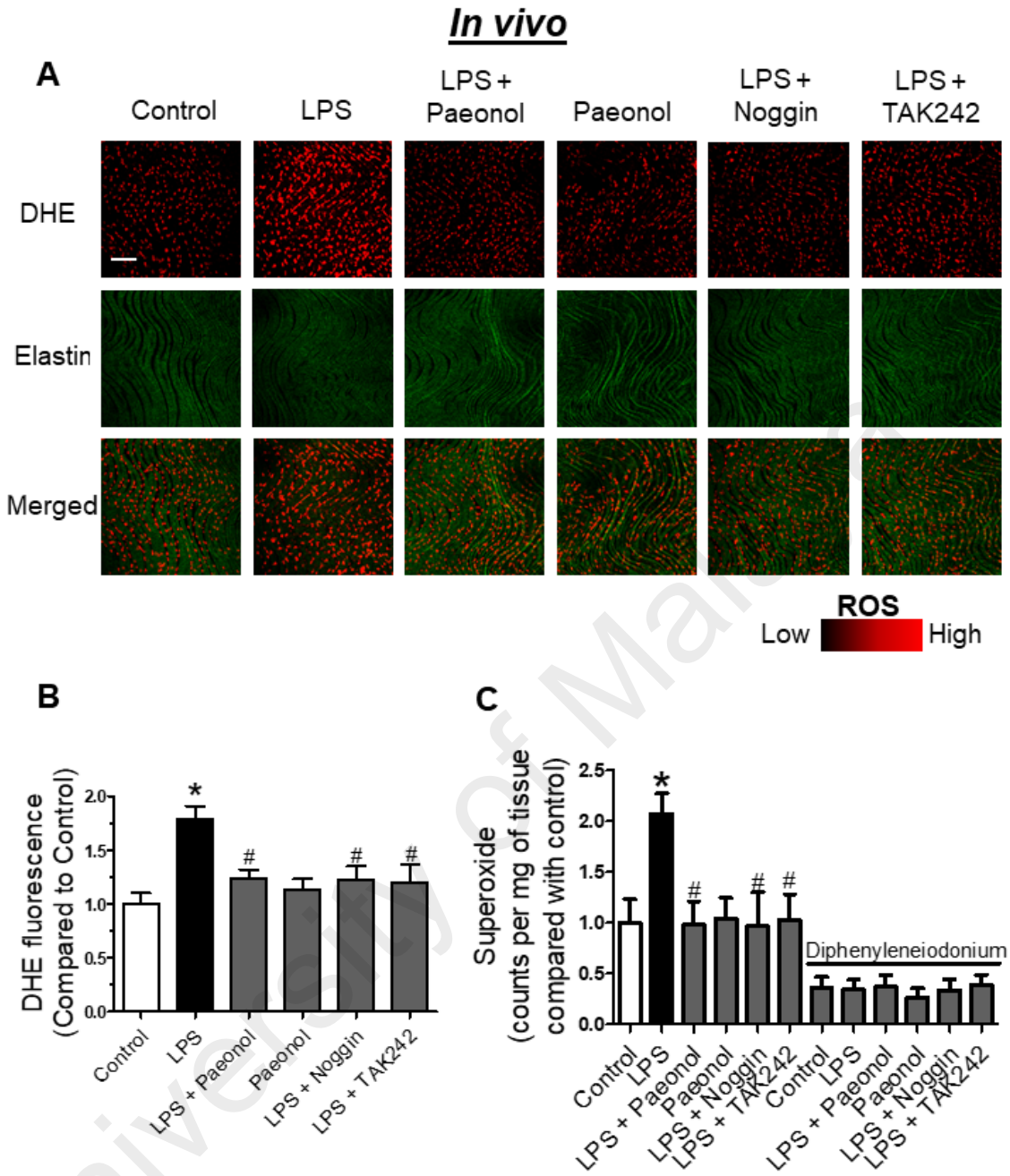

Figure 4.29: Paeonol reduced superoxide production in mouse aorta. Representative images and summarized results of superoxide anion production measured (A & B) in *en face* aortic endothelium with DHE and (C) LEC in the aortae mice treated with LPS, noggin and TAK242 for 24 hours. Red: DHE fluorescence in the nucleus. Green: autofluorescence of elastin underneath the endothelium. Lower panel, merged. Bar: 100 µm. Results are means± SEM of seven experiments. *P< 0.05 compared with control, #P< 0.05 when compared with LPS.

4.3.9 Paeonol reduced NO and cytokines levels in mice treated with LPS

Macrophages will produce nitric oxide when activated by LPS. Nitric oxide can react with oxygen to produce the stable products nitrate and nitrite, which can be determined with Griess reagent. As shown in Figure 4.30, paeonol, noggin and TAK242 suppressed NO production in serum of mice exposed to LPS as measured by total nitrate/nitrite assay.

To investigate the immunosuppressive role of paeonol on the production of cytokines *in vivo*, cytokine levels of IL-6 and TNFα were measured by ELISA. The level of IL-6 (Figure 4.31A) and TNFα (Figure 4.31B) in LPS group increased significantly after LPS was given compared to those in the control group ($P<0.01$). Paeonol, noggin and TAK242 significantly reduced IL-6 and TNFα production compared to those in the LPS group.

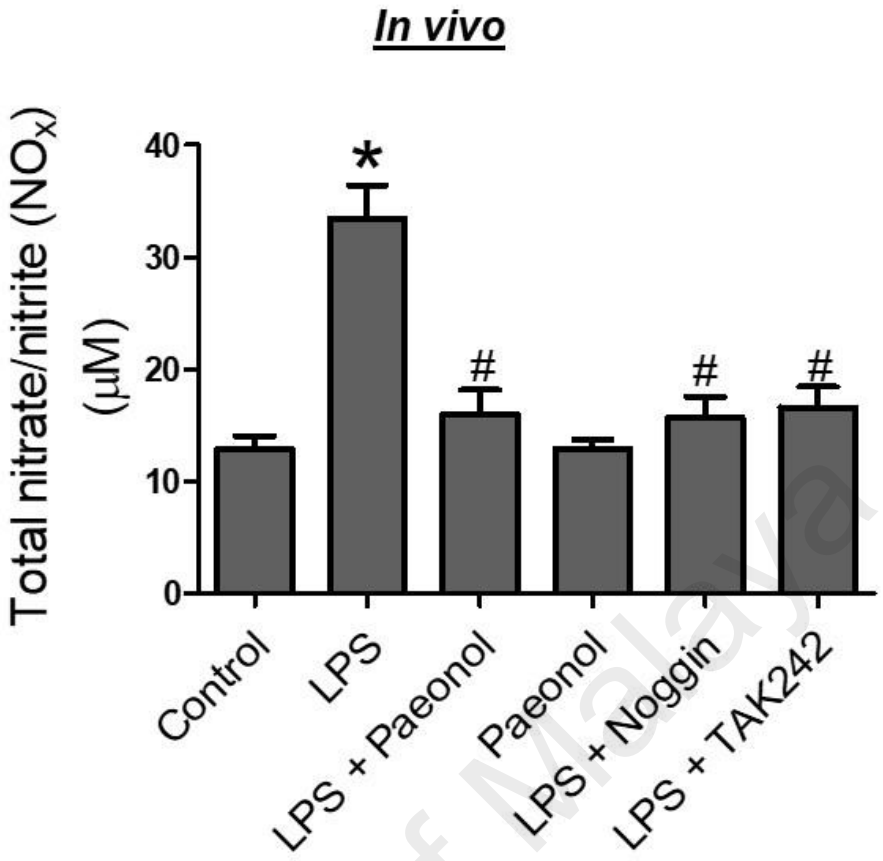

Figure 4.30: Paeonol (20 mg/kg), noggin (0.5 mg/kg) and TAK242 (3 mg/kg) treatment ameliorated serum total nitrite/nitrate level increased by LPS-treated mice as measured by colorimetric assay kit. Data are expressed as means ± SEM of seven experiments. *P< 0.05 compared to control; #P< 0.05 compared to mice induced with LPS.

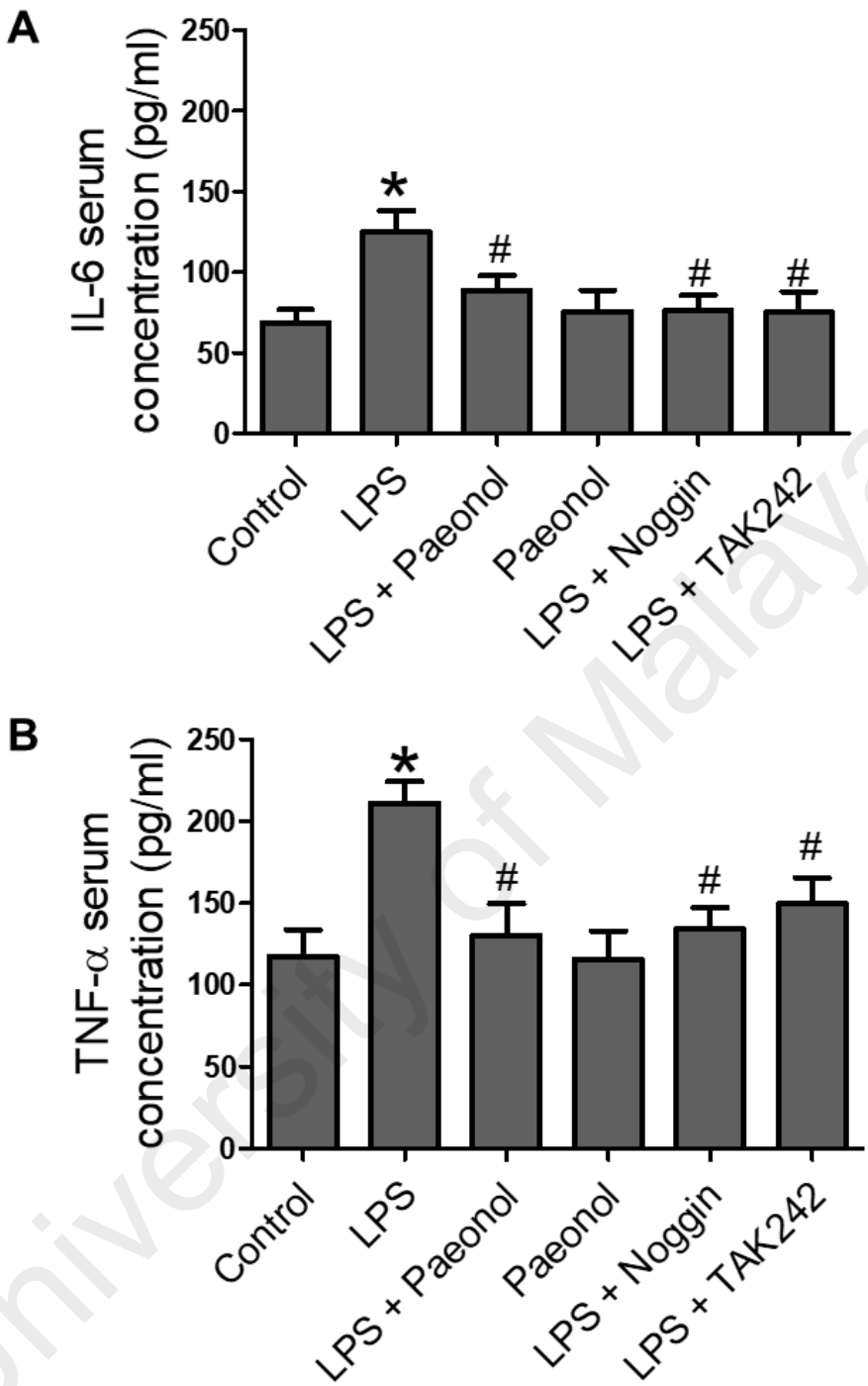

Figure 4.31: Paeonol (20 mg/kg), noggin (0.5 mg/kg) and TAK242 (3 mg/kg) reduced the production of pro-inflammatory cytokines of (A) IL-6 and (B) TNF-α elevated in blood serum of LPS-induced mice. Data are expressed as means ± SEM of six experiments. *P< 0.05 compared to control; #P< 0.05 compared to mice induced with LPS.

4.4 Discussion

Inflammation of endothelial cells leads to endothelial dysfunction and is involved in the pathogenesis of several cardiovascular diseases such as obesity, diabetes mellitus and atherosclerosis (Hung *et al.*, 2017). Controlling inflammation at the level of endothelial cells may efficiently retard or reverse the pathogenetic process (Mako *et al.*, 2010). The present study examined the anti-inflammatory action and mechanism of paeonol in reversing LPS-induced apoptosis and endothelial dysfunction. The major finding of the present study showed that paeonol inhibited LPS-induced apoptosis and endothelial dysfunction through inhibition of both TLR4 and BMP4 signalling pathway independently.

During infection, endothelial cells are constantly exposed to mediators such as bacterial LPS, a highly pro-inflammatory agent and a component of the outer membrane of gram-negative bacteria (Bannerman & Goldblum, 1999). LPS induces apoptosis by activating the TLR4/ROS/MAPK-dependent pathway (Bannerman & Goldblum, 2003; Lee *et al.*, 2012; Zhang *et al.*, 2016). Components of MAPK such as p38 and JNK are activated in response to environmental stress such as apoptosis, whereas ERK is involved in growth responses (Frey & Finlay, 1998; Kacimi *et al.*, 2011). During apoptosis, mitochondrial transmembrane potential is reduced followed by activation of caspase cascade (Bustamante *et al.*, 2004). The present study demonstrated that paeonol reversed LPS-induced apoptosis and depolarized MMP in endothelial cells *in vitro* and *in vivo.* In addition, Western blotting analysis shows that paeonol reduces the presence of BMP4 protein as well as several downstream kinases and transcription factors (JNK, p38 MAPK, iNOS, NOX2), and eventually attenuates the increased in cleaved caspase 3 activated by LPS or BMP4. However, current study showed that paeonol did not reduce H_2O_2-induced cell apoptosis, suggesting that the anti-apoptotic effect of paeonol is mainly due to anti-

inflammatory effect and not the direct consequent of scavenging effect (Bao *et al.*, 2013). H_2O_2-induced oxidative stress in endothelial cells by increasing intracellular superoxide levels through NOS and NADPH oxidase (Coyle *et al.*, 2006). Other studies demonstrated that paeonol reduced the apoptotic activity in cardiac myocytes following myocardial infarction (Li *et al.*, 2016) and suppressed ox-LDL induced endothelial cell apoptosis via initiation of the LOX-1/p38 MAPK/NF-κβ pathway (Bao *et al.*, 2013). Paeonol and danshensu combination attenuates apoptosis in rats with myocardial infarct rats by inhibiting oxidative stress pathway (Li *et al.*, 2016).

One of the prominent feature of inflammatory cardiovascular diseases is endothelial dysfunction (Didion *et al.*, 2004). LPS-induced TLR4 activation elevates adhesion molecules expression that recruits leucocytes (Lee *et al.*, 2012) as well as stimulate NADPH oxidase transcription, leading to elevated oxidative stress and endothelial dysfunction in arteries (Liang *et al.*, 2013b). LPS activate mononuclear phagocytes (monocytes and macrophages) to secrete inflammatory cytokines such as TNF-α and IL-6 (Soromou *et al.*, 2012). TNF-α has a crucial role in endothelial dysfunction in type II diabetic mice by activating the glycation end (AGE) product/receptor of AGE (RAGE) and the nuclear NF-kB signaling pathway (Zhang, 2008). Exogenous IL-6 treatment to C57BL/6J mice caused endothelial dysfunction in aorta through upregulation of angiotensin II type 1 receptor (Wassmann *et al.*, 2004). The interaction of TNF-α and IL-6 impaired endothelium-dependent vasodilation through exacerbation of oxidative stress that subsequent in impairment in NO-mediated signaling pathway (Lee *et al.*, 2017). In our model, mice induced with LPS showed a decreased low blood pressure. This is the effect of LPS-induced low grade inflammation that causes the immune system reacts by generating inflammatory cytokines, leading to a lowered total peripheral resistance of the circulatory system (Ehrentraut *et al.*, 2007). Present study also revealed

that mouse treated with paeonol *in vivo* showed improvement in endothelial function followed by normalization of iNOS, cleaved caspase 3 protein levels, ROS and inflammatory cytokines production increased by LPS. By inhibiting LPS-induced exaggerated NO production by iNOS, paeonol may additionally restore eNOS activity and improve endothelial function. Our result is in accordance with previous literature which stated that iNOS-generated NO exerts an inhibitory effect on eNOS and suppresses guanylate cyclase activity, thus induces endothelial dysfunction (Chauhan *et al.*, 2003). In addition, our study demonstrated *ex vivo* co-incubation with indomethacin (COX inhibitor) did not improve LPS-induced endothelial dysfunction in mouse thoracic aorta as reported previously (Franchi-Micheli *et al.*, 2000), suggesting that LPS signalling pathway is not dependent on COX (Wang *et al.*, 2009). The potent vasodilatory effect of paeonol was also reported via voltage-dependent and receptor-operated Ca^{2+} channel as well as intracellular Ca^{2+} release inhibition (Li *et al.*, 2010b). Chronic exposure of paeonol improved vascular reactivity in the cerebral basilar artery of diabetic rats through the reduction of oxidative stress and intracellular Ca^{2+} regulatory mechanisms (Hu *et al.*, 2012).

One of the sources of LPS-induced apoptosis in endothelial cells is the NADPH oxidase derived ROS, especially NOX 1, NOX 2, and NOX 4 (Basuroy *et al.*, 2009; Li *et al.*, 2007; Quagliaro *et al.*, 2003). Through the regulation of ROS in endothelial cells, MAPKs signalling components especially p38 MAPK and JNK/SAPK induce inflammation and cell apoptosis upon stress stimuli (Griendling *et al.*, 2000; Junttila *et al.*, 2008). In this study, paeonol reduced LPS and BMP4-induced NOX 2 protein up-regulation and superoxide production. These effects of paeonol are comparable to the effect of apocynin, which suggests that paeonol reduced apoptosis by scavenging free radicals, a consequences of its inhibitory effect on TLR4 and BMP4. Earlier performed

studies have also supported the potency of paeonol as a scavenger of different free radicals observed in several biological models (Ding *et al.*, 2016; Liu *et al.*, 2013; Matsuda *et al.*, 2001). Previous literature showed that paeonol reduced oxidative stress, inflammation, and fibrosis in the lungs induced by bleomycin *in vivo* and the suppression of the TGF-β1-induced fibrotic responses *in vitro* through inhibition of MAPKs/ SMAD3 signalling (Liu *et al.*, 2017).

BMP4 can be stimulated during oscillatory shear stress in endothelial cells (Sorescu *et al.*, 2003). BMP4 also induce local pro-inflammatory responses and is expressed abundantly in the myocardial tissue and aortae in obese mice (Wu *et al.*, 2015). Current result revealed that LPS-induced apoptosis and endothelial dysfunction is mediated through BMP4 in endothelial cells and mouse aorta based on the following observations: (a) LPS-induced up-regulation of BMP4 and BMPR1A was inhibited by noggin, (b) inhibition of BMP4 reduced LPS-induced inflammation and apoptosis; and (c) co-treatment with noggin improved acetylcholine and UK14304-induced relaxations following LPS treatment *ex vivo* and *in vivo*. In addition, silencing of BMP4 does not affect the LPS-induced upregulation of TLR4. Similarly, silencing of TLR4 inhibited LPS-induced apoptosis without affecting the LPS-induced augmentation of BMP4. This suggest that LPS mediated BMP4 up-regulation is independent of TLR4. Silencing of BMP4 and TLR4 abolished the effects of paeonol on LPS-induced up-regulation of cleaved caspase 3, which confirmed that paeonol protect endothelial cells against LPS-induced inflammation and apoptosis through BMP4 and TLR4 signalling independently.

4.5 Conclusion

In conclusion, paeonol reduced LPS-induced apoptosis and endothelial dysfunction by inhibiting independently both BMP4 and TLR4, subsequently reducing ROS and iNOS-

induced NO production as well as improving eNOS activity (Figure 4.32). The present findings provide a potential therapeutic use of paeonol to improve endothelial function during inflammation-related diseases by pharmacological modulation of either BMP4 or TLR4 activation.

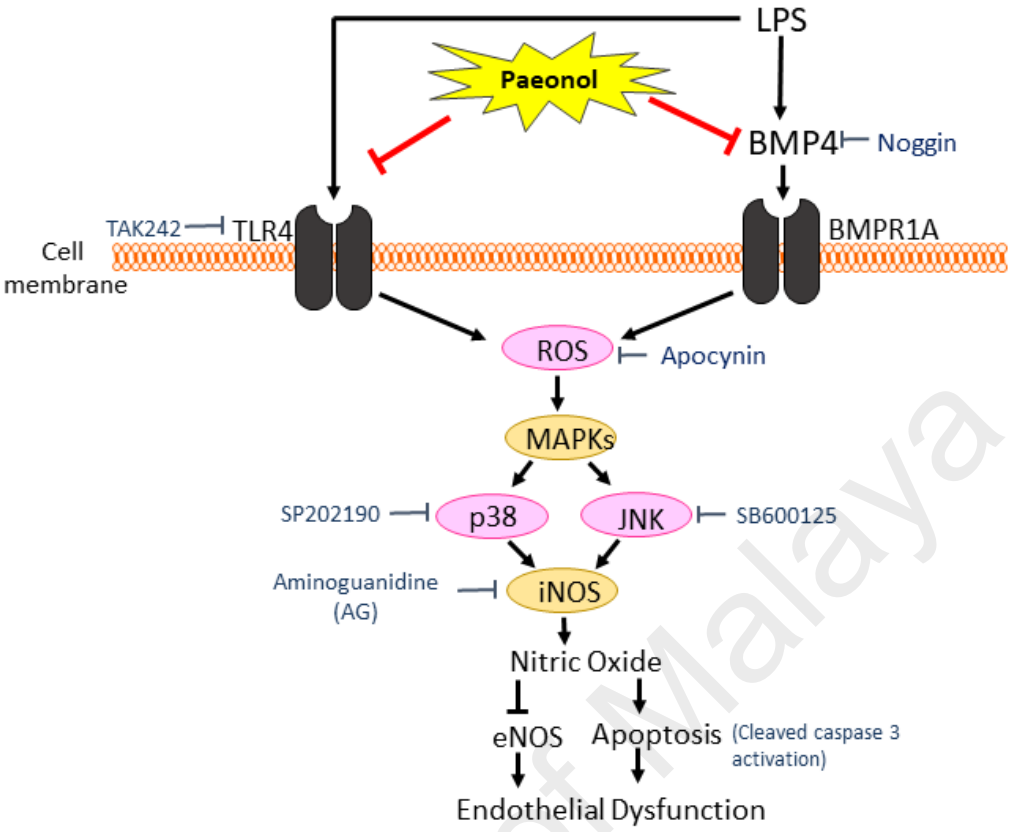

Figure 4.32: Diagram showing that paeonol treatment alleviates LPS-induced apoptosis and endothelial dysfunction *via* the TLR4 and BMP4 signalling pathways. The response to LPS is mediated *via* BMP4 activation independently of TLR4. LPS, lipopolysaccharides; BMP4, bone morphogenic protein 4; BMPR1A, bone morphogenetic protein receptor type IA; ROS, reactive oxygen species; MAPK, mitogen-activated protein kinases; iNOS, inducible nitric oxide synthase; eNOS, endothelial nitric oxide synthase.

CHAPTER 5: GENERAL CONCLUSION

ER stress and inflammation have been associated with augmentation of ROS and reduced NO bioavailability, leading to attenuation of EDR in blood vessels. The present study highlights the pharmacological effects of paeonol against ER stress and inflammation-induced endothelial dysfunction.

The first part of the study focused on the effects of paeonol against endothelial dysfunction induced by ER stress. Induction of ER stress by tunicamycin attenuated EDR in mouse aortas, leading to ROS over-production, and diminished NO production in the endothelial cells. Paeonol restored the impaired EDR *ex vivo* and *in vivo* through inhibition of ER stress in C57BL/6J and PPARδ WT mouse aorta, but not in PPARδ KO mouse aorta. Treatment with PPARδ antagonist, GSK0660 and AMPK antagonist, compound C abolished the protective effects of paeonol in HUVECs and C57BL/6J mouse aorta. Chronic treatment of paeonol reduced the elevated blood pressure induced by tunicamycin through a ROS-dependent mechanism; this is confirmed with the use of pharmacological ROS scavenger, tempol which prevented tunicamycin-induced up-regulation of ROS. These findings propose that paeonol protects against tunicamycin-induced endothelial dysfunction in mice via activation of AMPK/PPARδ pathway, thus inhibit ER stress and oxidative stress as well as augment NO bioavailability.

The second part of the study focused on the effects of paeonol against LPS-induced apoptosis and endothelial dysfunction. Exposure of HUVECs and C57BL/6J mouse aorta to LPS resulted in increased apoptosis and inflammatory markers, thus leading to impairment of EDR. We observed that paeonol reduced the TLR4 and BMP4 proteins increased by LPS exposure in HUVECs and mouse aortas. We demonstrated that in

addition of blocking TLR4 pathway, paeonol also reversed LPS induced-endothelial dysfunction and apoptosis by inhibiting BMP4 pathway. Our study demonstrated that silencing of TLR4 didn't affect the inhibitory effect of paeonol on BMP4 signalling pathway upon the exposure of LPS, suggesting that paeonol works against these two pathways independently. The current findings imply that paeonol reduces LPS-induced endothelial dysfunction and cell apoptosis by inhibiting BMP4 signalling independent of TLR4.

To summarize, the present investigation demonstrated the protective effects of paeonol in improving endothelial function via several mechanism including activation of AMPK/PPARδ to inhibit ER stress as well as inhibition of BMP4 and TLR4 signalling pathways to reduce vascular inflammation. These pharmacological actions of paeonol collectively reverse the imbalanced productions between ROS and NO, and improve the EDR. The present results further support the potential use of paeonol as a natural and effective antioxidant and anti-inflammatory agent which may protect against endothelial dysfunction associated with ER stress and inflammation.

Although the present study supports an endothelial protective effect of paeonol against ER stress and inflammation-induced endothelial dysfunction, there are several considerations which need to be further researched. Firstly, the effect of paeonol treatment in improving EDR may not reflect the overall effects of its treatment, as endothelium-dependant contraction may also play a role in the control of vascular tone. Further studies involving endothelial-dependent contractions should be incorporated to provide better understanding on the role of paeonol in improving the endothelial function. Effects of paeonol on other vascular modalities such as arterial stiffness, endothelial permeability or blood flow may similarly affect endothelial function and thus should be

investigated in future studies. Secondly, cells in our *in vitro* study are grown in monolayer with controlled environment and are devoid of influence of other cells in the proximity such as the absent of biological interactions between endothelial and vascular smooth muscle cells. These may not mimic the anatomical structure in the blood vessels which consists of various layers of cells. Therefore, the potential endothelial protective effect of paeonol could be further explore in 3D co-culture *in vitro* model using isolated primary endothelial cells and vascular smooth muscle cells from blood vessel of patients with other disease model such as diabetes mellitus or obesity which are also associated with altered vascular function. Thirdly, paeonol absorption, distribution and toxicity in whole animals *in vivo* are much lacking. To address this, pharmacokinetic and pharmacodynamics effect of paeonol during *in vivo* study should be performed further to enhance the discovery and development of paeonol as the potential therapeutic agent. In addition, further study should investigate the effects of other possible mechanism to support the potential of paeonol as a multi-target drug, including other mechanism such as autophagy and calcium signalling pathways. Finally, the synergistic effects of paeonol in combination with current drugs for cardiovascular disease related to ER stress and inflammation remains to be investigated.

REFERENCES

Acosta-Alvear, D., Zhou, Y., Blais, A., Tsikitis, M., Lents, N. H., Arias, C., Lennon, C. J., Kluger, Y., & Dynlacht, B. D. (2007). XBP1 controls diverse cell type- and condition-specific transcriptional regulatory networks. *Mol Cell, 27*(1), 53-66.

Aktan, F. (2004). iNOS-mediated nitric oxide production and its regulation. *Life Sci, 75*(6), 639-653.

Aliprantis, A. O., Yang, R. B., Weiss, D. S., Godowski, P., & Zychlinsky, A. (2000). The apoptotic signaling pathway activated by Toll-like receptor-2. *Embo J, 19*(13), 3325-3336.

Aljada, A. (2003). Endothelium, inflammation, and diabetes. *Metab Syndr Relat Disord, 1*(1), 3-21.

Assaly, R., Olson, D., Hammersley, J., Fan, P. S., Liu, J., Shapiro, J. I., & Kahaleh, M. B. (2001). Initial evidence of endothelial cell apoptosis as a mechanism of systemic capillary leak syndrome. *Chest, 120*(4), 1301-1308.

Augustin, H. G., Kozian, D. H., & Johnson, R. C. (1994). Differentiation of endothelial cells: analysis of the constitutive and activated endothelial cell phenotypes. *Bioessays, 16*(12), 901-906.

Babior, B. M. (2004). NADPH oxidase. *Curr Opin Immunol, 16*(1), 42-47.

Bannerman, D. D., & Goldblum, S. E. (1999). Direct effects of endotoxin on the endothelium: barrier function and injury. *Lab Invest, 79*(10), 1181-1199.

Bannerman, D. D., & Goldblum, S. E. (2003). Mechanisms of bacterial lipopolysaccharide-induced endothelial apoptosis. *Am J Physiol Lung Cell Mol Physiol, 284*(6), L899-914.

Bao, M. H., Zhang, Y. W., & Zhou, H. H. (2013). Paeonol suppresses oxidized low-density lipoprotein induced endothelial cell apoptosis via activation of LOX-1/p38MAPK/NF-kappaB pathway. *J Ethnopharmacol, 146*(2), 543-551.

Baradaran, A., Nasri, H., & Rafieian-Kopaei, M. (2014). Oxidative stress and hypertension: Possibility of hypertension therapy with antioxidants. *J Res Med Sci, 19*(4), 358-367.

Barish, G. D., Atkins, A. R., Downes, M., Olson, P., Chong, L. W., Nelson, M., Zou, Y., Hwang, H., Kang, H., Curtiss, L., Evans, R. M., & Lee, C. H. (2008). PPARdelta regulates multiple proinflammatory pathways to suppress atherosclerosis. *Proc Natl Acad Sci U S A, 105*(11), 4271-4276.

Barton, M., Shaw, S., d'Uscio, L. V., Moreau, P., & Luscher, T. F. (1997). Angiotensin II increases vascular and renal endothelin-1 and functional endothelin converting enzyme activity in vivo: role of ETA receptors for endothelin regulation. *Biochem Biophys Res Commun, 238*(3), 861-865.

Bassenge, E., Busse, R., & Pohl, U. (1988). Release of Endothelium-Derived Relaxing Factor(s) by Physicochemical Stimuli. In P. M. Vanhoutte (Ed.), *Relaxing and Contracting Factors: Biological and Clinical Research* (pp. 189-217). Totowa, NJ: Humana Press.

Basuroy, S., Bhattacharya, S., Leffler, C. W., & Parfenova, H. (2009). Nox4 NADPH oxidase mediates oxidative stress and apoptosis caused by TNF-alpha in cerebral vascular endothelial cells. *Am J Physiol Cell Physiol, 296*(3), C422-432.

Battson, M. L., Lee, D. M., & Gentile, C. L. (2017). Endoplasmic reticulum stress and the development of endothelial dysfunction. *American Journal of Physiology - Heart and Circulatory Physiology, 312*(3), H355-H367.

Bernales, S., Papa, F. R., & Walter, P. (2006). Intracellular signaling by the unfolded protein response. *Annu Rev Cell Dev Biol, 22*, 487-508.

Bhandary, B., Marahatta, A., Kim, H. R., & Chae, H. J. (2012). An involvement of oxidative stress in endoplasmic reticulum stress and its associated diseases. *Int J Mol Sci, 14*(1), 434-456.

Bijl, M. (2003). Endothelial activation, endothelial dysfunction and premature atherosclerosis in systemic autoimmune diseases. *Neth J Med, 61*(9), 273-277.

Bojic, L. A., & Huff, M. W. (2013). Peroxisome proliferator-activated receptor delta: a multifaceted metabolic player. *Curr Opin Lipidol, 24*(2), 171-177.

Bolisetty, S., & Jaimes, E. A. (2013). Mitochondria and reactive oxygen species: physiology and pathophysiology. *Int J Mol Sci, 14*(3), 6306-6344.

Bonfoco, E., Krainc, D., Ankarcrona, M., Nicotera, P., & Lipton, S. A. (1995). Apoptosis and necrosis: two distinct events induced, respectively, by mild and intense insults with N-methyl-D-aspartate or nitric oxide/superoxide in cortical cell cultures. *Proc Natl Acad Sci U S A, 92*(16), 7162-7166.

Bos, C. L., Richel, D. J., Ritsema, T., Peppelenbosch, M. P., & Versteeg, H. H. (2004). Prostanoids and prostanoid receptors in signal transduction. *Int J Biochem Cell Biol, 36*(7), 1187-1205.

Bostrom, K. I., Jumabay, M., Matveyenko, A., Nicholas, S. B., & Yao, Y. (2011). Activation of vascular bone morphogenetic protein signaling in diabetes mellitus. *Circ Res, 108*(4), 446-457.

Boulanger, C. M., Morrison, K. J., & Vanhoutte, P. M. (1994). Mediation by M3-muscarinic receptors of both endothelium-dependent contraction and relaxation to acetylcholine in the aorta of the spontaneously hypertensive rat. *Br J Pharmacol, 112*(2), 519-524.

Bowyer, D. E., Davies, P. F., Reidy, M. A., Goode, T. B., & Green, E. S. (1977). Scanning electron microscopy of arterial endothelium. *Prog Biochem Pharmacol, 13*, 164-170.

Braakman, I., & Bulleid, N. J. (2011). Protein folding and modification in the mammalian endoplasmic reticulum. *Annu Rev Biochem, 80*, 71-99.

Brozovic, A., Vukovic, L., Polancac, D. S., Arany, I., Koberle, B., Fritz, G., Fiket, Z., Majhen, D., Ambriovic-Ristov, A., & Osmak, M. (2013). Endoplasmic reticulum stress is involved in the response of human laryngeal carcinoma cells to Carboplatin but is absent in Carboplatin-resistant cells. *PLoS One, 8*(9), e76397.

Bustamante, J., Caldas Lopes, E., Garcia, M., Di Libero, E., Alvarez, E., & Hajos, S. E. (2004). Disruption of mitochondrial membrane potential during apoptosis induced by PSC 833 and CsA in multidrug-resistant lymphoid leukemia. *Toxicol Appl Pharmacol, 199*(1), 44-51.

Cahill, P. A., & Redmond, E. M. (2016). Vascular endothelium – Gatekeeper of vessel health. *Atherosclerosis, 248*, 97-109.

Cai, H. (2005). Hydrogen peroxide regulation of endothelial function: origins, mechanisms, and consequences. *Cardiovasc Res, 68*(1), 26-36.

Cai, H., & Harrison, D. G. (2000). Endothelial dysfunction in cardiovascular diseases: the role of oxidant stress. *Circ Res, 87*(10), 840-844.

Cai, J., Pardali, E., Sanchez-Duffhues, G., & ten Dijke, P. (2012). BMP signaling in vascular diseases. *FEBS Lett, 586*(14), 1993-2002.

Cakir, Y., & Ballinger, S. W. (2005). Reactive species-mediated regulation of cell signaling and the cell cycle: the role of MAPK. *Antioxid Redox Signal, 7*(5-6), 726-740.

Cannon, R. O., 3rd. (1998). Role of nitric oxide in cardiovascular disease: focus on the endothelium. *Clin Chem, 44*(8 Pt 2), 1809-1819.

Cao, M., Tong, Y., Lv, Q., Chen, X., Long, Y., Jiang, L., Wan, J., Zhang, Y., Zhang, F., & Tong, N. (2012). PPARdelta Activation Rescues Pancreatic beta-Cell Line INS-1E from Palmitate-Induced Endoplasmic Reticulum Stress through Enhanced Fatty Acid Oxidation. *PPAR Res, 2012*, 680684.

Cao, S. S., & Kaufman, R. J. (2014). Endoplasmic reticulum stress and oxidative stress in cell fate decision and human disease. *Antioxid Redox Signal, 21*(3), 396-413.

Cao, S. S., Luo, K. L., & Shi, L. (2016). Endoplasmic Reticulum Stress Interacts With Inflammation in Human Diseases. *J Cell Physiol, 231*(2), 288-294.

Caso, J. R., Pradillo, J. M., Hurtado, O., Lorenzo, P., Moro, M. A., & Lizasoain, I. (2007). Toll-like receptor 4 is involved in brain damage and inflammation after experimental stroke. *Circulation, 115*(12), 1599-1608.

Chakravortty, D., Koide, N., Kato, Y., Sugiyama, T., Kawai, M., Fukada, M., Yoshida, T., & Yokochi, T. (2000). Cytoskeletal alterations in lipopolysaccharide-induced bovine vascular endothelial cell injury and its prevention by sodium arsenite. *Clin Diagn Lab Immunol, 7*(2), 218-225.

Chang, K., Weiss, D., Suo, J., Vega, J. D., Giddens, D., Taylor, W. R., & Jo, H. (2007). Bone morphogenic protein antagonists are coexpressed with bone morphogenic protein 4 in endothelial cells exposed to unstable flow in vitro in mouse aortas and in human coronary arteries: role of bone morphogenic protein antagonists in inflammation and atherosclerosis. *Circulation, 116*(11), 1258-1266.

Chauhan, S. D., Seggara, G., Vo, P. A., Macallister, R. J., Hobbs, A. J., & Ahluwalia, A. (2003). Protection against lipopolysaccharide-induced endothelial dysfunction in resistance and conduit vasculature of iNOS knockout mice. *Faseb j, 17*(6), 773-775.

Cheang, W. S., Tian, X. Y., Wong, W. T., Lau, C. W., Lee, S. S., Chen, Z. Y., Yao, X., Wang, N., & Huang, Y. (2014). Metformin protects endothelial function in diet-induced obese mice by inhibition of endoplasmic reticulum stress through 5' adenosine monophosphate-activated protein kinase-peroxisome proliferator-activated receptor delta pathway. *Arterioscler Thromb Vasc Biol, 34*(4), 830-836.

Chen, D., Zhao, M., & Mundy, G. R. (2004). Bone morphogenetic proteins. *Growth Factors, 22*(4), 233-241.

Choi, K. B., Wong, F., Harlan, J. M., Chaudhary, P. M., Hood, L., & Karsan, A. (1998). Lipopolysaccharide mediates endothelial apoptosis by a FADD-dependent pathway. *J Biol Chem, 273*(32), 20185-20188.

Choi, S. K., Lim, M., Byeon, S. H., & Lee, Y. H. (2016). Inhibition of endoplasmic reticulum stress improves coronary artery function in the spontaneously hypertensive rats. *Sci Rep, 6*, 31925.

Choy, K. W., Lau, Y. S., Murugan, D., & Mustafa, M. R. (2017). Chronic treatment with paeonol improves endothelial function in mice through inhibition of endoplasmic reticulum stress-mediated oxidative stress. *PLoS One, 12*(5), 1-18.

Choy, K. W., Mustafa, M. R., Lau, Y. S., Liu, J., Murugan, D., Lau, C. W., Wang, L., Zhao, L., & Huang, Y. (2016). Paeonol protects against endoplasmic reticulum stress-induced endothelial dysfunction via AMPK/PPARdelta signaling pathway. *Biochem Pharmacol, 116*, 51-62.

Chuaiphichai, S., Starr, A., Nandi, M., Channon, K. M., & McNeill, E. (2016). Endothelial cell tetrahydrobiopterin deficiency attenuates LPS-induced vascular dysfunction and hypotension. *Vascul Pharmacol, 77*, 69-79.

Cines, D. B., Pollak, E. S., Buck, C. A., Loscalzo, J., Zimmerman, G. A., McEver, R. P., Pober, J. S., Wick, T. M., Konkle, B. A., Schwartz, B. S., Barnathan, E. S., McCrae, K. R., Hug, B. A., Schmidt, A. M., & Stern, D. M. (1998). Endothelial cells in physiology and in the pathophysiology of vascular disorders. *Blood, 91*(10), 3527-3561.

Coyle, C. H., Martinez, L. J., Coleman, M. C., Spitz, D. R., Weintraub, N. L., & Kader, K. N. (2006). Mechanisms of H2O2-induced oxidative stress in endothelial cells. *Free Radic Biol Med, 40*(12), 2206-2213.

Csiszar, A., Ahmad, M., Smith, K. E., Labinskyy, N., Gao, Q., Kaley, G., Edwards, J. G., Wolin, M. S., & Ungvari, Z. (2006). Bone morphogenetic protein-2 induces proinflammatory endothelial phenotype. *Am J Pathol, 168*(2), 629-638.

Csiszar, A., Labinskyy, N., Smith, K. E., Rivera, A., Bakker, E. N., Jo, H., Gardner, J., Orosz, Z., & Ungvari, Z. (2007). Downregulation of bone morphogenetic protein 4 expression in coronary arterial endothelial cells: role of shear stress and the cAMP/protein kinase A pathway. *Arterioscler Thromb Vasc Biol, 27*(4), 776-782.

Cullinan, S. B., Zhang, D., Hannink, M., Arvisais, E., Kaufman, R. J., & Diehl, J. A. (2003). Nrf2 is a direct PERK substrate and effector of PERK-dependent cell survival. *Mol Cell Biol, 23*(20), 7198-7209.

Cuschleri, J., Gourlay, D., Garcia, I., Jelacic, S., & Maier, R. V. (2003). Endotoxin-induced endothelial cell proinflammatory phenotypic differentiation requires stress fiber polymerization. *Shock, 19*(5), 433-439.

Dalman, R. L., & Porter, J. M. (1990). The endothelium: Modulator of cardiovascular function. *Journal of Vascular Surgery, 17*(2), 457.

Davis, B. J., Xie, Z., Viollet, B., & Zou, M. H. (2006). Activation of the AMP-activated kinase by antidiabetes drug metformin stimulates nitric oxide synthesis in vivo by promoting the association of heat shock protein 90 and endothelial nitric oxide synthase. *Diabetes, 55*(2), 496-505.

Davis, C., Fischer, J., Ley, K., & Sarembock, I. J. (2003). The role of inflammation in vascular injury and repair. *J Thromb Haemost, 1*(8), 1699-1709.

De Martin, R., Hoeth, M., Hofer-Warbinek, R., & Schmid, J. A. (2000). The transcription factor NF-kappa B and the regulation of vascular cell function. *Arterioscler Thromb Vasc Biol, 20*(11), E83-88.

Deanfield, J. E., Halcox, J. P., & Rabelink, T. J. (2007). Endothelial function and dysfunction: testing and clinical relevance. *Circulation, 115*(10), 1285-1295.

DeLeo, F. R., Renee, J., McCormick, S., Nakamura, M., Apicella, M., Weiss, J. P., & Nauseef, W. M. (1998). Neutrophils exposed to bacterial lipopolysaccharide upregulate NADPH oxidase assembly. *J Clin Invest, 101*(2), 455-463.

Demirtas, L., Guclu, A., Erdur, F. M., Akbas, E. M., Ozcicek, A., Onk, D., & Turkmen, K. (2016). Apoptosis, autophagy & endoplasmic reticulum stress in diabetes mellitus. *Indian J Med Res, 144*(4), 515-524.

Didion, S. P., Kinzenbaw, D. A., Fegan, P. E., Didion, L. A., & Faraci, F. M. (2004). Overexpression of CuZn-SOD prevents lipopolysaccharide-induced endothelial dysfunction. *Stroke, 35*(8), 1963-1967.

Diez, J. (2000). Apoptosis in cardiovascular diseases. *Rev Esp Cardiol, 53*(2), 267-274.

Ding, Y., Li, Q., Xu, Y., Chen, Y., Deng, Y., Zhi, F., & Qian, K. (2016). Attenuating Oxidative Stress by Paeonol Protected against Acetaminophen-Induced Hepatotoxicity in Mice. *PLoS One, 11*(5), e0154375.

Dong, Y., Zhang, M., Liang, B., Xie, Z., Zhao, Z., Asfa, S., Choi, H. C., & Zou, M. H. (2010a). Reduction of AMP-activated protein kinase alpha2 increases endoplasmic reticulum stress and atherosclerosis in vivo. *Circulation, 121*(6), 792-803.

Dong, Y., Zhang, M., Wang, S., Liang, B., Zhao, Z., Liu, C., Wu, M., Choi, H. C., Lyons, T. J., & Zou, M. H. (2010b). Activation of AMP-activated protein kinase inhibits oxidized LDL-triggered endoplasmic reticulum stress in vivo. *Diabetes, 59*(6), 1386-1396.

Dornas, W. C., Cardoso, L. M., Silva, M., Machado, N. L., Chianca-Jr, D. A., Alzamora, A. C., Lima, W. G., Lagente, V., & Silva, M. E. (2017). Oxidative stress causes hypertension and activation of nuclear factor-kappaB after high-fructose and salt treatments. *Sci Rep, 7*, 46051.

Du, Q., Feng, G. Z., Shen, L., Cui, J., & Cai, J. K. (2010). Paeonol attenuates airway inflammation and hyperresponsiveness in a murine model of ovalbumin-induced asthma. *Can J Physiol Pharmacol, 88*(10), 1010-1016.

Duan, X. H., Qi, Y. F., & Tang, C. S. (2009). Endoplasmic reticulum stress and cardiovascular diseases. *Journal of Geriatric Cardiology 6*(1).

Dunn, D. L. (1991). Role of Endotoxin and Host Cytokines in Septic Shock. *CHEST, 100*(3), 164S-168S.

Dyer, L. A., Pi, X., & Patterson, C. (2014). The role of BMPs in endothelial cell function and dysfunction. *Trends Endocrinol Metab, 25*(9), 472-480.

Ehrentraut, S., Frede, S., Stapel, H., Mengden, T., Grohe, C., Fandrey, J., Meyer, R., & Baumgarten, G. (2007). Antagonism of lipopolysaccharide-induced blood pressure attenuation and vascular contractility. *Arterioscler Thromb Vasc Biol, 27*(10), 2170-2176.

Eid, A. A., Ford, B. M., Block, K., Kasinath, B. S., Gorin, Y., Ghosh-Choudhury, G., Barnes, J. L., & Abboud, H. E. (2010). AMP-activated protein kinase (AMPK) negatively regulates Nox4-dependent activation of p53 and epithelial cell apoptosis in diabetes. *J Biol Chem, 285*(48), 37503-37512.

Emre, Y., Hurtaud, C., Nubel, T., Criscuolo, F., Ricquier, D., & Cassard-Doulcier, A. M. (2007). Mitochondria contribute to LPS-induced MAPK activation via uncoupling protein UCP2 in macrophages. *Biochem J, 402*(2), 271-278.

Endemann, D. H., & Schiffrin, E. L. (2004). Endothelial dysfunction. *J Am Soc Nephrol, 15*(8), 1983-1992.

Fan, H. Y., Qi, D., Yu, C., Zhao, F., Liu, T., Zhang, Z. K., Yang, M. Y., Zhang, L. M., Chen, D. Q., & Du, Y. (2016). Paeonol protects endotoxin-induced acute kidney injury: potential mechanism of inhibiting TLR4-NF-kappaB signal pathway. *Oncotarget, 7*(26), 39497-39510.

Fan, L., Song, B., Sun, G., Ma, T., Zhong, F., & Wei, W. (2012). Endoplasmic Reticulum Stress–Induced Resistance to Doxorubicin Is Reversed by Paeonol Treatment in Human Hepatocellular Carcinoma Cell. *PLOS ONE, 8* (5), 1-11.

Fan, L., Song, B., Sun, G., Ma, T., Zhong, F., & Wei, W. (2013). Endoplasmic reticulum stress-induced resistance to doxorubicin is reversed by paeonol treatment in human hepatocellular carcinoma cells. *PLoS One, 8*(5), e62627.

Faraci, F. M., & Heistad, D. D. (1998). Regulation of the Cerebral Circulation: Role of Endothelium and Potassium Channels. *Physiological Reviews, 78*(1), 53-97.

Farley, K. S., Wang, L. F., Razavi, H. M., Law, C., Rohan, M., McCormack, D. G., & Mehta, S. (2006). Effects of macrophage inducible nitric oxide synthase in murine septic lung injury. *Am J Physiol Lung Cell Mol Physiol, 290*(6), L1164-1172.

Faure, E., Equils, O., Sieling, P. A., Thomas, L., Zhang, F. X., Kirschning, C. J., Polentarutti, N., Muzio, M., & Arditi, M. (2000). Bacterial lipopolysaccharide activates NF-kappaB through toll-like receptor 4 (TLR-4) in cultured human dermal endothelial cells. Differential expression of TLR-4 and TLR-2 in endothelial cells. *J Biol Chem, 275*(15), 11058-11063.

Favero, T. G., Zable, A. C., & Abramson, J. J. (1995). Hydrogen peroxide stimulates the Ca2+ release channel from skeletal muscle sarcoplasmic reticulum. *J Biol Chem, 270*(43), 25557-25563.

Feletou. (2011). Integrated Systems Physiology: from Molecule to Function to Disease *The Endothelium: Part 1: Multiple Functions of the Endothelial Cells-Focus on Endothelium-Derived Vasoactive Mediators*. San Rafael (CA): Morgan & Claypool Life Sciences.

Feletou, M., & Vanhoutte, P. M. (2006). Endothelium-Derived Hyperpolarizing Factor. *Where Are We Now?, 26*(6), 1215-1225.

Feletou, V. P. (2006). EDHF: the complete story. *Boca Raton, Taylor & Francis CRC press*, 1–298.

Fiorentino, T. V., Procopio, T., Mancuso, E., Arcidiacono, G. P., Andreozzi, F., Arturi, F., Sciacqua, A., Perticone, F., Hribal, M. L., & Sesti, G. (2015). SRT1720 counteracts glucosamine-induced endoplasmic reticulum stress and endothelial dysfunction. *Cardiovasc Res, 107*(2), 295-306.

Fonseca, D. A., Antunes, P. E., & Cotrim, M. D. (2016). The Morphology, Physiology and Pathophysiology of Coronary Microcirculation. *Intech, 2*, 14-47.

Forstermann, U., & Sessa, W. C. (2012). Nitric oxide synthases: regulation and function. *Eur Heart J, 33*(7), 829-837, 837a-837d.

Franchi-Micheli, S., Failli, P., Mazzetti, L., Bani, D., Ciuffi, M., & Zilletti, L. (2000). Mechanical stretch reveals different components of endothelial-mediated vascular tone in rat aortic strips. *Br J Pharmacol, 131*(7), 1355-1362.

Frey, E. A., & Finlay, B. B. (1998). Lipopolysaccharide induces apoptosis in a bovine endothelial cell line via a soluble CD14 dependent pathway. *Microb Pathog, 24*(2), 101-109.

Fu, H. Y., Okada, K., Liao, Y., Tsukamoto, O., Isomura, T., Asai, M., Sawada, T., Okuda, K., Asano, Y., Sanada, S., Asanuma, H., Asakura, M., Takashima, S., Komuro, I., Kitakaze, M., & Minamino, T. (2010). Ablation of C/EBP homologous protein attenuates endoplasmic reticulum-mediated apoptosis and cardiac dysfunction induced by pressure overload. *Circulation, 122*(4), 361-369.

Furchgott, R. F., & Zawadzki, J. V. (1980). The obligatory role of endothelial cells in the relaxation of arterial smooth muscle by acetylcholine. *Nature, 288*(5789), 373-376.

Galan, M., Kassan, M., Choi, S. K., Partyka, M., Trebak, M., Henrion, D., & Matrougui, K. (2012). A novel role for epidermal growth factor receptor tyrosine kinase and its downstream endoplasmic reticulum stress in cardiac damage and microvascular dysfunction in type 1 diabetes mellitus. *Hypertension, 60*(1), 71-80.

Galan, M., Kassan, M., Kadowitz, P. J., Trebak, M., Belmadani, S., & Matrougui, K. (2014). Mechanism of endoplasmic reticulum stress-induced vascular endothelial dysfunction. *Biochim Biophys Acta, 1843*(6), 1063-1075.

Geng, H., Wang, A., Rong, G., Zhu, B., Deng, Y., Chen, J., & Zhong, R. (2010). The effects of ox-LDL in human atherosclerosis may be mediated in part via the toll-like receptor 4 pathway. *Mol Cell Biochem, 342*(1-2), 201-206.

Golia, E., Limongelli, G., Natale, F., Fimiani, F., Maddaloni, V., Pariggiano, I., Bianchi, R., Crisci, M., D'Acierno, L., Giordano, R., Di Palma, G., Conte, M., Golino, P., Russo, M. G., Calabro, R., & Calabro, P. (2014). Inflammation and cardiovascular disease: from pathogenesis to therapeutic target. *Curr Atheroscler Rep, 16*(9), 435.

Gong, X., Yang, Y., Huang, L., Zhang, Q., Wan, R. Z., Zhang, P., & Zhang, B. (2017). Antioxidation, anti-inflammation and anti-apoptosis by paeonol in LPS/d-GalN-induced acute liver failure in mice. *Int Immunopharmacol, 46*, 124-132.

Gorlach, A., Klappa, P., & Kietzmann, T. (2006). The endoplasmic reticulum: folding, calcium homeostasis, signaling, and redox control. *Antioxid Redox Signal, 8*(9-10), 1391-1418.

Gougerot-Podicalo, M. A., Elbim, C., & Chollet-Martin, S. (1996). Modulation of the oxidative burst of human neutrophils by pro- and anti-inflammatory cytokines. *Pathol Biol (Paris), 44*(1), 36-41.

Griendling, K. K., Sorescu, D., Lassegue, B., & Ushio-Fukai, M. (2000). Modulation of protein kinase activity and gene expression by reactive oxygen species and their role in vascular physiology and pathophysiology. *Arterioscler Thromb Vasc Biol, 20*(10), 2175-2183.

Griffith, T. M., Lewis, M. J., Newby, A. C., & Henderson, A. H. (1988). Endothelium-derived relaxing factor. *Journal of the American College of Cardiology, 12*(3), 797-806.

Gross, S. S., & Levi, R. (1992). Tetrahydrobiopterin synthesis. An absolute requirement for cytokine-induced nitric oxide generation by vascular smooth muscle. *J Biol Chem, 267*(36), 25722-25729.

Guzman, A., Zelman-Femiak, M., Boergermann, J. H., Paschkowsky, S., Kreuzaler, P. A., Fratzl, P., Harms, G. S., & Knaus, P. (2012). SMAD versus non-SMAD signaling is determined by lateral mobility of bone morphogenetic protein (BMP) receptors. *J Biol Chem, 287*(47), 39492-39504.

Hadi, H. A., Carr, C. S., & Al Suwaidi, J. (2005). Endothelial dysfunction: cardiovascular risk factors, therapy, and outcome. *Vasc Health Risk Manag, 1*(3), 183-198.

Haimovitz-Friedman, A., Cordon-Cardo, C., Bayoumy, S., Garzotto, M., McLoughlin, M., Gallily, R., Edwards, C. K., 3rd, Schuchman, E. H., Fuks, Z., & Kolesnick, R. (1997). Lipopolysaccharide induces disseminated endothelial apoptosis requiring ceramide generation. *J Exp Med, 186*(11), 1831-1841.

Hamilton, C. A., Brosnan, M. J., McIntyre, M., Graham, D., & Dominiczak, A. F. (2001). Superoxide Excess in Hypertension and Aging. *A Common Cause of Endothelial Dysfunction, 37*(2), 529-534.

Hampton, R. Y. (2002). ER-associated degradation in protein quality control and cellular regulation. *Curr Opin Cell Biol, 14*(4), 476-482.

Hardie, D. G. (1999). Roles of the AMP-activated/SNF1 protein kinase family in the response to cellular stress. *Biochem Soc Symp, 64*, 13-27.

Hardie, D. G. (2007). AMP-activated/SNF1 protein kinases: conserved guardians of cellular energy. *Nat Rev Mol Cell Biol, 8*(10), 774-785.

Hardie, D. G., Carling, D., & Halford, N. (1994). Roles of the Snf1/Rkin1/AMP-activated protein kinase family in the response to environmental and nutritional stress. *Semin Cell Biol, 5*(6), 409-416.

Harding, H. P., Novoa, I., Zhang, Y., Zeng, H., Wek, R., Schapira, M., & Ron, D. (2000). Regulated translation initiation controls stress-induced gene expression in mammalian cells. *Mol Cell, 6*(5), 1099-1108.

Harding, H. P., Zhang, Y., Zeng, H., Novoa, I., Lu, P. D., Calfon, M., Sadri, N., Yun, C., Popko, B., Paules, R., Stojdl, D. F., Bell, J. C., Hettmann, T., Leiden, J. M., & Ron, D. (2003). An integrated stress response regulates amino acid metabolism and resistance to oxidative stress. *Mol Cell, 11*(3), 619-633.

Harrison, D. G., Marvar, P. J., & Titze, J. M. (2012). Vascular inflammatory cells in hypertension. *Front Physiol, 3*, 128.

Helbing, T., Rothweiler, R., Ketterer, E., Goetz, L., Heinke, J., Grundmann, S., Duerschmied, D., Patterson, C., Bode, C., & Moser, M. (2011). BMP activity

controlled by BMPER regulates the proinflammatory phenotype of endothelium. *Blood, 118*(18), 5040-5049.

Hibbs, J. B., Jr., Taintor, R. R., Vavrin, Z., & Rachlin, E. M. (1988). Nitric oxide: a cytotoxic activated macrophage effector molecule. *Biochem Biophys Res Commun, 157*(1), 87-94.

Higashi, Y., Maruhashi, T., Noma, K., & Kihara, Y. (2014). Oxidative stress and endothelial dysfunction: clinical evidence and therapeutic implications. *Trends Cardiovasc Med, 24*(4), 165-169.

Hink, U., Li, H., Mollnau, H., Oelze, M., Matheis, E., Hartmann, M., Skatchkov, M., Thaiss, F., Stahl, R. A. K., Warnholtz, A., Meinertz, T., Griendling, K., Harrison, D. G., Forstermann, U., & Munzel, T. (2001). Mechanisms Underlying Endothelial Dysfunction in Diabetes Mellitus. *Circulation Research, 88*(2), e14-e22.

Hogan, B. L. (1996). Bone morphogenetic proteins in development. *Curr Opin Genet Dev, 6*(4), 432-438.

Hong, J., Kim, K., Kim, J.-H., & Park, Y. (2017). The Role of Endoplasmic Reticulum Stress in Cardiovascular Disease and Exercise. *International Journal of Vascular Medicine, 2017*, 9.

Hotamisligil, G. S. (2010). Endoplasmic reticulum stress and the inflammatory basis of metabolic disease. *Cell, 140*(6), 900-917.

Hsieh, C. L., Cheng, C. Y., Tsai, T. H., Lin, I. H., Liu, C. H., Chiang, S. Y., Lin, J. G., Lao, C. J., & Tang, N. Y. (2006). Paeonol reduced cerebral infarction involving the superoxide anion and microglia activation in ischemia-reperfusion injured rats. *J Ethnopharmacol, 106*(2), 208-215.

Hu, J., Li, Y. L., Li, Z. L., Li, H., Zhou, X. X., Qiu, P. C., Yang, Q., & Wang, S. W. (2012). Chronic supplementation of paeonol combined with danshensu for the improvement of vascular reactivity in the cerebral basilar artery of diabetic rats. *Int J Mol Sci, 13*(11), 14565-14578.

Huang, P. L. (2009). eNOS, metabolic syndrome and cardiovascular disease. *Trends Endocrinol Metab, 20*(6), 295-302.

Hull, C., McLean, G., Wong, F., Duriez, P. J., & Karsan, A. (2002). Lipopolysaccharide signals an endothelial apoptosis pathway through TNF receptor-associated factor 6-mediated activation of c-Jun NH2-terminal kinase. *J Immunol, 169*(5), 2611-2618.

Hung, Y. L., Fang, S. H., Wang, S. C., Cheng, W. C., Liu, P. L., Su, C. C., Chen, C. S., Huang, M. Y., Hua, K. F., Shen, K. H., Wang, Y. T., Suzuki, K., & Li, C. Y. (2017). Corylin protects LPS-induced sepsis and attenuates LPS-induced inflammatory response. *Sci Rep, 7*, 46299.

Hwa, J. J., Ghibaudi, L., Williams, P., & Chatterjee, M. (1994). Comparison of acetylcholine-dependent relaxation in large and small arteries of rat mesenteric vascular bed. *Am J Physiol, 266*(3 Pt 2), H952-958.

Ikegawa, R., Matsumura, Y., Tsukahara, Y., Takaoka, M., & Morimoto, S. (1990). Phosphoramidon, a metalloproteinase inhibitor, suppresses the secretion of endothelin-1 from cultured endothelial cells by inhibiting a big endothelin-1 converting enzyme. *Biochem Biophys Res Commun, 171*(2), 669-675.

Inagi, R., Ishimoto, Y., & Nangaku, M. (2014). Proteostasis in endoplasmic reticulum--new mechanisms in kidney disease. *Nat Rev Nephrol, 10*(7), 369-378.

Isodono, K., Takahashi, T., Imoto, H., Nakanishi, N., Ogata, T., Asada, S., Adachi, A., Ueyama, T., Oh, H., & Matsubara, H. (2010). PARM-1 is an endoplasmic reticulum molecule involved in endoplasmic reticulum stress-induced apoptosis in rat cardiac myocytes. *PLoS One, 5*(3), e9746.

Jacobson, J., & Duchen, M. R. (2002). Mitochondrial oxidative stress and cell death in astrocytes--requirement for stored Ca2+ and sustained opening of the permeability transition pore. *J Cell Sci, 115*(Pt 6), 1175-1188.

Jo, H., Song, H., & Mowbray, A. (2006). Role of NADPH oxidases in disturbed flow- and BMP4- induced inflammation and atherosclerosis. *Antioxid Redox Signal, 8*(9-10), 1609-1619.

Junttila, M. R., Li, S. P., & Westermarck, J. (2008). Phosphatase-mediated crosstalk between MAPK signaling pathways in the regulation of cell survival. *FASEB J, 22*(4), 954-965.

Kacimi, R., Giffard, R. G., & Yenari, M. A. (2011). Endotoxin-activated microglia injure brain derived endothelial cells via NF-kappaB, JAK-STAT and JNK stress kinase pathways. *J Inflamm (Lond), 8*, 7.

Kadowaki, H., & Nishitoh, H. (2013). Signaling pathways from the endoplasmic reticulum and their roles in disease. *Genes (Basel), 4*(3), 306-333.

Kalinowski, L., & Malinski, T. (2004). Endothelial NADH/NADPH-dependent enzymatic sources of superoxide production: relationship to endothelial dysfunction. *Acta Biochim Pol, 51*(2), 459-469.

Kang, K. T. (2014). Endothelium-derived Relaxing Factors of Small Resistance Arteries in Hypertension. *Toxicol Res, 30*(3), 141-148.

Kaplan, R. C., & Frishman, W. H. (2001). Systemic inflammation as a cardiovascular disease risk factor and as a potential target for drug therapy. *Heart Dis, 3*(5), 326-332.

Kapoor, A., Shintani, Y., Collino, M., Osuchowski, M. F., Busch, D., Patel, N. S., Sepodes, B., Castiglia, S., Fantozzi, R., Bishop-Bailey, D., Mota-Filipe, H., Yaqoob, M. M., Suzuki, K., Bahrami, S., Desvergne, B., Mitchell, J. A., & Thiemermann, C. (2010). Protective role of peroxisome proliferator-activated

receptor-beta/delta in septic shock. *Am J Respir Crit Care Med, 182*(12), 1506-1515.

Kassan, M., Galan, M., Choi, S. K., & Matrougui, K. (2011). Endoplasmic Reticulum Stress and Microvascular Endothelial Dysfunction in Diabetes. *J Diabetes Metab, 2*.

Kassan, M., Galan, M., Partyka, M., Saifudeen, Z., Henrion, D., Trebak, M., & Matrougui, K. (2012). Endoplasmic reticulum stress is involved in cardiac damage and vascular endothelial dysfunction in hypertensive mice. *Arterioscler Thromb Vasc Biol, 32*(7), 1652-1661.

Katusic, Z. S., Santhanam, A. V., & He, T. (2012). Vascular effects of prostacyclin: does activation of PPARδ play a role? *Trends in Pharmacological Sciences, 33*(10), 559-564.

Katusic, Z. S., & Vanhoutte, P. M. (1989). Superoxide anion is an endothelium-derived contracting factor. *Am J Physiol, 257*(1 Pt 2), H33-37.

Kaufman, R. J., Back, S. H., Song, B., Han, J., & Hassler, J. (2010). The unfolded protein response is required to maintain the integrity of the endoplasmic reticulum, prevent oxidative stress and preserve differentiation in beta-cells. *Diabetes Obes Metab, 12 Suppl 2*, 99-107.

Kietadisorn, R., Juni, R. P., & Moens, A. L. (2012). Tackling endothelial dysfunction by modulating NOS uncoupling: new insights into its pathogenesis and therapeutic possibilities. *Am J Physiol Endocrinol Metab, 302*(5), E481-E495.

Kim, Yeo, S., Shin, D. G., Bae, Y. S., Lee, J. J., Chin, B. R., Lee, C. H., & Baek, S. H. (2010). Glycogen synthase kinase 3beta and beta-catenin pathway is involved in toll-like receptor 4-mediated NADPH oxidase 1 expression in macrophages. *Febs J, 277*(13), 2830-2837.

Kim, H., Moon, S. Y., Kim, J. S., Baek, C. H., Kim, M., Min, J. Y., & Lee, S. K. (2015). Activation of AMP-activated protein kinase inhibits ER stress and renal fibrosis. *Am J Physiol Renal Physiol, 308*(3), F226-236.

Kim, I., Xu, W., & Reed, J. C. (2008). Cell death and endoplasmic reticulum stress: disease relevance and therapeutic opportunities. *Nat Rev Drug Discov, 7*(12), 1013-1030.

Kockx, M. M. (1998). Apoptosis in the Atherosclerotic Plaque Quantitative and Qualitative Aspects. *Arterioscler Thromb Vasc Biol, 18*, 1519-1522

Kohno, M., Murakawa, K., Yokokawa, K., Yasunari, K., Horio, T., Kurihara, N., & Takeda, T. (1989). Production of endothelin by cultured porcine endothelial cells: modulation by adrenaline. *J Hypertens Suppl, 7*(6), S130-131.

Kondo, S., Murakami, T., Tatsumi, K., Ogata, M., Kanemoto, S., Otori, K., Iseki, K., Wanaka, A., & Imaizumi, K. (2005). OASIS, a CREB/ATF-family member, modulates UPR signalling in astrocytes. *Nat Cell Biol, 7*(2), 186-194.

Kramer, B., Ferrari, D. M., Klappa, P., Pohlmann, N., & Soling, H. D. (2001). Functional roles and efficiencies of the thioredoxin boxes of calcium-binding proteins 1 and 2 in protein folding. *Biochem J, 357*(Pt 1), 83-95.

Landmesser, U., Spiekermann, S., Dikalov, S., Tatge, H., Wilke, R., Kohler, C., Harrison, D. G., Hornig, B., & Drexler, H. (2002). Vascular oxidative stress and endothelial dysfunction in patients with chronic heart failure: role of xanthine-oxidase and extracellular superoxide dismutase. *Circulation, 106*(24), 3073-3078.

Lau, Y. S., Tian, X. Y., Mustafa, M. R., Murugan, D., Liu, J., Zhang, Y., Lau, C. W., & Huang, Y. (2013). Boldine improves endothelial function in diabetic db/db mice through inhibition of angiotensin II-mediated BMP4-oxidative stress cascade. *Br J Pharmacol, 170*(6), 1190-1198.

Lau, Y. S., Tian, X. Y., Mustafa, M. R., Murugan, D., Liu, J., Zhang, Y., Lau, C. W., Huang, Y. (2013). Boldine improves endothelial function in diabetic db/db mice through inhibition of angiotensin II-mediated BMP4-oxidative stress cascade. *Br J Pharmacol, 170*(6), 1190-1198.

Laurindo, F. R., Araujo, T. L., & Abrahao, T. B. (2014). Nox NADPH oxidases and the endoplasmic reticulum. *Antioxid Redox Signal, 20*(17), 2755-2775.

Lee, Choi, H. M., Park, H. J., Ko, S. K., & Lee, H. Y. (2014a). Amlodipine and cardiovascular outcomes in hypertensive patients: meta-analysis comparing amlodipine-based versus other antihypertensive therapy. *Korean J Intern Med, 29*(3), 315-324.

Lee, A. H., Iwakoshi, N. N., & Glimcher, L. H. (2003). XBP-1 regulates a subset of endoplasmic reticulum resident chaperone genes in the unfolded protein response. *Mol Cell Biol, 23*(21), 7448-7459.

Lee, H., Lee, G., Kim, H., & Bae, H. (2013). Paeonol, a major compound of moutan cortex, attenuates Cisplatin-induced nephrotoxicity in mice. *Evid Based Complement Alternat Med, 2013*, 310989.

Lee, I. T., Shih, R. H., Lin, C. C., Chen, J. T., & Yang, C. M. (2012). Role of TLR4/NADPH oxidase/ROS-activated p38 MAPK in VCAM-1 expression induced by lipopolysaccharide in human renal mesangial cells. *Cell Commun Signal, 10*(1), 33.

Lee, J., Lee, S., Zhang, H., Hill, M. A., Zhang, C., & Park, Y. (2017). Interaction of IL-6 and TNF-alpha contributes to endothelial dysfunction in type 2 diabetic mouse hearts. *PLoS One, 12*(11), e0187189.

Lee, K. S., Kim, J., Kwak, S. N., Lee, K. S., Lee, D. K., Ha, K. S., Won, M. H., Jeoung, D., Lee, H., Kwon, Y. G., & Kim, Y. M. (2014b). Functional role of NF-kappaB in expression of human endothelial nitric oxide synthase. *Biochem Biophys Res Commun, 448*(1), 101-107.

Lenna, S., Townsend, D. M., Tan, F. K., Kapanadze, B., Markiewicz, M., Trojanowska, M., & Scorza, R. (2010). HLA-B35 upregulates endothelin-1 and downregulates endothelial nitric oxide synthase via endoplasmic reticulum stress response in endothelial cells. *J Immunol, 184*(9), 4654-4661.

Lerman, A., & Burnett, J. C., Jr. (1992). Intact and altered endothelium in regulation of vasomotion. *Circulation, 86*(6 Suppl), Iii12-19.

Levi, M., ten Cate, H., & van der Poll, T. (2002). Endothelium: interface between coagulation and inflammation. *Crit Care Med, 30*(5 Suppl), S220-224.

Li, G., Scull, C., Ozcan, L., & Tabas, I. (2010a). NADPH oxidase links endoplasmic reticulum stress, oxidative stress, and PKR activation to induce apoptosis. *J Cell Biol, 191*(6), 1113-1125.

Li, H., & Förstermann, U. (2013). Uncoupling of endothelial NO synthase in atherosclerosis and vascular disease. *Current Opinion in Pharmacology, 13*(2), 161-167.

Li, H., Song, F., Duan, L. R., Sheng, J. J., Xie, Y. H., Yang, Q., Chen, Y., Dong, Q. Q., Zhang, B. L., & Wang, S. W. (2016). Paeonol and danshensu combination attenuates apoptosis in myocardial infarcted rats by inhibiting oxidative stress: Roles of Nrf2/HO-1 and PI3K/Akt pathway. *Sci Rep, 6*, 23693.

Li, H., Xie, Y. H., Yang, Q., Wang, S. W., Zhang, B. L., Wang, J. B., Cao, W., Bi, L. L., Sun, J. Y., Miao, S., Hu, J., Zhou, X. X., & Qiu, P. C. (2012). Cardioprotective effect of paeonol and danshensu combination on isoproterenol-induced myocardial injury in rats. *PLoS One, 7*(11), e48872.

Li, J. M., Fan, L. M., George, V. T., & Brooks, G. (2007). Nox2 regulates endothelial cell cycle arrest and apoptosis via p21cip1 and p53. *Free Radic Biol Med, 43*(6), 976-986.

Li, Y. J., Bao, J. X., Xu, J. W., Murad, F., & Bian, K. (2010b). Vascular dilation by paeonol-a mechanism study. *Vascul Pharmacol, 53*(3-4), 169-176.

Liang, B., Wang, S. X., Wang, Q. L., Zhang, W. C., Viollet, B., Zhu, Y., & Zou, M. H. (2013a). Aberrant Endoplasmic Reticulum Stress in Vascular Smooth Muscle Increases Vascular Contractility and Blood Pressure in Mice Deficient of AMP-Activated Protein Kinase- a2 In Vivo. *Arterioscler Thromb Vasc Biol, 33* 595-604.

Liang, C. F., Liu, J. T., Wang, Y., Xu, A., & Vanhoutte, P. M. (2013b). Toll-like receptor 4 mutation protects obese mice against endothelial dysfunction by decreasing NADPH oxidase isoforms 1 and 4. *Arterioscler Thromb Vasc Biol, 33*(4), 777-784.

Liao, W. Y., Tsai, T. H., Ho, T. Y., Lin, Y. W., Cheng, C. Y., & Hsieh, C. L. (2016). Neuroprotective Effect of Paeonol Mediates Anti-Inflammation via Suppressing Toll-Like Receptor 2 and Toll-Like Receptor 4 Signaling Pathways in Cerebral Ischemia-Reperfusion Injured Rats. *Evid Based Complement Alternat Med, 2016*, 3704647.

Lien, E., Means, T. K., Heine, H., Yoshimura, A., Kusumoto, S., Fukase, K., Fenton, M. J., Oikawa, M., Qureshi, N., Monks, B., Finberg, R. W., Ingalls, R. R., & Golenbock, D. T. (2000). Toll-like receptor 4 imparts ligand-specific recognition of bacterial lipopolysaccharide. *J Clin Invest, 105*(4), 497-504.

Lin, C., Lin, H. Y., Chen, J. H., Tseng, W. P., Ko, P. Y., Liu, Y. S., Yeh, W. L., & Lu, D. Y. (2015). Effects of paeonol on anti-neuroinflammatory responses in microglial cells. *Int J Mol Sci, 16*(4), 8844-8860.

Lindner, H., Holler, E., Ertl, B., Multhoff, G., Schreglmann, M., Klauke, I., Schultz-Hector, S., & Eissner, G. (1997). Peripheral blood mononuclear cells induce programmed cell death in human endothelial cells and may prevent repair: role of cytokines. *Blood, 89*(6), 1931-1938.

Liu, Lin, A. H., Ko, H. K., Perng, D. W., Lee, T. S., & Kou, Y. R. (2017). Prevention of Bleomycin-Induced Pulmonary Inflammation and Fibrosis in Mice by Paeonol. *Front Physiol, 8*, 193.

Liu, Mu, J., Zheng, C., Chen, X., Guo, Z., Huang, C., Fu, Y., Tian, G., Shang, H., & Wang, Y. (2016a). Systems-Pharmacology Dissection of Traditional Chinese Medicine Compound Saffron Formula Reveals Multi-scale Treatment Strategy for Cardiovascular Diseases. *Sci Rep, 6*, 19809.

Liu, Yang, J., Li, L., Shi, W., Yuan, X., & Wu, L. (2016b). The Natural Occurring Compounds Targeting Endoplasmic Reticulum Stress. *Evid Based Complement Alternat Med, 2016*, 7831282.

Liu, J., Wang, S., Feng, L., Ma, D., Fu, Q., Song, Y., Jia, X., & Ma, S. (2013). Hypoglycemic and antioxidant activities of paeonol and its beneficial effect on diabetic encephalopathy in streptozotocin-induced diabetic rats. *J Med Food, 16*(7), 577-586.

Liu, L., Liu, J., Huang, Z., Yu, X., Zhang, X., Dou, D., & Huang, Y. (2015). Berberine improves endothelial function by inhibiting endoplasmic reticulum stress in the carotid arteries of spontaneously hypertensive rats. *Biochem Biophys Res Commun, 458*(4), 796-801.

Liu, M.-H., Lee, H.-F., Lee, T.-S., & Kou, Y. R. (2014a). Therapeutic effects and mechanisms of paeonol on cigarette smoke-induced lung inflammation *The FASEB J, 28*(1).

Liu, M. H., Lin, A. H., Lee, H. F., Ko, H. K., Lee, T. S., & Kou, Y. R. (2014b). Paeonol attenuates cigarette smoke-induced lung inflammation by inhibiting ROS-sensitive inflammatory signaling. *Mediators Inflamm, 2014*, 651890.

Liu, Y. R., Chen, J. J., & Dai, M. (2014c). Paeonol protects rat vascular endothelial cells from ox-LDL-induced injury in vitro via downregulating microRNA-21 expression and TNF-alpha release. *Acta Pharmacol Sin, 35*(4), 483-488.

Loinard, C., Zouggari, Y., Rueda, P., Ramkhelawon, B., Cochain, C., Vilar, J., Recalde, A., Richart, A., Charue, D., Duriez, M., Mori, M., Arenzana-Seisdedos, F., Levy, B. I., Heymes, C., & Silvestre, J. S. (2012). C/EBP homologous protein-10

(CHOP-10) limits postnatal neovascularization through control of endothelial nitric oxide synthase gene expression. *Circulation, 125*(8), 1014-1026.

Loo, B., Labugger, R., Skepper, J. N., Bachschmid, M., Kilo, J., Powell, J. M., Palacios-Callender, M., Erusalimsky, J. D., Quaschning, T., Malinski, T., Gygi, D., Ullrich, V., & Luscher, T. F. (2000). Enhanced peroxynitrite formation is associated with vascular aging. *J Exp Med, 192*(12), 1731-1744.

Lüscher, T. F., Boulanger, C. M., Dohi, Y., & Yang, Z. H. (1992). Endothelium-derived contracting factors. *Hypertension, 19*(2), 117-130.

Luscher, T. F., Yang, Z., Tschudi, M., von Segesser, L., Stulz, P., Boulanger, C., Siebenmann, R., Turina, M., & Buhler, F. R. (1990). Interaction between endothelin-1 and endothelium-derived relaxing factor in human arteries and veins. *Circ Res, 66*(4), 1088-1094.

Ma, Y., & Hendershot, L. M. (2003). Delineation of a negative feedback regulatory loop that controls protein translation during endoplasmic reticulum stress. *J Biol Chem, 278*(37), 34864-34873.

MacMicking, J. D., Nathan, C., Hom, G., Chartrain, N., Fletcher, D. S., Trumbauer, M., Stevens, K., Xie, Q. W., Sokol, K., Hutchinson, N., & et al. (1995). Altered responses to bacterial infection and endotoxic shock in mice lacking inducible nitric oxide synthase. *Cell, 81*(4), 641-650.

Macmillan-Crow, L. A., & Cruthirds, D. L. (2001). Invited review: manganese superoxide dismutase in disease. *Free Radic Res, 34*(4), 325-336.

Mako, V., Czucz, J., Weiszhar, Z., Herczenik, E., Matko, J., Prohaszka, Z., & Cervenak, L. (2010). Proinflammatory activation pattern of human umbilical vein endothelial cells induced by IL-1beta, TNF-alpha, and LPS. *Cytometry A, 77*(10), 962-970.

Malhi, H., & Kaufman, R. J. (2011). Endoplasmic reticulum stress in liver disease. *J Hepatol, 54*(4), 795-809.

Malhotra, J. D., & Kaufman, R. J. (2007). Endoplasmic reticulum stress and oxidative stress: a vicious cycle or a double-edged sword? *Antioxid Redox Signal, 9*(12), 2277-2293.

Malhotra, J. D., Miao, H., Zhang, K., Wolfson, A., Pennathur, S., Pipe, S. W., & Kaufman, R. J. (2008). Antioxidants reduce endoplasmic reticulum stress and improve protein secretion. *Proc Natl Acad Sci U S A, 105*(47), 18525-18530.

Mathewson, A. M., & Wadsworth, R. M. (2004). Induction of iNOS restricts functional activity of both eNOS and nNOS in pig cerebral artery. *Nitric Oxide, 11*(4), 331-339.

Matsuda, H., Ohta, T., Kawaguchi, A., & Yoshikawa, M. (2001). Bioactive constituents of chinese natural medicines. VI. Moutan cortex. (2): structures and radical scavenging effects of suffruticosides A, B, C, D, and E and galloyl-oxypaeoniflorin. *Chem Pharm Bull (Tokyo), 49*(1), 69-72.

McCullough, K. D., Martindale, J. L., Klotz, L. O., Aw, T. Y., & Holbrook, N. J. (2001). Gadd153 sensitizes cells to endoplasmic reticulum stress by down-regulating Bcl2 and perturbing the cellular redox state. *Mol Cell Biol, 21*(4), 1249-1259.

McNeill, E., Crabtree, M. J., Sahgal, N., Patel, J., Chuaiphichai, S., Iqbal, A. J., Hale, A. B., Greaves, D. R., & Channon, K. M. (2015). Regulation of iNOS function and cellular redox state by macrophage Gch1 reveals specific requirements for tetrahydrobiopterin in NRF2 activation. *Free Radic Biol Med, 79*, 206-216.

Medvedev, A. E., Kopydlowski, K. M., & Vogel, S. N. (2000). Inhibition of lipopolysaccharide-induced signal transduction in endotoxin-tolerized mouse macrophages: dysregulation of cytokine, chemokine, and toll-like receptor 2 and 4 gene expression. *J Immunol, 164*(11), 5564-5574.

Merkus, D., Duncker, D. J., & Chilian, W. M. (2002). Metabolic regulation of coronary vascular tone: role of endothelin-1. *Am J Physiol Heart Circ Physiol, 283*(5), H1915-1921.

Mihalj, M., Tadzic, R., Vcev, A., Rucevic, S., & Drenjancevic, I. (2016). Blood Pressure Reduction is Associated With the Changes in Oxidative Stress and Endothelial Activation in Hypertension, Regardless of Antihypertensive Therapy. *Kidney Blood Press Res, 41*(6), 721-735.

Minamino, T., & Kitakaze, M. (2010). ER stress in cardiovascular disease. *J Mol Cell Cardiol, 48*(6), 1105-1110.

Minamino, T., Komuro, I., & Kitakaze, M. (2010). Endoplasmic reticulum stress as a therapeutic target in cardiovascular disease. *Circ Res, 107*(9), 1071-1082.

Miriyala, S., Gongora Nieto, M. C., Mingone, C., Smith, D., Dikalov, S., Harrison, D. G., & Jo, H. (2006). Bone morphogenic protein-4 induces hypertension in mice: role of noggin, vascular NADPH oxidases, and impaired vasorelaxation. *Circulation, 113*(24), 2818-2825.

Miyazono, K., Kamiya, Y., & Morikawa, M. (2010). Bone morphogenetic protein receptors and signal transduction. *J Biochem, 147*(1), 35-51.

Miyazono, K., Maeda, S., & Imamura, T. (2005). BMP receptor signaling: transcriptional targets, regulation of signals, and signaling cross-talk. *Cytokine Growth Factor Rev, 16*(3), 251-263.

Mohebbi, N., Shalviri, G., Salarifar, M., Salamzadeh, J., & Gholami, K. (2010). Adverse drug reactions induced by cardiovascular drugs in cardiovascular care unit patients. *Pharmacoepidemiol Drug Saf, 19*(9), 889-894.

Mollnau, H., Wendt, M., Szöcs, K., Lassègue, B., Schulz, E., Oelze, M., Li, H., Bodenschatz, M., August, M., Kleschyov, A. L., Tsilimingas, N., Walter, U., Förstermann, U., Meinertz, T., Griendling, K., & Münzel, T. (2002). Effects of Angiotensin II Infusion on the Expression and Function of NAD(P)H Oxidase and Components of Nitric Oxide/cGMP Signaling. *Circ Res, 90*(4), e58-e65.

Mombouli, J. V., & Vanhoutte, P. M. (1993). Purinergic endothelium-dependent and -independent contractions in rat aorta. *Hypertension, 22*(4), 577-583.

Moncada, S., Palmer, R. M., & Higgs, E. A. (1991). Nitric oxide: physiology, pathophysiology, and pharmacology. *Pharmacol Rev, 43*(2), 109-142.

Moncada, S., & Vane, J. R. (1978). Pharmacology and endogenous roles of prostaglandin endoperoxides, thromboxane A2, and prostacyclin. *Pharmacol Rev, 30*(3), 293-331.

Montezano, A. C., & Touyz, R. M. (2012). Oxidative stress, Noxs, and hypertension: experimental evidence and clinical controversies. *Ann Med, 44 Suppl 1*, S2-16.

Mudau, M., Genis, A., Lochner, A., & Strijdom, H. (2012). Endothelial dysfunction: the early predictor of atherosclerosis. *Cardiovasc J Afr, 23*(4), 222-231.

Murugan, D., Lau, Y. S., Lau, C. W., Mustafa, M. R., & Huang, Y. (2015). Angiotensin 1-7 Protects against Angiotensin II-Induced Endoplasmic Reticulum Stress and Endothelial Dysfunction via Mas Receptor. *PLoS One, 10*(12), e0145413.

Nagao, T., & Vanhoutte, P. M. (1993). Endothelium-derived hyperpolarizing factor and endothelium-dependent relaxations. *Am J Respir Cell Mol Biol, 8*(1), 1-6.

Narkar, V. A., Downes, M., Yu, R. T., Embler, E., Wang, Y. X., Banayo, E., Mihaylova, M. M., Nelson, M. C., Zou, Y., Juguilon, H., Kang, H., Shaw, R. J., & Evans, R. M. (2008). AMPK and PPARdelta agonists are exercise mimetics. *Cell, 134*(3), 405-415.

Nishitoh, H., Matsuzawa, A., Tobiume, K., Saegusa, K., Takeda, K., Inoue, K., Hori, S., Kakizuka, A., & Ichijo, H. (2002). ASK1 is essential for endoplasmic reticulum stress-induced neuronal cell death triggered by expanded polyglutamine repeats. *Genes Dev, 16*(11), 1345-1355.

Ohlstein, E. H. (2010). The grand challenges in cardiovascular drug discovery and development. *Front Pharmacol, 1*, 125.

Omori, Y., Imai, J., Watanabe, M., Komatsu, T., Suzuki, Y., Kataoka, K., Watanabe, S., Tanigami, A., & Sugano, S. (2001). CREB-H: a novel mammalian transcription factor belonging to the CREB/ATF family and functioning via the box-B element with a liver-specific expression. *Nucleic Acids Res, 29*(10), 2154-2162.

Oslowski, C. M., & Urano, F. (2011). Measuring ER stress and the unfolded protein response using mammalian tissue culture system. *Methods Enzymol, 490*, 71-92.

Osto, E., Matter, C. M., Kouroedov, A., Malinski, T., Bachschmid, M., Camici, G. G., Kilic, U., Stallmach, T., Boren, J., Iliceto, S., Luscher, T. F., & Cosentino, F. (2008). c-Jun N-terminal kinase 2 deficiency protects against hypercholesterolemia-induced endothelial dysfunction and oxidative stress. *Circulation, 118*(20), 2073-2080.

Ou, Y., Li, Q. W., Wang, J. J., Gao, D. W., & Li, K. (2014). Antidiabetic Nephropathy Effects of Paeonol on Streptozotocin Induced Diabetic Rats. *Lat Am J Pharm, 33* (2), 210-217.

Ozcan, U., Cao, Q., Yilmaz, E., Lee, A. H., Iwakoshi, N. N., Ozdelen, E., Tuncman, G., Gorgun, C., Glimcher, L. H., & Hotamisligil, G. S. (2004). Endoplasmic reticulum stress links obesity, insulin action, and type 2 diabetes. *Science, 306*(5695), 457-461.

Ozkor, M. A., & Quyyumi, A. A. (2011). Endothelium-Derived Hyperpolarizing Factor and Vascular Function. *Cardiol Res Pract, 2011*, 12.

Padilla, J., & Jenkins, N. T. (2013). Induction of endoplasmic reticulum stress impairs insulin-stimulated vasomotor relaxation in rat aortic rings: role of endothelin-1. *J Physiol Pharmacol, 64*(5), 557-564.

Palomer, X., Capdevila-Busquets, E., Botteri, G., Salvado, L., Barroso, E., Davidson, M. M., Michalik, L., Wahli, W., & Vazquez-Carrera, M. (2014). PPARbeta/delta attenuates palmitate-induced endoplasmic reticulum stress and induces autophagic markers in human cardiac cells. *Int J Cardiol, 174*(1), 110-118.

Paolocci, N., Biondi, R., Bettini, M., Lee, C. I., Berlowitz, C. O., Rossi, R., Xia, Y., Ambrosio, G., L'Abbate, A., Kass, D. A., & Zweier, J. L. (2001). Oxygen radical-mediated reduction in basal and agonist-evoked NO release in isolated rat heart. *J Mol Cell Cardiol, 33*(4), 671-679.

Park, S. W., Zhou, Y., Lee, J., Lu, A., Sun, C., Chung, J., Ueki, K., & Ozcan, U. (2010). The regulatory subunits of PI3K, p85alpha and p85beta, interact with XBP-1 and increase its nuclear translocation. *Nat Med, 16*(4), 429-437.

Peters, J. M., Lee, S. S., Li, W., Ward, J. M., Gavrilova, O., Everett, C., Reitman, M. L., Hudson, L. D., & Gonzalez, F. J. (2000). Growth, adipose, brain, and skin alterations resulting from targeted disruption of the mouse peroxisome proliferator-activated receptor beta(delta). *Mol Cell Biol, 20*(14), 5119-5128.

Pierce, G. L., Lesniewski, L. A., Lawson, B. R., Beske, S. D., & Seals, D. R. (2009). Nuclear factor-{kappa}B activation contributes to vascular endothelial dysfunction via oxidative stress in overweight/obese middle-aged and older humans. *Circulation, 119*(9), 1284-1292.

Piqueras, L., Reynolds, A. R., Hodivala-Dilke, K. M., Alfranca, A., Redondo, J. M., Hatae, T., Tanabe, T., Warner, T. D., & Bishop-Bailey, D. (2007). Activation of PPARbeta/delta induces endothelial cell proliferation and angiogenesis. *Arterioscler Thromb Vasc Biol, 27*(1), 63-69.

Pober, J. S. (1998). Activation and injury of endothelial cells by cytokines. *Pathol Biol (Paris), 46*(3), 159-163.

Pryor, W. A., & Squadrito, G. L. (1995). The chemistry of peroxynitrite: a product from the reaction of nitric oxide with superoxide. *Am J Physiol, 268*(5 Pt 1), L699-722.

Quagliaro, L., Piconi, L., Assaloni, R., Martinelli, L., Motz, E., & Ceriello, A. (2003). Intermittent high glucose enhances apoptosis related to oxidative stress in human umbilical vein endothelial cells: the role of protein kinase C and NAD(P)H-oxidase activation. *Diabetes, 52*(11), 2795-2804.

Quintela, A. M., Jimenez, R., Gomez-Guzman, M., Zarzuelo, M. J., Galindo, P., Sanchez, M., Vargas, F., Cogolludo, A., Tamargo, J., Perez-Vizcaino, F., & Duarte, J. (2012). Activation of peroxisome proliferator-activated receptor-beta/-delta (PPARbeta/delta) prevents endothelial dysfunction in type 1 diabetic rats. *Free Radic Biol Med, 53*(4), 730-741.

Radomski, M. W., Palmer, R. M., & Moncada, S. (1990). Glucocorticoids inhibit the expression of an inducible, but not the constitutive, nitric oxide synthase in vascular endothelial cells. *Proc Natl Acad Sci U S A, 87*(24), 10043-10047.

Rajendran, P., Rengarajan, T., Thangavel, J., Nishigaki, Y., Sakthisekaran, D., Sethi, G., & Nishigaki, I. (2013). The vascular endothelium and human diseases. *Int J Biol Sci, 9*(10), 1057-1069.

Rapoport, R. M., & Murad, F. (1983). Endothelium-dependent and nitrovasodilator-induced relaxation of vascular smooth muscle: role of cyclic GMP. *J Cyclic Nucleotide Protein Phosphor Res, 9*(4-5), 281-296.

Read, M. A., Whitley, M. Z., Williams, A. J., & Collins, T. (1994). NF-kappa B and I kappa B alpha: an inducible regulatory system in endothelial activation. *J Exp Med, 179*(2), 503-512.

Reinhart, K., Bayer, O., Brunkhorst, F., & Meisner, M. (2002). Markers of endothelial damage in organ dysfunction and sepsis. *Crit Care Med, 30*(5 Suppl), S302-312.

Richards, A. M. (2010). New biomarkers in heart failure: applications in diagnosis, prognosis and guidance of therapy. *Rev Esp Cardiol, 63*(6), 635-639.

Rodgers, A. (2003). A cure for cardiovascular disease? *BMJ, 326*(7404), 1407-1408.

Roifman, I., Beck, P. L., Anderson, T. J., Eisenberg, M. J., & Genest, J. (2011). Chronic inflammatory diseases and cardiovascular risk: a systematic review. *Can J Cardiol, 27*(2), 174-182.

Ron, D., & Walter, P. (2007). Signal integration in the endoplasmic reticulum unfolded protein response. *Nat Rev Mol Cell Biol, 8*(7), 519-529.

Salvado, L., Barroso, E., Gomez-Foix, A. M., Palomer, X., Michalik, L., Wahli, W., & Vazquez-Carrera, M. (2014). PPARbeta/delta prevents endoplasmic reticulum stress-associated inflammation and insulin resistance in skeletal muscle cells through an AMPK-dependent mechanism. *Diabetologia, 57*(10), 2126-2135.

San Cheang, W., Yuen Ngai, C., Yen Tam, Y., Yu Tian, X., Tak Wong, W., Zhang, Y., Wai Lau, C., Chen, Z. Y., Bian, Z. X., Huang, Y., & Ping Leung, F. (2015). Black tea protects against hypertension-associated endothelial dysfunction through alleviation of endoplasmic reticulum stress. *Sci Rep, 5*, 10340.

Sanlioglu, S., Williams, C. M., Samavati, L., Butler, N. S., Wang, G., McCray, P. B., Jr., Ritchie, T. C., Hunninghake, G. W., Zandi, E., & Engelhardt, J. F. (2001). Lipopolysaccharide induces Rac1-dependent reactive oxygen species formation and coordinates tumor necrosis factor-alpha secretion through IKK regulation of NF-kappa B. *J Biol Chem, 276*(32), 30188-30198.

Santos, C. X., Nabeebaccus, A. A., Shah, A. M., Camargo, L. L., Filho, S. V., & Lopes, L. R. (2014). Endoplasmic reticulum stress and Nox-mediated reactive oxygen species signaling in the peripheral vasculature: potential role in hypertension. *Antioxid Redox Signal, 20*(1), 121-134.

Santos, C. X., Tanaka, L. Y., Wosniak, J., & Laurindo, F. R. (2009). Mechanisms and implications of reactive oxygen species generation during the unfolded protein response: roles of endoplasmic reticulum oxidoreductases, mitochondrial electron transport, and NADPH oxidase. *Antioxid Redox Signal, 11*(10), 2409-2427.

Sasaki, H., Asanuma, H., Fujita, M., Takahama, H., Wakeno, M., Ito, S., Ogai, A., Asakura, M., Kim, J., Minamino, T., Takashima, S., Sanada, S., Sugimachi, M., Komamura, K., Mochizuki, N., & Kitakaze, M. (2009). Metformin Prevents Progression of Heart Failure in Dogs. *Role of AMP-Activated Protein Kinase, 119*(19), 2568-2577.

Scheuner, D., Song, B., McEwen, E., Liu, C., Laybutt, R., Gillespie, P., Saunders, T., Bonner-Weir, S., & Kaufman, R. J. (2001). Translational control is required for the unfolded protein response and in vivo glucose homeostasis. *Mol Cell, 7*(6), 1165-1176.

Schindler, A. J., & Schekman, R. (2009). In vitro reconstitution of ER-stress induced ATF6 transport in COPII vesicles. *Proc Natl Acad Sci U S A, 106*(42), 17775-17780.

Schroder, M., & Kaufman, R. J. (2005). ER stress and the unfolded protein response. *Mutat Res, 569*(1-2), 29-63.

Schuck, S., Prinz, W. A., Thorn, K. S., Voss, C., & Walter, P. (2009). Membrane expansion alleviates endoplasmic reticulum stress independently of the unfolded protein response. *J Cell Biol, 187*(4), 525-536.

Schwartz, Economides, C., Mayeda, G. S., Burstein, S., & Kloner, R. A. (2010). The endothelial cell in health and disease: its function, dysfunction, measurement and therapy. *Int J Impot Res, 22*(2), 77-90.

Schwartz, B. R., Karsan, A., Bombeli, T., & Harlan, J. M. (1999). A novel beta 1 integrin-dependent mechanism of leukocyte adherence to apoptotic cells. *J Immunol, 162*(8), 4842-4848.

ScottBurden, T., & Vanhoutte, P. M. (1993). The endothelium as a regulator of vascular smooth muscle proliferation. *Circulation, 87*(5 SUPPL. V), V51.

Scull, C. M., & Tabas, I. (2011). Mechanisms of ER stress-induced apoptosis in atherosclerosis. *Arterioscler Thromb Vasc Biol, 31*(12), 2792-2797.

Senft, D., & Ronai, Z. A. (2015). UPR, autophagy, and mitochondria crosstalk underlies the ER stress response. *Trends Biochem Sci, 40*(3), 141-148.

Shen, Zhang, K., & Kaufman, R. J. (2004). The unfolded protein response--a stress signaling pathway of the endoplasmic reticulum. *J Chem Neuroanat, 28*(1-2), 79-92.

Shen, J., Chen, X., Hendershot, L., & Prywes, R. (2002). ER stress regulation of ATF6 localization by dissociation of BiP/GRP78 binding and unmasking of Golgi localization signals. *Dev Cell, 3*(1), 99-111.

Shi, X., Chen, Y. H., Liu, H., & Qu, H. D. (2016). Therapeutic effects of paeonol on methyl-4-phenyl-1,2,3,6-tetrahydropyridine/probenecid-induced Parkinson's disease in mice. *Mol Med Rep, 14*(3), 2397-2404.

Shi, Y., & Vanhoutte, P. M. (2008). Oxidative stress and COX cause hyper-responsiveness in vascular smooth muscle of the femoral artery from diabetic rats. *Br J Pharmacol, 154*(3), 639-651.

Shi, Y., Vattem, K. M., Sood, R., An, J., Liang, J., Stramm, L., & Wek, R. C. (1998). Identification and characterization of pancreatic eukaryotic initiation factor 2 alpha-subunit kinase, PEK, involved in translational control. *Mol Cell Biol, 18*(12), 7499-7509.

Shimada, K., Takahashi, M., & Tanzawa, K. (1994). Cloning and functional expression of endothelin-converting enzyme from rat endothelial cells. *J Biol Chem, 269*(28), 18275-18278.

Shimokawa, H., Flavahan, N. A., Lorenz, R. R., & Vanhoutte, P. M. (1988). Prostacyclin releases endothelium-derived relaxing factor and potentiates its action in coronary arteries of the pig. *Br J Pharmacol, 95*(4), 1197-1203.

Shioiri, T., Muroi, M., Hatao, F., Nishida, M., Ogawa, T., Mimura, Y., Seto, Y., Kaminishi, M., & Tanamoto, K. (2009). Caspase-3 is activated and rapidly released from human umbilical vein endothelial cells in response to lipopolysaccharide. *Biochim Biophys Acta, 1792*(10), 1011-1018.

Simon, F., & Fernandez, R. (2009). Early lipopolysaccharide-induced reactive oxygen species production evokes necrotic cell death in human umbilical vein endothelial cells. *J Hypertens, 27*(6), 1202-1216.

Sorescu, G. P., Song, H., Tressel, S. L., Hwang, J., Dikalov, S., Smith, D. A., Boyd, N. L., Platt, M. O., Lassegue, B., Griendling, K. K., & Jo, H. (2004). Bone morphogenic protein 4 produced in endothelial cells by oscillatory shear stress induces monocyte adhesion by stimulating reactive oxygen species production from a nox1-based NADPH oxidase. *Circ Res, 95*(8), 773-779.

Sorescu, G. P., Sykes, M., Weiss, D., Platt, M. O., Saha, A., Hwang, J., Boyd, N., Boo, Y. C., Vega, J. D., Taylor, W. R., & Jo, H. (2003). Bone morphogenic protein 4 produced in endothelial cells by oscillatory shear stress stimulates an inflammatory response. *J Biol Chem, 278*(33), 31128-31135.

Soromou, L. W., Zhang, Z., Li, R., Chen, N., Guo, W., Huo, M., Guan, S., Lu, J., & Deng, X. (2012). Regulation of inflammatory cytokines in lipopolysaccharide-stimulated RAW 264.7 murine macrophage by 7-O-methyl-naringenin. *Molecules, 17*(3), 3574-3585.

Sozen, E., & Ozer, N. K. (2017). Impact of high cholesterol and endoplasmic reticulum stress on metabolic diseases: An updated mini-review. *Redox Biol, 12*, 456-461.

Spitler, K. M., Matsumoto, T., & Webb, R. C. (2013). Suppression of endoplasmic reticulum stress improves endothelium-dependent contractile responses in aorta of the spontaneously hypertensive rat. *Am J Physiol Heart Circ Physiol, 305*(3), H344-353.

Staehr, M., Madsen, K., Vanhoutte, P. M., Hansen, P. B., & Jensen, B. L. (2011). Disruption of COX-2 and eNOS does not confer protection from cardiovascular failure in lipopolysaccharide-treated conscious mice and isolated vascular rings. *Am J Physiol Regul Integr Comp Physiol, 301*(2), R412-420.

Steyers, C., & Miller, F. (2014). Endothelial Dysfunction in Chronic Inflammatory Diseases. *Int J Mol Sci, 15*(7), 11324.

Sugawara, T., Fujimura, M., Noshita, N., Kim, G. W., Saito, A., Hayashi, T., Narasimhan, P., Maier, C. M., & Chan, P. H. (2004). Neuronal death/survival signaling pathways in cerebral ischemia. *NeuroRx, 1*(1), 17-25.

Szabo, C., Cuzzocrea, S., Zingarelli, B., O'Connor, M., & Salzman, A. L. (1997). Endothelial dysfunction in a rat model of endotoxic shock. Importance of the activation of poly (ADP-ribose) synthetase by peroxynitrite. *J Clin Invest, 100*(3), 723-735.

Tabas, I. (2010). The role of endoplasmic reticulum stress in the progression of atherosclerosis. *Circ Res, 107*(7), 839-850.

Tabet, F., Savoia, C., Schiffrin, E. L., & Touyz, R. M. (2004). Differential calcium regulation by hydrogen peroxide and superoxide in vascular smooth muscle cells from spontaneously hypertensive rats. *J Cardiovasc Pharmacol, 44*(2), 200-208.

Takata, Y., Liu, J., Yin, F., Collins, A. R., Lyon, C. J., Lee, C. H., Atkins, A. R., Downes, M., Barish, G. D., Evans, R. M., Hsueh, W. A., & Tangirala, R. K. (2008). PPARdelta-mediated antiinflammatory mechanisms inhibit angiotensin II-accelerated atherosclerosis. *Proc Natl Acad Sci U S A, 105*(11), 4277-4282.

Takimoto, E., Champion, H. C., Li, M., Ren, S., Rodriguez, E. R., Tavazzi, B., Lazzarino, G., Paolocci, N., Gabrielson, K. L., Wang, Y., & Kass, D. A. (2005). Oxidant stress from nitric oxide synthase-3 uncoupling stimulates cardiac pathologic remodeling from chronic pressure load. *J Clin Invest, 115*(5), 1221-1231.

Tang, E. H., Leung, F. P., Huang, Y., Feletou, M., So, K. F., Man, R. Y., & Vanhoutte, P. M. (2007). Calcium and reactive oxygen species increase in endothelial cells in response to releasers of endothelium-derived contracting factor. *Br J Pharmacol, 151*(1), 15-23.

Tang, E. H., & Vanhoutte, P. M. (2009). Prostanoids and reactive oxygen species: team players in endothelium-dependent contractions. *Pharmacol Ther, 122*(2), 140-149.

Taniyama, Y., & Griendling, K. K. (2003). Reactive oxygen species in the vasculature: molecular and cellular mechanisms. *Hypertension, 42*(6), 1075-1081.

Terai, K., Hiramoto, Y., Masaki, M., Sugiyama, S., Kuroda, T., Hori, M., Kawase, I., & Hirota, H. (2005). AMP-activated protein kinase protects cardiomyocytes against hypoxic injury through attenuation of endoplasmic reticulum stress. *Mol Cell Biol, 25*(21), 9554-9575.

Tian, X. Y., Wong, W. T., Wang, N., Lu, Y., Cheang, W. S., Liu, J., Liu, L., Liu, Y., Lee, S. S., Chen, Z. Y., Cooke, J. P., Yao, X., & Huang, Y. (2012a). PPARdelta activation protects endothelial function in diabetic mice. *Diabetes, 61*(12), 3285-3293.

Tian, X. Y., Wong, W. T., Xu, A., Lu, Y., Zhang, Y., Wang, L., Cheang, W. S., Wang, Y., Yao, X., & Huang, Y. (2012b). Uncoupling protein-2 protects endothelial function in diet-induced obese mice. *Circ Res, 110*(9), 1211-1216.

Tian, X. Y., Yung, L. H., Wong, W. T., Liu, J., Leung, F. P., Liu, L., Chen, Y., Kong, S. K., Kwan, K. M., Ng, S. M., Lai, P. B., Yung, L. M., Yao, X., & Huang, Y. (2012c). Bone morphogenic protein-4 induces endothelial cell apoptosis through oxidative stress-dependent p38MAPK and JNK pathway. *J Mol Cell Cardiol, 52*(1), 237-244.

Toth, A., Nickson, P., Mandl, A., Bannister, M. L., Toth, K., & Erhardt, P. (2007). Endoplasmic reticulum stress as a novel therapeutic target in heart diseases. *Cardiovasc Hematol Disord Drug Targets, 7*(3), 205-218.

Touyz, R. M. (2004). Reactive oxygen species, vascular oxidative stress, and redox signaling in hypertension: what is the clinical significance? *Hypertension, 44*(3), 248-252.

Touyz, R. M., Yao, G., Quinn, M. T., Pagano, P. J., & Schiffrin, E. L. (2005). p47phox associates with the cytoskeleton through cortactin in human vascular smooth muscle cells: role in NAD(P)H oxidase regulation by angiotensin II. *Arterioscler Thromb Vasc Biol, 25*(3), 512-518.

Tseng, Y. T., Hsu, Y. Y., Shih, Y. T., & Lo, Y. C. (2012). Paeonol attenuates microglia-mediated inflammation and oxidative stress-induced neurotoxicity in rat primary microglia and cortical neurons. *Shock, 37*(3), 312-318.

Tu, B. P., & Weissman, J. S. (2004). Oxidative protein folding in eukaryotes: mechanisms and consequences. *J Cell Biol, 164*(3), 341-346.

Ulevitch, R. J., & Tobias, P. S. (1995). Receptor-dependent mechanisms of cell stimulation by bacterial endotoxin. *Annu Rev Immunol, 13*, 437-457.

Urano, F., Wang, X., Bertolotti, A., Zhang, Y., Chung, P., Harding, H. P., & Ron, D. (2000). Coupling of stress in the ER to activation of JNK protein kinases by transmembrane protein kinase IRE1. *Science, 287*(5453), 664-666.

Van der Poll, T., & Opal, S. M. (2008). Host-pathogen interactions in sepsis. *Lancet Infect Dis, 8*(1), 32-43.

Vanhoutte, P. M. (1989). Endothelium and control of vascular function. State of the Art lecture. *Hypertension, 13*(6 Pt 2), 658-667.

Vanhoutte, P. M., Boulanger, C. M., & Mombouli, J. V. (1995). Endothelium-derived relaxing factors and converting enzyme inhibition. *Am J Cardiol, 76*(15), 3E-12E.

Vanhoutte, P. M., Feletou, M., & Taddei, S. (2005). Endothelium-dependent contractions in hypertension. *Br J Pharmacol, 144*(4), 449-458.

Vanhoutte, P. M., Shimokawa, H., Tang, E. H., & Feletou, M. (2009). Endothelial dysfunction and vascular disease. *Acta Physiol (Oxf), 196*(2), 193-222.

Vanhoutte, P. M., & Tang, E. H. (2008). Endothelium-dependent contractions: when a good guy turns bad! *J Physiol, 586*(22), 5295-5304.

Varani, J., & Ward, P. A. (1994). Mechanisms of endothelial cell injury in acute inflammation. *Shock, 2*(5), 311-319.

Viner, R. I., Williams, T. D., & Schoneich, C. (2000). Nitric oxide-dependent modification of the sarcoplasmic reticulum Ca-ATPase: localization of cysteine target sites. *Free Radic Biol Med, 29*(6), 489-496.

Virag, L., Szabo, E., Gergely, P., & Szabo, C. (2003). Peroxynitrite-induced cytotoxicity: mechanism and opportunities for intervention. *Toxicol Lett, 140-141*, 113-124.

Virdis, A., Ghiadoni, L., & Taddei, S. (2010). Human endothelial dysfunction: EDCFs. *Pflugers Arch, 459*(6), 1015-1023.

Virdis, A., & Schiffrin, E. L. (2003). Vascular inflammation: a role in vascular disease in hypertension? *Curr Opin Nephrol Hypertens, 12*(2), 181-187.

Waller, B. F., Orr, C. M., Slack, J. D., Pinkerton, C. A., Van Tassel, J., & Peters, T. (1992). Anatomy, histology, and pathology of coronary arteries: a review relevant to new interventional and imaging techniques--Part IV. *Clin Cardiol, 15*(9), 675-687.

Walsh, C., Barrow, S., Voronina, S., Chvanov, M., Petersen, O. H., & Tepikin, A. (2009). Modulation of calcium signalling by mitochondria. *Biochimica et Biophysica Acta (BBA) - Bioenergetics, 1787*(11), 1374-1382.

Wang, Wang, H. Y., Ouyang, J., Yu, L., Chen, B., Qin, J. Q., & Qiu, X. Z. (2009). Low concentration of lipopolysaccharide acts on MC3T3-E1 osteoblasts and induces proliferation via the COX-2-independent NFkappaB pathway. *Cell Biochem Funct, 27*(4), 238-242.

Wang, D., Wang, H., Guo, Y., Ning, W., Katkuri, S., Wahli, W., Desvergne, B., Dey, S. K., & DuBois, R. N. (2006). Crosstalk between peroxisome proliferator-activated receptor delta and VEGF stimulates cancer progression. *Proc Natl Acad Sci U S A, 103*(50), 19069-19074.

Wang, S., & Kaufman, R. J. (2012). The impact of the unfolded protein response on human disease. *J Cell Biol, 197*(7), 857-867.

Wang, X., Zhu, G., Yang, S., Wang, X., Cheng, H., Wang, F., Li, X., & Li, Q. (2011). Paeonol prevents excitotoxicity in rat pheochromocytoma PC12 cells via downregulation of ERK activation and inhibition of apoptosis. *Planta Med, 77*(15), 1695-1701.

Wassmann, S., Stumpf, M., Strehlow, K., Schmid, A., Schieffer, B., Bohm, M., & Nickenig, G. (2004). Interleukin-6 induces oxidative stress and endothelial dysfunction by overexpression of the angiotensin II type 1 receptor. *Circ Res, 94*(4), 534-541.

White, R. M., Rivera, C. O., & Davison, C. B. (1996). Differential contribution of endothelial function to vascular reactivity in conduit and resistance arteries from deoxycorticosterone-salt hypertensive rats. *Hypertension, 27*(6), 1245-1253.

Widlansky, M. E., Gokce, N., Keaney, J. F., & Vita, J. A. (2003). The clinical implications of endothelial dysfunction. *J Am Coll Cardiol, 42*(7), 1149-1160.

Willerson, J. T., & Ridker, P. M. (2004). Inflammation as a cardiovascular risk factor. *Circulation, 109*(2), 2-10.

Wolfram, J. A., & Donahue, J. K. (2013). Gene Therapy to Treat Cardiovascular Disease. *J Am Heart Assoc, 2*(4).

Wong, M. S., & Vanhoutte, P. M. (2010). COX-mediated endothelium-dependent contractions: from the past to recent discoveries. *Acta Pharmacol Sin, 31*(9), 1095-1102.

Wong, W. T., Tian, X. Y., Chen, Y., Leung, F. P., Liu, L., Lee, H. K., Ng, C. F., Xu, A., Yao, X., Vanhoutte, P. M., Tipoe, G. L., & Huang, Y. (2010). Bone morphogenic protein-4 impairs endothelial function through oxidative stress-dependent cyclooxygenase-2 upregulation: implications on hypertension. *Circ Res, 107*(8), 984-991.

Woods, M., Bishop-Bailey, D., Pepper, J. R., Evans, T. W., Mitchell, J. A., & Warner, T. D. (1998). Cytokine and lipopolysaccharide stimulation of endothelin-1 release from human internal mammary artery and saphenous vein smooth-muscle cells. *J Cardiovasc Pharmacol, 31 Suppl 1*, S348-350.

Wu, B. (1966). Studies on the Chinese drug cortex moutan radicis. Assay of paeonol in cortex moutan radicis. *Yao Xue Xue Bao, 13*(2), 145-148.

Wu, J., Xue, X., Wu, Z., Zhao, H.-L., Cao, H.-M., Sun, D.-Q., Wang, R.-M., Sun, J., Liu, Y., & Guo, R.-C. (2014). Anti-tumor effect of paeonol via regulating NF-κB,

AKT and MAPKs activation: A quick review. *Biomedicine & Preventive Nutrition, 4*(1), 9-14.

Wu, T., Ling, Q.-Y., Zhong, C., Wang, T.-X., Wang, L.-L., Wang, X.-Y., Su, Z.-L., & Zong, G.-J. (2015). Expression of BMP4 in myocardium and vascular tissue of obese mice. *Int J Inflam, 12*(1), 8.

Xie, Q., Khaoustov, V. I., Chung, C. C., Sohn, J., Krishnan, B., Lewis, D. E., & Yoffe, B. (2002). Effect of tauroursodeoxycholic acid on endoplasmic reticulum stress-induced caspase-12 activation. *Hepatology, 36*(3), 592-601.

Xie, Q. W., Kashiwabara, Y., & Nathan, C. (1994). Role of transcription factor NF-kappa B/Rel in induction of nitric oxide synthase. *J Biol Chem, 269*(7), 4705-4708.

Xu, J., Wang, S., Wu, Y., Song, P., & Zou, M. H. (2009). Tyrosine nitration of PA700 activates the 26S proteasome to induce endothelial dysfunction in mice with angiotensin II-induced hypertension. *Hypertension, 54*(3), 625-632.

Yanagisawa, M., Kurihara, H., Kimura, S., Tomobe, Y., Kobayashi, M., Mitsui, Y., Yazaki, Y., Goto, K., & Masaki, T. (1988). A novel potent vasoconstrictor peptide produced by vascular endothelial cells. *Nature, 332*(6163), 411-415.

Yang, D., Feletou, M., Boulanger, C. M., Wu, H. F., Levens, N., Zhang, J. N., & Vanhoutte, P. M. (2002). Oxygen-derived free radicals mediate endothelium-dependent contractions to acetylcholine in aortas from spontaneously hypertensive rats. *Br J Pharmacol, 136*(1), 104-110.

Yang, X., Long, L., Southwood, M., Rudarakanchana, N., Upton, P. D., Jeffery, T. K., Atkinson, C., Chen, H., Trembath, R. C., & Morrell, N. W. (2005). Dysfunctional Smad signaling contributes to abnormal smooth muscle cell proliferation in familial pulmonary arterial hypertension. *Circ Res, 96*(10), 1053-1063.

Yoon, Y. M., Lee, J. H., Yun, S. P., Han, Y. S., Yun, C. W., Lee, H. J., Noh, H., Lee, S. J., Han, H. J., & Lee, S. H. (2016). Tauroursodeoxycholic acid reduces ER stress by regulating of Akt-dependent cellular prion protein. *Sci Rep, 6*, 39838.

Yoshida, H. (2007). ER stress and diseases. *Febs J, 274*(3), 630-658.

Yoshizumi, M., Kurihara, H., Sugiyama, T., Takaku, F., Yanagisawa, M., Masaki, T., & Yazaki, Y. (1989). Hemodynamic shear stress stimulates endothelin production by cultured endothelial cells. *Biochem Biophys Res Commun, 161*(2), 859-864.

Young, C. N., Cao, X., Guruju, M. R., Pierce, J. P., Morgan, D. A., Wang, G., Iadecola, C., Mark, A. L., & Davisson, R. L. (2012). ER stress in the brain subfornical organ mediates angiotensin-dependent hypertension. *J Clin Invest, 122*(11), 3960-3964.

Zeeshan, H. M., Lee, G. H., Kim, H. R., & Chae, H. J. (2016). Endoplasmic Reticulum Stress and Associated ROS. *Int J Mol Sci, 17*(3), 327.

Zhang, Syed, T. W., Liu, R., & Yu, J. (2017). Role of Endoplasmic Reticulum Stress, Autophagy, and Inflammation in Cardiovascular Disease. *Front Cardiovasc Med, 4*, 29.

Zhang, C. (2008). The role of inflammatory cytokines in endothelial dysfunction. *Basic Res Cardiol, 103*(5), 398-406.

Zhang, H., Park, Y., Wu, J., Chen, X., Lee, S., Yang, J., Dellsperger, K. C., & Zhang, C. (2009). Role of TNF-alpha in vascular dysfunction. *Clin Sci (Lond), 116*(3), 219-230.

Zhang, L. H., Xiao, P. G., & Huang, Y. (1996). Recent progresses in pharmacological and clinical studies of paeonol. *Zhongguo Zhong Xi Yi Jie He Za Zhi, 16*(3), 187-190.

Zhang, X., Wang, C., Shan, S., Liu, X., Jiang, Z., & Ren, T. (2016). TLR4/ROS/miRNA-21 pathway underlies lipopolysaccharide instructed primary tumor outgrowth in lung cancer patients. *Oncotarget, 7*(27), 42172-42182.

Zhang, Y., Liu, J., Tian, X. Y., Wong, W. T., Chen, Y., Wang, L., Luo, J., Cheang, W. S., Lau, C. W., Kwan, K. M., Wang, N., Yao, X., & Huang, Y. (2014). Inhibition of Bone Morphogenic Protein 4 Restores Endothelial Function in db/db Diabetic Mice. *Arterioscler Thromb Vasc Biol, 34*(1), 152-159.

Zhang, Y., & Ren, J. (2011). Thapsigargin triggers cardiac contractile dysfunction via NADPH oxidase-mediated mitochondrial dysfunction: Role of Akt dephosphorylation. *Free Radic Biol Med, 51*(12), 2172-2184.

Zhao, H., Liao, Y., Minamino, T., Asano, Y., Asakura, M., Kim, J., Asanuma, H., Takashima, S., Hori, M., & Kitakaze, M. (2008). Inhibition of cardiac remodeling by pravastatin is associated with amelioration of endoplasmic reticulum stress. *Hypertens Res, 31*(10), 1977-1987.

Zhu, Y.-P. (1998). Chinese Materia Medica: Chemistry, Pharmacology and Applications. *CRC Press*.

Zorov, D. B., Juhaszova, M., & Sollott, S. J. (2014). Mitochondrial reactive oxygen species (ROS) and ROS-induced ROS release. *Physiol Rev, 94*(3), 909-950.

Zou, M. H., & Wu, Y. (2008). AMP-activated protein kinase activation as a strategy for protecting vascular endothelial function. *Clin Exp Pharmacol Physiol, 35*(5-6), 535-545.

Zuo, L., Zhou, T., Pannell, B. K., Ziegler, A. C., & Best, T. M. (2015). Biological and physiological role of reactive oxygen species--the good, the bad and the ugly. *Acta Physiol (Oxf), 214*(3), 329-348.

LIST OF PUBLICATIONS AND PAPERS PRESENTED

1. Academic Awards

a) Best Oral Presentation Award (Molecular Biology Category) in International Postgraduate Research Awards Seminar (INPRAS), University Malaya, 7-8th March 2016.

b) Young Investigator Award, 7th Scientific International Meeting of the Asian Society for Vascular Biology, Taiwan, 27-29 Oct 2016.

c) 3rd prize winner, 3 minute thesis competition, Department Level, University Malaya, 2nd March 2017.

d) The Best Oral Scientific Presentation Award, International Conference on Scientific Frontiers in Natural Product Based Drug, National University of Singapore, 6-7 July 2017.

e) Third Place Winner, 31st Scientific Meeting of the Malaysia Society of Pharmacology & Physiology (MSPP), School of Medical Sciences, University Science Malaysia, 18-19 August 2017.

2. List of Publications

a) Ker Woon Choy, Mohd Rais Mustafa, Yeh Siang Lau, Jian Liu, Dharmani Murugan, Chi Wai Lau, Li Wang, Lei Zhao, Yu Huang, Paeonol Protects Against Endoplasmic Reticulum Stress-Induced Endothelial Dysfunction via AMPK/PPARδ Signaling Pathway, *Biochemical Pharmacology*, 2016.

b) Ker Woon Choy, Yeh Siang Lau, Dharmani Murugan, Mohd Rais Mustafa, Chronic treatment with paeonol improves endothelial function in mice through inhibition of endoplasmic reticulum stress-mediated oxidative stress, *Plos One*, 2017

c) Ker Woon Choy, Yeh Siang Lau, Dharmani Murugan, Paul M. Vanhoutte, Mohd Rais Mustafa, Paeonol attenuates LPS-induced endothelial dysfunction and apoptosis through inhibition of BMP4 signalling pathway independent of TLR4, Journal of Pharmacology and Experimental Therapeutics, December 2017.

d) Ker Woon Choy, Dharmani Murugan, Mohd Rais Mustafa, Natural products targeting ER stress pathway in cardiovascular diseases, Pharmacological Research.

3. Conference abstracts

a. Oral presentation

i. Mohd Rais Mustafa, Ker Woon Choy, Yeh Siang Lau, Jian Liu, Chi Wai Lau, Dharmani Murugan and Yu Huang, and Paeonol Protects Against Tunicamycin-Induced Oxidative Stress And Endothelial Dysfunction Via AMPK/PPARδ Pathway, *The 13th Asia Pacific Federation Of Pharmacologist (APFP) Meeting "New Paradigms In Pharmacology For Global Health"*, 1-3 Febuary 2016

ii. Ker Woon Choy, Yeh Siang Lau, Jian Liu, Chi Wai Lau, Dharmani Murugan, Yu Huang and Mohd Rais Mustafa, Paeonol Protects Against Endoplasmic Reticulum Stress-Induced Endothelial Dysfunction via AMPK/PPARδ Signalling Pathway. *International Postgraduate Research Awards Seminar (INPRAS)*, University Malaya, 7-8th March 2016.

iii. Ker Woon Choy, Mohd Rais Mustafa, Yeh Siang Lau, Jian Liu, Dharmani Murugan, Chi Wai Lau, Li Wang, Lei Zhou and Yu Huang, Protective Effects Of Paeonol Against Endoplasmic Reticulum Stress-Induced Endothelial Dysfunction And Oxidative Stress Through AMPK/ PPARδ Pathway, *7th*

Scientific International Meeting of the Asian Society for Vascular Biology, Taiwan, 27-29 Oct 2016.

iv. Ker-Woon Choy, Yeh Siang Lau, Dharmani Murugan, Mohd Rais Mustafa, Paeonol attenuates lipopolysaccharide-induced apoptosis in human umbilical vein endothelial cells by inhibiting BMP4/ROS/MAPK signalling, *International Conference on Scientific Frontiers in Natural Product Based Drug*, National University of Singapore, 6-7 July 2017.

v. Mohd Rais Mustafa, Ker Woon Choy, Yeh Siang Lau, Dharmani Murugan Chronic treatment with paeonol protects against tunicamycin-induced endothelial dysfunction through attenuating Oxidative Stress and Endoplasmic Reticulum Stress, *International Conference on Scientific Frontiers in Natural Product Based Drug*, National University of Singapore, 6-7 July 2017.

vi. Ker Woon Choy, Yeh Siang Lau, Dharmani Murugan, Mohd Rais Mustafa, Paeonol Attenuates Lipopolysaccharide-Induced Apoptosis In Human Umbilical Vein Endothelial Cells By Inhibiting BMP4/ROS/MAPK Signalling, *31st Scientific Meeting of the Malaysia Society of Pharmacology & Physiology (MSPP)*, School of Medical Sciences, University Science Malaysia, Malaysia18-19 August 2017.

b. Poster presentation

i. Ker Woon Choy, Mohd Rais Mustafa, Yeh Siang Lau, Jian Liu, Dharmani Murugan, Chi Wai Lau, Li Wang, Lei Zhou and Yu Huang. Paeonol Protects Against Endoplasmic Reticulum Stress-Induced Endothelial Dysfunction via AMPK/PPARδ Signalling Pathway. *International Conference by British Pharmacological Society*, London, 15-17 December 2015.

ii. Mohd Rais Mustafa, Ker Woon Choy, Dharmani Murugan, Yeh Siang Lau, Paul M. Vanhoutte, Vascular protective effect of Paeonol inhibits the bone morphogenetic protein 4 (BMP4)/ MAPK dependent pathway in the mouse aorta and protects against lipopolysaccharide-induced endothelial dysfunction, *International Symposium on Mechanisms of Vasodilatation*, Rochester, United Kingdom, 7th- 9th November 2016.